

**Natural Product-Like Furopyranones:  
Synthesis and Biological Activity in Human Cancer Cells**

Inauguraldissertation  
der Philosophisch-naturwissenschaftlichen Fakultät  
der Universität Bern

vorgelegt von  
**Cyril Adrian Fuhrer**  
von Langnau i. E. (BE)

Leiter der Arbeit:  
Prof. Dr. Robert Häner  
Departement für Chemie und Biochemie der Universität Bern

**Natural Product-Like Furopyranones:  
Synthesis and Biological Activity in Human Cancer Cells**

Inauguraldissertation  
der Philosophisch-naturwissenschaftlichen Fakultät  
der Universität Bern

vorgelegt von  
**Cyril Adrian Fuhrer**  
von Langnau i. E. (BE)

Leiter der Arbeit:  
Prof. Dr. Robert Häner  
Departement für Chemie und Biochemie der Universität Bern

Von der Philosophisch-naturwissenschaftlichen Fakultät angenommen.

Bern, 1. November 2007

Der Dekan:  
Prof. Dr. Paul Messerli

*Für meine Eltern,  
Nadja und Philipp*

*„ Dosis sola facit venenum“*

*Theophrastus Bombastus von Hohenheim*

*(1493 – 1541)*

## List of Publications:

- C. Fuhrer, R. Messer, R. Häner:  
,Stereoselective synthesis of 3a,7a-dihydro-3H,4H-furo[3,4-c]pyran-1-ones via intramolecular hetero-Diels-Alder reaction'  
*Tetrahedron Lett.* **2004**, *45*, 4297-4300.
  
- P. Gerner, C. Fuhrer, Ch. Reinhard, H. U. Güdel:  
'Near-infrared to visible photon upconversion in Mn<sup>2+</sup> and Yb<sup>3+</sup> containing materials'  
*J. Alloys Comp.* **2004**, *380*, 39-44.
  
- R. Messer, C. A. Fuhrer, R. Häner:  
'Natural product-like libraries based on non-aromatic, polycyclic motifs'  
*Curr. Opin. Chem. Biol.* **2005**, *9*, 259-265.
  
- N. Guiblin, C. A. Fuhrer, R. Häner, H. Stöckli-Evans, K. Schenk, G. Chapuis:  
'The incommensurately modulated structure of a tricyclic natural-product-like compound of empirical formula C<sub>22</sub>H<sub>20</sub>O<sub>3</sub>'  
*Acta Cryst.* **2006**, *B62*, 506-512.
  
- C. A. Fuhrer, E. Grüter, S. Ruetz, R. Häner:  
'Cis-Stilbene Derived Furopyranones Show Potent Antiproliferative Activity by Inducing G2/M Arrest'  
*ChemMedChem* **2007**, *2*, 441-444.
  
- R. Messer, C. A. Fuhrer, R. Häner:  
'Lewis acid catalysed synthesis of a tricyclic scaffold from D-(-)-ribose'  
*Nucleosides, Nucleotides & Nucleic Acids* **2007**, in press.

## Acknowledgements

First of all I would like to thank Prof. Dr. Robert Häner for the opportunity to do my Ph. D. in his research group. I strongly appreciate his great support, the fruitful discussions and the possibility to collaborate with the 'Novartis Institutes for BioMedical Research' in Basel. I would like to thank him very much for his confidence and the opportunity to supervise several Bachelor- and Master-Students as well as educating apprentices.

Special thanks go to Prof. Dr. Peter Gmeiner for being my co-referee and examiner and to Prof. Dr. Philippe Renaud who agreed to supervise the final examination.

Many thanks go to Dr. Holger Bittermann, Dr. Volodimir Malinovskii, Luzia Moesch, Dr. Eric Grüter, Dr. Roland Messer and Dr. Simon Langenegger for the helpful suggestions and interesting discussions. Furthermore I would like to thank Sarah Maria Biner, Alina Nussbaumer, Sandro Manni, Florian Garo, Michael Locher and Fabian Wenger, whom I supervised. Special thanks go to Zoe Clerc and again to Dr. Holger Bittermann as well as to Dr. Volodimir Malinovskii for critical reading of this dissertation.

Sincere thanks go to Dr. Stephan Ruetz, Dr. Bahaa Salem, Dr. Philipp Grosche, Dr. Hans-Jörg Roth, Dr. Jürg Zimmermann, Hélène Kiesler, Stephanie Pickett, Halil Koc, Raphael Gattlen, Urs Rindisbacher, Felix Thommen and their teams at the 'Novartis Institutes for BioMedical Research' in Basel for the successful collaboration, the instructive internship and the helpful suggestions.

Furthermore I would like to thank the University of Bern, Prof. Dr. Helen Stoeckli-Evans and Dr. Antonia Neels for the x-ray crystallographic analyses, Prof. Dr. Peter Bigler and his team for the NMR measurements and their help concerning NMR related questions, Dr. Stefan Schürch and his team for MS measurements and the group of Prof. Dr. Silvio Decurtins for the use of their equipment. Also many thanks to the 'Ausgabe' team, the technical and electronic team and the administration of the Department of Chemistry and Biochemistry for various help.

Special thanks go to all the past and current members of the Häner and the Leumann group for help, support and good spirits.

Finally, I would like to thank those who I failed to mention, but who in one way or another have contributed to the present thesis.

# Table of Contents

<b>Summary</b>	<b>1</b>
<b>1 Introduction</b>	<b>3</b>
1.1 Drug Discovery	3
1.1.1 A Brief Historical Perspective of Drug Discovery	5
1.1.2 Medicinal Chemistry	9
1.1.3 Tools of the Trade	11
1.1.3.1 Combinatorial Chemistry	14
1.1.4 Natural Products and Chemical Genetics in Drug Discovery	15
1.1.5 A Diversity-Oriented Synthesis (DOS) Approach to Natural Product-Like Compounds	17
1.2 Approaches to the Medical Treatment of Cancer	19
1.2.1 Some Facts about Cancer	19
1.2.2 Genetic Faults Leading to Cancer: Proto-Oncogenes and Oncogenes	20
1.2.3 Treatment and Resistance of Cancer	23
1.3 Natural Product Leads for Discovering New Anticancer Agents	25
1.3.1 Iridoids	25
1.3.1.1 Antitumor Activity of Iridoids and Their Derivatives	28
1.3.2 Stilbenes Including Resveratrol and Combretastatin A-4	31
1.3.2.1 Antitumor Activity of Resveratrol, Combretastatin A-4 and Its Derivatives	32
1.3.3 Natural Products with Anticancer Properties Containing Lactones	36
1.4 The Diels-Alder Reaction	38
1.4.1 Intramolecular <i>hetero</i> Diels-Alder Reactions	40
1.5 Solid Support Chemistry	44
1.6 References for Chapter 1	47
<b>2 Aim of the Work</b>	<b>51</b>
<b>3 Synthesis and Antiproliferative Properties of Furopyranones</b>	<b>53</b>
3.1 Development of a Synthetic Route for Furopyranones	53
3.2 Stereoselective Synthesis of 3a,7a-Dihydro-3H,4H-furo[3,4-c]pyran-1-ones <i>via</i> an Intramolecular <i>hetero</i> Diels-Alder Reaction	55
3.3 Syntheses of Furo[3,4-c]pyranones for Implementation of a Detailed Structure-Activity Relationship (SAR) Study	59
3.3.1 Synthesis of C(7)-Desphenyl Derivatives	59

---

3.3.2	Aminolysis of the Lactone	62
3.3.3	Synthesis of a Tricyclic Derivative	64
3.3.4	Attempted Replacement of the $\gamma$ -Lactone by a $\delta$ -Lactone	68
3.3.5	Carboxy- and Nitro-substituted Furopyranones	69
3.3.5.1	Nitro-substituted Furopyranones	69
3.3.5.2	Carboxy-substituted Furopyranones	71
3.3.6	Variation of the Substitution Pattern of the <i>cis</i> -Stilbene Motif	74
3.3.6.1	Synthesis from 4,4'-Dibromobenzil	74
3.3.6.2	Synthesis from 2,2'-Dichlorobenzil	74
3.3.6.3	Further Furopyranones from different $\alpha$ -Diketones	76
3.3.7	<i>Hetero</i> Diels-Alder <i>versus</i> Diels-Alder Reaction	77
3.4	Antiproliferative Properties of Natural Product-Like Furopyranones	83
3.4.1	<i>Cis</i> -Stilbene Derived Furopyranones and Their Antiproliferative Properties in A549 and KB31 Cells	83
3.4.2	<i>Cis</i> -Stilbene Derived Furopyranones and Their Antiproliferative Properties in K562 Cells	87
3.4.3	Further <i>Cis</i> -Stilbene Derived Furopyranones and Their Antiproliferative Properties in A549 and KB31 Cells	89
3.5	References for Chapter 3	96
<b>4</b>	<b>Preparation of Furopyranone-Libraries</b>	<b>98</b>
4.1	Preparation of Furopyranones Containing a Linker Group and a Protected Amine Function	99
4.2	Elaboration of Conditions for the Solid Phase Synthesis	105
4.2.1	Conditions for the Coupling Step	105
4.2.2	Determination of the Loading Efficiency by UV Quantification	106
4.2.3	Application of the Conditions to Different BAL-aminomethyl-PS Solid Supports	107
4.2.4	Configurational Stability of the Final Products Under Cleavage Conditions	109
4.3	Synthesis of Prototypes for Each Scaffold	110
4.4	Aminolysis of the Lactone Ring	115
4.5	References for Chapter 4	116
<b>5</b>	<b>Conclusions &amp; Outlook</b>	<b>117</b>
5.1	Antiproliferative Activity of Natural Product-Like Furopyranones	117
5.2	Solid Support Chemistry of Furopyranones	118
5.3	Outlook	119



---

5.4	References for Chapter 5	121
<b>6</b>	<b>Experimental Part</b>	<b>122</b>
6.1	Instrumentation	122
6.1.1	NMR Spectroscopy	122
6.1.2	Mass Spectrometry	123
6.1.3	IR –Spectroscopy	123
6.1.4	UV-VIS Spectroscopy	123
6.1.5	Melting Point Measurement	123
6.1.6	Analytical TLC and Preparative Column Chromatography	124
6.1.7	High Performance Liquid Chromatography (HPLC)	124
6.1.8	X-Ray Crystal Structure Analyses	124
6.1.9	Autoclave	125
6.1.10	Cellular Assays and Cell Cycle Analysis (KB31 and A549 Cells)	125
6.2	Solvents, Chemicals and Consumables	125
6.3	Solid Support Chemistry	126
6.3.1	Loading Efficiency and Loading Capacity	126
6.3.2	UV-Spectroscopic Quantification of the Loading Efficiency	126
6.3.3	Absorbance and Extinction Coefficient	126
6.3.4	General Methods for the Solid Phase Chemistry	127
6.3.4.1	Initial Tests with Compounds <b>53</b> , <b>54</b> , <b>55</b> and <b>56</b>	127
6.3.4.2	Testing of Different Solid Supports with Compound <b>53</b>	128
6.3.4.3	Fmoc-Determination of the Loading of the Resin	129
6.3.4.4	Synthesis of Prototypes Starting From Compounds <b>53</b> and <b>56</b>	130
6.3.4.5	Synthesis of Prototypes Starting From Compounds <b>54</b> and <b>55</b>	132
6.4	Experimental Procedures and Characterisation Data	134
6.4.1	Synthesis of Esters <b>6a-f</b>	134
6.4.2	Synthesis of Furopyranones <b>7a-f</b>	140
6.4.3	Aminolysis of Furopyranone <b>3g (8a-e)</b>	146
6.4.4	Synthesis of the Tricyclic Scaffold <b>16</b>	151
6.4.5	Attempted Synthesis of Pyranopyranone <b>21</b>	155
6.4.6	Synthesis of Furopyranone <b>26</b> and the Tricyclic Scaffold <b>27</b>	159
6.4.7	Synthesis of Cinnamyl Alcohol Derivatives <i>meta</i> - <b>32</b> and <i>para</i> - <b>32</b>	166
6.4.8	Synthesis of Furopyranone <b>36</b>	170
6.4.9	Synthesis of Furopyranone <b>39</b>	174
6.4.10	Synthesis of Furopyranone <b>41</b>	176
6.4.11	Synthesis of Furopyranone <b>51</b> and the Tricyclic Scaffold <b>52</b>	178

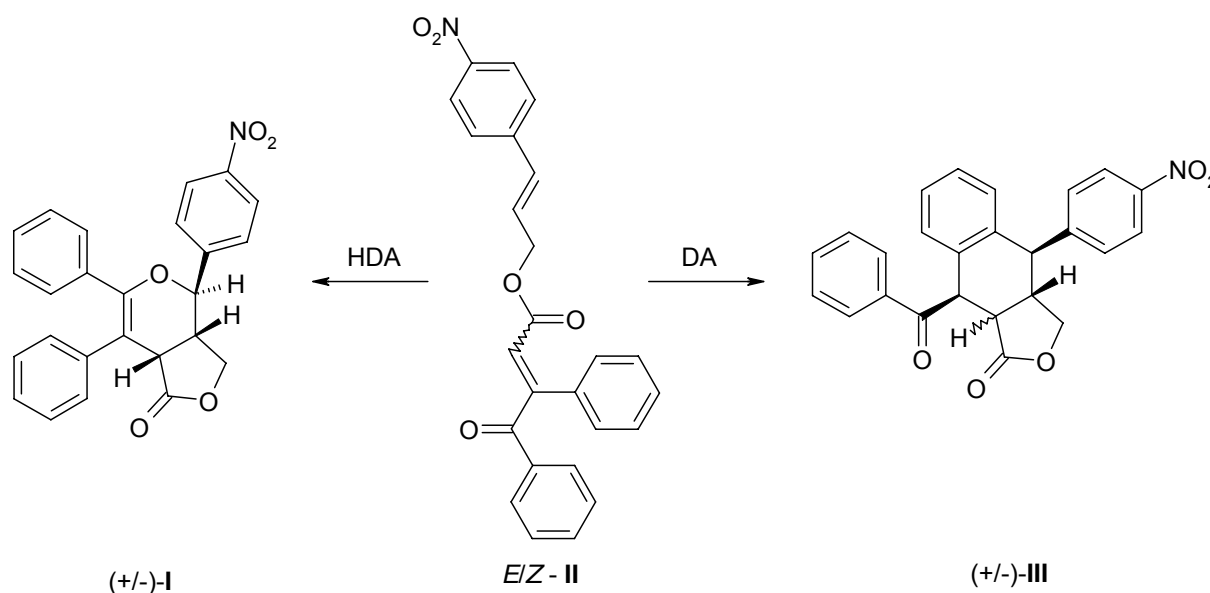
---

6.4.12	Synthesis of Furopyranones <b>53-56</b> for Solid Phase Chemistry	183
6.4.13	Products <b>72-85</b> obtained by Solid Phase Chemistry	196
6.4.14	Cellular Assays (K562 Cells)	207
6.5	References for Chapter 6	210
<b>7</b>	<b>Appendix</b>	<b>211</b>
7.1	Abbreviations	211
7.2	X-Ray Crystallography of Compound <b>3g</b>	216
7.3	X-Ray Crystallography of Compound <b>41</b>	219
7.4	Synthesis of ( <i>E/Z</i> )-4-Oxo-3,4-diphenyl-but-2-enoic acid 3-methyl-cyclohex-2-enyl ester	222
7.5	Synthesis of ( <i>E/Z</i> )-4-Oxo-3,4-diphenyl-but-2-enoic acid 3,5,5-trimethyl-cyclohex-2-enyl ester	225
7.6	4-Oxo-3,4-diphenyl-but-2-enoic acid ( <b>12</b> )	228
7.7	Cellular Assays (KB31 and A549 Cells)	229
7.8	Cell Cycle Analysis (KB31 and A549 Cells)	230
	<b>Curriculum Vitae</b>	<b>233</b>

## Summary

New drugs are constantly required to combat drug resistance, for improvement in the treatment of existing diseases, the treatment of newly identified diseases and the production of safer drugs by the reduction or removal of adverse side effects. The drug discovery process is devoted to the identification of compounds that cure or help to treat diseases. The current work is focused on the hit/lead identification process of novel natural product-like compounds with potential application in cancer treatment. Since natural products have been the mainstay of cancer therapy for more than 30 years, several natural product-like furopyranones like **I** were synthesised. These compounds contain several structural motifs from natural products (*cis*-stilbene, iridoid structure,  $\gamma$ -lactone) with anticancer properties.

The most important step for the synthesis of furopyranones like **I** was an intramolecular *hetero* Diels-Alder (HDA) reaction with an inverse electron demand. Herewith it was possible to synthesise these dihydropyran derivatives and to build up to three stereogenic centers in one reaction step. In selected cases formation of tricyclic products **III** via a normal Diels-Alder (DA) reaction involving a phenyl ring was observed under relatively harsh reaction conditions (autoclave,  $\sim 200^\circ\text{C}$ ). While the bicyclic furopyranones can be synthesised from the *E*- and *Z*-isomer of the corresponding  $\alpha,\beta$ -unsaturated  $\gamma$ -ketoesters **II** the tricyclic compounds were only formed *via* the *Z*-isomer.



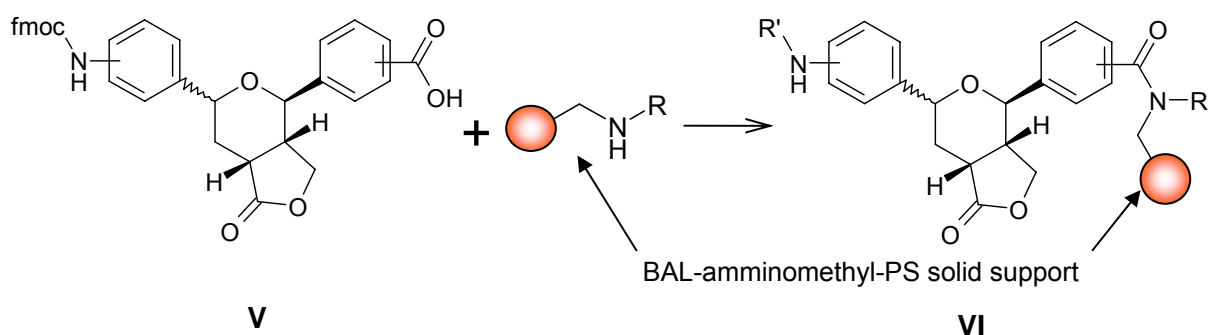
Several of the compounds showed anticancer activity in the low  $\mu\text{M}$  range in different human cancer cell lines (A549, KB31 and K562). Cell cycle analysis of cells treated with compound **IV** showed a significant and dose dependent cell cycle arrest in the G2/M-phase.

Furthermore, the compounds induced apoptosis in KB31 cells while no programmed cell death was observed in A549 cells.



A detailed structure-activity relationship study (SAR) revealed the *cis*-stilbene moiety as an essential element of the pharmacophore. The additional aryl ring next to the *cis*-stilbene moiety increased the activity. Aminolysis of the lactone decreased or eliminated the biological activity, which showed that the bicyclic nature of the structure also contributes to the activity.

In collaboration with the 'Novartis Institutes for BioMedical Research' in Basel, suitable furopyranones for solid phase chemistry were developed. Thus, furopyranones of type V containing amine and carboxylic acid groups were synthesised, in which the amine was Fmoc-protected. The BAL-aminomethyl-PS solid support used featured the advantage of yielding N-substituted carboxyamides upon release from the support.



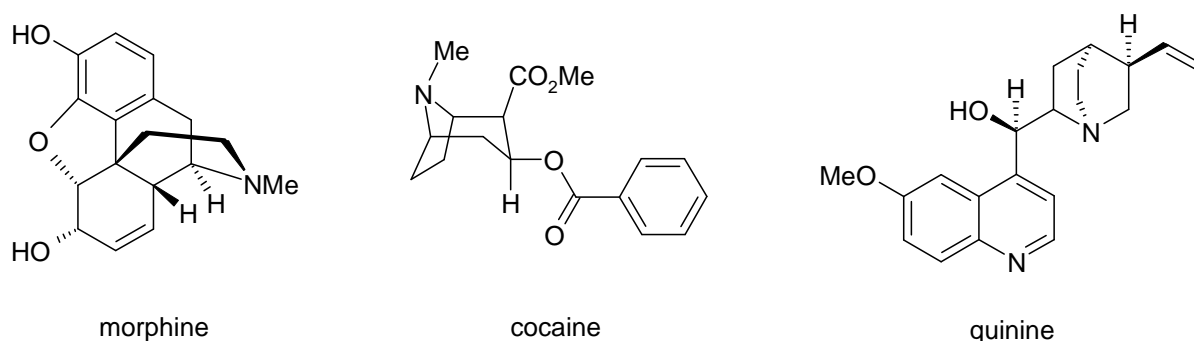
The synthesis of different derivatives (acylation, urea and sulfonic acid derivatives, aminolysis of the lactone) showed that formation of urea and acylation derivatives worked well while the synthesis of sulfonic acid derivatives and aminolysis of the lactone gave the product in only moderate yields. In cases where the amine of the aniline part was in *para*-position, a single diastereomer was isolated after an elongated cleaving procedure due to a possible ring opening-closing reaction of the pyrane ring under acidic conditions.

# 1. Introduction

The rich structural diversity and complexity of natural products have inspired chemists through the ages and have prompted them to produce these compounds in the laboratory, often with therapeutic applications in mind. Overall many drugs used today are natural products or natural product derivatives. A lot of these pharmaceuticals improved the quality and expectancy of life mainly of the people living in the developed world. Nevertheless there are still many severe diseases where no satisfactory therapies exist including cancer, autoimmune diseases (e.g. multiple sclerosis), infections by viruses and protozoans (e.g. AIDS, malaria, toxoplasmosis) and neurodegenerative diseases (e.g. Alzheimer's and Parkinson's disease). New danger also arises from bacterial pathogens: Many bacteria have developed a resistance against several antibiotics. Some pathogens show more and more resistance even against the antibiotic Vancomycin which is only used in hospitals as the last resort. New drugs are constantly required to combat drug resistance even though it can be minimised by the correct use of medicines by patients. They are also required for the improvement in the treatment of existing diseases, the treatment of newly identified diseases and the production of safer drugs by the reduction or elimination of adverse side effects.

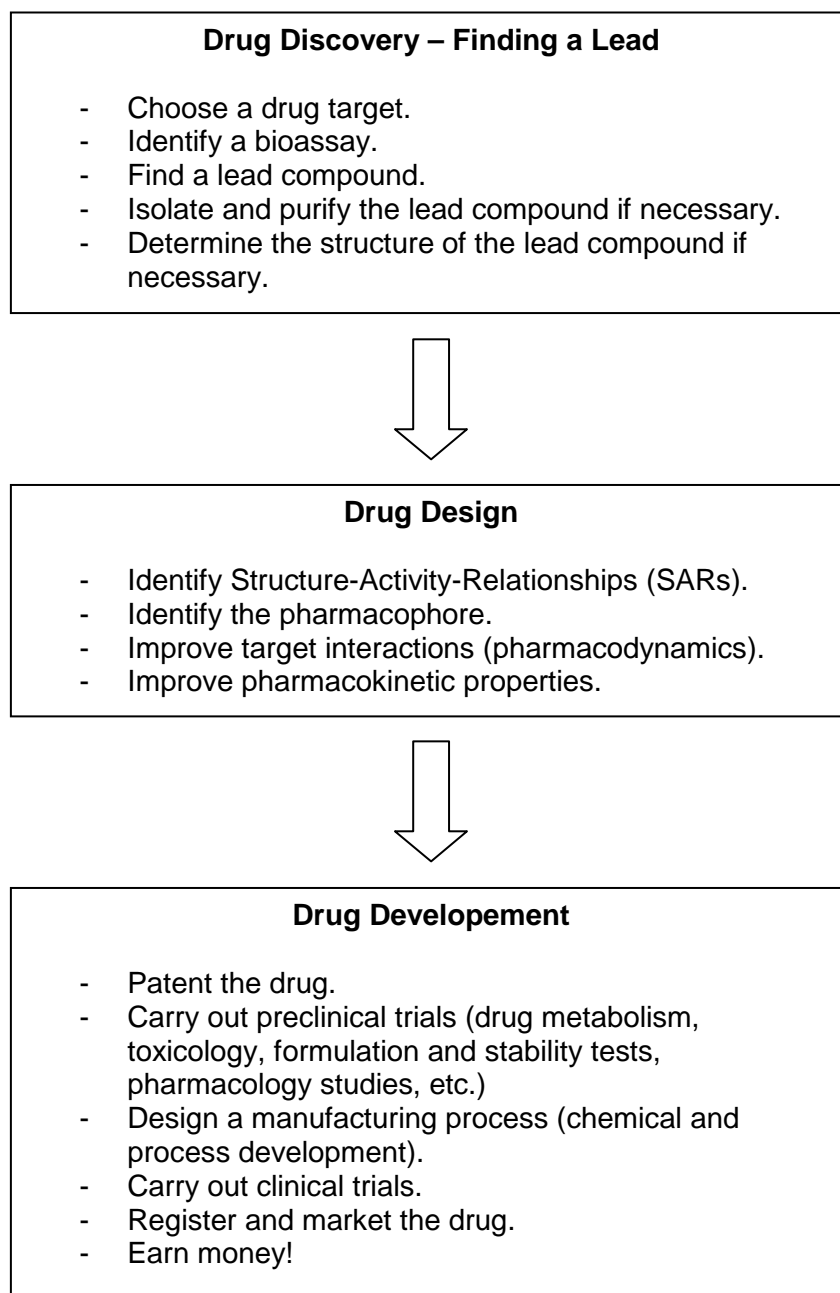
## 1.1 Drug Discovery

Before the twentieth century, medicines consisted mainly of herbs and potions. It was not until the mid-nineteenth century that first serious efforts were made to isolate and purify the active principle of these remedies (i.e. the pure chemicals responsible for the medicinal properties).



**Figure 1.1.** The structure of the alkaloids morphine (analgesic activity), cocaine (stimulant of the central nervous system and an appetite suppressant) and quinine (antipyretic, anti-malarial with analgesic and anti-inflammatory properties).

The success of these efforts led to the birth of many of the pharmaceutical companies we know today. Since then, many naturally occurring drugs have been obtained and their structures determined (e.g. morphine from opium, cocaine from coca leaves, quinine from the bark of the cinchona tree, see Figure 1.1). These natural products led to a major synthetic effort where chemists made literally thousands of analogues in an attempt to improve on what nature had done. Much of this work was carried out on a trial and error basis, but the results obtained revealed several general principles behind drug design.



**Figure 1.2.** General stages in drug discovery, design and development (adapted from cited ref.).<sup>1</sup>

An overall pattern for drug discovery and drug development also evolved, but there was still a high element of trial and error involved in the process. The mechanism by which a drug worked at the molecular level was rarely understood and drug research very much focused on what is known as the lead compound – an active principle isolated from a natural source or a synthetic compound prepared in the laboratory.

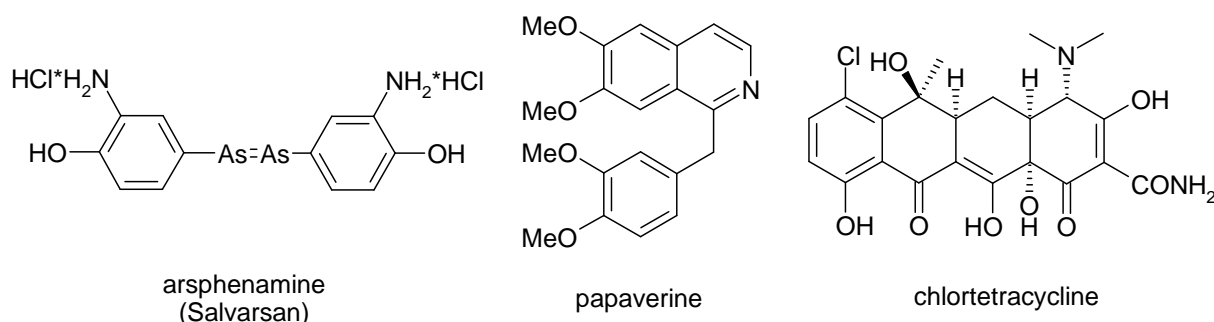
In recent years, medicinal chemistry has undergone a revolutionary change. Rapid advances in the biological sciences have resulted in a much better understanding of how the body functions at the cellular and the molecular level. As a result, many research projects in the academic sector or the pharmaceutical industry now begin by identifying a suitable target in the body and designing a drug to interact with that target. An understanding of the structure and function of the target, as well as the mechanism by which it interacts with potential drugs is crucial to this approach. Generally, one can identify the following stages in drug discovery, design and development as presented in Figure 1.2. Many of these stages run concurrently and are dependent on each other. For example, preclinical trials are usually carried out in parallel with the development of a manufacturing process. Even so, the discovery, design and development of a new drug can take 15 years or more, involve the synthesis of over 10000 compounds and cost in the region of \$800 million.<sup>1,2</sup>

### 1.1.1 A Brief Historical Perspective of Drug Discovery

Drug research, as we know it today, is not much older than a century. This kind of research began its career when chemistry was able to apply its principles and methods to problems outside of chemistry itself and when pharmacology had become a well-defined scientific discipline in its own right.<sup>3</sup>

**1800s to 1919:** Since ancient times the peoples of the world have had a wide range of natural products that they use for medicinal purposes. These products, obtained from animal, vegetable and mineral sources, were sometimes very effective. However, many of these products were very toxic and information about these remedies was not readily available to users until the invention of the printing press in the fifteenth century. The usage of such remedies reached its height in the seventeenth century. However, improved communication between practitioners in the eighteenth and nineteenth centuries resulted in the progressive removal of preparations that were either ineffective or too toxic from herbals and pharmacopoeias. It also led to a more rational development of new drugs.<sup>4</sup> In 1815, F. W. Sertürner isolated morphine from opium extracts and papaverine (see Figure 1.3) was isolated in 1848, but its antispasmodic properties were not discovered until 1917. By 1883, the first commercial drug antipyrine was produced and in 1897, Felix Hoffmann (Bayer)

synthesised Aspirin<sup>®</sup> which was first marketed in 1899. With the discovery of X-rays in 1895, the first step was taken toward X-ray crystallography, which would become the ultimate arbiter of complex molecular structures, including proteins and DNA.



**Figure 1.3.** The structure of Salvarsan as assumed by Ehrlich on the left, but recent investigations show that Salvarsan exists as cyclic trimer and pentamer. In the middle the structure of papaverine and on the right the structure of chlortetracycline are shown.

The benzene theory, which was pioneered by August Kekulé in 1865, gave an essential impulse to research on coal-tar derivatives, particularly dyes. In turn, the evolution of dye chemistry had a profound influence on medicine. The selective affinity of dyes for biological tissues led Paul Ehrlich, a medical student in the laboratory of the anatomist Wilhelm Waldeyer (between 1872 and 1874) at the University of Strasbourg, to postulate the existence of “chemoreceptors”. Ehrlich later argued that certain chemoreceptors on parasites, microorganisms, and cancer cells would be different from analogous structures in host tissues, and that these differences could be exploited therapeutically. It was the birth of chemotherapy, a particular type of drug therapy, that in the course of the 20th century led to unprecedented therapeutic triumphs. Ehrlich and Sacachiro Hata, who produced arsphenamine (Salvarsan, see Figure 1.3) to treat syphilis in 1910 by combining synthesis with reliable biological screening and evaluation procedures, carried out the first rational development of synthetic drugs. However, the influenza pandemic of 1918-1920, which killed more than 20 million people worldwide, clearly demonstrated the inability of medical science to stand up against disease.<sup>3,4,5</sup>

**1920s to 1930s:** These two decades were mainly characterised by the discovery of vitamins and developments in chemistry. The developments of the previous decades led to new drugs and new vaccines. Sulfa drugs became the first of the antibacterial wonder drugs promising broad-spectrum cures. One of the most important discoveries was the almost accidentally found penicillin by Alexander Fleming in 1928. New instruments such as the ultracentrifuge and refined techniques of X-ray crystallography paralleled the development of virology as a science. Isoelectric precipitation and electrophoresis first became important for drug purification and analysis.<sup>5</sup>



**1940s:** World War II played an important role for the development and production of Penicillin and antibiotics. There was the important need to cure the infected soldiers. So this era is commonly known as the *antibiotic era*. During these years, drugs were discovered in a less serendipitous fashion. Researchers started looking for specific drugs and often managed to find them. The treatment of malaria was another important topic and therefore William E. Doering and Robert B. Woodward synthesized quinine from coal tar in 1944. Woodward's achievements in the art of organic synthesis earned him the Nobel Prize in Chemistry in 1958. In 1948, Benjamin M. Duggar, a professor at the University of Wisconsin, isolated chlortetracycline from *Streptomyces aureofaciens*. Chlortetracycline, also called Aureomycin<sup>®</sup> (see Figure 1.3), was the first tetracycline antibiotic and the first broad-spectrum antibiotic.<sup>5</sup>

**1950s:** Drug discovery during this decade was also influenced by world events (e.g. Cold War, Korean conflict, the launch of the first orbital satellite in 1957). Technologies previously used for scientific purposes or for warfare were now being used for civilian needs. New technology and new instrumentation coupled with an understanding of how the human body worked and the publication of the structure of DNA by James Watson and Francis Crick in *Nature* in 1953 opened new windows of opportunity for the development of new drugs. So a large number of new drugs were discovered, among them cortisone and oral contraceptives. Breakthroughs were made in the instrumentation that led to the development of biotechnology. Human cell culture and radioimmunoassays developed as key research technologies and ultrasound was adapted for fetal monitoring. *Gas chromatography* (GC), *mass spectrometry* (MS), and polyacrylamide gel electrophoresis began transforming drug research. The main characteristics and contributions of this decade were mainly the vast amount of knowledge about human biology and chemistry, the development of sophisticated instrumentation, and the shift of the drug discovery process to a less serendipitous pattern.<sup>5</sup>

**1960s:** The 1960s was the pharmaceutical decade of the century where people became conscious about pills in all aspects of their lives. A plethora of new drugs was suddenly available: the Pill (oral contraceptives) was first marketed; Valium<sup>®</sup> and Librium<sup>®</sup> debuted to calm the nerves of housewives and businessmen; blood-pressure drugs and other heart-aiding medications were developed. Another emblem of the 1960s was the development of worldwide drug abuse, including the popularization of psychotropic drugs such as LSD. The social expansion of drugs for use and abuse in the 1960s forever changed not only the nature of medicine but also the politics of nations. The technology of drug discovery, analysis, and manufacture also proliferated. New forms of chromatography became available, including *high performance liquid chromatography* (HPLC), capillary GC, GC/MS, and the rapid expansion of thin-layer chromatography techniques. Proton NMR was developed to analyze complex biomolecules. By the end of the decade, amino acid analyzers

were commonplace, and the ultracentrifuge was fully adapted to biomedical uses. Analytical chemistry and biology joined as never before in the search for new drugs and analysis of old ones.<sup>5</sup>

**1970s:** New chemistries and the war on cancer were the most important stages during this decade. In 1978, for example, the cancer suppressor gene P53 was first discovered and by the end of the decade bone marrow transplants together with chemotherapeutics had become available. New drugs appeared. Cyclosporin provided a long-sought breakthrough with its ability to prevent immune rejection of tissue grafts and organ transplants. Rifampicin proved its worth for treating tuberculosis; cimetidine (Tagamet<sup>®</sup>), the first histamine blocker, became available for treating peptic ulcers. Throughout the decade, improvements in analytical instrumentation, HPLC and MS, made drug purification and analysis easier than ever before. In this period, NMR became transformed into the medical imaging system, MRI.<sup>5,6</sup>

**1980s:** The appearance of new diseases like AIDS motivated the development of immunology i.e. the study of the body's resistance to infections. Another phenomenon that triggered novel research was the resistance of old diseases to conventional drugs. Molecular biology and the use of computers gave rise to a new approach to innovation. Another significant step was the development of combinatorial chemistry in order to produce thousands of organic compounds that are then screened for biological activity.<sup>5,6</sup>

**1990s:** Miniaturisation of robotics and computers allowed manipulation of thousands of samples and processing the information gained therefrom in short time. High-throughput processes became state of the art. Especially the screening processes saw an enormous progress not only in instrumentation but also in techniques like fluorescence labelling and micro array scanning. The knowledge on disease underlying causes started to grow exponentially with initiatives like the Human Genome Project and studies of the proteome. Bioinformatic tools were put into place to process the vast amount of information and to recognise patterns within the data. The large amount of information and scientists from various disciplines had to be effectively managed in order to increase the efficiency of the drug discovery process. At the same time traditional antibiotics began to lose their power due to resistances in bacteria and the ongoing battle against AIDS had proven the failure of technology to master some of its problems.<sup>5,6</sup>

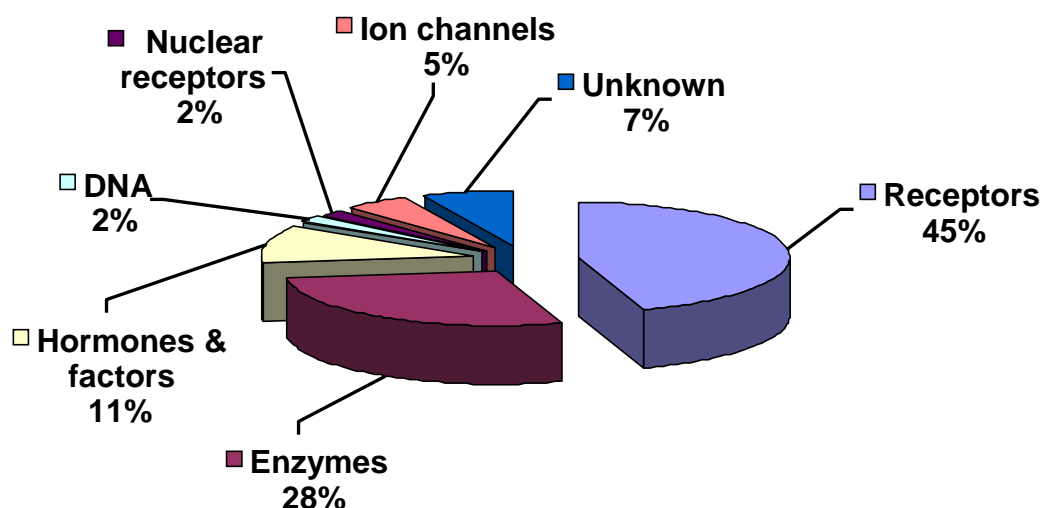
Finally it has to be said that serendipity as in the case of Penicillin has always played a part in the development of drugs. In spite of our increased knowledge base, it is still necessary to pick the correct starting point if a successful outcome is to be achieved and luck still plays a part in selecting that point. This state of affairs will not change and undoubtedly luck will also lead to new discoveries in the future. However, modern techniques such as computer

modelling and combinatorial chemistry are likely to reduce the number of intuitive discoveries.

### 1.1.2 Medicinal Chemistry

The primary objective of medicinal chemistry is the design and discovery of new compounds that are suitable for use as drugs. This process requires a team effort. It not only involves chemists but also scientists from a wide range of disciplines such as biology, biochemistry, pharmacology, mathematics, computing and medicine, amongst others.<sup>4,7</sup>

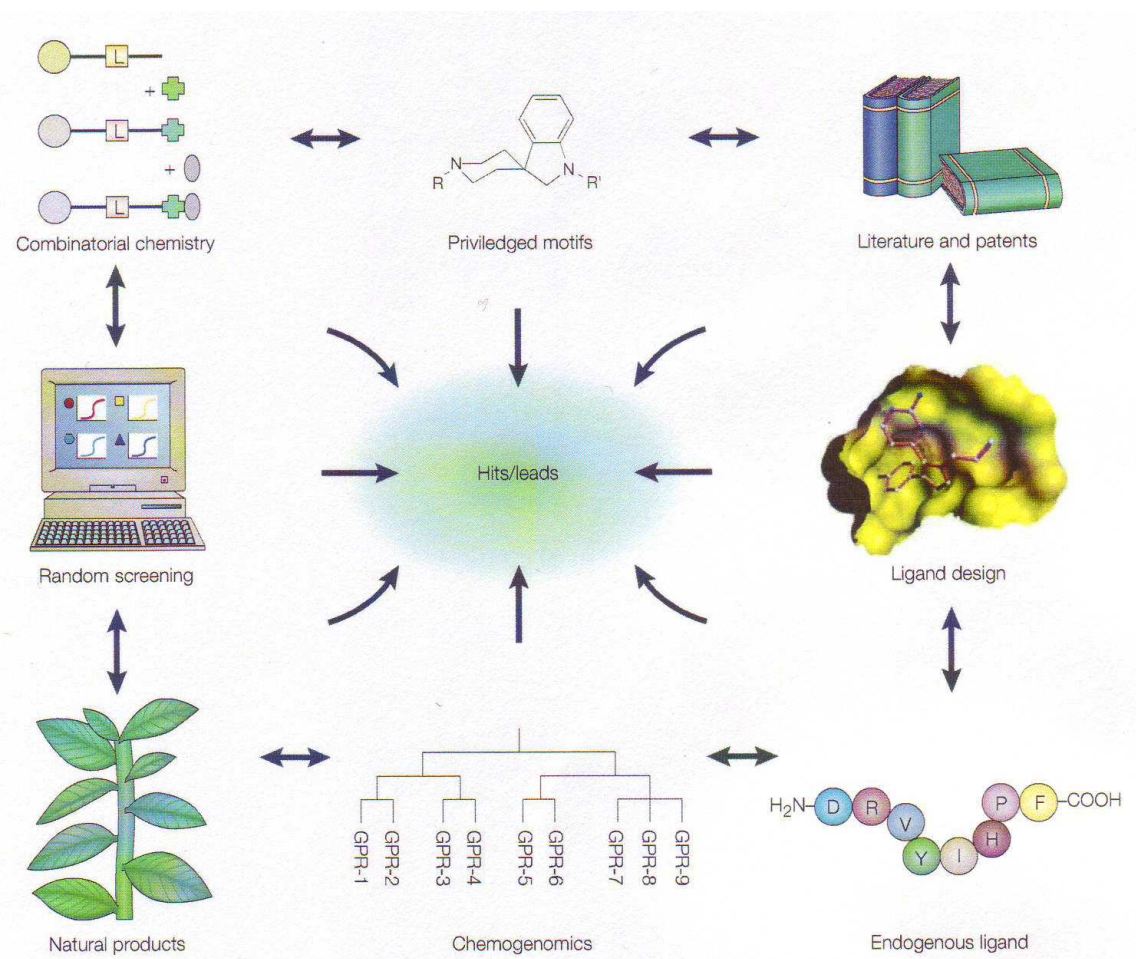
The role of the medicinal chemist is to design and synthesize new drugs.<sup>2</sup> In order to carry out that role, it is important to identify the particular target for a specific drug, and to establish how the drug interacts with that target to produce a biological effect. This is an area of study known as pharmacodynamics. The major drug targets in the body are normally large molecules (macromolecules) such as proteins, nucleic acids and carbohydrates. A comprehensive analysis of the drug targets underlying current drug therapy undertaken in 1996 showed that present-day therapy addresses only about 500 molecular targets. According to the analysis, cell membrane receptors, largely heterotrimeric GTP-binding protein (G-protein)-coupled receptors, constitute the largest subgroup with 45% of all targets, and enzymes account for 28% of all current drug targets (see Figure 1.4).<sup>3</sup>



**Figure 1.4.** Molecular targets of drug therapy (N=483). The therapeutic targets can be subdivided in seven main classes, wherein enzymes and receptors represent the largest part (adapted from cited ref.).<sup>3</sup>

Knowing the structure, properties, and functions of a specific macromolecular target goes a long way to understanding how a drug works in the body. This is also crucial in helping to design better or novel drugs.

Drugs are normally small molecules with molecular weight less than 500 atomic mass units, much smaller than their macromolecular targets. As a result, they interact directly with only a small portion of the macromolecule. This is called a binding site. The binding site usually has a defined shape into which a drug must fit if it is to have an effect, and so it is important that the drug has the correct size and shape. However, there is more to drug action than just a good fit. Once an active drug enters a binding site, a variety of intermolecular bonding interactions are set up which hold it there and lead to further changes, culminating eventually in a biological effect. For this to occur, the drug must have the correct functional groups and molecular skeleton capable of participating in these interactions.<sup>1</sup>



**Figure 1.5.** Different hit-identification strategies. The most common strategies today range from knowledge-based approaches (literature- and patent-derived molecular entities, endogenous ligands, biostructural information) to purely serendipity-based “brute-force” methods (combinatorial chemistry, high-throughput screening). The combination of both extremes is anticipated to deliver more high-content chemical leads in a shorter period of time (taken from cited ref.).<sup>8</sup>

Generally any chemistry programme within drug discovery research starts with the identification of specifically acting low molecular weight modulators showing an adequate activity in a suitable target assay. Such initial hits can be generated in many different ways, depending on the level of information available. These hit-identification strategies can be subdivided into those that require very detailed ligand and/or target information and those that do not (see Figure 1.5). The former include techniques such as mutagenesis, NMR and X-ray crystallography, as well as the recognition information that can be derived from endogenous ligands or non-natural small-molecule surrogates retrieved from literature and patents. At the other extreme are the technologies that do not require any prior information on target or ligand, and which use serendipity-based search strategies in either a given physical or virtual compound subset. Examples of so called 'random' hit-identification strategies include biophysical and biochemical testing which employ specific methods for detecting a molecular-binding event, usually in a high-throughput format.<sup>8</sup>

Between these extremes are more integrated approaches, including target libraries and chemogenomics. The combination of HTS with computational chemistry methods has allowed a move away from purely random-based testing, towards more meaningful and directed iterative rapid-feedback searches of subsets and focused libraries. The prerequisite for success of both approaches is the availability of the highest-quality compounds possible for screening, either real or virtual (see Figure 1.5).<sup>8</sup>

### 1.1.3 Tools of the Trade

Several invaluable tools for supporting drug discovery like quantitative *structure-activity relationships* (QSAR), combinatorial chemistry, the use of computers, and special *in vitro* tests are essential for medicinal chemistry. QSAR, which attempts to relate the physicochemical properties of compounds to their biological activity in a quantitative fashion by the use of equations, has been around for many years and it is a well-established tool in medicinal chemistry. In traditional QSAR, this typically involves studying a series of analogues with different substituents and studying how the physicochemical properties of the substituents affect the biological activities of the analogues. Typically, the hydrophobic, steric, and electronic properties of each substituent are considered when setting up a QSAR equation. With the advent of computers and suitable software programmes, traditional QSAR studies have been largely superseded by *three-dimensional quantitative structure-activity relationships* (3D QSAR), where the physicochemical properties of the complete molecule are calculated and then related to biological activity.

Combinatorial chemistry is a method for the rapid preparation of large numbers of compounds in an automated or semi-automated fashion, usually by solid phase synthetic

methods. The technique was developed to meet the urgent need for new lead compounds for the ever increasing number of novel targets discovered by genomic and proteomic projects. It is now an effective method of producing large numbers of analogues for drug development and for studies into SARs.

Computers and molecular modelling software packages have now become an integral part of the drug design process and have been instrumental in a more scientific approach to medicinal chemistry.<sup>1</sup>

The emphasis on *in vitro* screening of compounds against molecularly defined targets, although rapid and specific, has additional consequences for today's medicinal chemists. As the primary screen used to guide SAR studies, *in vitro* data do not help chemists to overcome the pharmacokinetic liabilities of their compounds. On the other hand, relying on *in vivo* animal models for the evaluation of pharmacokinetic performance suffers from a potentially serious drawback: differences between absorption and metabolism of drugs in humans and rats (a common test species) can lead to the development of drugs that work only in rats and not in humans. To help overcome this limitation, *in vitro* assays have been developed that are predictive of human pharmacokinetic performance, for example, by measuring a compound's degradation by preparations of human microsomes or hepatocytes or by recombinant human cytochrome P450 enzymes. Final testing might involve a disease-relevant animal model, although these data must be interpreted cautiously owing to several limitations. For example, many diseases, such as stroke, atherosclerosis and Alzheimer's disease, do not have clinically effective drugs that can validate a disease-progression-relevant animal model. Also, older models are based on drugs that work by certain mechanisms, and might not fairly assess drugs that are developed against a new mechanism. As such, the disease-relevant animal model is only one of many assays used to evaluate new compounds and, coming later in the testing sequence, has less impact on decisions made by today's chemists.<sup>2</sup>

Another strategy to overcome pharmacokinetic liabilities is the prediction and synthesis of compounds with 'drug-like' properties. Highly lipophilic, high-molecular-mass compounds tend to have more potent *in vitro* binding activity, because of displacement of water from the enzyme or receptor surface and thereby picking up additional hydrophobic interactions. But these compounds are usually not drug-like because of their low water solubility, and they generally fail in further development because of poor pharmacokinetics and oral bioavailability. Lipinski *et al.* formulated the 'Rule of Five' to predict drug-likeness, which consists of four important properties, each related to the number 5. The rule is based on data in the literature for a large number of compounds, including all known drugs that correlate physical properties with oral bioavailability. Support for the rule as a predictor of drug-likeness comes from observing weaknesses in the development pipelines of major

pharmaceutical companies owing to failure to adhere to the 'Rule of Five'. Computational calculations routinely predict 'rule of five' properties for prospective compounds in a chemist's SAR plans to guide compound selection, although this guidance comes at the cost of adding complexity to an already complex set of *in vitro* data.

---

### Lipinski's 'Rule of Five'<sup>9</sup>

Poor absorption or permeation are more likely when:

- There are more than 5 H-bond donors (expressed as the sum of OHs and NHs)
- The molecular weight (MW) is over 500
- The Log P (cLog P) is over 5
- There are more than 10 H-bond acceptors (expressed as the sum of Ns and Os)

Compound classes that are substrates for biological transporters are exceptions to the rule.

---

Completing the *in vitro* screens that the chemist uses to select the next compound to synthesize are the toxicity screens that weed out compounds predicted to fail for safety reasons.

**Table 1.1.** A typical battery of tests for a modern drug discovery programme (from ref. [2]).

<i>In vitro</i> target	<i>In vitro</i> ADME	Physical properties	<i>In vivo</i>	Toxicity
<ul style="list-style-type: none"> <li>• Primary</li> <li>• Whole cell</li> <li>• Functional</li> <li>• Selectivity assays</li> </ul>	<ul style="list-style-type: none"> <li>• Microsomal stability</li> <li>• Hepatocyte stability</li> <li>• P450 substrate</li> <li>• P450 inhibitor</li> <li>• Permeability</li> <li>• Transporter efflux (for example, P-glycoprotein)</li> <li>• Protein binding</li> </ul>	<ul style="list-style-type: none"> <li>• Rule-of-five</li> <li>• <i>In silico</i> ADME</li> </ul>	<ul style="list-style-type: none"> <li>• Functional</li> <li>• Secondary (behavioural, chronic)</li> </ul>	<ul style="list-style-type: none"> <li>• Ames test</li> <li>• Micronucleus test</li> <li>• hERG half-maximal inhibitory concentration (IC<sub>50</sub>)</li> <li>• P450 induction</li> <li>• Broad screening</li> <li>• Others (depending on project)</li> </ul>

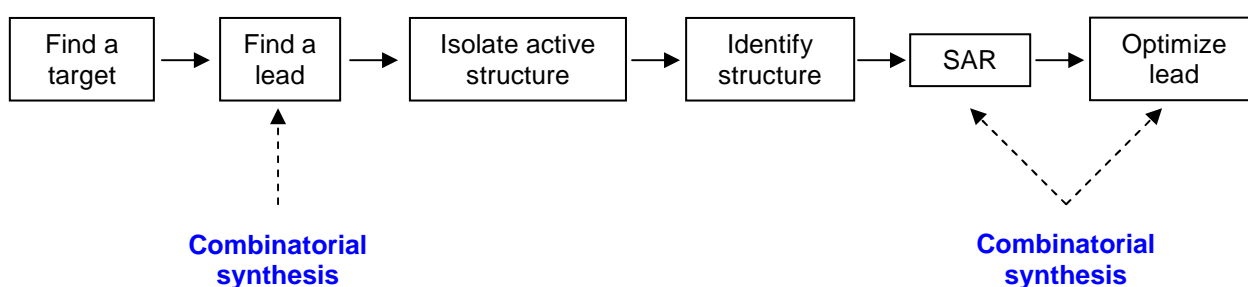
---

The Ames test, and related *in vitro* tests for mutagenicity and carcinogenicity, has a long history, but recent additions to this list include the hERG (human Ether-a-go-go-Related Gene) channel, a cardiac potassium ion channel involved in cardiac repolarization following ventricle contraction during the heartbeat. Drugs that bind to and inhibit the hERG channel can cause heart problems such as loss of a synchronous heartbeat and even death. Most

pharmaceutical companies now have hERG screening in place to afford chemists an indication of the therapeutic index of their compounds for this end point.<sup>10,11</sup> Table 1.1 summarizes the various criteria that today's chemist must follow to develop a successful drug candidate.

### 1.1.3.1 Combinatorial Chemistry

Combinatorial synthesis can be carried out such that a single product is obtained in each different reaction flask – a process known as parallel synthesis. Alternatively, the process can be designed such that mixtures of compounds are produced in each reaction vessel. Medicinal chemistry requires the rapid synthesis of a large number of compounds for a variety of reasons (see Figure 1.6).<sup>1</sup>



**Figure 1.6.** The use of combinatorial chemistry in drug discovery and drug optimization (taken from cited ref.).<sup>1</sup>

Before the advent of combinatorial chemistry, the need to find a lead compound was often the limiting factor in the whole process. Herein is the real need for combinatorial synthesis. Whereas in the past the driving force was the discovery of a lead compound, the driving force now is the discovery of new drug targets. It has been stated that a pharmaceutical company might expect to set up and carry out lead discovery programmes against about 100 targets per year and will need to screen over a million compounds if it is to find a lead compound quickly and efficiently. Combinatorial synthesis provides a means of producing that many compounds.<sup>1</sup>

Both parallel and mixed combinatorial syntheses can be used to generate large quantities of structures. In the procedure, mixtures of compounds are deliberately produced in separate reaction flasks, allowing chemists to produce thousands and even millions of novel structures in the time that they would need to synthesise a few dozen by conventional means. The structures in each reaction vessel of a mixed combinatorial synthesis are not separated and purified, but are tested for their biological activity as a whole. If activity is observed, the



challenge is to identify which component of the mixture is the active compound. Overall, there is an economy of effort, as a negative result for a mixture of 100 compounds saves the effort of synthesising, purifying, and identifying each component of that mixture. On the other hand, identifying the active component of an active mixture is not straightforward.<sup>1</sup>

In a sense, a mixed combinatorial synthesis can be looked upon as the synthetic equivalent of a fraction of nature's chemical pool. Through evolution, nature has produced a huge number and variety of chemical structures, some of which are biologically active. Traditional medicinal chemistry dips into that pool to pick out the active principles and develop them. A mixed combinatorial synthesis produces pools of purely synthetic structures that we can explore for active compounds. The diversity of structures from the natural pool is by far greater than that likely to be achieved by combinatorial synthesis, but isolating, purifying, and identifying new agents from natural sources is a relatively slow process and there is no guarantee that a lead compound will be discovered against a specific drug target. The advantage of combinatorial chemistry is the fact that it produces new compounds faster than those derived from natural sources and can produce a diversity not found in the traditional libraries of synthetic compounds held by pharmaceutical companies.

The other two areas of medicinal chemistry where a large number of compounds have to be synthesised are SAR studies and drug optimization. Parallel rather than mixed syntheses are used here, as each compound has to be tested individually.

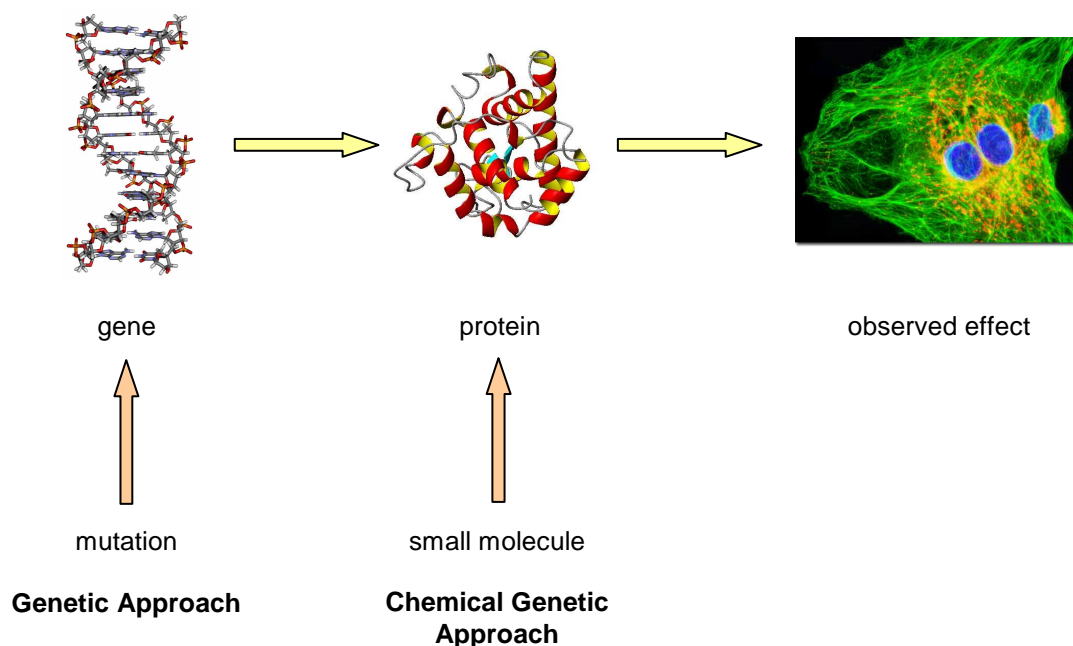
Combinatorial chemistry and high-throughput screening have emerged as powerful tools to generate and evaluate large compound libraries for activity against many different targets. However, initial expectations that large compound libraries should result in the discovery of many new hit and lead structures for drug development have not been fulfilled thus far.<sup>1</sup>

#### **1.1.4 Natural Products and Chemical Genetics in Drug Discovery**

Natural products have been invaluable as tools for deciphering the logic of biosynthesis and as platforms for developing drugs. These products have evolved to interact with biomolecules, which is why so many can be found in pharmacopoeias and why these compounds are still a major source of innovative therapeutic agents for infectious diseases (both bacterial and fungal), cancer, lipid disorders and immunomodulation. There are several general distinctions between natural products and synthetic drugs or drug candidates: First, natural products typically have more stereogenic centers and more architectural complexity than synthetic molecules generated by medicinal chemists, although several important natural products that act with potency and specificity at protein receptors (e.g. adrenaline and noradrenaline) have simple structures. Second, natural products contain relatively more carbon, hydrogen and oxygen, and less nitrogen and other elements than synthetic medicinal

agents.<sup>12</sup> Third, many useful natural products have molecular masses in excess of 500 daltons and high polarities (greater water solubility), and therefore violate Lipinski's "rule-of-five". The uniqueness of natural products and their special properties make this class of compounds very interesting for finding new drugs that alter protein functions.<sup>12,13,14</sup>

Where classical geneticists use mutations to perturb gene expression and thereby indirectly affect gene products, chemists can use small molecules to directly activate or inactivate proteins (see Figure 1.7).



**Figure 1.7.** Genetic and chemical genetic approaches.

Chemical genetics involves exposing cells to a combinatorial library of small molecules, selecting a molecule in the library that induces a phenotypic change of interest. If possible, the protein responsible for that phenotypic change is identified. Chemical genetics is more amenable to high throughput screening than classical genetics and hence has the potential to allow a systematic analysis of the function and role of proteins in the cell. In *reverse* chemical genetics a known protein of interest is selected and by screening a library of small molecules the best ligand that will bind to the protein is identified. Then the phenotypic effect is observed by exposing the cells to that ligand. Reverse genetics involves targeting a gene of interest with a mutation and then observing the phenotypic consequences of the loss or alteration of that gene product.

Chemical genetics has proven to be a very powerful tool in identifying new cellular targets and modes of drug action. The success of such screening methods depends strongly on the quality of the used small molecules. Natural products and natural product-like compounds have proven to be invaluable tools in this area.<sup>15,16,17</sup>

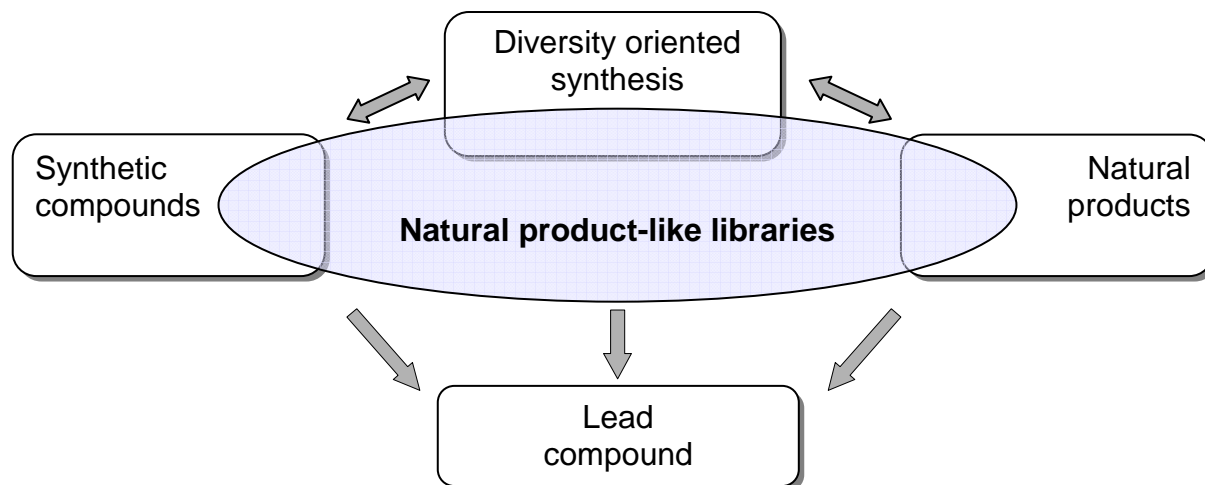
### 1.1.5 A Diversity-Oriented Synthesis (DOS) Approach to Natural Product-Like Compounds

Natural products have played an eminent role in the discovery and development of new drugs. Over half of the nearly 1000 small-molecule drugs introduced on the market over the past two decades are either natural products or in some way related to natural products.<sup>18a</sup>

The pharmaceutical industry depends on the generation of new drugs. The drug discovery process is devoted to the identification of compounds that cure or help to treat diseases. The past decade has seen tremendous progress in many of the different aspects of the drug-discovery process. These aspects include the development of combinatorial chemistry technologies, the implementation of high-throughput screens and bioinformatics tools, the sequencing of the human and other genomes, as well as the integration of functional genomics platforms. Although rendering many new potential biological target molecules, this route of industrialising the drug-discovery process failed, however, to deliver the number of lead compounds required to maintain the necessary productivity of pharmaceutical R&D. The efforts aimed at increasing the output of lead compounds relied too strongly on a quantitative increase of compounds to enter the screening process, while qualitative aspects were neglected.<sup>18b</sup>

Nature provides us with a vast pool of highly potent compounds. According to evolutionary theory, each species is optimally adapted to life in its environment, leading to a highly diverse system. Only the best organisms can survive and, eventually, the ones functioning better will supersede them. Yet the basis of all biological function resides in the molecules that organisms are built of. The ever ongoing selection of the best adapted species can be viewed, in the given context, as the largest possible effort on this earth towards the synthesis of new molecular entities followed by their screening for biological usefulness, ultimately resulting in a pool of highly potent and diverse compounds. It is not surprising that humans have tapped into this pool of compounds in their quest for cures, from the times of ancient cultures to modern medicine. On the other hand, one of the recurrent drawbacks associated with natural products is a limited access to the material. Isolation of sufficient quantities from natural resources is often not possible, and chemical synthesis is usually a lengthy and low-yielding process. In light of all this, the synthesis of large numbers of compounds that are based on a naturally occurring structural motif with demonstrated biological activity is an appealing idea. This provides the process of lead identification with a starting point that has a likelihood of producing compounds with natural product-like activities, and all compounds with interesting activity are definitely accessible through chemical synthesis. A further recent development is the concept of diversity-oriented libraries. DOS is a skilful approach towards generating a large number of different molecules and, at the same time, introducing a maximal degree of structural diversity into the library.<sup>19, 20, 21</sup> In view of the difficulties

encountered on the way to lead compounds, diversity-oriented, natural product-like libraries appear to be an ideal approach for the generation of high-quality structures. By combining positive features from several different areas, such libraries are expected to add value to the lead identification process (see Figure 1.8).<sup>18b</sup>



**Figure 1.8.** Natural product-like libraries bring value to the drug-discovery process by combining positive aspects from several different areas.<sup>18b</sup>

Because of the attractiveness of the concept, a significant effort has been devoted to the chemical synthesis of natural product-like scaffolds and libraries over the past few years. A large number of chemical libraries based on motifs of natural compounds with proven biological and pharmaceutical activity have been reported. Similarity to natural products is ensured by synthesizing structurally diverse derivatives of privileged substructures, or hybrid structures, rather than arbitrarily chosen scaffolds. The number of reports is rapidly increasing, and several reviews have addressed the topic of natural product-like libraries.<sup>18b</sup>

19, 20, 21, 22

## 1.2 Approaches to the Medical Treatment of Cancer

Cancer is a leading cause of death worldwide next to the cardiovascular diseases (CVDs) which are the number one cause of death globally. Cancer cells are formed when normal cells lose the natural regulatory mechanisms that control growth and multiplication. They become 'rogue cells' and often lose the specialized characteristics that distinguish one type of cell from another (for example a liver cell from a blood cell). This is called a loss of differentiation. The term neoplasm means new growth and is a more accurate terminology for the disease. The terms cancer and tumour, however, are more commonly accepted and will be used in this dissertation. If the tumour is localized it is said to be benign. If the tumour cells invade other parts of the body and set up secondary tumours – a process called metastasis – it is defined as malignant. It is the latter form of cancer which is life threatening. A major problem in treating cancer is the fact that it is not a single disease. There are more than 200 different cancers known resulting from different cellular defects, and so a treatment that is effective against one type of cancer may be ineffective on another.<sup>1</sup>

### 1.2.1 Some Facts about Cancer

From a total of 58 million deaths worldwide in 2005, cancer accounts for 7.6 million (or 13%) of all deaths. In the case of the CVDs an estimated 17.5 million people died in 2005, representing 30% of all global deaths. The main types of cancer leading to overall cancer mortality are:<sup>23</sup>

- Lung (1.3 million deaths/year)
- Stomach (almost 1 million deaths/year)
- Liver (662'000 deaths/year)
- Colon (655'000 deaths/year)
- Breast (502'000 deaths/year)

More than 70% of all cancer deaths in 2005 occurred in low and middle income countries. Deaths from cancer in the world are projected to continue rising, with an estimated 9 million people dying from cancer in 2015 and 11.4 million dying in 2030.<sup>23</sup>

The most frequent cancer types world wide are:<sup>23</sup>

- Among men (in order of number of global deaths): lung, stomach, liver, colorectal, oesophagus and prostate.

- Among women (in order of number of global deaths): breast, lung, stomach, colorectal and cervical.

Possibly as many as 30% of cancers are caused by smoking, while another 30% are diet related. Carcinogenic chemicals in smoke, food and the environment (UV and ionizing radiation) may cause cancer by inducing gene mutations or interfering with normal cell differentiation. The 'birth of cancer' (carcinogenesis) can be initiated by chemicals – usually a mutagen – but other triggering events such as exposure to further mutagens are usually required before cancer develops.<sup>1</sup>

Viruses (e.g. Epstein-Barr virus or Human papillomaviruses) have been implicated in at least six human cancers and are the cause of about 15% of the world's cancer deaths. They may bring oncogenes into the cell and insert them into the genome. Some viruses carry one or more promoters or enhancers. If these are integrated next to a cellular oncogene, the promoter stimulates its transcription leading to cancer. The bacterium *Helicobacter pylori* is responsible for many stomach ulcers and is also implicated in stomach cancer.<sup>1</sup>

Some patients are prone to certain cancers for genetic reasons. Damaged genes can be passed from one generation to another, increasing the risk of cancer in subsequent generations. On the other hand 40% of cancer can be prevented by healthy diet, physical activity and not using tobacco. Tobacco use is the single largest preventable cause of cancer in the world and it causes cancer of the lung (as passive smoking), throat, mouth, pancreas, bladder, stomach, liver, kidney and other types.<sup>1, 23</sup>

### 1.2.2 Genetic Faults Leading to Cancer: Proto-Oncogenes and Oncogenes

Proto-oncogenes are genes which normally code for proteins involved in the control of cell division and differentiation. If they are mutated, this disrupts the normal function and the cell can become cancerous. The proto-oncogene is then defined as an oncogene. The *ras* gene which codes for a protein called Ras is one example. Ras is involved in the signalling pathway leading to cell division and if the gene becomes mutated, uncontrolled cell division can result. It has been shown that mutation of the *ras* gene is present in 20 – 30% of human cancers. As mentioned before, oncogenes may also be introduced to the cell by viruses.<sup>1</sup>

If DNA is damaged in a normal cell, there are cellular mechanisms that can detect the damage and block DNA replication. This gives the cell time to repair the damaged DNA before the next cell division. If repair does not prove possible, the cell commits suicide (apoptosis). Tumour suppression genes (anti-oncogenes) are genes which code for proteins that are involved in these processes of checking, repair and suicide. The gene which codes for the p53 protein is an important example of such a gene. If this gene is damaged, the

repair mechanisms become less efficient, defects are carried forward from one cell generation to another and as the damage increases, the chances of the cell becoming cancerous increase.<sup>1</sup> In over 50% of all cancers this gene is altered.<sup>23</sup>

Genetic defects can lead to the following cellular defects, all of which are associated with cancer:

- **Abnormal signalling pathways:**

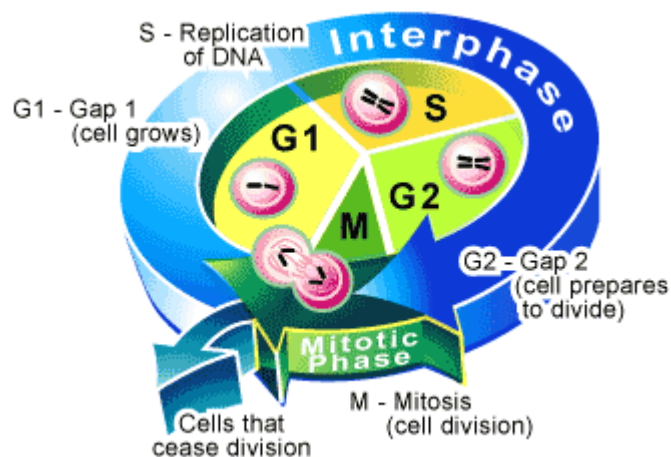
The most important of these signals come from hormones called growth factors, extracellular chemical messengers which activate protein kinase receptors in the cell membrane (e.g. platelet-derived growth factor (PDGF), transforming growth factor  $\alpha$  (TGF- $\alpha$ )).<sup>1, 23</sup>

- **Insensitivity to growth-inhibitory signals:**

Several external hormones such as transforming growth factor  $\beta$  (TGF- $\beta$ ) counteract the effects of stimulatory growth factors, and signal the inhibition of cell growth and division. Insensitivity to these signals raises the risk of a cell becoming cancerous. This can arise from damage to the genes coding for the receptors for these inhibitory hormones – the tumour suppression genes.<sup>1, 23</sup>

- **Abnormalities in cell cycle regulation:**

The cell cycle consists of four phases (G1, S, G2 and M, see Figure 1.9). Progression through the cell cycle is controlled by cyclins and cyclin-dependent kinases, moderated by restraining proteins. Defects in this system have been detected in 90% of cancers. Knowledge of the cell cycle is important in chemotherapy because some drugs are more effective during one part of the cell cycle than another.



**Figure 1.9.** Graphical representation of the cell cycle. In the case of G1 there also exists a so called G0 phase which means a resting stage without growth. Every phase has specific checkpoints, where the cell decides to go on or not. Source: [www.scq.ubc.ca/wp-content/cellcycle.gif](http://www.scq.ubc.ca/wp-content/cellcycle.gif)

For example, drugs which affect microtubules like colchicine, podophyllotoxin and combretastatin A-4 are effective when cells are actively dividing (M phase), whereas drugs acting on DNA like Doxorubicin (see Figure 1.10) are more effective in the S phase. Some drugs are effective regardless of the phase like cisplatin (see Figure 1.10).<sup>1, 23</sup>

- **Evasion of programmed cell death (apoptosis):**

Apoptosis is a destructive process leading to cell death. Cells have monitoring systems which check the general health of the cell and trigger the process of apoptosis if there are too many defects. Regulatory proteins (e.g. p53) have a moderating influence on apoptosis. Defects in apoptosis increase the chances of defective cells developing into cancerous cells and reduce the effectiveness of several drugs.<sup>1, 23</sup>

- **Limitless cell division (immortality):**

Telomeres act as splices to stabilize the ends of DNA. Normally, they decrease in size at each replication until they are too short to be effective, resulting in cell death. Cancer cells activate the expression of an enzyme called telomerase to maintain the telomere and become immortal.<sup>1</sup> More than 85% of all cancers achieve this by expressing a telomerase that synthesises new telomeric DNA to replace the sequences lost during cell division.<sup>23</sup>

- **Ability to develop new blood vessels (angiogenesis):**

Angiogenesis is the process by which tumours stimulate the growth of new blood vessels to provide the nutrients required for continued growth. Agents which inhibit angiogenesis are useful in anticancer therapy to inhibit tumour growth and to enhance the effectiveness of other drugs.<sup>1, 23</sup>

- **Tissue invasion and metastasis:**

Metastasis is the process by which cancer cells break free of the primary tumour, enter the blood stream or lymphatic system, and set up secondary tumours in other tissues. To do this, the regulatory controls which fix cells to a specific environment, and which destroy cells that become detached, are overruled.<sup>1, 23</sup>

Since so many cellular safeguards are involved, it is unlikely that tackling one specific cellular defect is going to be totally effective. As a result, traditional anticancer drugs have tended to be highly toxic agents and act against a variety of different cellular targets by different mechanisms. Unfortunately, since they are potent cellular poisons, they also affect normal cells and produce serious side effects. Such agents are said to be cytotoxic, and dose levels have to be chosen which are bearable to the patient. In recent years, anticancer drugs have been developed which target specific abnormalities in a cancer cell, allowing them to be more selective and have less serious side effects. However, bearing in mind the number of

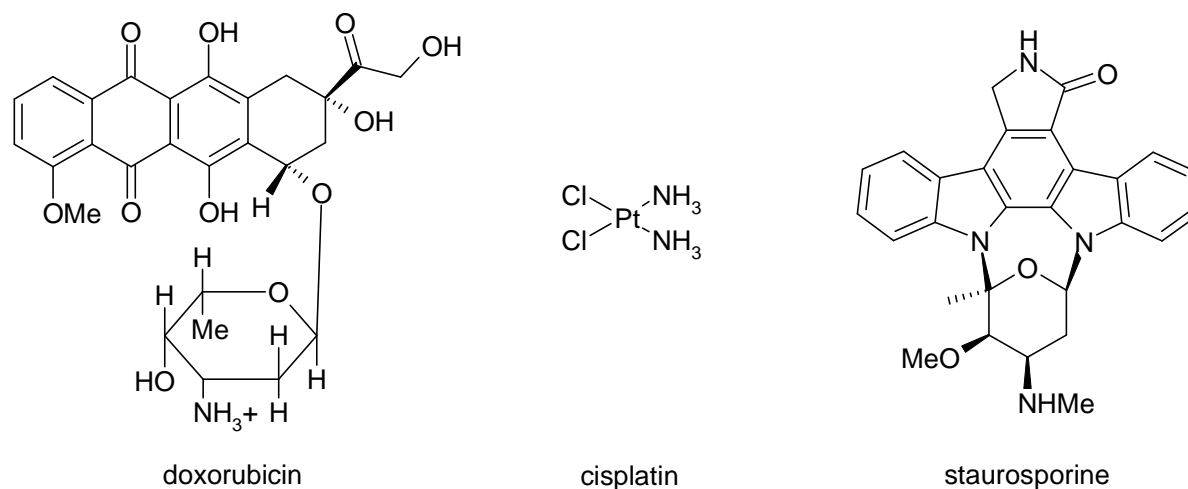


defects in a cancer cell, it is unlikely that a single agent of this kind will be totally effective and it is more likely that these new agents will be most effective when they are used in combination with other drugs having different mechanisms of action, or surgery and radiotherapy.<sup>1, 23</sup>

### 1.2.3 Treatment and Resistance of Cancer

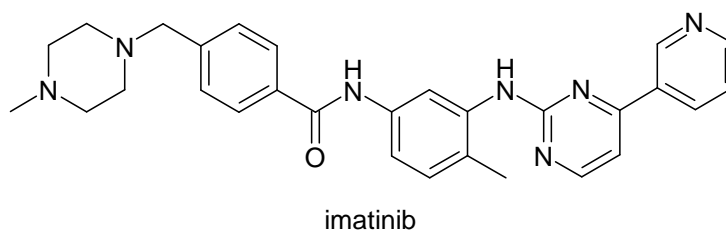
There are three traditional approaches to the treatment of cancer – surgery, radiotherapy, and chemotherapy. It is often the case that combination therapy (the simultaneous use of various anticancer drugs with different mechanisms of action combined with radiotherapy and if possible surgery) is more effective than using a single drug.<sup>1, 23</sup>

Identifying targets that are unique to cancer cells is difficult, because cancer cells are derived from normal cells. As a result, most traditional anticancer agents act against targets which are present in both types of cell. Cancer cells are generally growing faster than normal cells, and so they accumulate nutrients, synthetic building blocks, and drugs more quickly.



**Figure 1.10.** Three examples of anticancer agents: Doxorubicin (an anthracycline), a natural product produced by bacteria cultures of *Streptomyces peucetius*, is a DNA intercalating agent; cisplatin, a very useful drug for intravenous treatment of testicular and ovarian tumours, is a DNA cross-linking agent; staurosporine, a natural compound from *Streptomyces staurosporeus*, is an inhibitor of cyclin-dependent kinases (CDKs).

Many traditional anticancer drugs work by disrupting the function of DNA and are classed as cytotoxic (see Figure 1.10). Some act on DNA directly, others (antimetabolites) act indirectly by inhibiting the enzymes involved in DNA synthesis. A better understanding of the cellular chemistry involved in particular cancer cells allowed to create highly selective agents which aim at specific molecular targets that are abnormal or over-expressed in the cancer cell.



**Figure 1.11.** The structure of imatinib (Glivec<sup>®</sup>) which is a selective inhibitor of a protein kinase found in a blood cancer called chronic myeloid leukaemia (CML).

The development of kinase inhibitors such as Imatinib (Glivec<sup>®</sup>, see Figure 1.11), which is used for chronic myeloid leukaemia, is an example of this approach.<sup>1</sup>

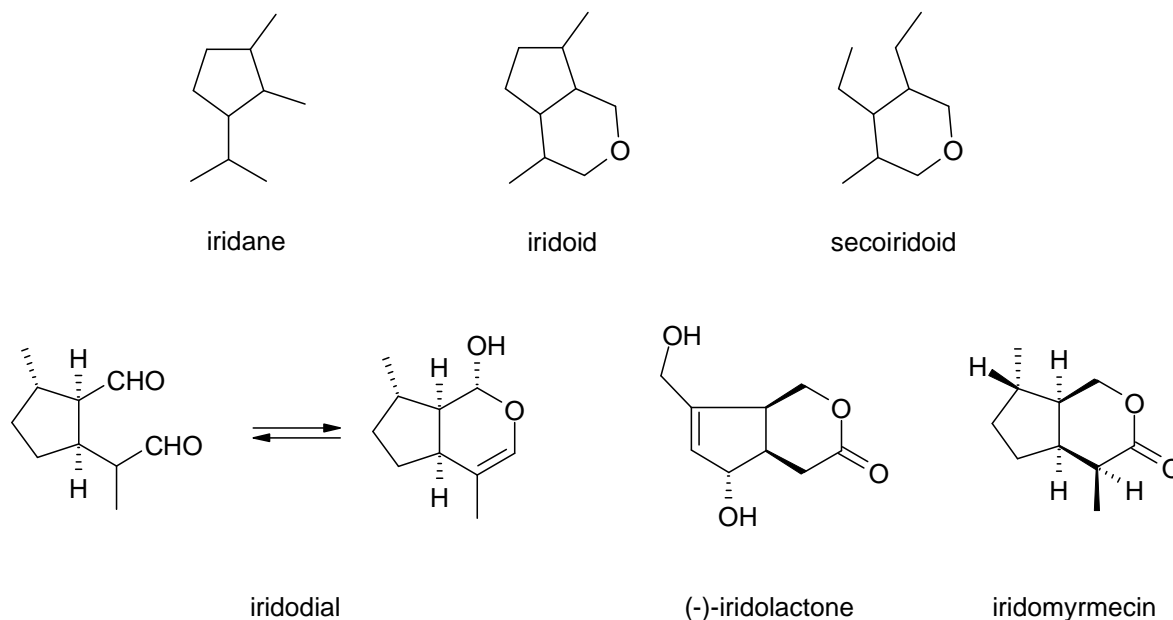
The resistance of cancer cells to anticancer drugs is a serious problem. This resistance can be intrinsic (the tumour shows little response to an anticancer agent from the very start) or acquired (when a tumour is initially susceptible to a drug but becomes resistant).<sup>1</sup> Resistance may be due to poor uptake of the drug as mentioned before, increased production of the target protein, mutations which prevent the drug binding to its target, alternative metabolic pathways, or efflux systems which expel drugs from the cell. This is known as *multidrug resistance* (MDR).<sup>1</sup> Since it is likely that a drug-resistant cell may be present in a cancer, it makes sense to use combinations of anticancer drugs with different targets to increase the chance of finding a weakness in every cell.<sup>1, 23 – 30</sup>

### 1.3 Natural Product Leads for Discovering New Anticancer Agents

Most biologically active natural products are secondary metabolites with quite complex structures. This has the advantage in that they are novel compounds. On the other hand, this complexity also makes their synthesis difficult and the compound usually has to be extracted from its natural source – very often a slow, expensive and inefficient process. As a result, there is usually an advantage in designing simpler analogues which may also be suitable for applying combinatorial methods like solid support chemistry.<sup>1, 18b</sup> During our work aimed at the synthesis and biological evaluation of natural product-like scaffolds as novel anticancer agents, we became attracted to different natural compounds like iridoids, stilbenes and  $\gamma$ -butyrolactones, which are a very common structural elements in biologically active natural products.<sup>18b, 31, 32, 33, 34</sup>

#### 1.3.1 Iridoids

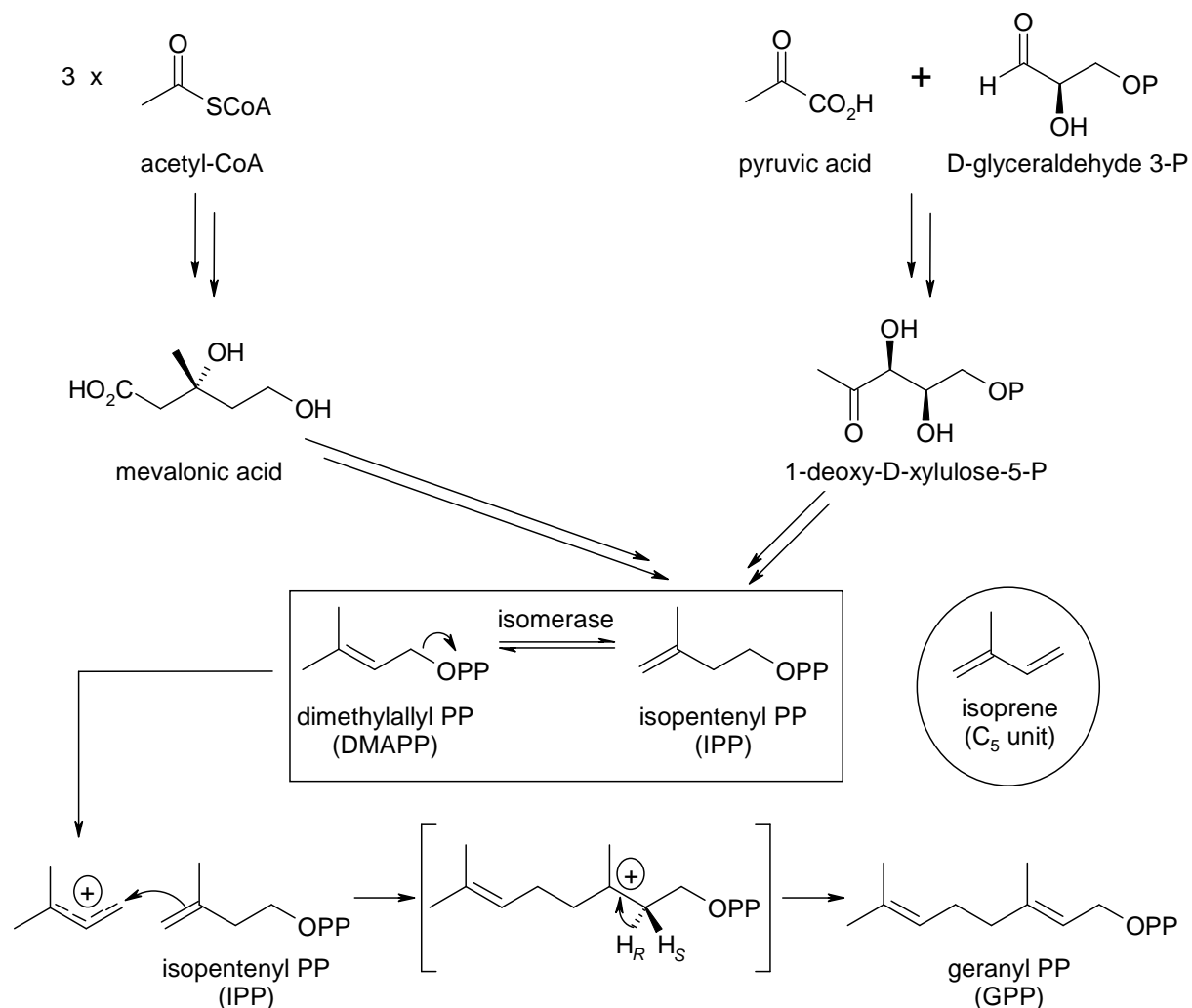
Iridoids are monoterpenes based on the cyclopenta[*c*]pyran skeleton as shown in Figure 1.12. They are found in a large number of plant families, usually, but not invariably, as glycosides.<sup>35</sup>



**Figure 1.12.** Different examples of iridoid monoterpenes: Above the general structures of iridane, iridoid and secoiridoid; below the structures of iridodial, iridolactone and iridomyrmecin.

The name iridoid is a generic term derived from the names iridomyrmecin, iridolactone and iridodial, compounds isolated from some species of *Iridomyrmex*, a genus of ants, in which

they occur as defensive secretions.<sup>35</sup> The latter and the key role played by secologanin in the biosynthesis of many alkaloids stimulated the chemical interest in the iridoids. Naturally occurring iridoids and secoiridoids and their derivatives are known to have interesting biological and pharmacological activity, for example cardiovascular, antihepatotoxic, anti-inflammatory, antitumor and antiviral activity.<sup>35, 36, 37, 38</sup>

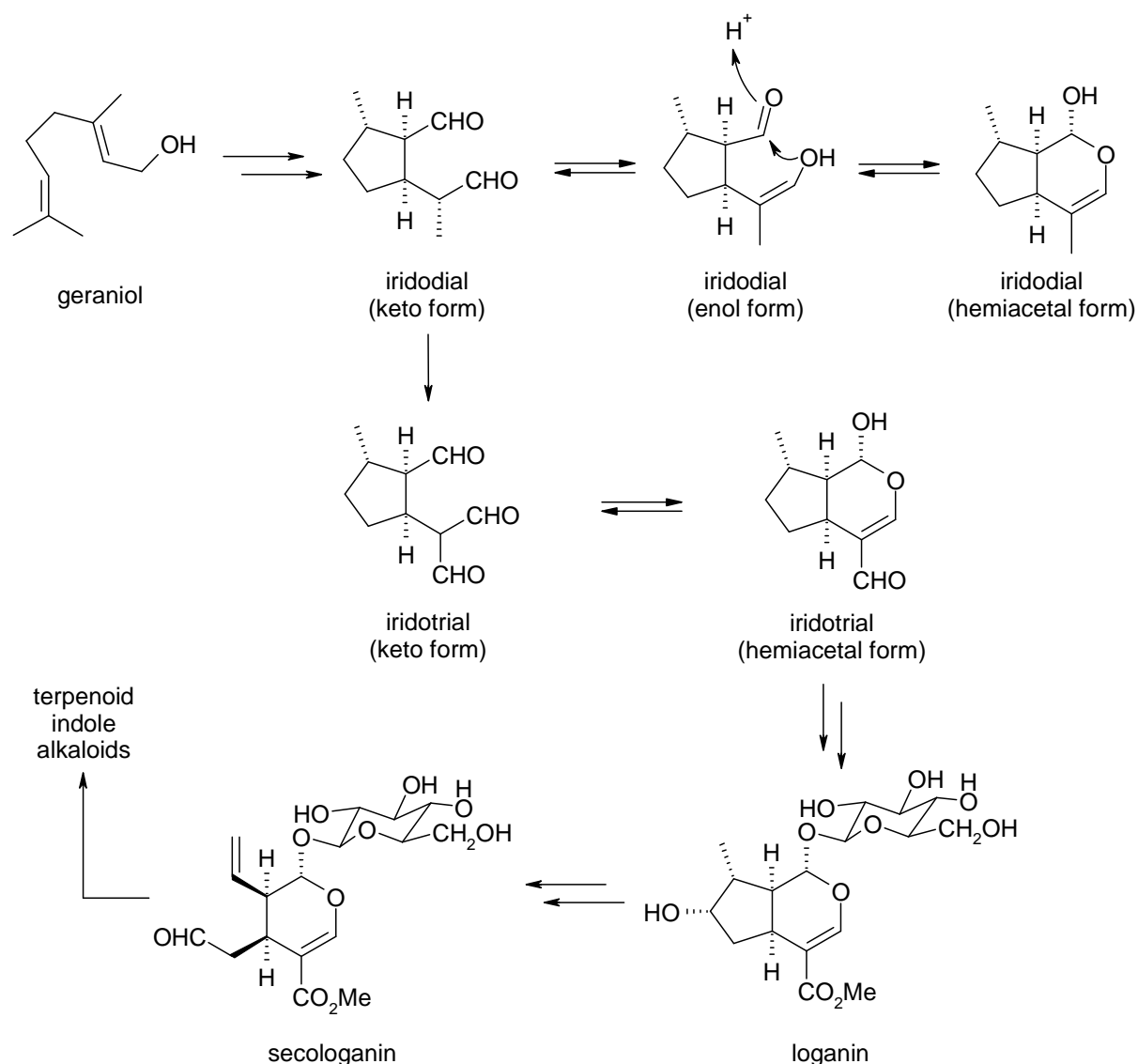


**Scheme 1.1.** Biosynthesis of geranyl PP from mevalonic acid or 1-deoxy-xylulose-5-P *via* dimethylallyl PP.

Monoterpenes are metabolic products of the mevalonate and deoxyxylulose phosphate pathways. Mevalonic acid itself is formed from three molecules of acetyl-CoA and deoxyxylulose phosphate is a product of two glycolytic pathway intermediates, namely pyruvic acid and glyceraldehyde 3-phosphate (see Scheme 1.1). These intermediates are transformed in a convergent biosynthesis into isopentenyl diphosphate (IPP). This is further isomerised into dimethylallyl diphosphate (DMAPP), which represents together with IPP the key intermediates in terpene biosynthesis. Combination of DMAPP and IPP via the enzyme

prenyl transferase yields geranyl diphosphate (GPP) from which the alcohol geraniol is formed.<sup>38</sup>

The terpenoids form a large and structurally diverse family of natural products derived from  $C_5$  isoprene units. Typical structures contain carbon skeletons represented by  $(C_5)_n$ , and are classified as hemiterpenes ( $C_5$ ), monoterpenes ( $C_{10}$ , e.g. iridoids), sesquiterpenes ( $C_{15}$ ), diterpenes ( $C_{20}$ ), sesterterpenes ( $C_{25}$ ), triterpenes [ $C_{30}$ ], steroids ( $C_{18}$ - $C_{30}$ ) and tetraterpenes ( $C_{40}$ , carotenoids).<sup>38</sup>



**Scheme 1.2.** Further biosynthetic transformation of geraniol to iridoids like iridotrial, loganin and secologanin (adapted from cited ref.).<sup>38</sup>

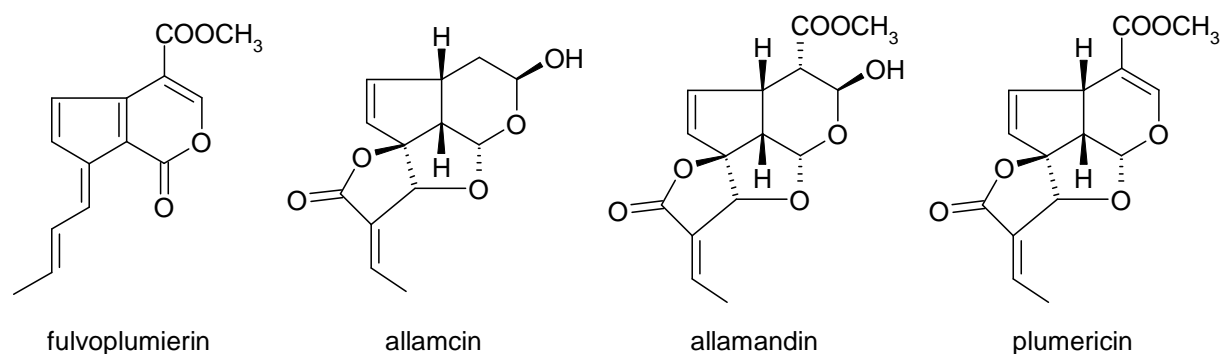
The iridoid system arises from geraniol by a cyclisation to iridodial, which is produced by a series of hydroxylation and oxidation reactions on geraniol (see Scheme 1.2). Further oxidation of the keto form gives iridotrial, in which hemiacetal formation then leads to production of the heterocyclic ring. A large number of iridoids are found as glycosides (e.g. loganin). Glycosylation transforms the hemiacetal linkage into an acetal. The pathway to

loganin involves a sequence of reactions in which the remaining aldehyde group is oxidized to the acid and methylated. The final step is a hydroxylation reaction. Logaganin, which shows hepatoprotective and anti-inflammatory activity, is a key intermediate in the biosynthesis of many other iridoid structures. Secologaganin is the parent compound of secoiridoids and a key intermediate in the biosynthesis of many alkaloids. Many compounds derived from Secologaganin display a high degree of biological activity and are employed as pharmaceuticals.<sup>38, 39</sup>

### 1.3.1.1 Antitumor Activity of Iridoids and Their Derivatives

Several iridoids from the bark of *Plumeria rubra* collected in Indonesia have been isolated and some of them exhibited cytotoxic activity against different human cancer cell lines (e.g. breast, colon, lung, KB). The isolated iridoids fulvoplumierin, allamcin, allamandin and plumericin showed efficient cytotoxic activity (see Table 1.2).<sup>40</sup>

**Table 1.2.** Evaluation of the cytotoxic potential of the compounds isolated from *Plumeria rubra* in different cancer cell lines.

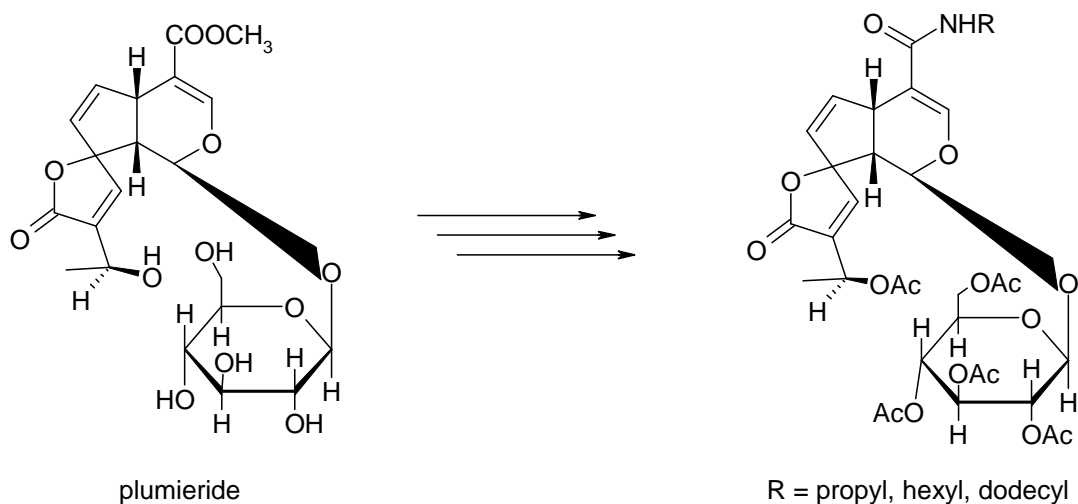


Compound	Cancer Cell Lines [ $\mu\text{g/ml}$ ] <sup>a</sup>			
	Breast	Lung	Colon	KB (cervix)
fulvoplumierin	3.5	3.0	1.3	4.6
allamcin	0.1	1.2	0.3	0.3
allamandin	0.4	0.7	0.3	0.4
plumericin	0.4	0.2	0.1	0.3

<sup>a</sup>Results are expressed as ED<sub>50</sub> values [ $\mu\text{g/ml}$ ]

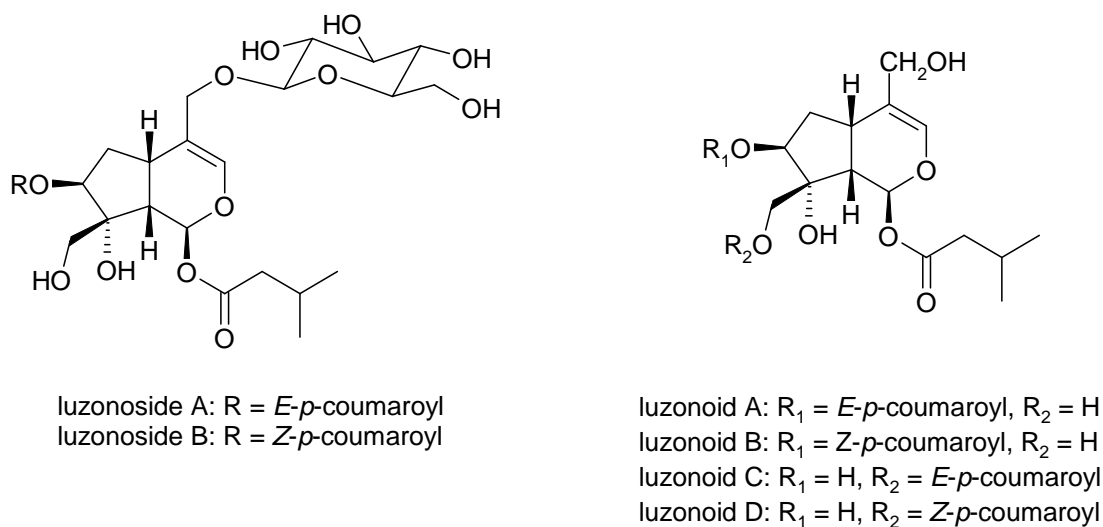
Plumieride (see Scheme 1.3) was isolated as one of the major components of the bark of *Plumeria bicolor* (family Apocynaceae). For optimisation of the cytotoxic activity of plumieride the compound was modified into a series of compounds. The *in vitro* cytotoxicity of these analogues was determined in radiation induced fibrosarcoma (RIF) tumour cells. Replacing the methyl ester functionality of plumieride with alkyl amides of variable carbon

units improved the cytotoxic activity, and a correlation between overall lipophilicity and cytotoxic activity was observed. Among all of the derivatives, the naturally occurring plumieride showed the least cytotoxicity ( $IC_{50} = 49.5 \mu\text{g/ml}$ ), and the amide analogues of plumieride pentaacetate showed the best efficacy (R = propyl:  $IC_{50} = 12.2 \mu\text{g/ml}$ ; R = hexyl:  $IC_{50} = 18.5 \mu\text{g/ml}$ ; R = dodecyl:  $IC_{50} = 11.8 \mu\text{g/ml}$ ).<sup>41</sup>



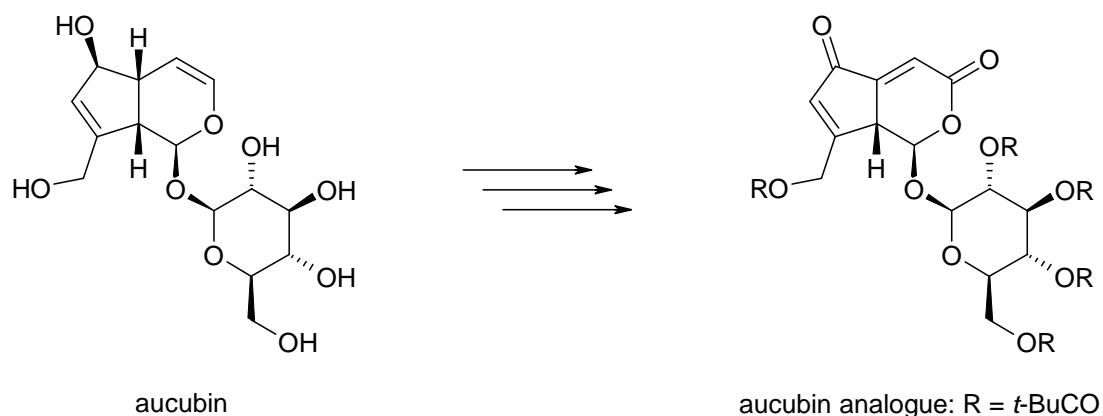
**Scheme 1.3.** Modification of plumieride to different derivatives with cytotoxic activity.

Several iridoid glucosides and iridoid aglycones bearing *E*- or *Z*-*p*-coumaroyl groups were isolated from dried leaves of *Viburnum luzonicum* collected in Taiwan. In a cytotoxicity assay with the HeLa S3 (human epithelial cancer) cell line, iridoid glycosides luzonoside A and B and their aglycons luzonoid A – D (see Figure 1.13) exhibited inhibitory activity, with  $IC_{50}$  values of 3 – 7  $\mu\text{M}$ . Furthermore these iridoids inhibited the growth and the cell viability in primary-cultured rat cortical neurons at 10  $\mu\text{M}$ .<sup>42</sup>



**Figure 1.13.** Structures of luzonosides and luzonoids (two types of iridoids).

The iridoid aucubin (see Scheme 1.4), which can be extracted in large amounts from fresh fruits and leaves of *Aucuba japonica* Thunb (Cornaceae), has been employed as starting material for the synthesis of various biologically relevant derivatives, including insect antifeedants, carbocyclic nucleoside analogues, aminocyclopentitol glycosidase inhibitors and numerous prostaglandins. Aucubin itself does not exhibit significant cytotoxic activity, so this compound was modified to improve this activity. The cytotoxic activity of the aucubin analogue was determined against the L1210 murine leukaemia cell line and an  $IC_{50}$  value of  $3.0 \mu\text{M}$  was found.<sup>43</sup>

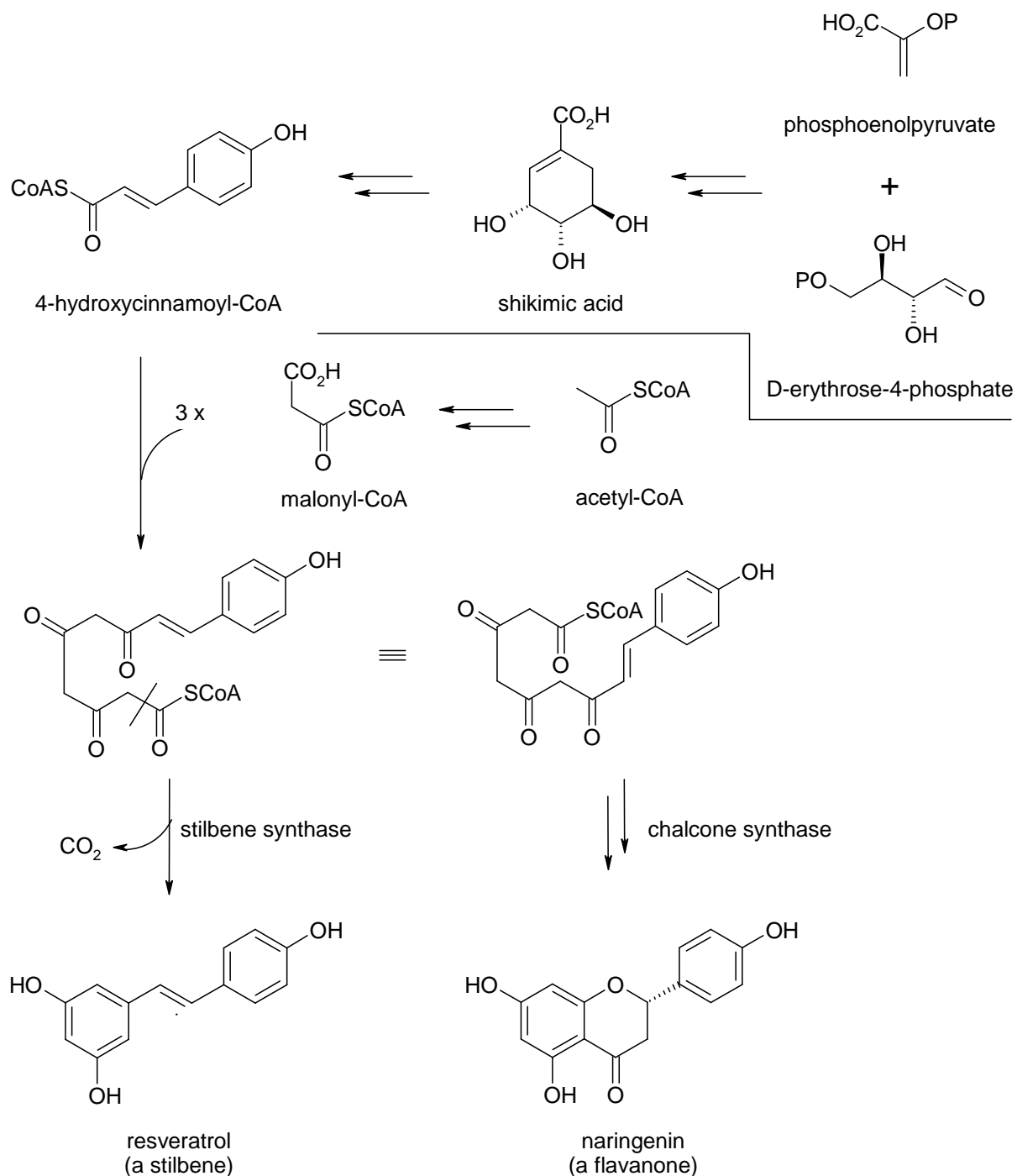


**Scheme 1.4.** Modification of aucubin.



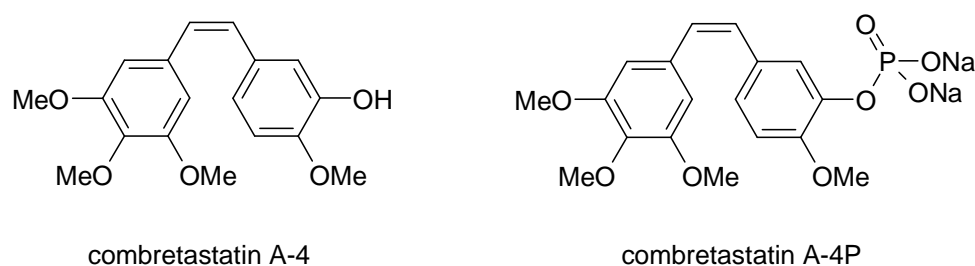
### 1.3.2 Stilbenes Including Resveratrol and Combretastatin A-4

Stilbenes and flavonoids are products from a cinnamoyl-CoA starter unit, with chain extension using three molecules of malonyl-CoA. The cinnamoyl-CoA is synthesised *via* the shikimate pathway, starting from phosphoenolpyruvate and D-erythrose-4-phosphate *via* shikimic acid. This leads to a polyketide which, depending on the nature of the enzyme involved, can be folded in two different ways (see Scheme 1.5).



**Scheme 1.5.** Biosynthesis of resveratrol from phosphoenolpyruvate and D-erythrose-4-phosphate.

The enzymes stilbene synthase and chalcone synthase couple a cinnamoyl-CoA unit with three malonyl-CoA units giving stilbenes (e.g. resveratrol, see Scheme 1.5) or flavonoids *via* chalcones, respectively. With stilbenes, it is noted that the terminal ester function is no longer present, and therefore hydrolysis and decarboxylation have also taken place during this transformation. No intermediates have been observed, and the transformation from cinnamoyl-CoA / malonyl-CoA to stilbene is catalysed by a single enzyme.<sup>38</sup> Resveratrol became more interesting in recent years as a constituent of grapes and wine, as well as other food products, with antioxidant, anti-inflammatory and cancer preventative properties.<sup>38</sup> Coupled with the cardiovascular benefits of moderate amounts of alcohol, and the beneficial antioxidant effects of flavonoids, red wine has now emerged as an unlikely but most acceptable medicinal agent.<sup>38</sup> Although a detailed knowledge of the mode of action for the antiproliferative effects of resveratrol is still elusive, several reports indicate that inhibition of cell growth is a consequence of interference with cell-cycle progression, and induction of apoptosis. Several structural aspects, such as the nature of the aryl substituents and geometrical isomerism were shown to have a significant influence on the inhibitory effects.<sup>34</sup> The *cis*-stilbenoid combretastatin A-4 (see Figure 1.14) is a natural product isolated from the South African bush willow tree *Combretum caffrum* and strongly inhibits the polymerization of tubulin by binding to the colchicine-binding site. The natural compound also exerts potent cytotoxicity against a variety of human cancer cells including multidrug-resistant (MDR) cancer cell lines. Combretastatin A-4 is the most potent member of the combretastatin family and has reached clinical trials as its more water-soluble phosphate pro-drug for the treatment of solid tumours. As a result of its high biological activity combretastatin A-4 (CA-4) serves as a starting point for the development of new antitubulin agents with a potential for cancer treatment.<sup>1, 34, 38</sup>

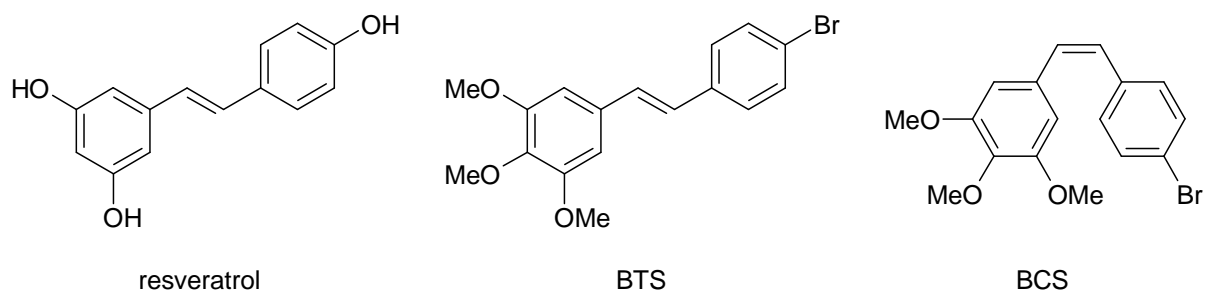


**Figure 1.14.** Structures of combretastatin A-4 and its more water-soluble phosphate pro-drug.

### 1.3.2.1 Antitumor Activity of Resveratrol, Combretastatin A-4 and Its Derivatives

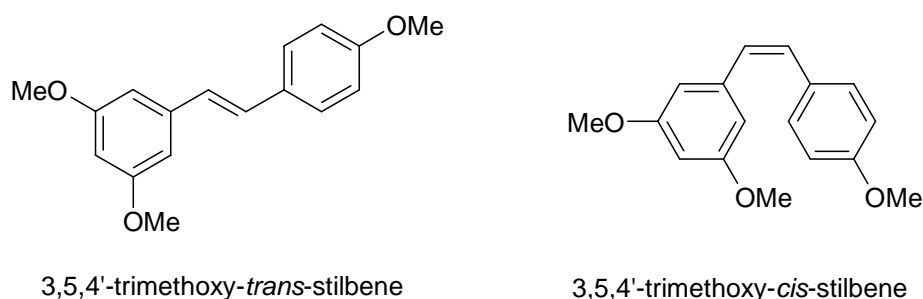
Lee *et al.* investigated the effect of resveratrol and two other stilbenoids with *cis*- and *trans*-configuration on human lung cancer cells (A549).<sup>44</sup> They showed that one of the stilbenoid analogues, 3,4,5-trimethoxy-4'-bromo-*cis*-stilbene (BCS, see Figure 1.15), was more

effective than its corresponding *trans*-isomer and resveratrol on the inhibition of cancer cell growth. Prompted by the strong growth inhibition of BCS ( $IC_{50} = 0.03 \mu\text{M}$ ) compared to its *trans*-isomer ( $IC_{50} = 6.36 \mu\text{M}$ ), 3,4,5-trimethoxy-4'-bromo-*trans*-stilbene (BTS), and resveratrol ( $IC_{50} = 33.0 \mu\text{M}$ ) in cultured A549 cells, they investigated its mechanism of action. BCS induced G2/M cell cycle arrest and subsequently increased DNA contents in the sub-G1 phase in a time dependent manner, indicating induction of apoptosis.



**Figure 1.15.** Structures of resveratrol, 3,4,5-trimethoxy-4'-bromo-*trans*-stilbene (BTS) and 3,4,5-trimethoxy-4'-bromo-*cis*-stilbene (BCS).

In another study Schneider *et al.* compared the activity of resveratrol in human colon cancer cells (Caco-2) to its *cis*- and *trans*-trimethoxy derivatives (3,5,4'-trimethoxy-*cis*-stilbene and 3,5,4'-trimethoxy-*trans*-stilbene, see Figure 1.16).<sup>45</sup> The *cis*-derivative was 100-fold more active than the *trans*-derivative and arrested growth of the Caco-2 cells completely at  $0.4 \mu\text{M}$ . This 3,5,4'-trimethoxy-*cis*-stilbene also caused cell cycle arrest at the G2/M phase transition and inhibited tubulin polymerisation in a dose dependent manner.

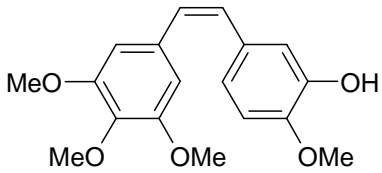
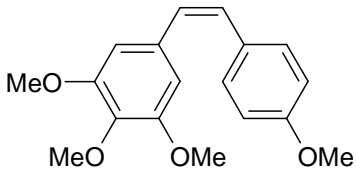
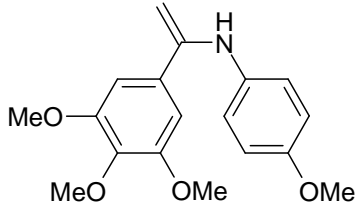


**Figure 1.16.** Structures of the 3,5,4'-trimethoxy-*trans*-stilbene and 3,5,4'-trimethoxy-*cis*-stilbene.

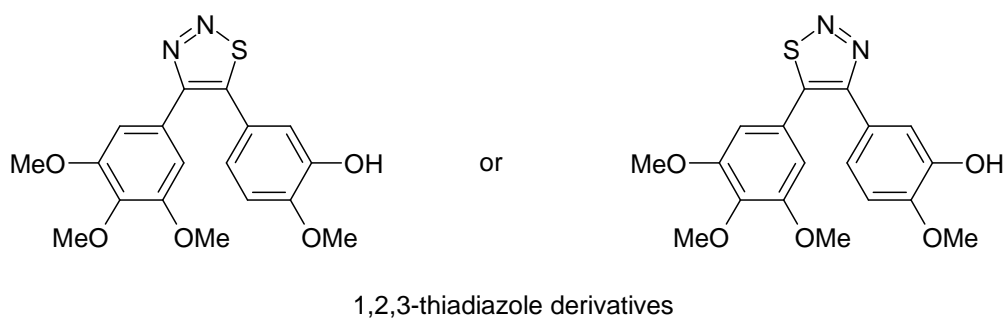
Chushman *et al.* synthesized an array of *cis*-, *trans*-, and dihydrostilbenes and some *N*-arylbenzylamines and evaluated their cytotoxicity in different cancer cell cultures like A549 lung carcinoma, MCF-7 breast carcinoma and HT-29 colon adenocarcinoma cells.<sup>46</sup> Several *cis*-stilbenes, structurally similar to combretastatins, were highly cytotoxic in all cell lines and

these were also found to be active as inhibitors of tubulin polymerization (see Table 1.3). The most active compounds also inhibited the binding of colchicine to tubulin.

**Table 1.3.** Cytotoxicity of the compounds in different cancer cell cultures ( $ED_{50}$  in  $\mu\text{M}$ ) and the effect on tubulin polymerization.

			
	combretastatin A-4	(Z)-1-(4-methoxyphenyl)-2-(3,4,5-trimethoxyphenyl)ethene	(4-Methoxy-phenyl)-[1-(3,4,5-trimethoxy-phenyl)-vinyl]-amine
A-549	$1.2 \times 10^{-6}$	$2.2 \times 10^{-5}$	$1.9 \times 10^{-3}$
MCF-7	$3.8 \times 10^{-6}$	$1.2 \times 10^{-6}$	$2.4 \times 10^{-3}$
HT-29	$1.2 \times 10^{-5}$	$2.7 \times 10^{-5}$	$1.0 \times 10^{-3}$
Effects on tubulin polymerization ( $IC_{50}$ in $\mu\text{M} \pm \text{SD}$ )			
	$1.9 \pm 0.2$	$2.2 \pm 0.1$	$23 \pm 0.5$

Wu *et al.* synthesised a series of 1,2,3-thiadiazole derivatives related to CA-4 (see Figure 1.17).<sup>47</sup>



**Figure 1.17.** Structures of one 1,2,3-thiadiazole derivative related to combretastatin A-4.

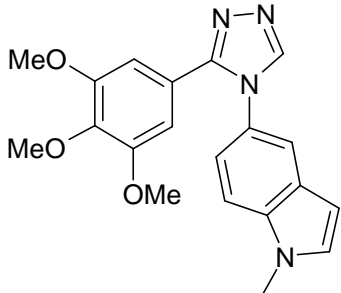
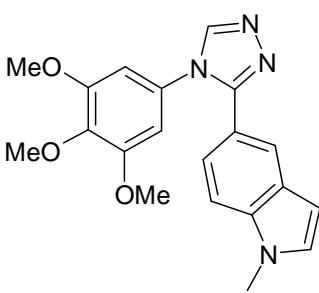
They investigated the *in vitro* and *in vivo* (mice) cytotoxic activity of these compounds as well as their effect on the inhibition of tubulin polymerization. The compounds were evaluated for their antiproliferative activities against three types of human cancer cell lines (human myeloid leukaemia cells HL-60, human colon adenocarcinoma cells HCT-116 and human microvascular endothelial cells HMEC-1, see Table 1.4).

**Table 1.4.** IC<sub>50</sub> values (nM ± SD) of the 1,2,3-thiadiazole derivative and combretastatin A-4. The inhibitory effect on tubulin polymerization is shown on the right.

	Cell Line			Anti-tubulin activity
	HL-60	HCT116	HMEC-1	IC <sub>50</sub> (μM)
1,2,3-thiadiazole derivatives	1.5 ± 0.1	3.0 ± 1.3	3.9 ± 2.8	0.7
CA-4	1.9 ± 0.7	3.0 ± 1.2	3.5 ± 0.9	0.81

Zhang and co-workers described the synthesis and biological evaluation of a series of tubulin polymerization inhibitors that contain the 1,2,4-triazole ring to retain the bioactive configuration afforded by the *cis* double bond in combretastatin A-4.<sup>48</sup>

**Table 1.5.** Cytotoxicity of the 1,2,4-triazole derivatives in different human cancer cell lines (IC<sub>50</sub> in nM) and the effect on tubulin polymerization.

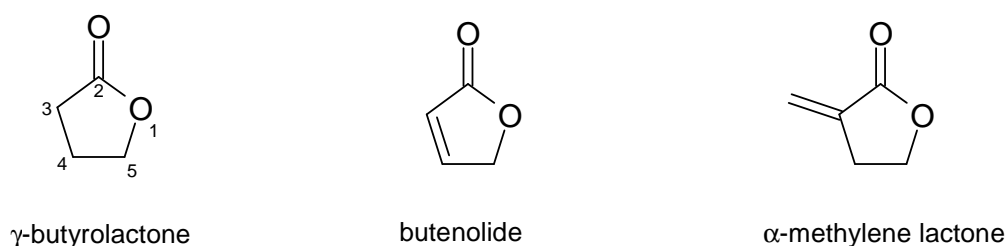
			CA-4
	1-methyl-5-[3-(3,4,5-trimethoxyphenyl)-4H-1,2,4-triazol-4-yl]-1H-indole	1-methyl-5-[4-(3,4,5-trimethoxyphenyl)-4H-1,2,4-triazol-3-yl]-1H-indole	
HCT-116	7.39	24.3	0.35
ZR-75-1	23.8	ND <sup>b</sup>	0.24
HeLa	8.73	18.0	0.30
KB31	9.9	15.0	0.78
KB-V1 <sup>a</sup>	20.8	32.1	0.64

<sup>a</sup> MDR cancer cell line; <sup>b</sup> ND = not determined.

Several compounds exhibited potent tubulin polymerization inhibitory activity as well as cytotoxicity against a variety of human cancer cells including MDR cancer cell lines. Attachment of the N-methyl-5-indolyl moiety to the 1,2,4-triazole core conferred optimal properties.

### 1.3.3 Natural Products with Anticancer Properties Containing Lactones

Lactones are cyclic esters, of which  $\gamma$ -butyrolactone (a five-membered-ring cyclic ester, see Figure 1.18) is a specific example. Two subclasses of unsaturated derivatives may be defined. The butyrolactone may have an endocyclic double bond located on the C-3 and C-4 carbons. Such bonds will be conjugated with the carbonyl group. Butyrolactones of this type are called butenolides. When the double bond is exocyclic, starting at the C-3 carbon, the butyrolactone is often referred to as a  $\alpha$ -methylene lactone.<sup>49</sup>

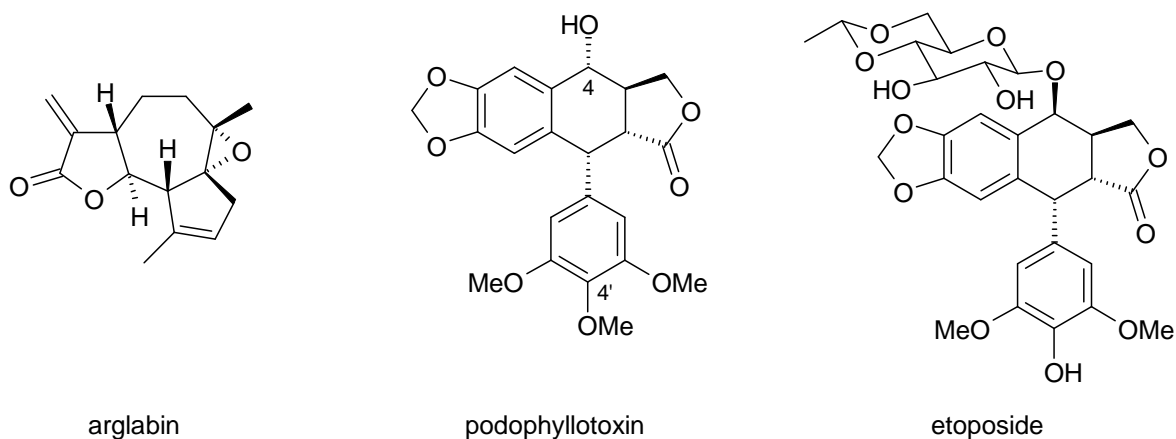


**Figure 1.18.** Structures of  $\gamma$ -butyrolactone, butenolides and  $\alpha$ -methylene lactone.

$\gamma$ -Butyrolactones, present in about 10% of all natural products, are a very common structural element in organic compounds.<sup>50</sup> A wide variety of naturally occurring mono-, di- and trisubstituted monocyclic  $\gamma$ -butyrolactones are known, but they are also found as part of more complex structures, especially in bicyclic and tricyclic ring systems. These compounds display a broad biological profile including strong antibiotic, antifungal, antitumor, antiviral, anti-inflammatory and cytostatic properties, which makes them interesting lead structures for new drugs. In many cases, a  $\alpha$ -methylene group in the lactone ring, being potentially able to bind the nucleophilic sites of biomolecules by conjugate addition, manifests their biological activity. Such Michael acceptors are generally avoided as a structural element in a potential drug because of the toxicity caused by unspecific binding. However, it does offer the possibility of generating adducts that can act as a prodrug with improved pharmacological properties. For example, the dimethylamino adduct of arglabin (see Figure 1.19), which is in clinical trials because of its promising activity against various cancer types, shows improved water solubility compared with the natural product itself, and can therefore be applied as an oral drug. On the other hand, the lactone unit represents a reactive functionality itself, being also a possible target for nucleophilic centers of biomolecules.<sup>50</sup>

Lignans which exist in a variety of plant species show a broad range of biological activities. Several lignans from natural sources like podophyllotoxin from *Podophyllum hexandrum* are proven to have antitumour activity. The antimetabolic effect of podophyllotoxin caused by binding to the protein tubulin in the mitotic spindle, preventing polymerization and assembly into microtubules. Podophyllotoxin and other *Podophyllum* lignans were found to be

unsuitable for clinical use as anticancer agents due to toxic side-effects, but the semi-synthetic derivatives etoposide and tenoposide (only etoposide is shown in Figure 1.19), which are synthesised from natural podophyllotoxin, are excellent antitumour agents. Etoposide is a very effective anticancer agent, and is used in the treatment of small cell lung cancer, testicular cancer and lymphomas, usually in combination therapies with other anticancer drugs. It may be given orally or intravenously. The water soluble pro-drug etopophos (etoposide 4'-phosphate) is also available.<sup>38</sup>



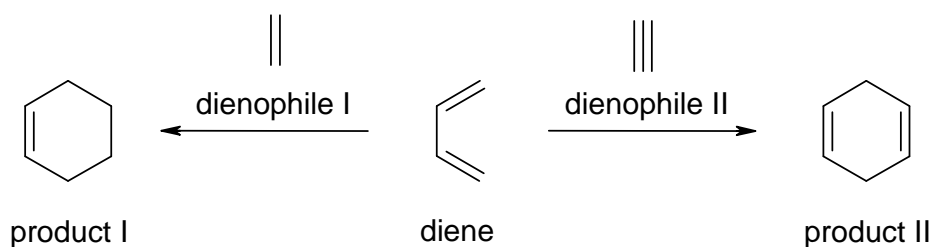
**Figure 1.19.** The structures of the anticancer compounds arglabin, podophyllotoxin and etoposide.

Remarkably, the 4'-demethylepipodophyllotoxin series of lignans do not act *via* a tubulin-binding mechanism like podophyllotoxin. Instead, these drugs inhibit the enzyme topoisomerase II, thus preventing DNA synthesis and replication. Topoisomerases are responsible for cleavage and resealing of the DNA strands during the replication process. Etoposide is believed to inhibit strand-rejoining ability by stabilising the topoisomerase II – DNA complex in a cleavage state, leading to double-strand breaks and cell death. Development of other topoisomerase inhibitors based on podophyllotoxin-related lignans is an active research area. Biological activity in this series of compounds is very dependent on the presence of the *trans*-fused five-membered lactone ring, this type of fusion producing a highly strained system. Ring strain is markedly reduced in the corresponding *cis*-fused system, and the natural compounds are easily and rapidly converted into these *cis*-fused lactones by treatment with very mild bases, via enol tautomers or enolate anions.<sup>38, 49</sup>

## 1.4 The Diels-Alder Reaction

The Diels-Alder (DA) cycloaddition, discovered by Professor Otto Diels and his student Karl Alder in 1928 and being awarded with the Nobel Prize in 1950, is one of the best-known organic reactions that is widely used to construct, in a regio- and stereo-controlled way, a six-membered ring with up to four stereogenic centers.<sup>51</sup> With the potential of forming carbon-carbon, carbon-heteroatom and hetero-heteroatom bonds, the reaction is a versatile synthetic tool for the construction of simple as well as complex molecules. Since its discovery in 1928, more than 17 000 papers have been published concerning synthetic, mechanistic and theoretical aspects of the reaction and about half of these publications have appeared in the last decade.<sup>52, 53, 54</sup>

The classical DA reaction is a cycloaddition between a conjugated diene and a dienophile, which has at least one  $\pi$ -bond (see Scheme 1.6). When one or more heteroatoms are present in the diene and/or the dienophile framework, the cycloaddition is called a *hetero* Diels-Alder reaction.

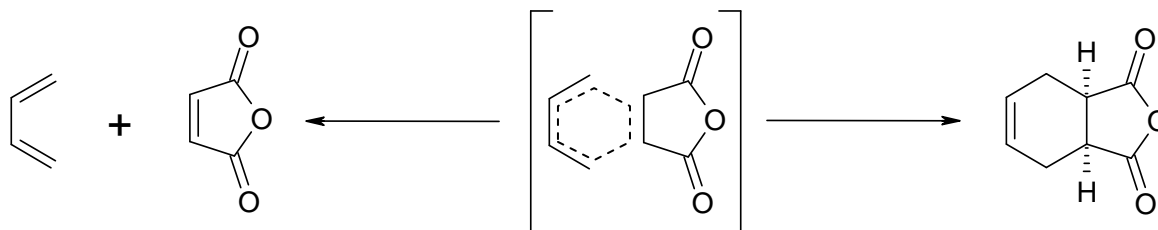


**Scheme 1.6.** Classical Diels-Alder reaction of a diene with a dienophile, which has one (left) or two (right)  $\pi$  bonds.

The reaction is classified as a  $[\pi 4_s + \pi 2_s]$  cycloaddition; 4 and 2 identify both the number of  $\pi$ -electrons involved in the electronic rearrangement and the number of atoms originating the unsaturated six-membered ring. The subscript *s* indicates that the reaction takes place suprafacially on both components. The DA reaction can be intermolecular or intramolecular and can be carried out under a variety of experimental conditions (e.g. thermal, Lewis-Acid catalyzed, solid support, high pressure).

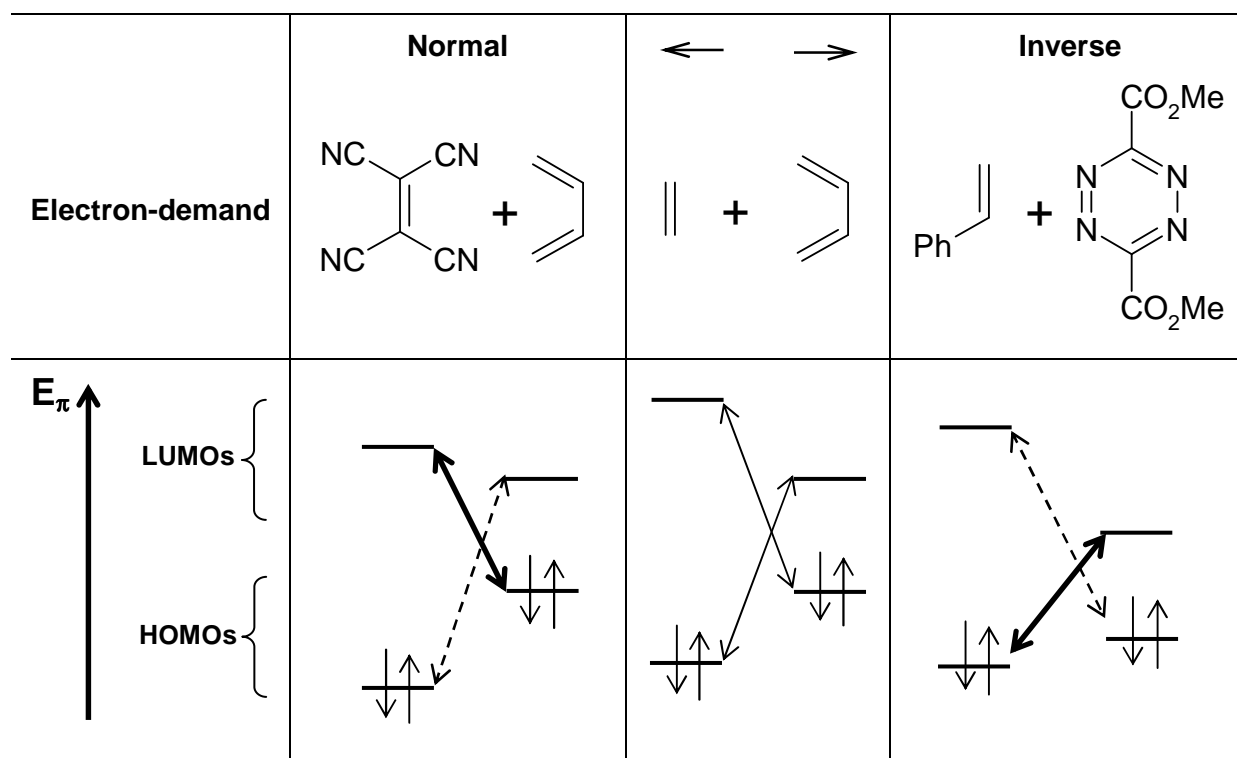
The DA reaction is a pericyclic cycloaddition when bond-forming and bond-breaking processes occur concertedly in a six-membered transition state (see Scheme 1.7). A concerted synchronous transition state (the formation of new bonds occurs simultaneously) and a concerted asynchronous transition state (the formation of one  $\sigma$ -bond proceeds in advance of the other) have been suggested, and the pathway of the reaction depends on the nature of the reagents and the experimental conditions.





**Scheme 1.7.** The Diels-Alder reaction of 1,3-butadiene and maleic anhydride. The bicyclic *cis*-product (*cis*-4-Cyclohexene-1,2-dicarboxylic anhydride) is formed stereoselectively via the six-membered transition state.

Most DA reactions, particularly the thermal ones and those involving apolar dienes and dienophiles, are described by a concerted mechanism. The high *syn* stereospecificity of the reaction, the low solvent effect on the reaction rate, and the large negative values of both activation entropy and activation volume comprise the chemical evidence usually given in favour of a pericyclic DA reaction.

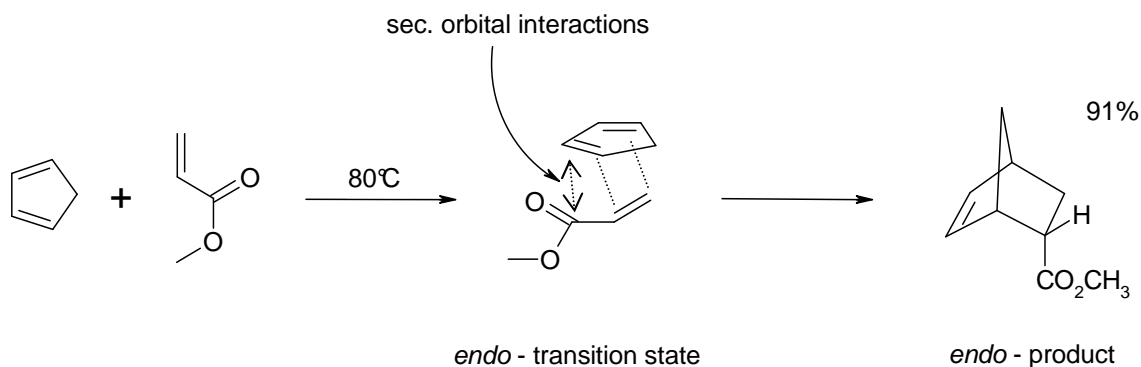


**Figure 1.20.** Examples of stabilizing  $\pi$ -frontier orbital interactions of Diels-Alder reactions with different electron demands. The bold arrows show the dominant interactions. Left: normal electron-demand; right: inverse electron-demand; HOMOs: **H**ighest **O**ccupied **M**olecular **O**rbitals; LUMOs: **L**owest **U**noccupied **M**olecular **O**rbitals.

According to the frontier molecular orbital theory (FMO), the reactivity, regiochemistry and stereochemistry of the DA reaction are controlled by the suprafacial in-phase interaction of the highest occupied molecular orbital (HOMO) of one component and the lowest

unoccupied molecular orbital (LUMO) of the other. These orbitals are the closest in energy. The reactivity of a DA reaction depends on the HOMO – LUMO energy separation of components: the lower the energy difference, the lower is the transition state energy of the reaction. Electron-withdrawing substituents lower the energy of both HOMO and LUMO, while electron-donating groups increase their energies. HOMO diene-controlled DA reactions are accelerated by electron-donating substituents in the diene and by electron-withdrawing substituents in the dienophile (normal electron-demand DA reaction). LUMO diene-controlled DA reactions are influenced by electronic effects of the substituents in the opposite way (inverse electron-demand DA reaction, see Figure 1.20).

The theory explains the kinetically favored *endo* approach considering an additional nonbonding interaction (see Scheme 1.8). This secondary orbital interaction does not give rise to a bond but contributes to lowering the energy of the *endo* transition state with respect to that of the *exo* one. The *endo* preference is known as Alder's rule.<sup>52</sup>

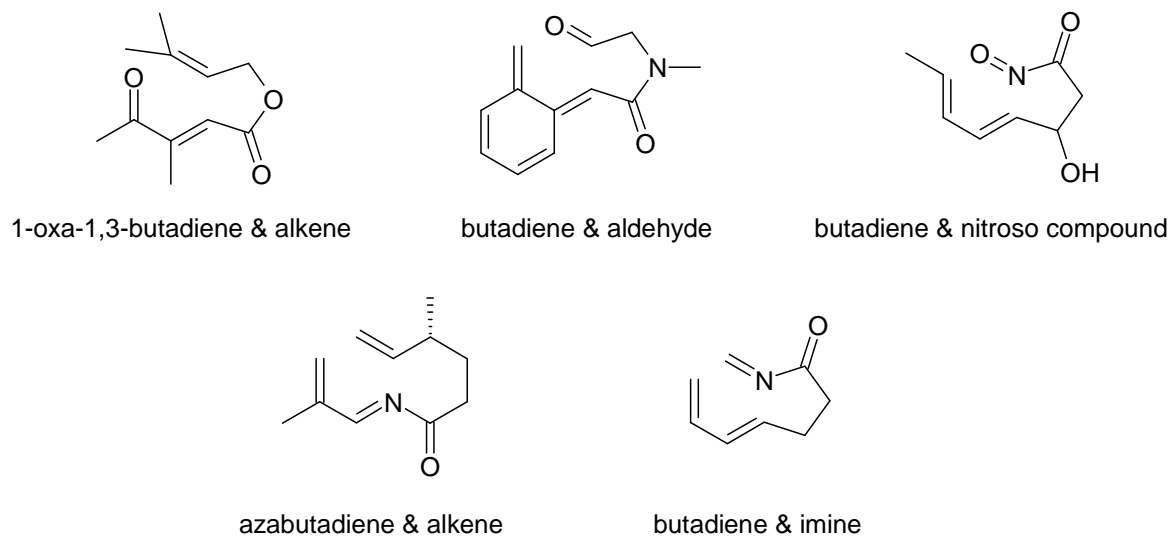


**Scheme 1.8.** The Diels-Alder reaction for the synthesis of the drawn bicyclic ester favours the *endo*-transition state because of secondary orbital interactions (nonbonding interactions).

#### 1.4.1 Intramolecular *hetero* Diels-Alder Reactions

When the diene and dienophile are connected by a chain the DA reaction can take place intramolecularly. The intramolecular DA reaction is a valuable tool in organic synthesis because it allows the formation of bicyclic derivatives and up to four chiral centers in one step. Both carbocyclic and heterocyclic rings may be generated depending on the nature of the interacting moieties; the size of the second ring depends on the length of the chain connecting the reaction partners. The hetero Diels-Alder (HDA) reaction allows the construction of heterocyclic six-membered rings by the interaction of heterodienes and/or heterodienophiles. Both the intermolecular and intramolecular versions of the HDA reaction are therefore very important methods for synthesizing heterocyclic compounds.<sup>33, 52, 55, 56, 57</sup>

There are many different types of intramolecular HDA reactions and only selected examples are presented in Figure 1.21.

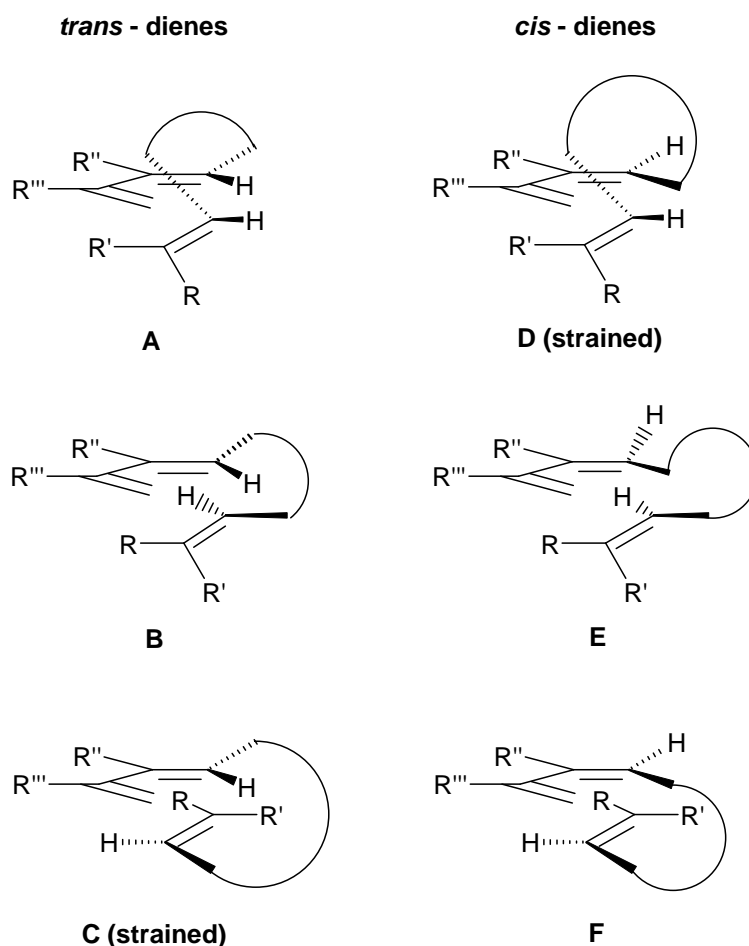


**Figure 1.21.** Examples of intramolecular *hetero* Diels-Alder reaction partners.

The first example of an intramolecular DA reaction appears to have been reported by Alder and Schumaker in 1953<sup>58</sup>, although it was not until the early sixties that isolated examples were published. The additional intramolecular advantages gained due to entropy, reactivity, regio-, stereo-, and diastereoselectivity account for the explosive growth in the study and application of this internal cycloaddition for the synthesis of complex molecules such as natural products or natural product-like compounds.<sup>33, 59, 60, 61</sup>

Due to the entropic influence intramolecular DA reactions proceed under milder conditions than their bimolecular analogues. Because of this reason even not activated dienophiles as well as poorly reacting 1,3-dienes can participate in intramolecular reactions. Figure 1.22 shows the possible transition states of the intramolecular DA reaction where the diene and dienophile are connected through a bridge of three or four atoms. The more flexible this bridge is, the more the reaction behaves like a bimolecular addition. The models show that the reaction of *trans*-dienes is forced in the direction of A or B, because orientation C is strained too strongly. With *cis*-dienes the preferred orientation is E, because D is also strained. In the case of the orientation F the bridge has to be long enough to allow this transition state and the connection of the closer ends of the diene and dienophile as shown in E may be entropically favoured over the orientation F.<sup>59</sup> The stereochemical outcome of an intramolecular DA reaction depends on the configurations of the diene and the dienophile, the length and substitution of the connecting bridge and the substitution of the reacting partners. Another strategy to control the absolute configuration of the product is the use of a chiral catalyst like chiral Lewis acids. To achieve catalytic enantioselective HDA reactions

(e.g. of carbonyl compounds), coordination of a chiral Lewis acid to the *hetero* atom is necessary. This coordination activates the substrate and provides the chiral environment that forces the approach of a diene to the substrate from the less sterically hindered face, introducing enantioselectivity in the reaction.

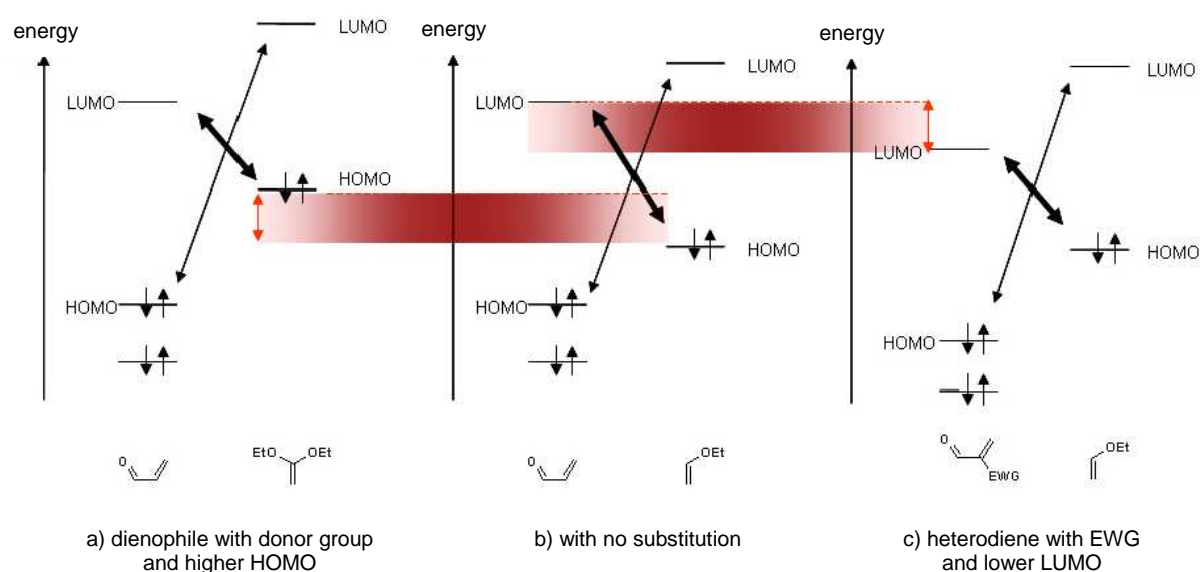


**Figure 1.22.** Possible transition states of the intramolecular DA reaction for *trans*- and *cis*-dienes in which the diene and dienophile are connected through a bridge of three or four atoms (adapted from cited ref.).<sup>59</sup>

HDA reactions with an oxygen bearing diene or dienophile are called oxa Diels-Alder reactions. In this case the oxygen atom among the reacting partners is either present in an aldehyde / ketone or in an oxa-1,3-butadiene. In the latter case this is an inverse electron demand controlled reaction with a dominant interaction between the LUMO of the 1-oxa-1,3-butadiene and the HOMO of the alkene. This reaction is usually a concerted nonsynchronous transformation with retention of the configuration of the dienophile and normally shows high regioselectivity, which is improved in the presence of Lewis acids. The HDA reaction of  $\alpha,\beta$ -unsaturated carbonyl compounds with electron-rich alkenes is a simple approach for the

synthesis of 3,4-dihydro-2*H*-pyrans, which are useful precursors for natural products such as carbohydrates.

In this oxa *hetero* Diels-Alder reactions, electron withdrawing groups at the oxa-1,3-butadiene greatly enhance their reactivity by lowering the energy of the LUMO and electron donating groups at the dienophile raise the energy of the HOMO and increase reactivity. The effect of substituents on the relative energy distribution of  $\pi$ -frontier orbital interactions of the HOMOs and LUMOs is graphically shown in the Figure 1.23 below. Again Lewis acids can enhance these effects even further.<sup>56</sup>



**Figure 1.23.** Influence of electron withdrawing groups (EWG) and donor groups on the  $\pi$ -frontier orbitals of oxa-HDA reactions with inverse electron demand (taken from cited ref.).<sup>62</sup>

Finally, there is the question if nature also knows the Diels-Alder reaction, this powerful synthesis to build up complex polycyclic natural products. This question can be answered with a clear yes. Studies on enzymes catalyzing the Diels-Alder reaction, often named “Diels-Alderase”, clearly demonstrated the involvement of this synthetically useful reaction in the biosynthesis of natural products like secondary metabolites.<sup>63, 64, 65</sup>

## 1.5 Solid Support Chemistry

In the case of solid-phase organic syntheses the starting material and synthetic intermediates are linked to an insoluble material (support) such as a resin bead, which enables easy mechanical separation of the intermediates from reactants and solvents. The solid phase synthesis was pioneered by Merrifield for the synthesis of peptides in 1963.<sup>66</sup>

The solid-support reaction has several advantages:<sup>1</sup>

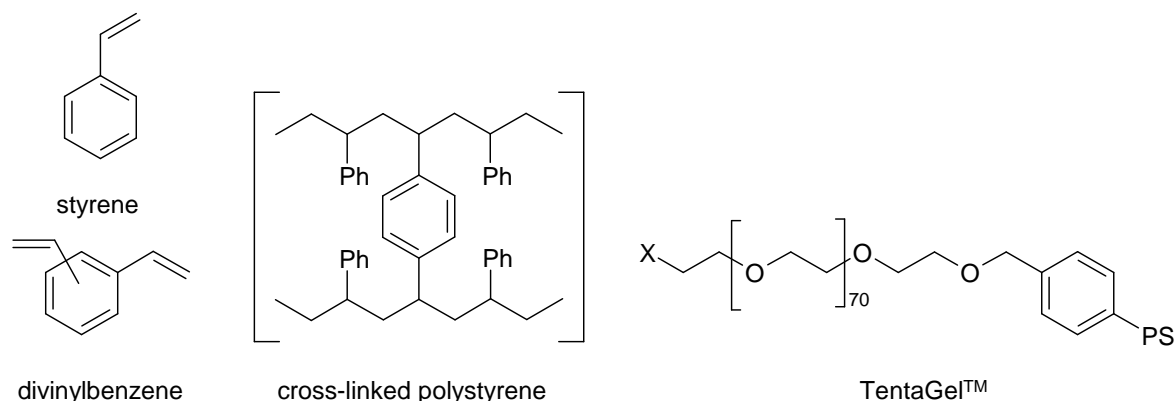
- A range of different starting materials can be bound to separate beads which can be mixed and treated with another reagent in a single experiment.
- Excess reagents or unbound by-products can be easily removed by washing the resin because the starting materials and products are bound to the solid support.
- The easy washing procedure allows the use of large excesses of reagents to drive the reaction to completion.
- Undesired side reactions like crosslinking can be suppressed if low loadings (less than 0.8 mmol/g support) are used.
- Intermediates do not need to be purified.
- At the end the individual beads can be separated to give individual products.
- Under suitable conditions and if appropriate anchor/linker groups are chosen the polymeric support can be regenerated.
- Automation is possible.

Especially the last point is an important advantage of solid-support chemistry. Today synthesizers for proteins, nucleic acids and small molecule libraries exist, saving time in otherwise repetitious work.

Several different support materials are suitable for solid-phase organic synthesis, but not all materials are compatible with all types of solvents and reagents. That's the reason why for each application the proper type of support has to be selected. The essential requirements for solid phase synthesis are:<sup>1</sup>

- a cross-linked insoluble polymeric support which is inert to the synthetic conditions
- an anchor or linker covalently linked to the resin, having functional groups where substrates can be attached
- a bond linking the substrate to the linker which will be stable to the reaction conditions used in the synthesis
- a means of cleaving the product or the intermediates from the linker
- protecting groups for functional groups not involved in the synthetic route.

Styrene-divinylbenzene copolymers (cross-linked polystyrene, see Figure 1.24) are one of the most frequently used supports.



**Figure 1.24.** Structures of hydrophobic cross-linked polystyrene (styrene & divinylbenzene) and the more hydrophilic TentaGel™ resin which has different swelling properties.

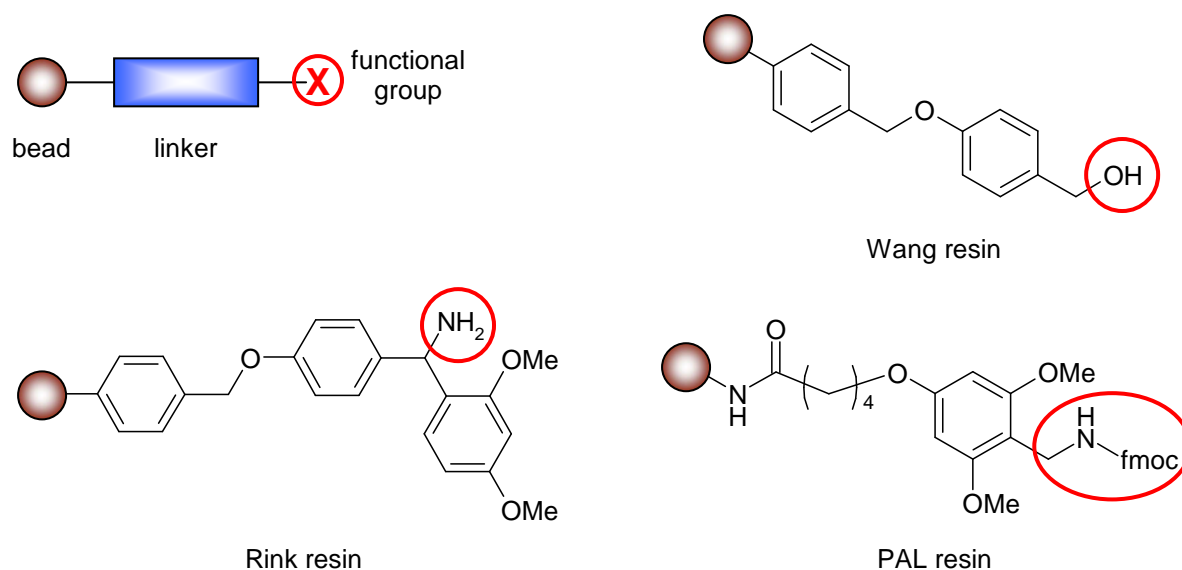
Copolymers of styrene and divinylbenzene were initially developed for the production of ion-exchange resins, and are still being used for this purpose. These polymers are essentially insoluble if cross-linking exceeds 0.2%, but can swell to variable extent in organic solvents. The swelling behaviour decreases with increasing cross-linking. The TentaGel™ resin is 80% polyethylene glycol (PEG) grafted to cross-linked polystyrene and provides an environment similar to ether or tetrahydrofuran (THF). This support is more hydrophilic than pure polystyrene, and swells in a broad variety of solvents.<sup>1, 67</sup>

Regardless of the polymer used, the bead should be capable of swelling in different solvents, yet remain stable. Swelling is important because most of the reactions involved in solid phase synthesis take place in the interior of the bead rather than on the surface. Each bead is a polymer and swelling involves unfolding of the polymer chains such that the solvent and reagents can move between the chains into the centre of the polymer.<sup>1, 67</sup>

Linkers are molecules which keep the intermediates in solid-phase synthesis bound to the support. These linkers should enable the easy attachment of the starting material to the support, be stable under a broad variety of reaction conditions, and yet enable selective cleavage at the end of a synthesis, without damage to the product. Different types of linkers have been developed and are used depending on the functional group which will be present on the starting material and on the functional group which is desired on the final product once it is released.

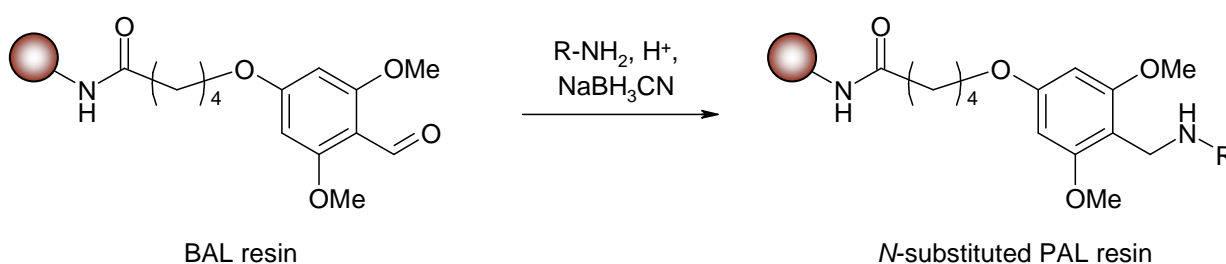
Resins having different linkers are given different names. For example, the Wang resin has a linker which is suitable for the attachment and release of carboxylic acids, whereas the Rink resin is suitable for the attachment of carboxylic acids and the release of carboxamides. The PAL (Peptide Amide Linker) was the first linker for solid-phase synthesis of peptide amides

by the Fmoc / *t*-Bu strategy (Fmoc: 9-fluorenylmethoxycarbonyl; *t*-Bu: *tert*-butyl; see Figure 1.25).



**Figure 1.25.** Typical resins used for solid-phase synthesis.

BAL (Backbone Amide Linker, see Figure 1.26), which is the aldehyde precursor of PAL, has been used for the preparation of hundreds of *C*-terminal modified peptides, heterocycles and other small organic molecules – always through amide/peptide bond anchoring. This approach involves the attachment of an amine nitrogen by reductive amination and further acylation. After cleavage from the solid support the *N*-substituted group stays on the final product.



**Figure 1.26.** Derivatisation of a BAL resin to a *N*-substituted PAL resin.

For the solid-phase synthesis it is necessary to protect important functional groups of the compound chosen for the synthesis which are not involved in the synthetic route. The selection of the right protecting group is important, because this group should be stable to the reaction conditions involved in the synthesis, but being removable in high yield under mild conditions once the synthesis is completed.<sup>1, 67, 68</sup>



## 1.6 References for Chapter 1

- [1] G. L. Patrick, *An Introduction to Medicinal Chemistry*, Oxford University Press: UK, third edition **2005**.
- [2] J. G. Lombardino, J. A. Lowe III, *Nature Rev. Drug Disc.* **2004**, 3, 853-862.
- [3] J. Drews, *Science* **2000**, 287, 1960-1964.
- [4] G. Thomas, *Medicinal Chemistry - An Introduction*; John Wiley & Sons, Ltd: Chichester, England, **2000**.
- [5] a) M. S. Lesney, Patents and Potions: Entering the Pharmaceutical Century, *The Pharmaceutical Century: Ten Decades of Drug Discovery Supplement to American Chemical Society*, **2000**, pp. 18-31; b) R. Pizzi, Salving with Science: The Roaring Twenties and the Great Depression, *The Pharmaceutical Century: Ten Decades of Drug Discovery Supplement to American Chemical Society*, **2000**, pp. 34-51; c) J. B. Miller, Antibiotics and Isotopes: Swingtime, *The Pharmaceutical Century: Ten Decades of Drug Discovery Supplement to American Chemical Society*, **2000**, pp. 52-72; d) B. D. Tweedy, M. S. Lesney, Prescription and Polio: Postwar Progress, *The Pharmaceutical Century: Ten Decades of Drug Discovery Supplement to American Chemical Society*, **2000**, pp. 72-91; e) R. Frey, M. S. Lesney, Anodynes and Estrogens: The Pharmaceutical Decade, *The Pharmaceutical Century: Ten Decades of Drug Discovery Supplement to American Chemical Society*, **2000**, pp. 92-109; f) M. S. Lesney, R. Frey, Chemistry, Cancer and Ecology: Environments of Health, *The Pharmaceutical Century: Ten Decades of Drug Discovery Supplement to American Chemical Society*, **2000**, pp. 110-129; g) C. S. W. Koehler, Aids, Arteries and Engineering: Epidemics and Entrepreneurs, *The Pharmaceutical Century: Ten Decades of Drug Discovery Supplement to American Chemical Society*, **2000**, pp. 130-147; h) M. S. Lesney, J. B. Miller, Harnessing Genes, Recasting Flesh: Closing the Pharmaceutical Century, *The Pharmaceutical Century: Ten Decades of Drug Discovery Supplement to American Chemical Society*, **2000**, pp. 148-167; all articles are available online at <http://pubs.acs.org/journals/pharmcent/index.html>
- [6] L. J. Gershell, J. H. Atkins, *Nature Rev. Drug Disc.* **2003**, 2, 321-327.
- [7] G. Wess, M. Urmann, B. Sickenberger, *Angew. Chem.* **2001**, 113, 3443-3453.
- [8] K. H. Bleicher, H.-J. Böhm, K. Müller, A. I. Alanine, *Nature Rev. Drug Disc.* **2003**, 2, 369-378.
- [9] C. A. Lipinski, F. Lombardo, B. W. Dominy, P. J. Feeney, *Adv. Drug Deliv. Rev.* **1997**, 23, 3-25.
- [10] A. Steinmeyer, *ChemMedChem* **2006**, 1, 31-36.
- [11] U. Norinder, Ch. A. S. Bergström, *ChemMedChem* **2006**, 1, 920-937.

- [12] J. Clardy, Ch. Walsh, *Nature* **2004**, 432, 829-837.
- [13] F. E. Koehn, G. T. Carter, *Nature Rev. Drug Disc.* **2005**, 4, 206-220.
- [14] R. Breinbauer, I. R. Vetter, H. Waldmann, *Angew. Chem. Int. Ed.* **2002**, 41, 2878-2890.
- [15] B. R. Stockwell, *Nature Rev. Genet.* **2000**, 1, 116-125.
- [16] A. M. Piggott, P. Karuso, *Comb. Chem. High Throughput Screen.* **2004**, 7, 607-630.
- [17] D. S. Tan, M. A. Foley, B. R. Stockwell, M. D. Shair, S. L. Schreiber, *J. Am. Chem. Soc.* **1999**, 121, 9073-9087.
- [18] a) D. J. Newman, G. M. Cragg, K. M. Snader, *J. Nat. Prod.* **2003**, 66, 1022-1037; b) R. Messer, C. A. Fuhrer, R. Häner, *Curr. Opin. Chem. Biol.* **2005**, 9, 259-265 (and references therein).
- [19] A. Reayi, P. Arya, *Curr. Opin. Chem. Biol.* **2005**, 9, 240-247.
- [20] S. Shang, D. S. Tan, *Curr. Opin. Chem. Biol.* **2005**, 9, 248-258.
- [21] G. L. Thomas, E. E. Wyatt, D. R. Spring, *Curr. Opin. Drug Discov. Dev.* **2006**, 9, 700-712.
- [22] F. J. Dekker, M. A. Koch, H. Waldmann, *Curr. Opin. Chem. Biol.* **2005**, 9, 232-239.
- [23] a) B. W. Stewart and P. Kleihues (Eds): *World Cancer Report*. IARC Press. Lyon **2003**; b) <http://www.who.int/en/> .
- [24] Ch. Sawyers, *Nature* **2004**, 432, 294-297.
- [25] J. Massagué, *Nature* **2004**, 432, 298-306.
- [26] S. W. Lowe, E. Cepero, G. Evan, *Nature* **2004**, 432, 307-315.
- [27] M. B. Kastan, J. Bartek, *Nature* **2004**, 432, 316-323.
- [28] H. Rajagopalan, Ch. Lengauer, *Nature* **2004**, 432, 338-341.
- [29] M. Arkin, *Curr. Opin. Chem. Biol.* **2005**, 9, 317-324.
- [30] R. S. DiPaola, *Clin. Cancer Res.* **2002**, 8, 3311-3314.
- [31] R. Messer, A. Schmitz, L. Moesch, R. Häner, *J. Org. Chem.* **2004**, 69, 8558-8560.
- [32] R. Messer, X. Pelle, A. L. Marzinzik, H. Lehmann, J. Zimmermann, R. Häner, *Synlett* **2005**, 2441-2444.
- [33] C. A. Fuhrer, R. Messer, R. Häner, *Tetrahedron Lett.* **2004**, 45, 4297-4300 (and references therein).
- [34] C. A. Fuhrer, E. Grüter, S. Ruetz, R. Häner, *ChemMedChem* **2007**, 2, 441-444 (and references therein).
- [35] E. L. Ghisalberti, *Phytomedicine* **1998**, 5, 147-163.
- [36] S. Mandal, R. Jain, S. Mukhopadhyay, *Indian J. Pharm. Sci.* **1998**, 60, 123-127.
- [37] L. J. El-Naggar, J. L. Beal, *J. Nat. Prod.* **1980**, 43, 649-707.
- [38] P. M. Dewick, *Medicinal Natural Products – A Biosynthetic Approach*; John Wiley & Sons Ltd: Chichester, **2003**.

- [39] L.-F. Tietze, *Angew. Chem.* **1983**, *95*, 840-853.
- [40] L. B. S. Kardono, S. Tsauri, K. Padmawinata, J. M. Pezzuto, D. A. Kinghorn, *J. Nat. Prod.* **1990**, *53*, 1447-1455.
- [41] M. P. Dobhal, G. Li, A. Gryshuk, A. Graham, A. K. Bhatanager, S. D. Khaja, Y. C. Joshi, M. C. Sharma, A. Oseroff, R. K. Pandey, *J. Org. Chem.* **2004**, *69*, 6165-6172.
- [42] Y. Fukuyama, Y. Minoshima, Y. Kishimoto, I. Chen, H. Takahashi, T. Esumi, *J. Nat. Prod.* **2004**, *67*, 1833-1838.
- [43] Ch. Mouriès, V. C. Rakotondramasy, F. Libot, M. Koch, F. Tillequin, B. Deguin, *Chem. Biodivers.* **2005**, *2*, 695-703.
- [44] E. Lee, H. Min, H. J. Park, H. Chung, S. Kim, Y. N. Han, S. K. Lee, *Life Sci.* **2004**, *75*, 2829-2839.
- [45] Y. Schneider, P. Chabert, J. Stutzman, D. Coelho, A. Fougerousse, F. Gossé, J.-F. Launay, R. Brouillard, F. Raul, *Int. J. Cancer* **2003**, *107*, 189-196.
- [46] M. Cushman, D. Nagarathnam, D. Gopal, A. K. Chakraborti, C. M. Lin, E. Hamel, *J. Med. Chem.* **1991**, *34*, 2579-2588.
- [47] M. Wu, Q. Sun, Ch. Yang, D. Chen, J. Ding, Y. Chen, L. Lin, Y. Xie, *Bioorg. Med. Chem. Lett.* **2007**, *17*, 869-873.
- [48] Q. Zhang, Y. Peng, X. I. Wang, S. M. Keenan, S. Arora, W. J. Welsh, *J. Med. Chem.* **2007**, *50*, 749-754.
- [49] S. H. Inayat-Hussain, N. F. Thomas, *Expert Opin. Ther. Patents* **2004**, *14*, 819-835.
- [50] M. Seitz, O. Reiser, *Curr. Opin. Chem. Biol.* **2005**, *9*, 285-292.
- [51] O. Diels, K. Alder, *Justus Liebigs Ann. Chem.* **1928**, *460*, 98-122 (as cited in [54]).
- [52] F. Fringuelli, A. Taticchi, *The Diels-Alder Reaction – Selected Practical Methods*; John Wiley & Sons Ltd: Chichester, **2002**.
- [53] E. J. Corey, *Angew. Chem.* **2002**, *114*, 1724-1741.
- [54] K. C. Nicolaou, S. A. Snyder, T. Montagnon, G. E. Vassilikogiannakis, *Angew. Chem.* **2002**, *114*, 1742-1773.
- [55] H. Waldmann, *Synthesis* **1994**, 535-551.
- [56] K. A. Jorgensen, *Angew. Chem. Int. Ed.* **2000**, *39*, 3558-3588.
- [57] K. A. Jorgensen, *Eur. J. Org. Chem.* **2004**, 2093-2102.
- [58] K. Alder, M. Schumaker, *Fortschr. Chem. Org. Naturst.* **1953**, *10*, 66.
- [59] W. Oppolzer, *Angew. Chem.* **1977**, *89*, 10-24.
- [60] A. G. Fallis, *Can. J. Chem.* **1984**, *62*, 183-234.
- [61] K. Takao, R. Munakata, K. Tadano, *Chem. Rev.* **2005**, *105*, 4779-4807.
- [62] Roland Messer, *Natural Product-like Compound Libraries from D-(-) Ribose*, Dissertation **2005**, Universität Bern, Schweiz.
- [63] G. Pohnert, *ChemBioChem* **2001**, *2*, 873-875.

- 
- [64] H. Oikawa, T. Tokiwano, *Nat. Prod. Rep.* **2004**, *21*, 321-352.
- [65] H. Oikawa, *Bull. Chem. Soc. Jpn.* **2005**, *78*, 537-554.
- [66] R. B. Merrifield, *J. Am. Chem. Soc.* **1963**, *85*, 2149-2154.
- [67] F. Z. Dörwald, *Organic Synthesis on Solid Support – Supports, Linkers, Reactions*; WILEY-VCH Verlag GmbH: Weinheim, **2000**.
- [68] F. Yraola, R. Ventura, M. Vendrell, A. Colombo, J.-C. Fernández, N. de la Figurea, D. Fernández-Forner, M. Royo, P. Forns, F. Albericio, *QSAR Comb. Sci.* **2004**, *23*, 145-152.

## 2. Aim of the Work

One of the most important steps in the drug discovery process is the identification of a biologically active molecular entity, a so called 'hit' or 'lead structure'. There are many approaches for finding such biologically active compounds as described earlier (Chapter 1.1.2). These approaches include the development of combinatorial chemistry technologies, the implementation of high-throughput screens (HTS) and bioinformatics tools, the sequencing of the human genome and other genomes, as well as the integration of functional genomics platforms.

Due to the many interesting biological activities of iridoids, such as anticancer properties, our group became attracted to this kind of structural element for synthesising natural product-like compound libraries. The successful library development of a tricyclic compound related to iridoids led to further investigations in this area. Therefore, the synthesis of natural product-like furopyranones (see Figure 2.1) was developed by combining several structural elements from biologically active natural products having anticancer properties (iridoids, *cis*-stilbenes,  $\gamma$ -butyrolactones). The screening process of the synthesised compounds was performed at a highly professional level in collaboration with the 'Novartis Institutes for BioMedical Research' in Basel (Switzerland). Thus, the natural product-like compounds were tested for their biological activity in different human cancer cell lines during this chemical genetic approach. Another part of this dissertation was the development of a suitable furopyranone scaffold(s) for solid phase synthesis. Next to the development of a suitable scaffold(s) for the attachment to substituted BAL (Backbone Amide Linker) resins, a small library of prototypes should be synthesised to prove the suitability of the scaffold(s) for solid phase synthesis. This part was done in collaboration with the 'Novartis Institutes for BioMedical Research' in Basel (Switzerland) where the suitability of the solid phase chemistry should be tested.

The aim of this work can be roughly subdivided into the two following projects:

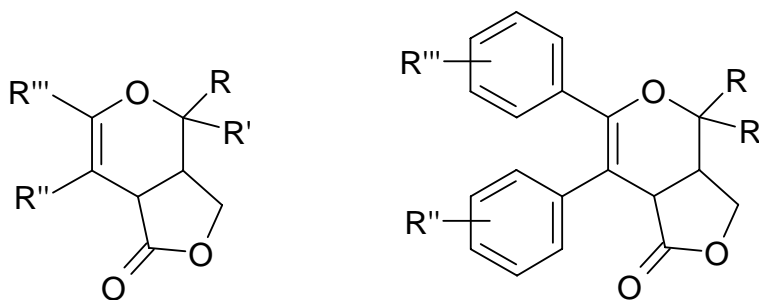
- 1. Development of the synthesis of natural product-like furopyranones by combining several structural elements of biologically active natural products for screening in different human cancer cell lines.**

The synthesis should be easy, selective as well as high yielding and the necessary structural elements should be easily implemented. The potential and the stereoselectivity of the *hetero* Diels-Alder reaction for the formation of the furopyranones should be investigated carefully. The integration of many different

functional groups into the system should be possible to conduct a detailed SAR study in the case of potent biological activity.

## 2. Development of a solid phase synthesis for the generation of natural product-like libraries.

For solid phase synthesis the suitable scaffold(s) needs a point of attachment and one or more functional group(s) for derivatisations. In the case of substituted BAL (Backbone Amide Linker) resins a carboxylic acid group is ideal for attachment. Furthermore, the furopyranone scaffold should be stable enough to resist all the chemical conditions during the solid phase synthesis. Reagents and conditions for the derivatisation of the scaffold on the solid support have to be found and some prototypes have to be synthesised for proving the suitability of the scaffold(s) for solid phase synthesis. The goal was, thus, to find suitable scaffolds and conditions for the generation of bicyclic furopyranone libraries.



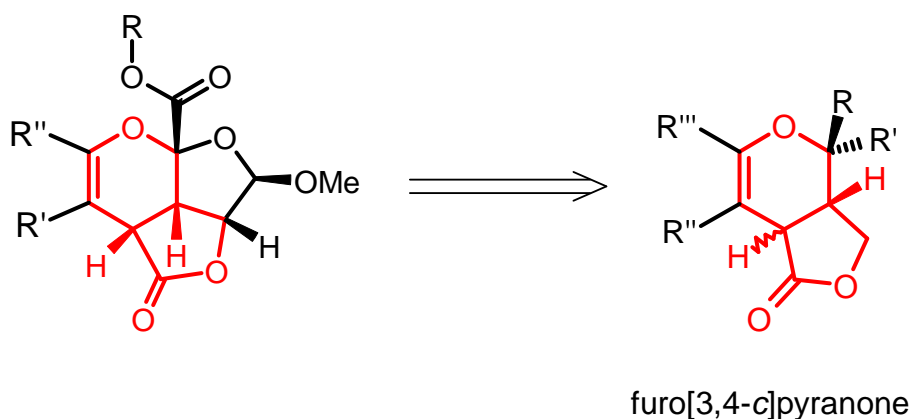
furopyranones

**Figure 2.1.** Structure of natural product-like furopyranones. On the left hand side the core structure without a *cis*-stilbene motif; on the right hand side the structure which contains a *cis*-stilbene motif. The integration of different functional groups for a SAR study or attachment to a solid support should be possible via the labelled positions (R, R', R'', R''').

### 3. Synthesis and Antiproliferative Properties of Furopyranones

#### 3.1 Development of a Synthetic Route for Furopyranones

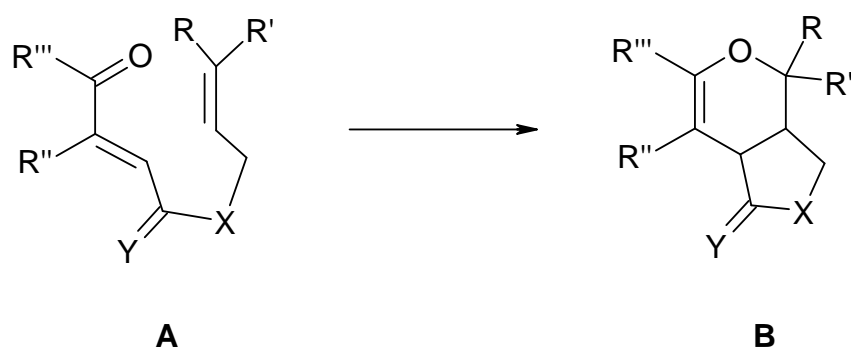
The rigid tricyclic compounds (see Scheme 3.1) related to iridoids and with a defined stereochemistry, containing a double ketal/acetal structure and a  $\gamma$ -lactone, were the first type of derivatives developed for building up natural product-like libraries in our group.<sup>1, 2, 3</sup> A long synthetic pathway and the existence of the acid labile acetal functions, however, led us to investigate the more easily accessible bicyclic scaffold – the furopyranone scaffold shown in Scheme 3.1.



**Scheme 3.1.** Furopyranone structure related to the tricyclic natural product-like scaffold developed for combinatorial chemistry in our group. The two compounds share a common part which is drawn in red.

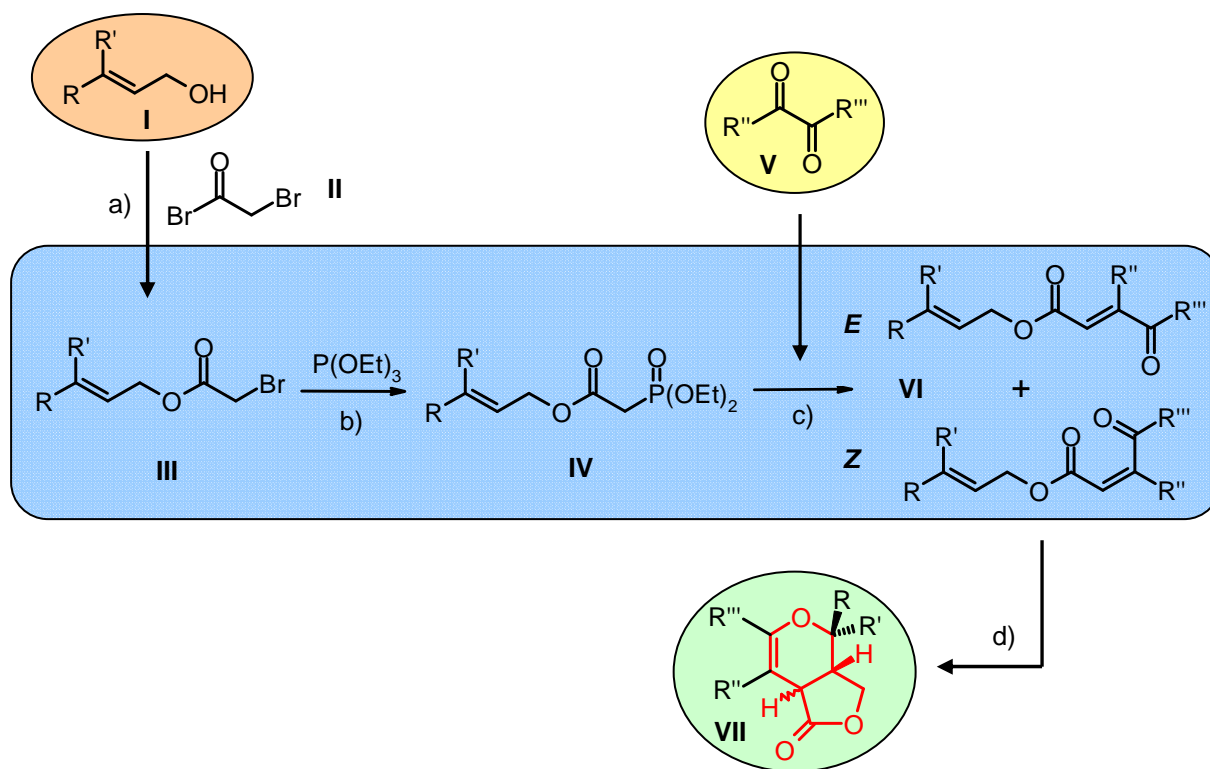
This bicyclic scaffold has several positions for the introduction of additional substituents. Introduction of substituted phenyl rings at the positions R'' and R''' leads to a *cis*-stilbene motif, a common structure in natural products with anticancer properties. This additional motif might influence the biological activity of furopyranones. Another possibility would be the opening of the  $\gamma$ -lactone for example by aminolysis, which would lead to monocyclic dihydropyran derivatives, which are useful precursors for natural products such as carbohydrates.<sup>4</sup>

As in the case of the tricyclic scaffold, an intramolecular *hetero* Diels-Alder reaction was to be used for the stereoselective construction of the furopyranones. Its concerted character allows the selective formation of up to three stereogenic centres in a single reaction step. The intramolecular version of the *hetero* Diels-Alder reaction (e.g., of  $\alpha,\beta$ -unsaturated ketones, such as **A** in Scheme 3.2) leads to the formation of bicyclic dihydropyran derivatives (**B**).



**Scheme 3.2.** Intramolecular *hetero* Diels-Alder reaction (e.g. X,Y=O).

For the synthesis of the intermediates we followed the strategy of the synthesis of the tricyclic scaffold (see Scheme 3.3):



**Scheme 3.3.** Synthetic route for the synthesis of furopyranones: a) esterification with bromoacetyl bromide; b) Arbusov reaction with triethyl phosphite; c) Horner-Wadsworth-Emmons reaction with different  $\alpha$ -diketones; d) thermal *hetero* Diels-Alder reaction.

Esterification of commercially available allyl alcohol derivatives **I** with bromoacetyl bromide (**II**) leads to the corresponding  $\alpha$ -bromoacetates **III**. Treatment of these intermediates with triethyl phosphite gives the phosphonates **IV**. At this point different  $\alpha$ -diketones **V** can be used for the synthesis of the  $\alpha,\beta$ -unsaturated  $\gamma$ -ketoesters **VI**. The final thermally induced



*hetero* Diels-Alder reaction should then result in the formation of the bicyclic furopyranones **VII**.

### 3.2 Stereoselective Synthesis of 3a,7a-Dihydro-3H,4H-furo[3,4-c]pyran-1-ones via an Intramolecular *hetero* Diels-Alder Reaction

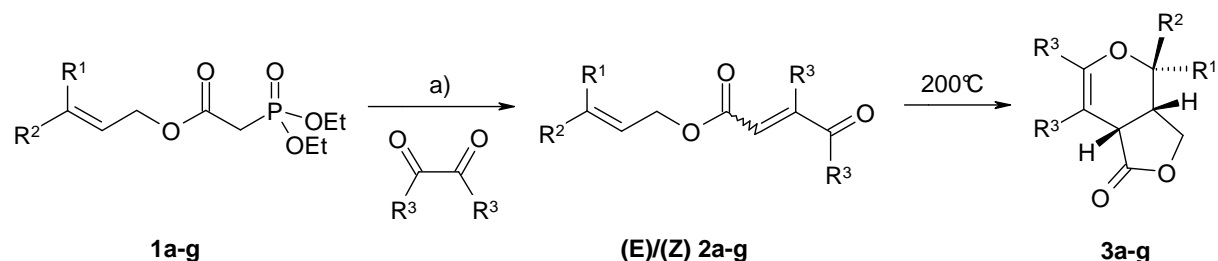
The synthesis of the required building blocks was straightforward. The diethyl phosphonate esters **1a-g** were prepared through an *Arbuzov* reaction of the corresponding  $\alpha$ -bromoacetates with triethyl phosphite. The phosphonates were converted into the  $\alpha,\beta$ -unsaturated  $\gamma$ -ketoesters **2a-g** via the *Horner-Wadsworth-Emmons* reaction using commercially available  $\alpha$ -diketones (see Table 3.1). Products **2a-g** were obtained as isomeric mixtures (*E:Z*-ratio approximately 1:2). In the cases where separation of the *E*- and *Z*-isomers (i.e. for **2a**, **2b** and **2e**) was possible, the pure isomers were used in the following cyclisation step. In all other cases, the obtained mixture of *E*- and *Z*-isomers was used.

We then investigated the thermal cyclisation of  $\alpha\beta$ -unsaturated  $\gamma$ -ketoesters **2a-g**. Generally, the reaction was carried out in an autoclave at a temperature of 200°C using toluene as the solvent. As can be seen from Table 3.1, the yield of the reaction increased with the number of substituents of the ene-moiety ( $R^1$  and  $R^2$ ). Only traces of product (<10%) were observed in the case of the allylesters *E*- and *Z*-**2a**. With the dimethyl and phenyl substituted derivatives, the reaction proceeded considerably better and, with one exception (*E*-**2e**), the expected products could be isolated in yields between 40 and 70%. The finding that alkyl or aryl substituents at the ene-part have a positive effect on this *inverse* electron demand *hetero* Diels-Alder reaction is well in agreement with the theory. Some decomposition (ester cleavage) of the starting material at the relatively high reaction temperature was observed, which partly explains the moderate yields in some cases. Attempts to facilitate the reaction with various *Lewis* acids (e.g. Cu(II), Zn(II), Al(III), BF<sub>3</sub>) were not successful and led to complex reaction mixtures at temperatures above 110°C. Furthermore, we could not observe any product arising from an ene-reaction (see Scheme 3.4), which is theoretically possible with compounds **2b**, **c** and **d**. An intramolecular ene-reaction was observed by Snider *et al.* in a related system.<sup>5,6</sup>

As expected, the cyclisation reaction turned out to be highly stereoselective. In all cases, formation of a single product was observed. Structural elucidation revealed a *cis*-configuration of the two rings. Furthermore, in the cases in which  $R^1$  and  $R^2$  were different (i.e. products **2e-g**) again a single diastereomer was formed. Most importantly, the formation of the product did not depend on the geometry of the diene moiety. The same isomer was

formed from either the *E*- or the *Z*-precursor. The relative configurations of the products **3c** and **3f** were established by x-ray crystallography.\* The structure of **3f** is shown in Figure 3.1.

**Table 3.1.** Preparation of furo[3,4-*c*]pyranones (+/-)-**3a-g** via intramolecular *hetero* Diels-Alder reaction of  $\alpha,\beta$ -unsaturated  $\gamma$ -ketoesters **2**.



R <sup>1</sup>	R <sup>2</sup>	R <sup>3</sup>	Compound (% yield; <i>E:Z</i> ) <sup>b)</sup>	Product	% yield <sup>c)</sup>
H	H	CH <sub>3</sub>	<b>2a</b> (62%; 1:2)	<b>3a</b>	(traces)
CH <sub>3</sub>	CH <sub>3</sub>	CH <sub>3</sub>	<b>2b</b> (73%; 1:2)	<b>3b</b>	37% from <i>E</i> - <b>2b</b> 46% from <i>Z</i> - <b>2b</b>
CH <sub>3</sub>	CH <sub>3</sub>	phenyl	<b>2c</b> (58%; 1:2.3)	<b>3c</b>	58%
CH <sub>3</sub>	CH <sub>3</sub>	4-fluorophenyl	<b>2d</b> (42%; 1:2.6)	<b>3d</b>	64%
H	phenyl	CH <sub>3</sub>	<b>2e</b> (67%; 1:2)	<b>3e</b>	21% from <i>E</i> - <b>2e</b> 69% from <i>Z</i> - <b>2e</b>
H	phenyl	phenyl	<b>2f</b> (38%; 1:2.4)	<b>3f</b>	72%
H	phenyl	4-fluorophenyl	<b>2g</b> (43%; 1:2)	<b>3g</b>	56%

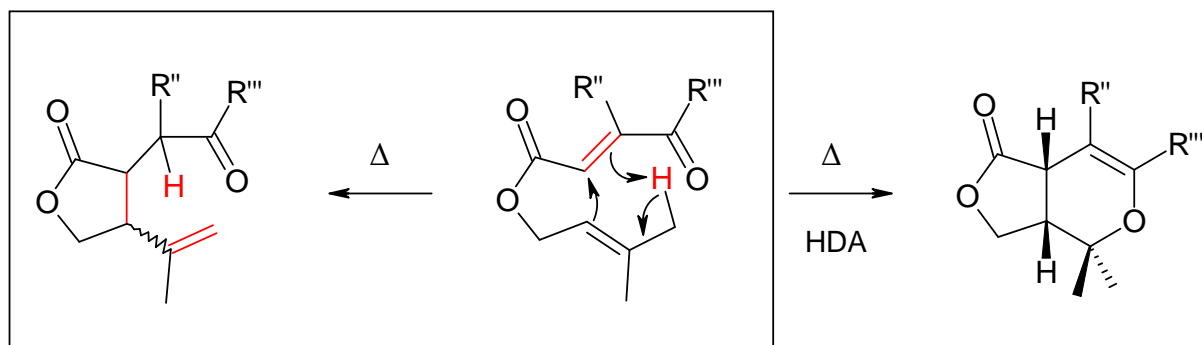
<sup>a)</sup> LiHMDS (1.1 eq.), THF, -78°C, 2.5h.

<sup>b)</sup> *E*- and *Z*-isomers could be separated in the case of **2a,b** and **e**; all other compounds **2** were isolated as *E/Z*-mixtures.

<sup>c)</sup> isolated yields of **3** starting either from the pure *E*- or *Z*-isomers of **2b** and **e** or, alternatively, from the *E/Z*-mixture.

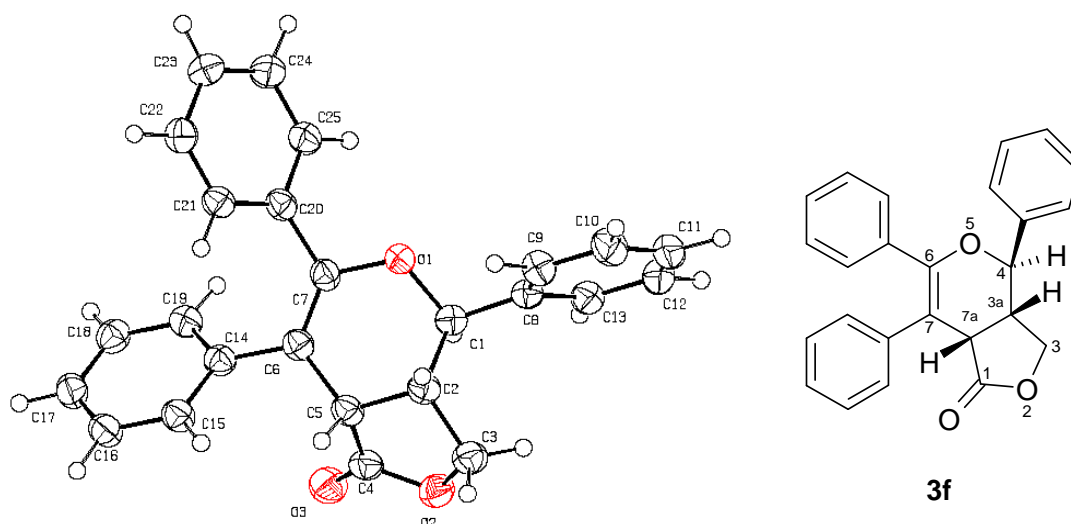
\* Crystallographic data (excluding structure factors) for the structures **3c** and **3f** have been deposited with the Cambridge Crystallographic Data Centre as supplementary publications numbers CCDC 233713 and CCDC 233714, respectively.

## ene-reaction



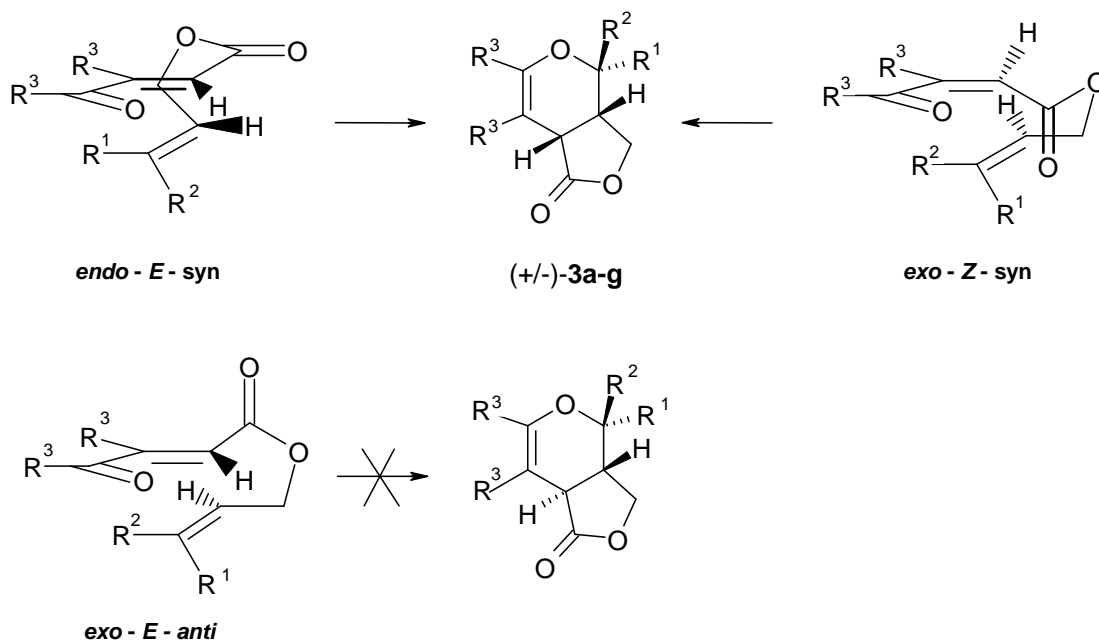
**Scheme 3.4.** Illustration of a possible ene-reaction. An allylic hydrogen (red) of a methyl group represents the ene while the double bond in  $\alpha$ -position (red) to the ester represents the enophile. On the right the observed *hetero* Diels-Alder (HDA) reaction is shown.

Based on the structural information, the stereochemical course of the *hetero* Diels-Alder reaction must proceed as illustrated in Scheme 3.5. Since both geometrical isomers afford the same product, the *E*-isomer reacts *via* the *endo-syn* and the *Z*-isomer *via* the *exo-syn* transition state. The formation of *trans*-fused products would require reaction through the *exo-E-anti* transition state. This has been observed in an intramolecular *hetero* Diels-Alder reaction of a more flexible system leading to two annulated six-membered rings.<sup>7</sup> In the present case, however, the sterically less flexible five membered linker seems to disfavor this transition state. The final fourth theoretical possibility (i.e. the *endo-Z-anti* transition state) is not possible for geometrical reasons (see Figure 1.22).<sup>5</sup>



**Figure 3.1.** Relative configuration of *hetero* Diels-Alder product (+/-)-**3f** as determined by x-ray crystallography. (Note that the crystallographic numbering, which has been kept for reasons of simplicity, is different from the systematic numbering).

Thus, *cis*-fused furo[3,4-*c*]pyranones can be synthesized from easily accessible  $\alpha,\beta$ -unsaturated  $\gamma$ -ketoesters *via* an intramolecular *hetero* Diels-Alder reaction. The reaction proceeds in a highly stereoselective way. Independently of the enone double bond configuration, a single product diastereomer is formed.<sup>5</sup>



**Scheme 3.5.** Stereochemical course of intramolecular *hetero* Diels-Alder reaction leading to *cis*-fused furo[3,4-*c*]pyranones.

The obtained compounds from this small library were screened for their biological activity in human cancer cell lines. In preliminary studies, compounds containing the *cis*-stilbene motif (**3c**, **3d**, **3f**, **3g**) indeed showed antiproliferative activity in the low  $\mu$ M range in different cell lines, whereas derivatives lacking the *cis*-stilbene motif (**3a**, **3b**, **3e**) were inactive (for a detailed discussion see Chapter 3.4). The promising results of this screening process prompted us to synthesise additional furopyranones for a more detailed SAR study.

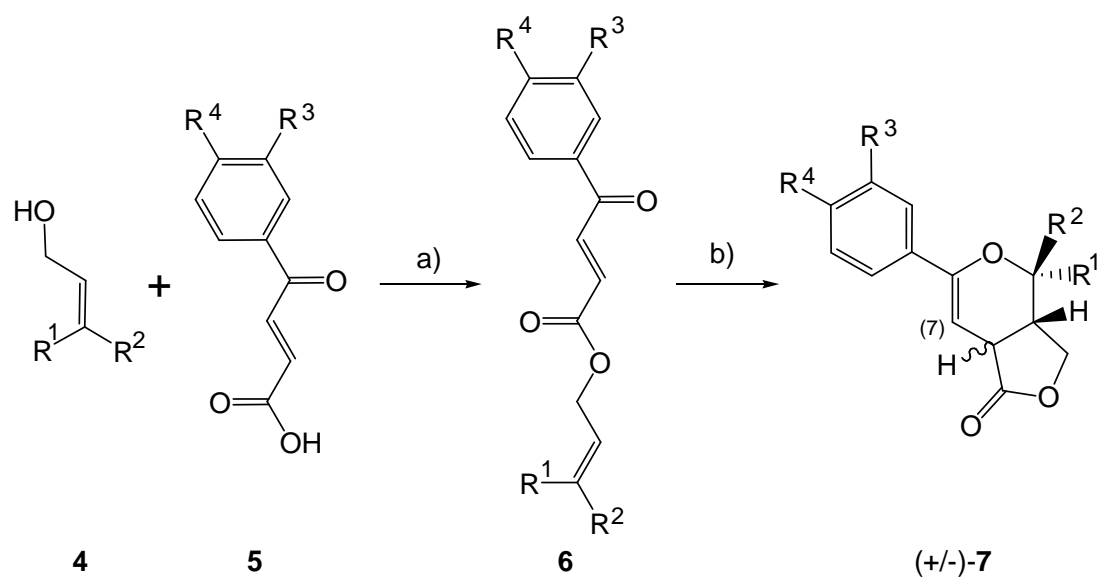
### 3.3 Syntheses of Furo[3,4-c]pyranones for Implementation of a Detailed Structure-Activity Relationship (SAR) Study

For the identification of the pharmacophore and for the improvement of the anticancer activity of the furo[3,4-c]pyranones, an extended SAR study was conducted. Therefore it was planned to introduce changes in the *cis*-stilbene motif, the lactone (opening and ring expansion), the furo[3,4-c]pyranone scaffold by additional ring implementation to a tricyclic scaffold and the substitution pattern of the *cis*-stilbene motif as well as of the additional phenyl ring. The synthesis of derivatives was carried out by considering the following questions: i) to what extent does the stilbene motif influence the biological activity and ii) is the bicyclic structure required for the biological effect observed?

#### 3.3.1 Synthesis of C(7)-Desphenyl Derivatives

To establish the importance of the *cis*-stilbenoid motif, several C(7)-desphenyl derivatives were synthesized (Scheme 3.6). Their preparation involved a similar route as the one used for the synthesis of compounds **3**.

Starting from the allylic alcohols **4** and the  $\gamma$ -oxo-butenoic acids **5**, the corresponding esters **6** were prepared *via* the mixed anhydride using pivaloyl chloride. Esters **6** were subsequently transformed into the furopyranones **7** through an intramolecular *hetero* Diels-Alder reaction. The cyclisation was carried out in refluxing *o*-xylene. Yields of isolated products varied between 40 and 70% (see Table 3.2), which is acceptable in view of the relatively harsh reaction conditions. The stereoselectivity of the *hetero* Diels-Alder reaction leading to products **7** varied greatly, depending on the substitution pattern of the allyl moiety of esters **6**. While the previously reported reaction leading to compounds **3** provided a *cis*-configuration of the two rings only, *cis/trans* ratios obtained in product **7a-f** varied between 97:3 and 34:66 (see Table 3.2). This indicates that the substituent at position C(7) has a significant influence on the relative configuration of the formed products. The results obtained do not allow drawing general conclusions on the governing aspects of the stereochemical course. The relative configurations of compounds *cis-7c*, *cis-7f* and *trans-7f* were confirmed by X-ray analysis as presented in Figures 3.2, 3.3 and 3.4.

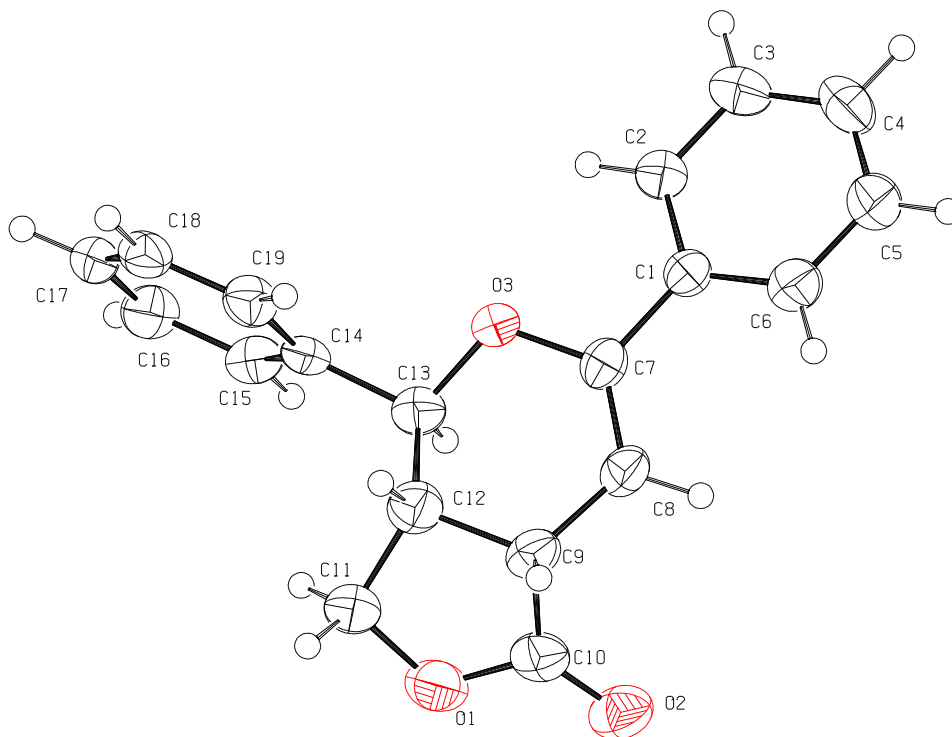


**Scheme 3.6.** Synthesis of furo[3,4-*c*]pyranones lacking the stilbene motif; a) pivaloyl chloride, triethylamine, DMAP, 1,2-dichloroethane, 0°C, 3 h; b) *o*-xylene, reflux, 24-48 h (for yields see Table 3.2).

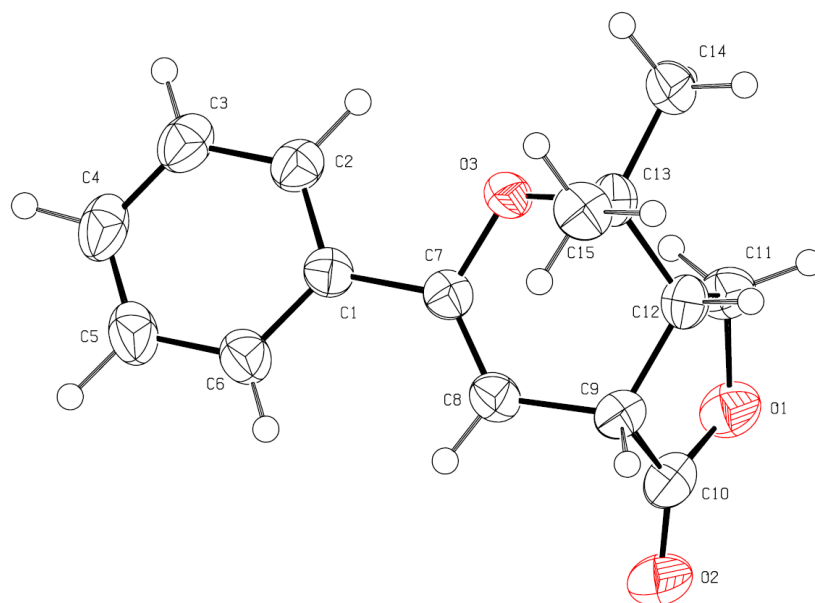
**Table 3.2.** Preparation of (±)-3a,7a-dihydro-3*H*,4*H*-furo[3,4-*c*]pyran-1-ones **7a-f** via intramolecular *hetero* Diels-Alder reaction of αβ-unsaturated γ-ketoesters.

R <sup>1</sup>	R <sup>2</sup>	R <sup>3</sup>	R <sup>4</sup>	compd. <b>6</b>	compd. <b>7</b>	
				(% yield)	(% yield) <sup>[a]</sup>	<i>cis/trans</i> ratio
H	C <sub>6</sub> H <sub>5</sub>	H	NO <sub>2</sub>	<b>6a</b> (63)	<b>7a</b> (55)	92:8
H	C <sub>6</sub> H <sub>5</sub>	NO <sub>2</sub>	H	<b>6b</b> (67)	<b>7b</b> (46)	42:58
H	C <sub>6</sub> H <sub>5</sub>	H	H	<b>6c</b> (80)	<b>7c</b> (39)	37:63
CH <sub>3</sub>	CH <sub>3</sub>	H	NO <sub>2</sub>	<b>6d</b> (58)	<b>7d</b> (66)	36:64
CH <sub>3</sub>	CH <sub>3</sub>	NO <sub>2</sub>	H	<b>6e</b> (69)	<b>7e</b> (44)	97:3
CH <sub>3</sub>	CH <sub>3</sub>	H	H	<b>6f</b> (92)	<b>7f</b> (73)	34:66

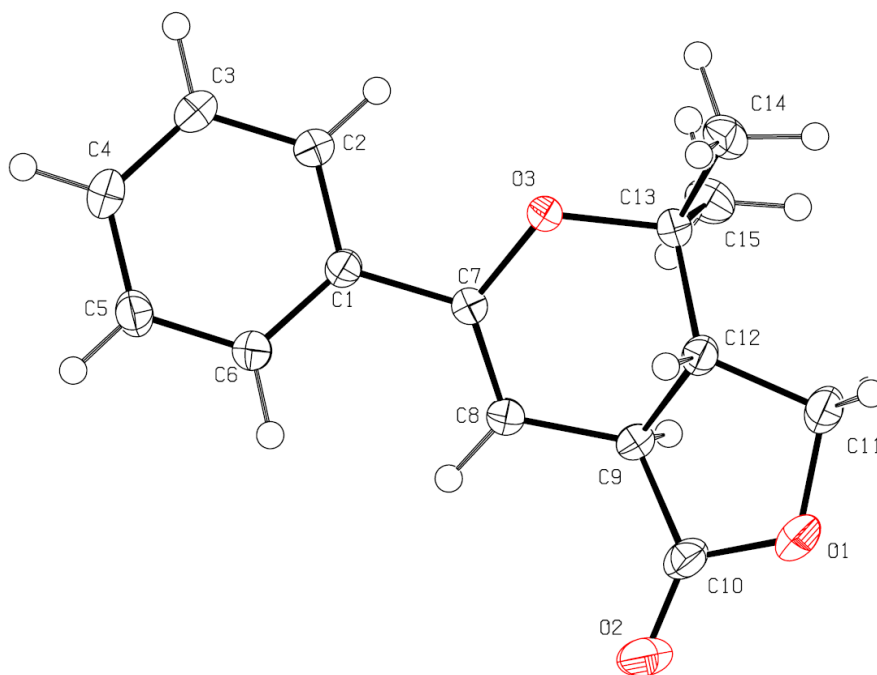
[a] Combined isolated yield of *cis*- and *trans*-isomers.



**Figure 3.2.** Relative configuration of *hetero* Diels-Alder product *cis-7c* as determined by x-ray crystallography.



**Figure 3.3.** Relative configuration of *hetero* Diels-Alder product *cis-7f* as determined by x-ray crystallography.



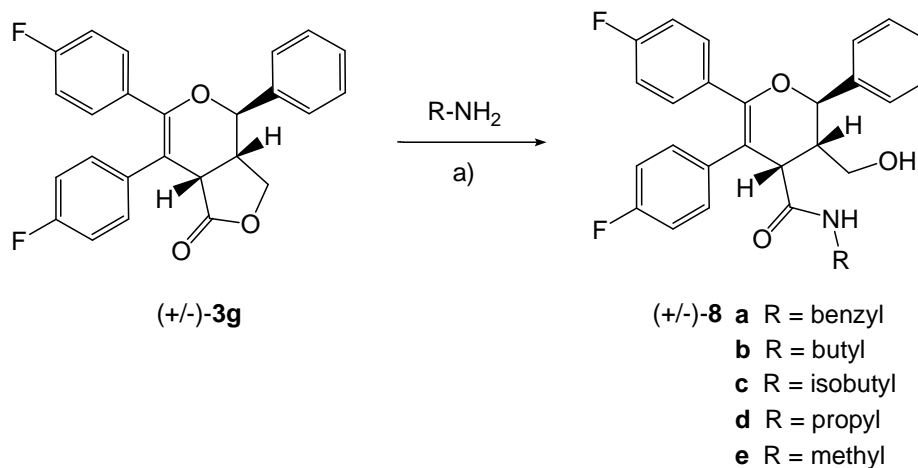
**Figure 3.4.** Relative configuration of *hetero* Diels-Alder product *trans*-7f as determined by x-ray crystallography.

CCDC 613296 (*cis*-7c), CCDC 613297 (*cis*-7f) and CCDC 613298 (*trans*-7f) contain the supplementary crystallographic data for the paper of Fuhrer *et al.*<sup>8</sup> These data can be obtained free of charge from *The Cambridge Crystallographic Data Centre* via [www.ccdc.cam.ac.uk/data\\_request/cif](http://www.ccdc.cam.ac.uk/data_request/cif).

### 3.3.2 Aminolysis of the Lactone

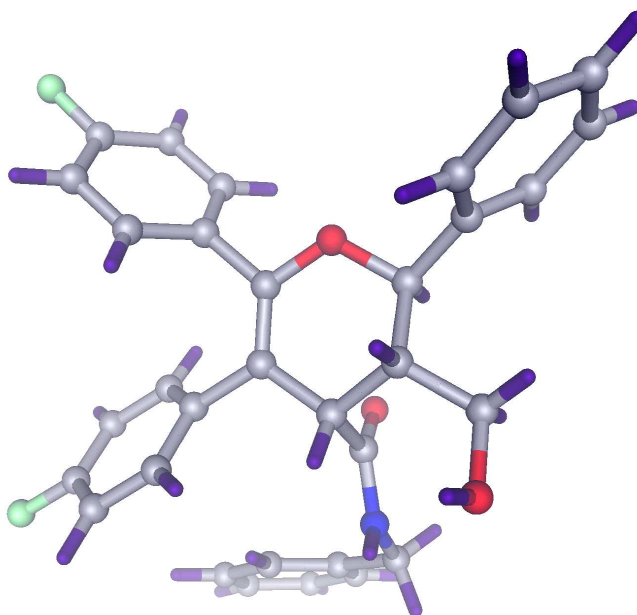
The bicyclic structure was further transformed into monocyclic compounds. To achieve the latter, the bicyclic compound **3g** was converted into monocyclic derivatives by ring opening aminolysis (Scheme 3.7).<sup>2, 3, 9</sup> Thus, treatment with benzyl-, butyl-, isobutyl-, propyl- or methyl amine in refluxing toluene in the presence of 2-hydroxypyridine gave the four monocyclic derivatives **8a-e**.





**Scheme 3.7.** Aminolysis of the  $\gamma$ -lactone ring of furo[3,4-*c*]pyranone **3g**; a) toluene, 2-hydroxypyridine, R-NH<sub>2</sub>, reflux, 20 h [yields: 47% (**8a**); 48% (**8b**); 52% (**8c**); 84% (**8d**); 27% (**8e**)].

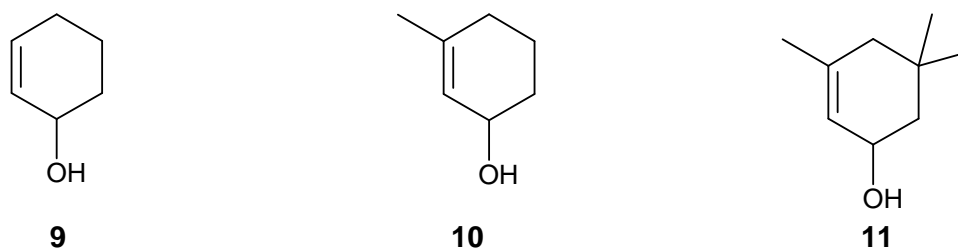
Treatment under the same conditions without a transacylation catalyst failed to give the ring-opened amides. The relative configuration of **8a** was verified by X-ray analysis as shown in Figure 3.5.



**Figure 3.5.** Relative configuration of aminolysis product **8a** as determined by x-ray crystallography. CCDC 613295 (**8a**), contain the supplementary crystallographic data for the paper of Fuhrer *et al.*<sup>8</sup> These data can be obtained free of charge from *The Cambridge Crystallographic Data Centre* via [www.ccdc.cam.ac.uk/data\\_request/cif](http://www.ccdc.cam.ac.uk/data_request/cif).

### 3.3.3 Synthesis of a Tricyclic Derivative

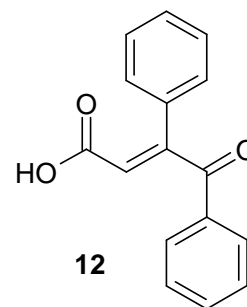
The strategy of extension involves the addition of another functional group to the lead compound in order to probe for extra binding interactions with the target.<sup>10</sup> We therefore investigated the synthesis of a tricyclic derivative starting from the cyclic allyl alcohols **9**, **10** and **11** as shown in Figure 3.6.



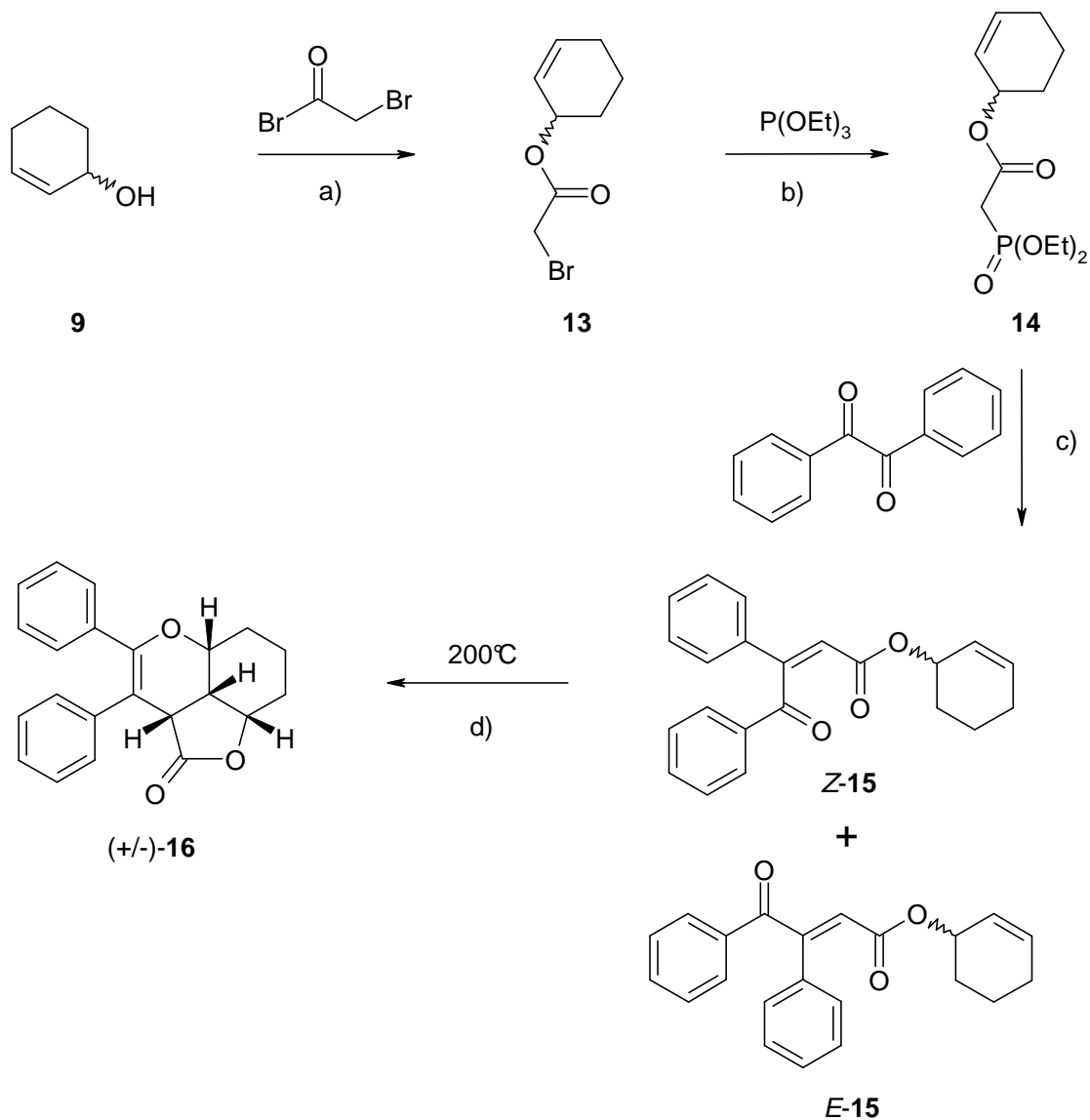
**Figure 3.6.** Structure of the cyclic alcohols (2-cyclohexen-1-ol **9**, 3-methyl-2-cyclohexen-1-ol **10** and 3,5,5-trimethyl-2-cyclohexen-1-ol **11**).

The cyclohexenols **9**, **10** and **11** were treated with bromoacetyl bromide to give the corresponding  $\alpha$ -bromoacetates. These products were converted into the phosphonates *via* an Arbuzov reaction followed by a Horner-Wadsworth-Emmons reaction with benzil. Again this reaction gave an isomeric mixture of *E*- and *Z*-isomers. The ratio of the two isomers can be influenced by the temperature. Thus, a low temperature leads to the kinetically more favoured *Z*-isomer while a higher temperature leads to the thermodynamically favoured *E*-isomer. The thermal *hetero* Diels-Alder reaction was performed in an autoclave (see Scheme 3.8).

The tricyclic product **16** was synthesised starting from alcohol **9**. Unfortunately the *hetero* Diels-Alder reaction with the precursors **10** and **11** did not work and the tricyclic products could not be isolated. The additional methyl groups led to sterical hindrance during the thermal cyclisation reaction and resulted in enhanced decomposition of the starting material. As a product of this decomposition (pyrolysis) carboxylic acid **12** (see Figure 3.7) was isolated:

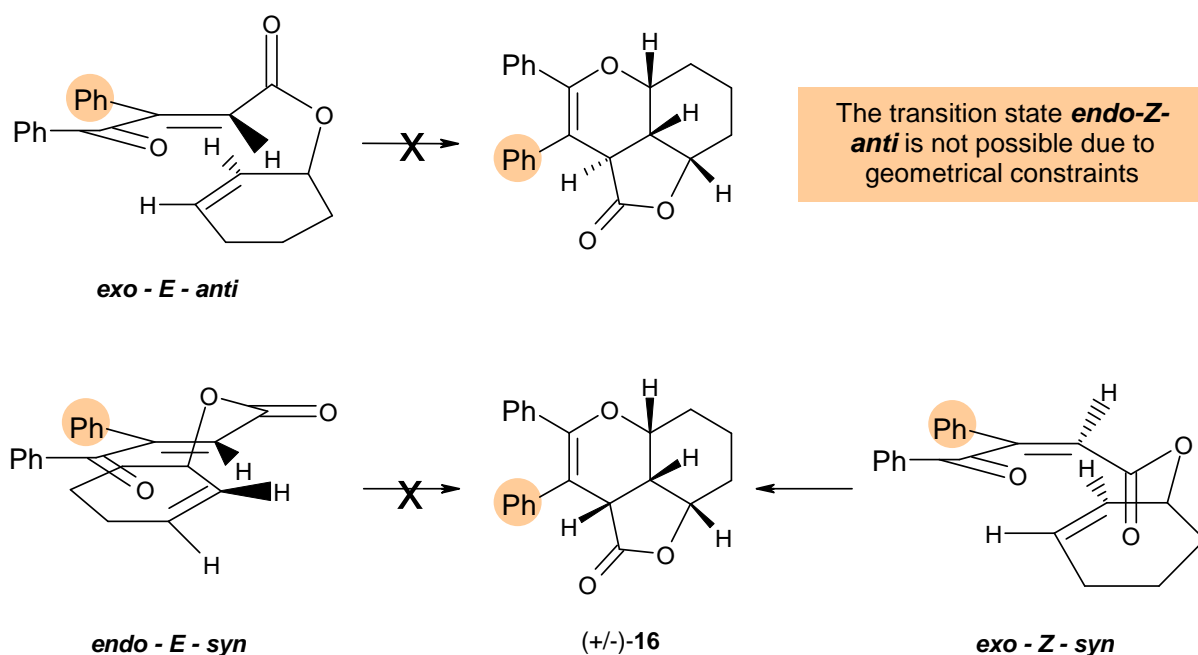


**Figure 3.7.** 4-Oxo-3,4-diphenyl-but-2-enoic acid **12** isolated after the *hetero* Diels-Alder reaction.



**Scheme 3.8.** Synthesis of 3,4-diphenyl-2a,5a,6,7,8,8a,8b-heptahydro-furo[4,3,2de]chromen-2-one (**16**); a)  $\text{CH}_2\text{Cl}_2$ , pyridine, 1h,  $0^\circ\text{C} \rightarrow \text{rt}$ , 1h, 78%; b) THF, reflux, 19h, 83%; c) *n*-BuLi, HMDS, THF,  $-78^\circ\text{C}$ , 3h, 90%; d) autoclave, toluene, 17 h, 41%.

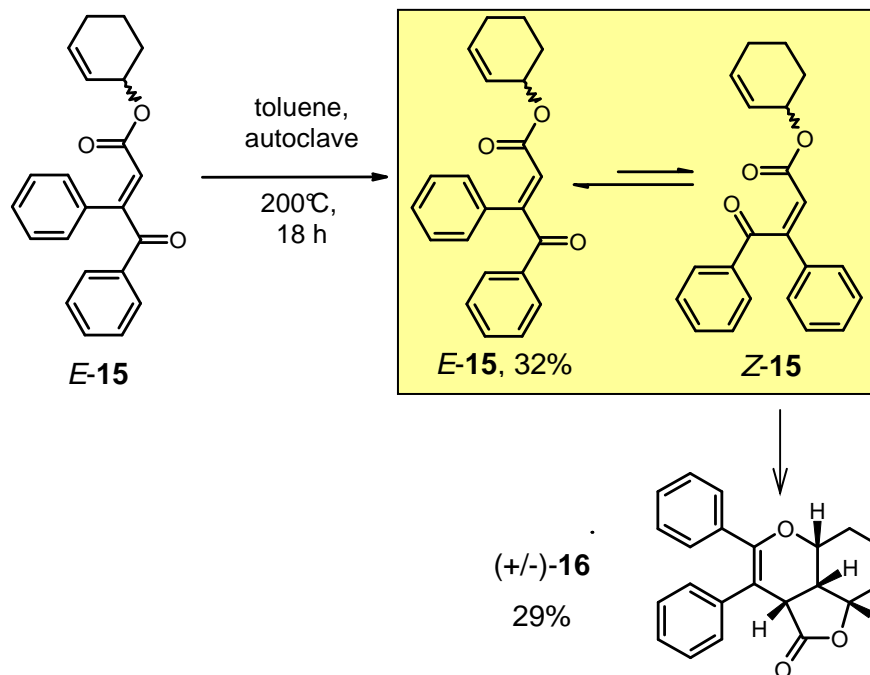
The thermal *hetero* Diels-Alder reaction of the isomeric mixture of **15** turned out to be highly selective. After purification of the final product **16** (yield: 41%), the starting material *E*-**15** (yield: 39%) was isolated as well. No *Z*-isomer of **15** was isolated indicating that **16** was formed *via* the *exo-Z-syn* transition state (see Scheme 3.9). The *endo-Z-anti* transition state is not possible because of geometrical constraints (see Figure 1.22).



**Scheme 3.9.** Stereochemical course of the intramolecular *hetero* Diels-Alder reaction leading to *cis*-fused **16**.

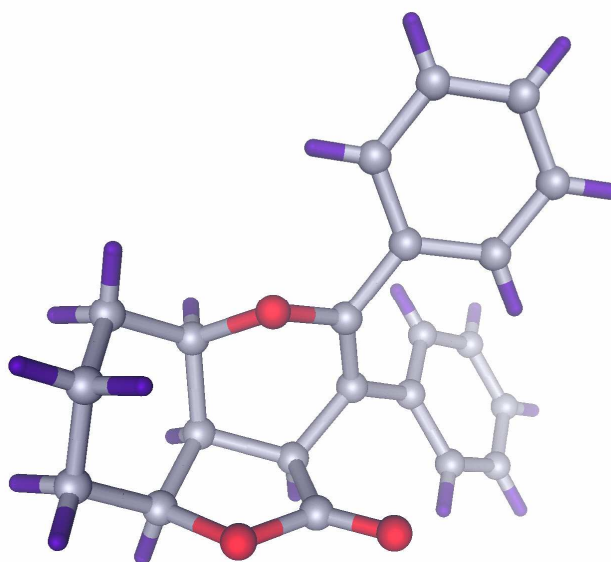
The stereoselective synthesis *via* the *hetero* Diels-Alder reaction resulted again only in the *cis*-configured product **16** indicating that the phenyl substituent (Ph) at the allyl moiety of ester **15** has a significant influence on the relative configuration of the formed product. Furthermore the presence of a ring on the linking chain introduces supplementary steric and torsional strain, which disfavours some of the possible transition states like the *endo-E-syn* transition state (see Scheme 3.9).<sup>11, 12, 13</sup>

Another experiment with the isolated *E*-isomer of **15** showed that the conditions in the autoclave for the *hetero* Diels-Alder reaction induced isomerisation. At a temperature of 200°C the equilibrium between the *E*- and *Z*-isomer of **15** should be on the side of the thermodynamically more stable *E*-isomer. But small amounts of the *Z*-isomer were able to react and to form compound **16** which was isolated (yield: 29%) after the reaction as well as the starting material **15** (*E*-isomer, yield: 32%, see Scheme 3.10). Due to the fact that product **16** was only formed *via* the *Z*-isomer of **15**, the Horner-Wadsworth-Emmons reaction was performed at low temperature to favour the synthesis of the *Z*-isomer. At a temperature of -78°C the ratio of *E*- to *Z*-isomer was about 1:2 while at a temperature of 0°C this ratio changed to about 1:1 (*E:Z*).



**Scheme 3.10.** The *hetero* Diels-Alder reaction with the isolated *E*-isomer of **15**. Under the conditions indicated, isomerisation took place and product **16** (29%) could be formed through small amounts of the *Z*-isomer of **15**. *E*-**15** (32%) was again isolated after the reaction.

Upon recrystallization of **16** from ethanol suitable crystals were obtained and analysed by x-ray crystallography (see Figure 3.8).

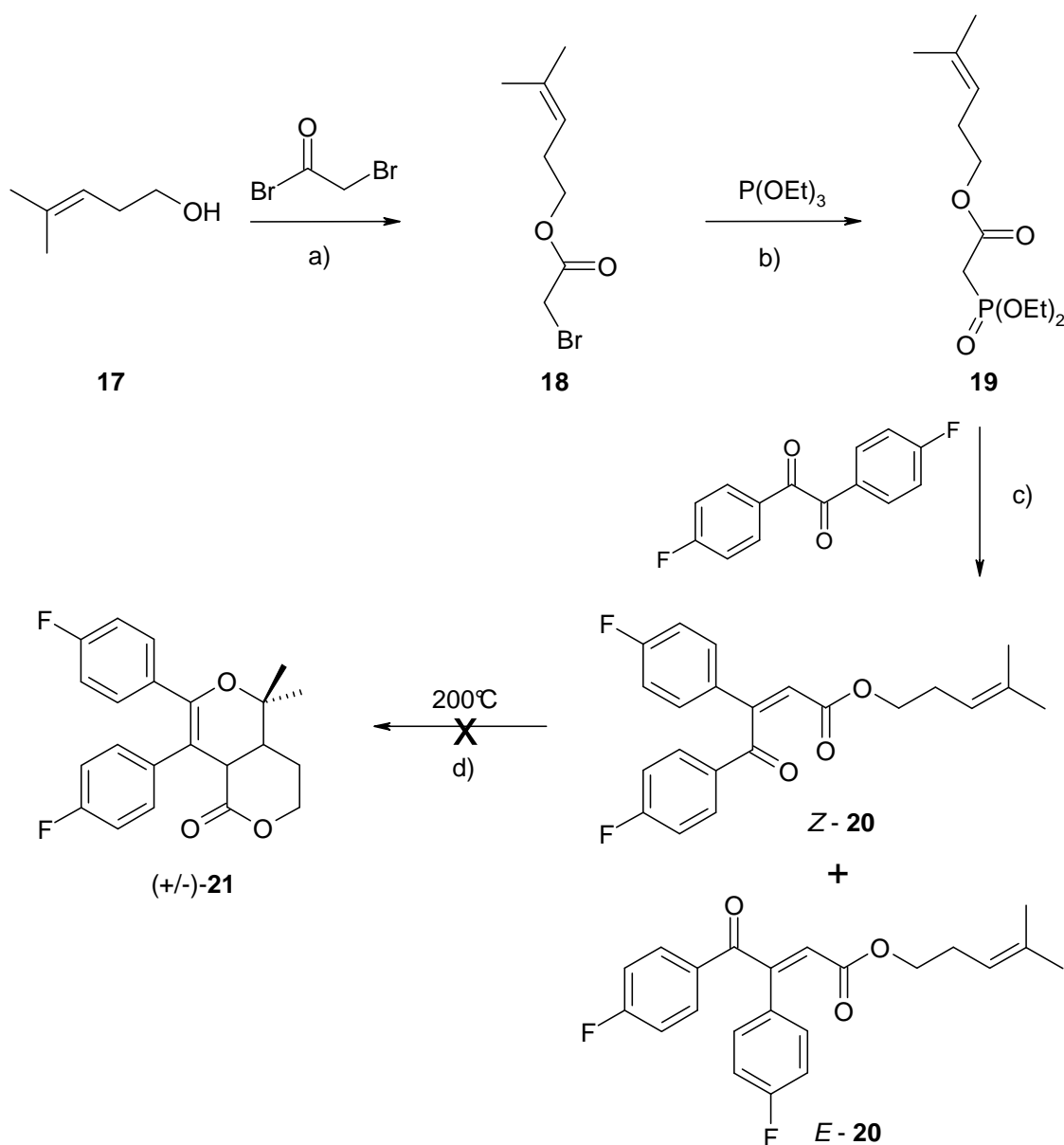


**Figure 3.8.** Relative configuration of product **16** as determined by x-ray crystallography.<sup>14</sup>

### 3.3.4 Attempted Replacement of the $\gamma$ -Lactone by a $\delta$ -Lactone

If a drug has one or more rings, it is generally worth synthesizing analogues where one of these rings is expanded or contracted. The principle behind this approach is much the same as varying the substitution pattern of an aromatic ring. Expanding or contracting the ring puts the binding groups in different positions relative to each other and may lead to better interactions with specific regions in the binding site.<sup>10</sup>

The strategy for the replacement of the  $\gamma$ -lactone to a  $\delta$ -lactone was straightforward. Thus, the commercially available 4-methyl-3-penten-1-ol (**17**) was chosen which should lead to the formation of a  $\delta$ -lactone during the final *hetero* Diels-Alder reaction (see Scheme 3.11).



**Scheme 3.11.** Attempted synthesis of pyranopyranone **21**; a)  $\text{CH}_2\text{Cl}_2$ , pyridine, 1 h, 0°C, 99%; b) THF, reflux, 22 h, 99%; c) *n*-BuLi, HMDS, THF, 0°C, 5 h, 60%; d) autoclave, toluene, 22 h.

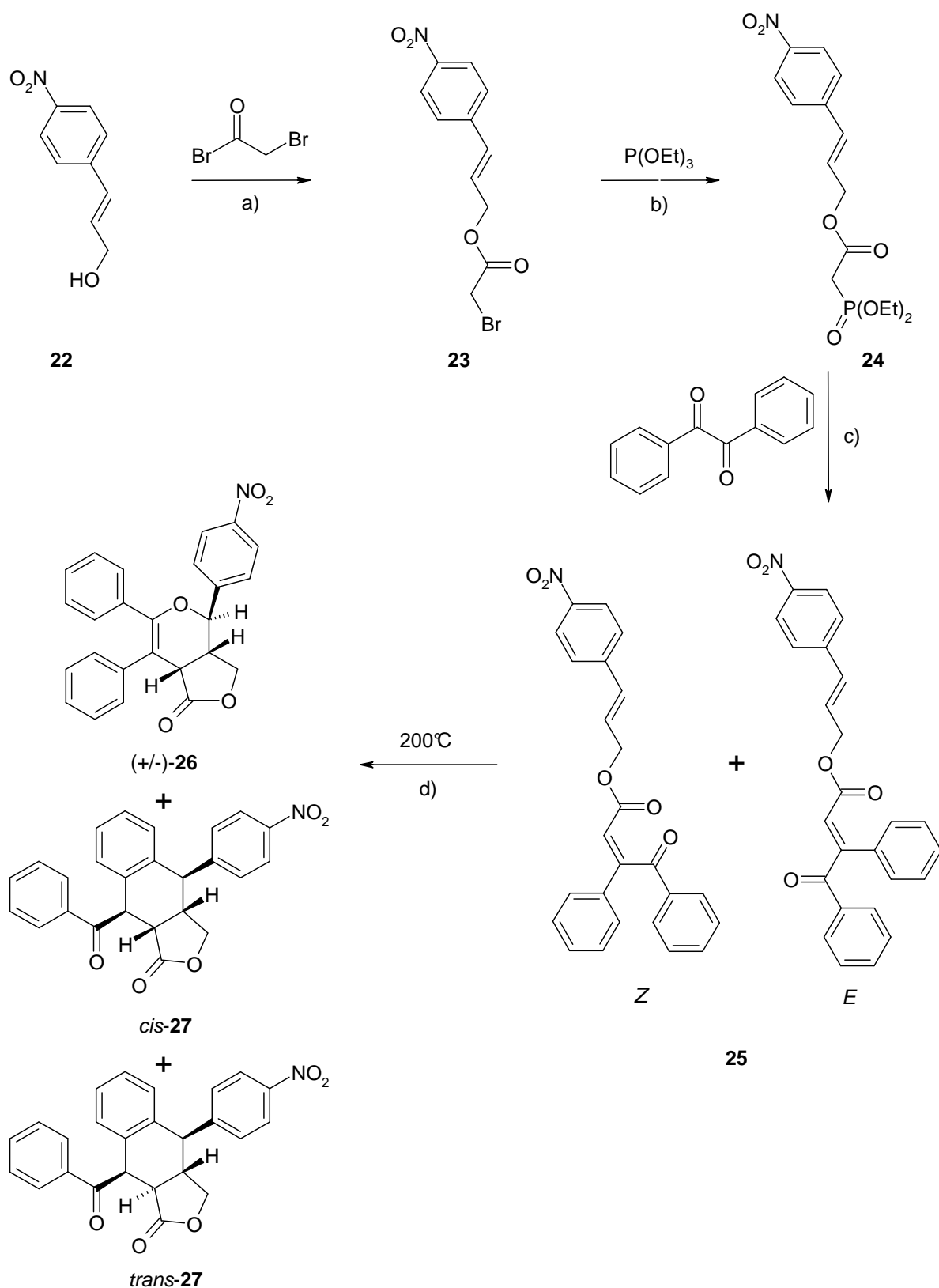
Esterification with bromoacetyl bromide gave the corresponding  $\alpha$ -bromoacetate **18** (yield: 99%) which were used without further purification for the following Arbuzov reaction. The obtained phosphonate **19** (yield: 99%) did not have to be purified for the Horner-Wadsworth-Emmons reaction which was carried out at a temperature of 0°C. Thus, the *E*- and *Z*-isomer of **20** were obtained in a ratio of about 9:10 (yield: 60%). Unfortunately the *hetero* Diels-Alder reaction did not form the expected product **21** (see Scheme 3.11). At the relatively harsh reaction conditions in the autoclave only isomerisation of the *Z*-isomer of **20** to the thermodynamically more stable *E*-isomer took place. After 22 h the ratio of *E*-**20** to *Z*-**20** changed from 9:10 in the beginning to 10:3 as determined by NMR of the crude reaction mixture. The diene and the dienophile in this case are connected through a bridge of 4 atoms (3 atoms in the case of furo[3,4-*c*]pyranone **3d**, see Table 3.1) which allows a greater flexibility of the molecule. Less flexibility in the case of furo[3,4-*c*]pyranone **3d** seems to force the diene and the dienophile to react with each other under the conditions indicated in Scheme 3.11.<sup>15</sup>

### 3.3.5 Carboxy- and Nitro-substituted Furopyranones

In order to bring additional functional groups into the furopyranone scaffold different strategies were investigated to synthesise functionalised cinnamyl alcohol derivatives. These starting materials would bring extra functionality into the scaffold for extension of a SAR study and bearing in mind the later work planned with BAL resins for solid phase chemistry, an additional carboxylic acid group was first choice.

#### 3.3.5.1 Nitro-substituted Furopyranones

In a first attempt the commercially available nitro-cinnamyl alcohol **22** was used (see Scheme 3.12). Esterification with bromoacetyl bromide (yield: 99%) followed by the Arbuzov reaction with triethyl phosphite (yield: 96%) worked well and the obtained products did not have to be purified. The Horner-Wadsworth-Emmons reaction was carried out at 0°C and gave the two isomers (*E*, *Z*) in a ratio of about 1:1 (yield: 59%). The outcome of the *hetero* Diels-Alder reaction was very surprising and led to the formation of the unexpected tricyclic products *cis*- and *trans*-**27** which were not observed in similar previous reactions (see Scheme 3.12). The strong electron withdrawing nitro-group in *para*-position was able to provide suitable electronic properties for a normal Diels-Alder reaction in which the phenyl ring in  $\beta$ -position of the ester was involved.



**Scheme 3.12.** Synthesis of furopyranone **26** and the tricyclic byproducts *cis*- and *trans*-**27** related to podophyllotoxin; a)  $\text{CH}_2\text{Cl}_2$ , pyridine, 2.5 h,  $0^\circ\text{C}$ , 1 h, 99%; b) THF, reflux, 24 h, 96%; c) LiHMDS, THF,  $0^\circ\text{C}$ , 4 h, 59%; d) autoclave, toluene, 20 h, yield of **26**: 40%.

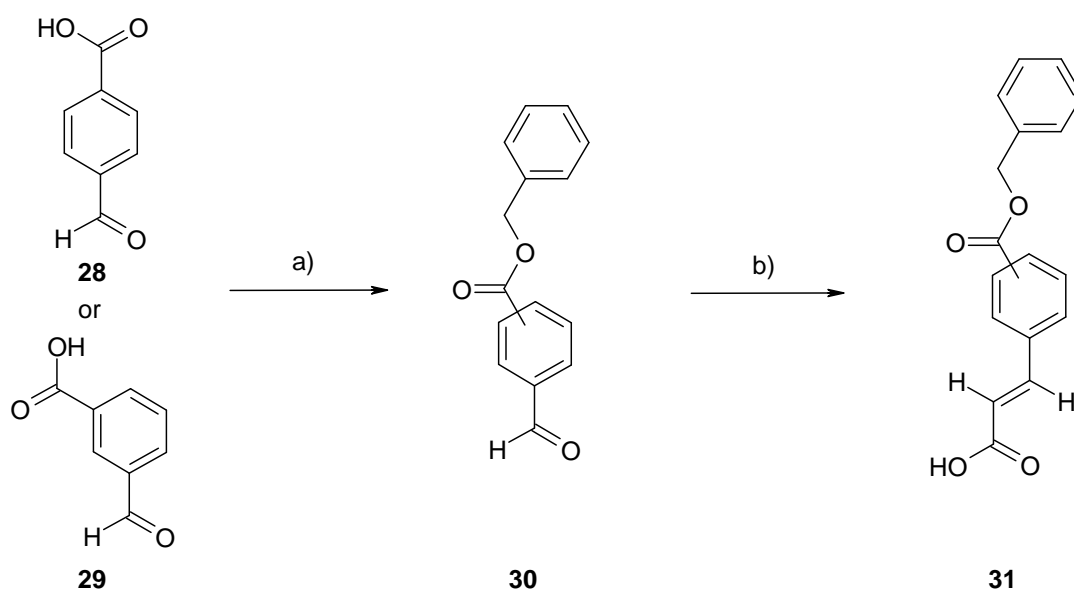


Further investigations showed that only the *Z*-isomer was able to form the tricyclic products **27** while the *E*-isomer was only able to form the bicyclic furopyranone **26**. Structural investigations and further experiments revealed the tricyclic structure with *cis*- and *trans*-configuration which has similarities to podophyllotoxin (see Chapter 1.3.3).<sup>16</sup>

Under the conditions described the major product was the bicyclic furopyranone followed by the tricyclic *cis*-configured byproduct and the tricyclic *trans*-configured byproduct. The crude NMR spectrum showed a ratio of about 5:2:1 (**26**:*cis*-**27**:*trans*-**27**) for these three products. Trace amounts (2-3 mg) of the pure tricyclic products could be isolated and analysed by HPLC. The pure products served as basis for further structural investigations by NMR (2D-NMR: <sup>1</sup>H/<sup>1</sup>H-COSY, NOE). The topic of the formation of these novel tricyclic scaffolds is discussed separately in Chapter 3.3.7.

### 3.3.5.2 Carboxy-substituted Furopyranones

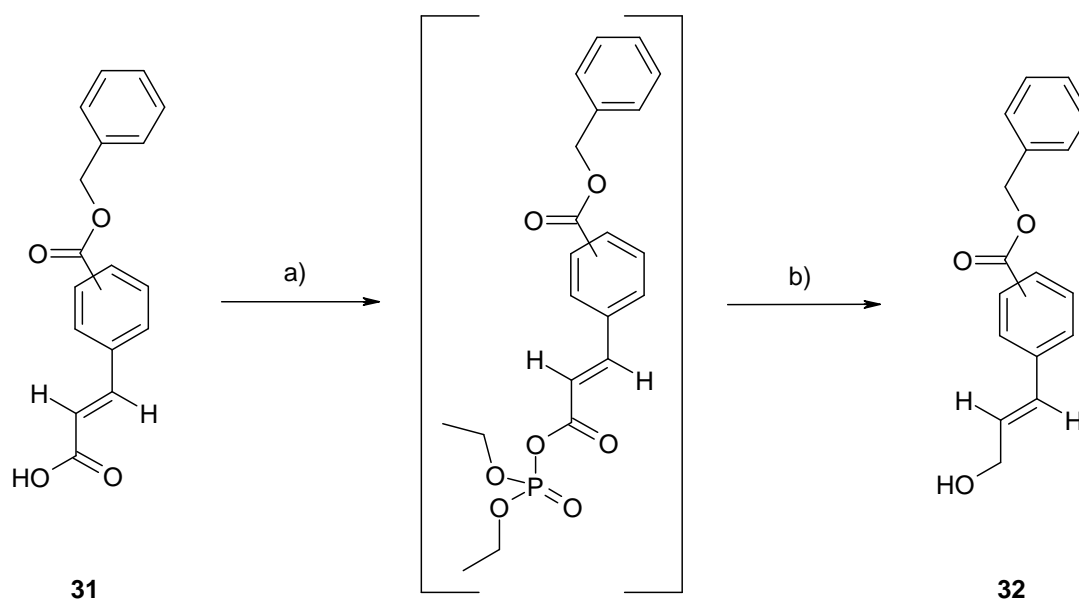
Since carboxyl containing cinnamyl alcohol derivatives were not commercially available, a synthesis for this starting material was developed. An already published procedure by Nagao *et al.* was adapted to our needs.<sup>17</sup> As starting materials 4-carboxybenzaldehyde **28** or 3-carboxybenzaldehyde **29** were used (see Scheme 3.13).



**Scheme 3.13.** Synthesis of carboxylic acid precursors *meta*- and *para*-**31**; a) BnBr, Cs<sub>2</sub>CO<sub>3</sub>, CH<sub>3</sub>CN, rt, 12 h, up to 99%; b) piperidine-pyridine (1:10), malonic acid, 100°C, 3h, >80%.

In a first step the carboxylic group of **28** and **29** was protected by conversion into benzyl esters *meta*- and *para*-**30**. This protecting group is very stable at high temperatures (up to

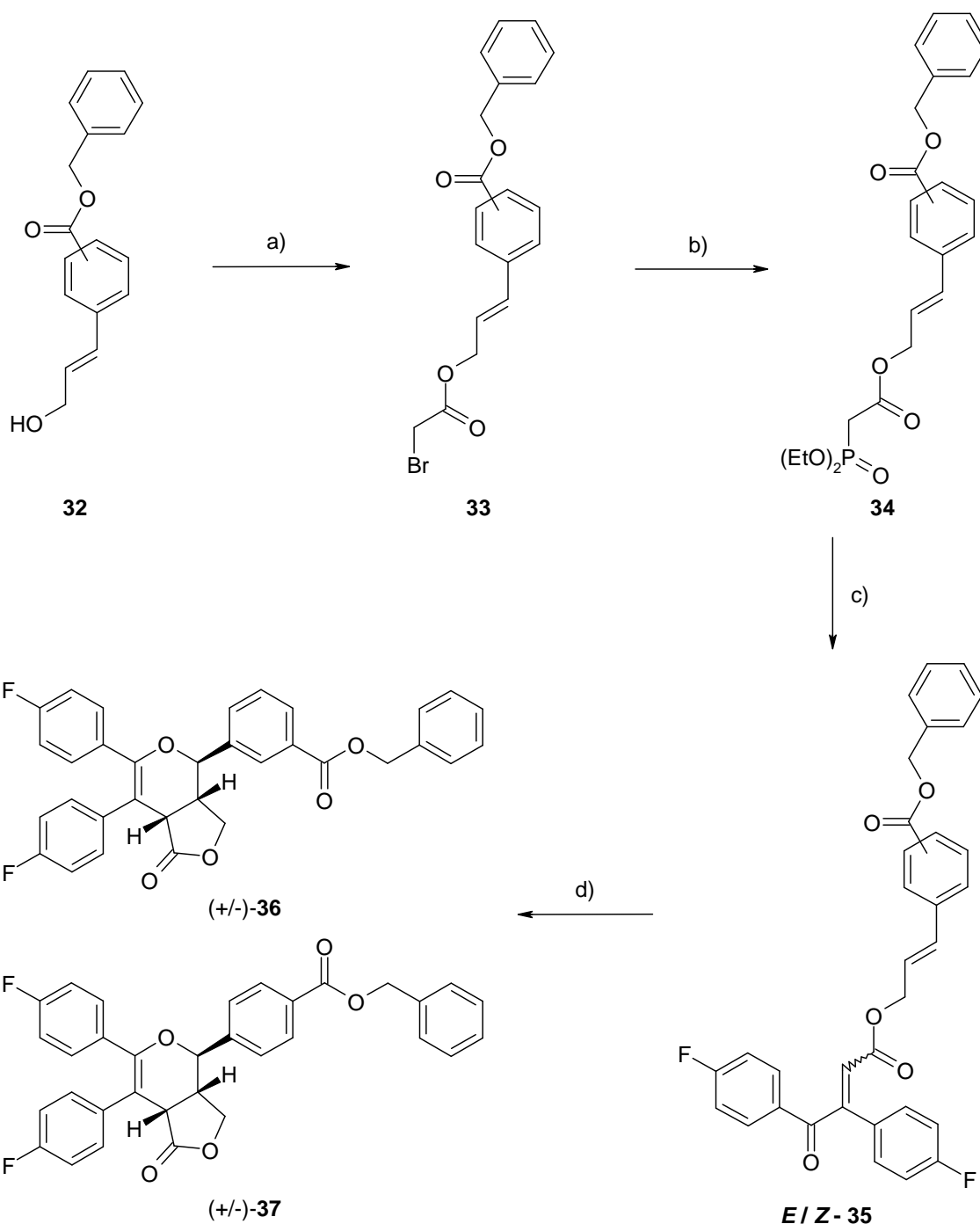
180°C) and easy to eliminate *via* a hydrogenation reaction.<sup>18</sup> The benzyl ester seemed to be the right choice for surviving the relatively harsh reaction conditions of the *hetero* Diels-Alder reaction. The synthesis of esters *meta*- and *para*-**30** was done according to the literature using benzyl bromide and Cs<sub>2</sub>CO<sub>3</sub>.<sup>18</sup> The second step was a Knoevenagel condensation with malonic acid to convert the aldehydes *meta*- and *para*-**30** into the carboxylic acids *meta*- and *para*-**31**. A mixture of piperidine-pyridine (1:10) was reagent as well as solvent. After recrystallisation from MeOH the pure acids **31** were obtained (yield: 81% and 85%). <sup>1</sup>H-NMR measurements clearly established the *trans*-configuration of *meta*- and *para*-**31**. The coupling constant of the two protons was about 16 Hz, a common value for *trans*-configured protons at a double bond.<sup>19</sup>



**Scheme 3.14.** Synthesis of *meta*- and *para*-benzyl ester cinnamyl alcohol derivatives **32**; a) NEt<sub>3</sub>, diethyl chlorophosphate, THF, 3 h, rt; b) NaBH<sub>4</sub>, THF, H<sub>2</sub>O, 0°C -> rt, 2 h, >50%.

The final reduction of the carboxylic acids **31** to the alcohols *meta*- and *para*-**32** was accomplished in two steps. First a mixed anhydride was formed using diethyl chlorophosphate, followed by treatment with NaBH<sub>4</sub> and aqueous work up (see Scheme 3.14).

The so obtained alcohols *meta*-**32** and *para*-**32** (yields: *meta*=56%, *para*=55%) were used for the synthesis of further furopyranones **36** and **37** to extend the SAR study and to implement solid phase chemistry. Therefore the deprotected carboxylic acid group will be useful as linker to attach the scaffold to the solid support (BAL resin, see Chapter 4).



**Scheme 3.15.** Synthesis of furopyranones **36** and **37**; a)  $\text{CH}_2\text{Cl}_2$ , bromoacetyl bromide, pyridine, 1.5 h,  $0^\circ\text{C}$ , *meta*-**33**: 74%, *para*-**33**: 76%; b)  $\text{P}(\text{OEt})_3$ , THF, reflux, 22 h, *meta/para*-**34**: 92%/99%; c) LiHMDS, 4,4'-difluorobenzil, THF,  $0^\circ\text{C}$ , 2 h, *meta*-**35**: 50%, *para*-**35**: 39%; d) autoclave, toluene, 24 h, **36**: 25%, **37**: 72%.

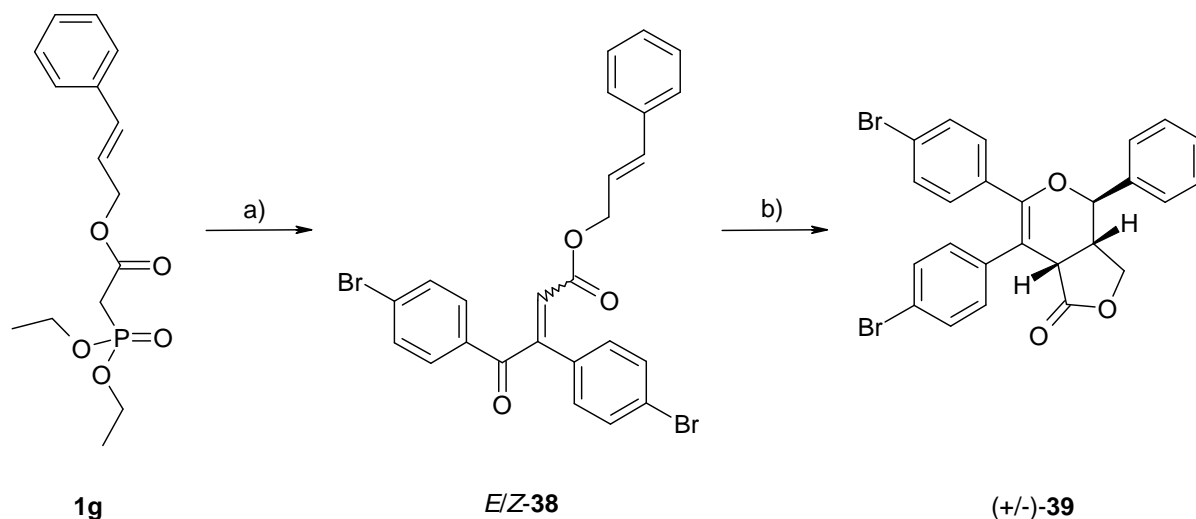
Furopyranones **36** and **37** were synthesised as shown in Scheme 3.15.<sup>20</sup> Esterification with bromoacetyl bromide and the Arbuzov reaction worked well as in the previously reported cases. The Horner-Wadsworth-Emmons reaction was carried out at a temperature of  $0^\circ\text{C}$  and gave the *E*- and *Z*-isomer of **35** in a ratio of about 1:1. The products **36** and **37** of the *hetero* Diels-Alder reaction were obtained after recrystallisation from MeOH.<sup>20</sup>

### 3.3.6 Variation of the Substitution Pattern of the *cis*-Stilbene Motif

Since the *cis*-stilbene motif was identified as the pharmacophore of the biologically active furopyranones (see Chapter 3.4), a detailed investigation of the substitution pattern of this part of the molecule was necessary. For this reason we synthesised further furopyranones starting from commercially available  $\alpha$ -diketones.

#### 3.3.6.1 Synthesis from 4,4'-Dibromobenzil

In a first attempt the phosphonate **1g** and 4,4'-dibromobenzil were used for the Horner-Wadsworth-Emmons reaction (see Scheme 3.16). The reaction was done at  $-78^{\circ}\text{C}$  and resulted an isomeric mixture of **38** with a ratio of 1:2 for the *E*- and *Z*-isomer. With a yield of 47% the outcome of the reaction was comparable to the previously reported ones. After the *hetero* Diels-Alder reaction furopyranone **39** was obtained with a yield of 27%. The lower yield of this reaction may result from the bromine substitution which had less electron withdrawing influence compared to fluorine (see Table 3.1). This should lead to an increase of the HOMO-LUMO energy gap for this *hetero* Diels-Alder reaction with an inverse electron demand.

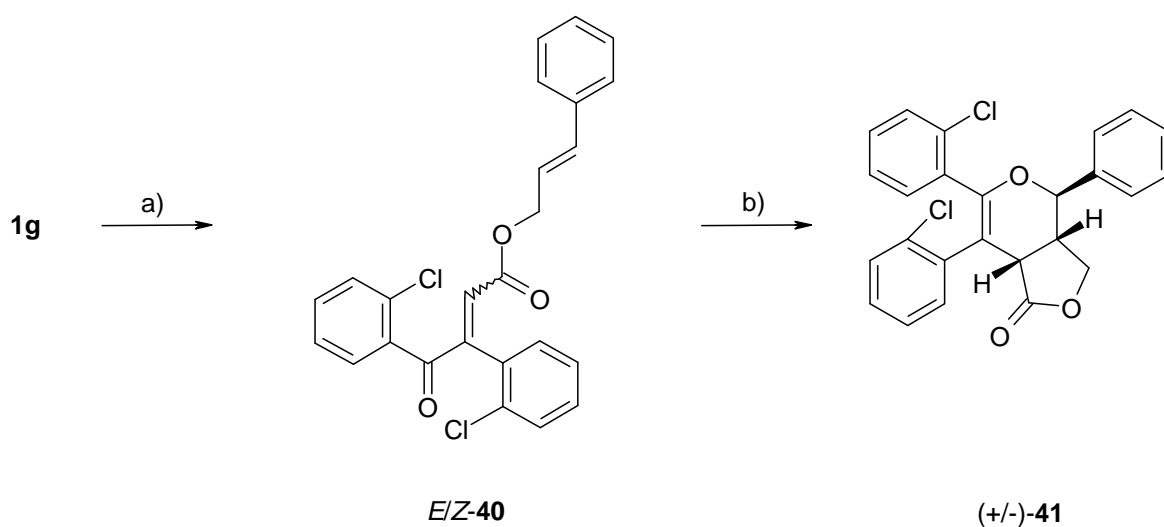


**Scheme 3.16.** Synthesis of furopyranone **38**; a) LiHMDS, 4,4'-dibromobenzil, THF,  $-78^{\circ}\text{C}$ , 4 h, 47%; b) autoclave, toluene,  $200^{\circ}\text{C}$ , 20 h, 27%.

#### 3.3.6.2 Synthesis from 2,2'-Dichlorobenzil

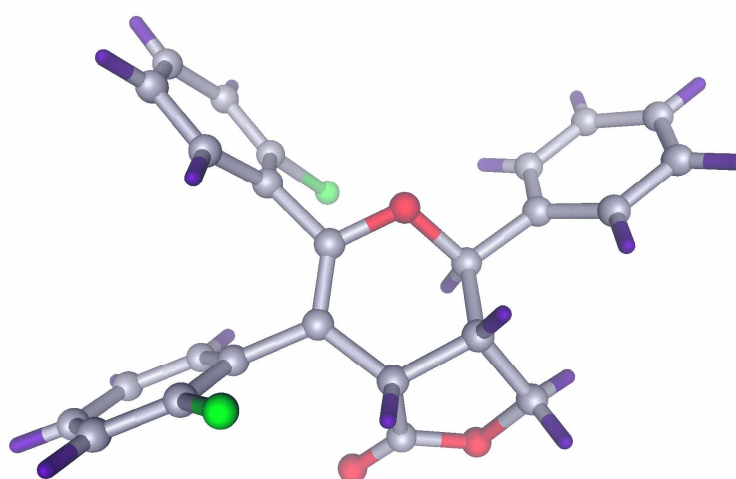
Another synthesis was performed using 2,2'-dichlorobenzil in the Horner-Wadsworth-Emmons reaction. The reaction was carried out at a temperature of  $0^{\circ}\text{C}$  and only the *E*-

isomer of **40** was isolated (yield: 24%). Possibly, the chlorine in *ortho*-position had a sterical influence, which could explain the selective outcome and the low yield of this reaction.



**Scheme 3.17.** Synthesis of furopyranone **38**; a) LiHMDS, 2,2'-dichlorobenzil, THF, 0°C, 4 h, 24 %; b) autoclave, toluene, 200°C, 20 h, 36%.

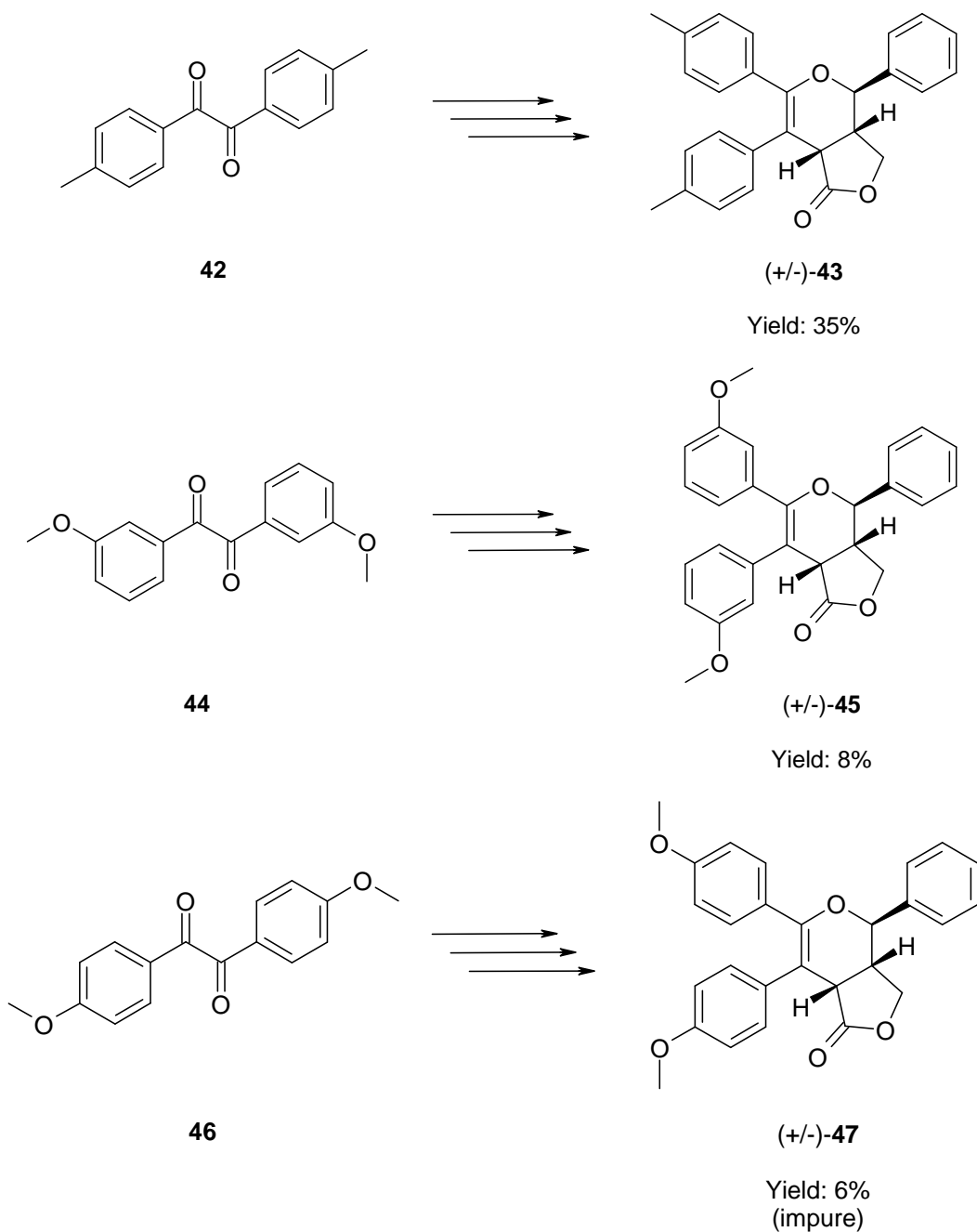
The *hetero* Diels-Alder reaction gave furopyranone **41** with a yield of 36% (see Scheme 3.17). The increased yield compared to **39** could be explained by the more electronegative chlorine compared to bromine which lowers the HOMO-LUMO energy gap. After recrystallisation of **41** from MeOH suitable crystals were obtained and analysed by x-ray (see Figure 3.9).



**Figure 3.9.** Relative configuration of furopyranone **41** as determined by x-ray crystallography.

### 3.3.6.3 Further Furopyranones from different $\alpha$ -Diketones

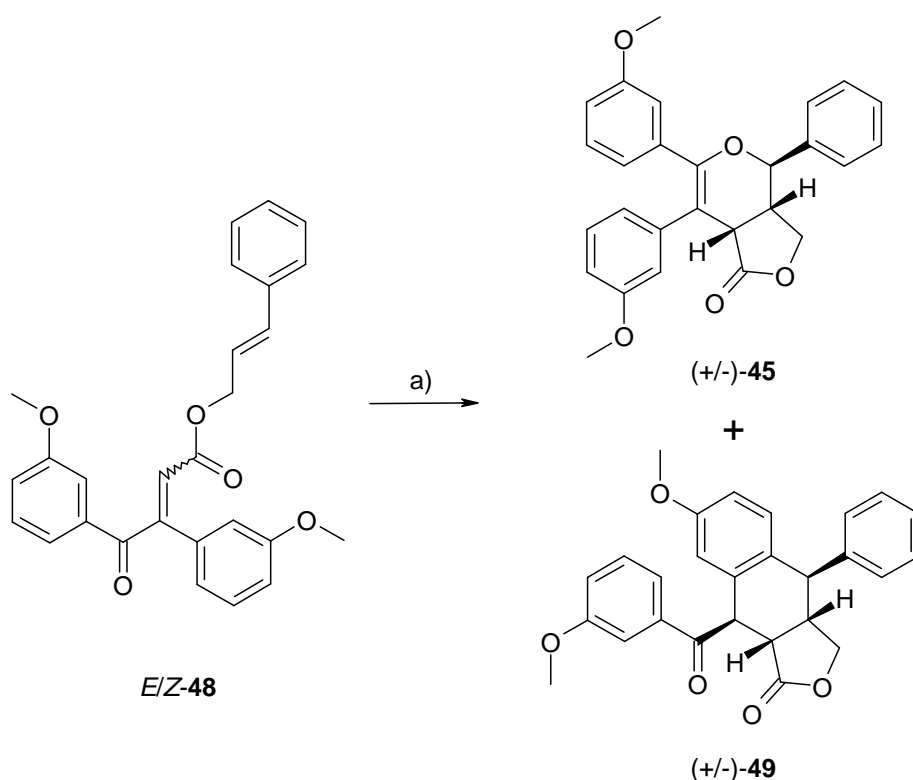
During a bachelor work on this medicinal chemistry project further furopyranones (**43**, **45**, **47**, see Scheme 3.18) were synthesised starting from several  $\alpha$ -diketones (**42**, **44**, **46**). The syntheses were similar to the already presented procedures.<sup>16</sup>



**Scheme 3.18.** Synthesis of furopyranones **43**, **45** and **47** starting from the  $\alpha$ -diketones **42**, **44**, **46**.<sup>16</sup>

### 3.3.7 *Hetero* Diels-Alder versus Diels-Alder Reaction

As presented in Scheme 3.12, not only the *hetero* Diels-Alder reaction, leading to bicyclic furopyranones, can take place during the thermal cyclisation. We observed that in special cases the aromatic phenyl ring in  $\beta$ -position took part in a normal Diels-Alder. This reaction led to tricyclic scaffolds related to podophyllotoxins. In all the cases where this Diels-Alder reaction was observed, the tricyclic side-products were formed in trace amounts and could be isolated in pure form by preparative HPLC purification. Thus, compound **49** was obtained along with **45** as shown in Scheme 3.19.<sup>16</sup>

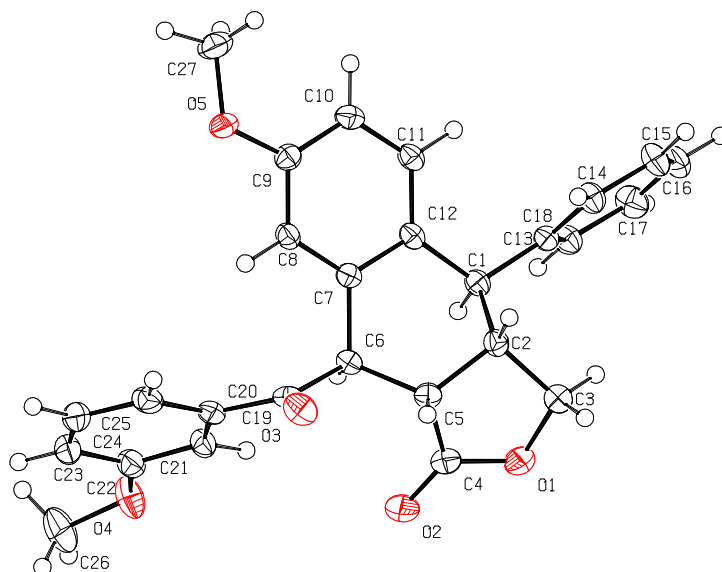


**Scheme 3.19.** Synthesis of furopyranone **45** (yield: 8%) and the tricyclic scaffold **49** (trace amounts) from the *E/Z*-mixture (ratio ~ 1:1) of ester **48**; a) autoclave, toluene, 220°C, 24 h.<sup>16</sup>

After recrystallisation from MeOH a mixture of suitable crystals of **45** and **49** was obtained and x-ray analysis revealed the so far unknown structure of the tricyclic compound **49** (see Figure 3.10).

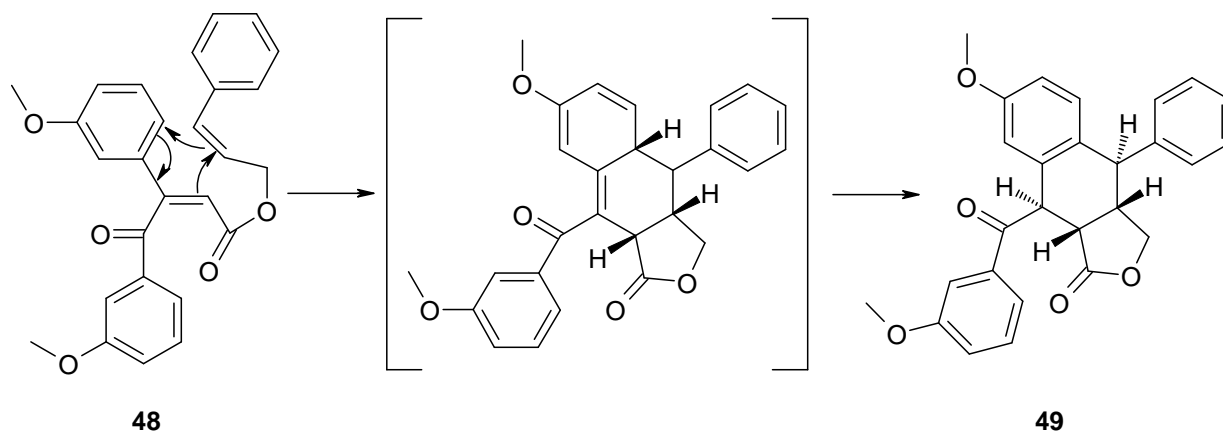
The thermal cyclisation reaction was done in an autoclave at a temperature of 220°C starting from a 1:1 (*E/Z*) isomeric mixture of ester **48**. The NMR spectrum of the crude product showed a ratio of about 3:1 for the products **45** and **49**. A doublet signal at about  $\delta$  5.43 ppm (ratio *cis:trans* = 2:1) indicated the existence of the *trans*-configured product of **49**, but unfortunately this compound could not be isolated. Due to the x-ray structure it was possible

to speculate how this tricyclic compound was formed. Apparently, the phenyl ring in  $\beta$ -position of ester **48** was part of the diene which reacted with the dienophile.



**Figure 3.10.** Structure of compound **49** as determined by x-ray crystallography.<sup>16</sup>

In a first step the Diels-Alder intermediate is formed and through proton rearrangement the aromatic ring is regenerated in a second step (see Scheme 3.20).

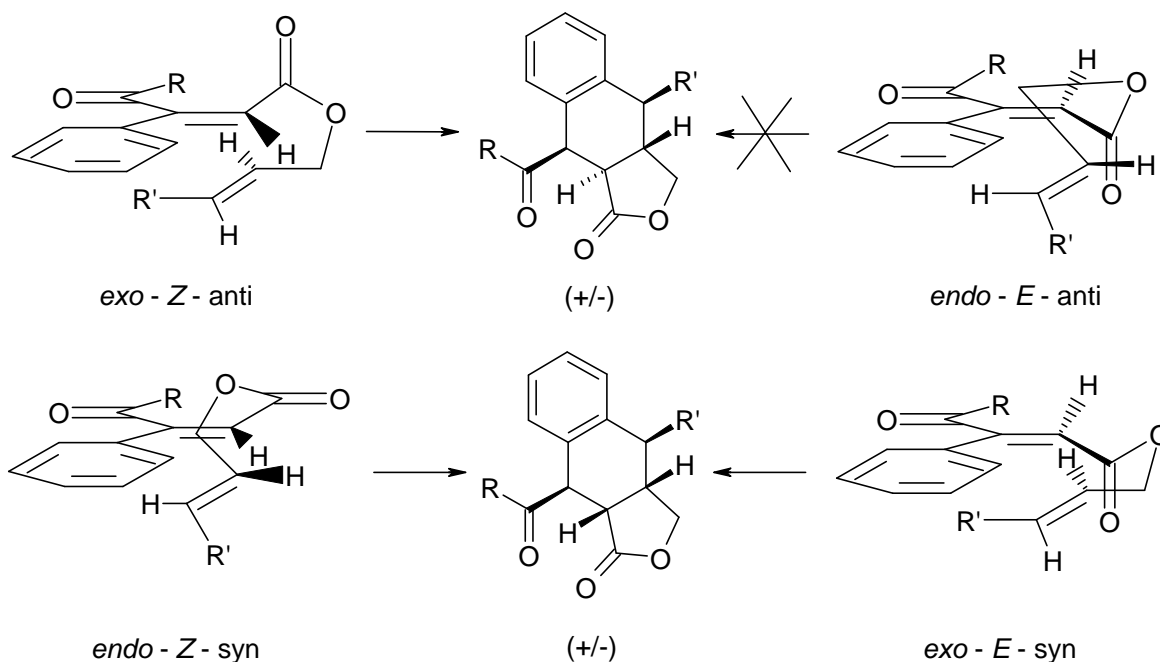


**Scheme 3.20.** Synthesis of compound **49** from ester **48**. After involvement of the aromatic ring in the *Diels-Alder* reaction an intermediate is formed which regenerates the aromatic system in a second step by rearrangement of a proton.

Scaffold **49** is the thermodynamically preferred configuration since the two large substituents are in an equatorial position in this boat-like cyclohexene ring. Analysis of the possible transition states (see Scheme 3.21) for this type of reaction showed that the *Z*-isomer of the starting material has more possibilities to form the tricyclic product than the corresponding *E*-



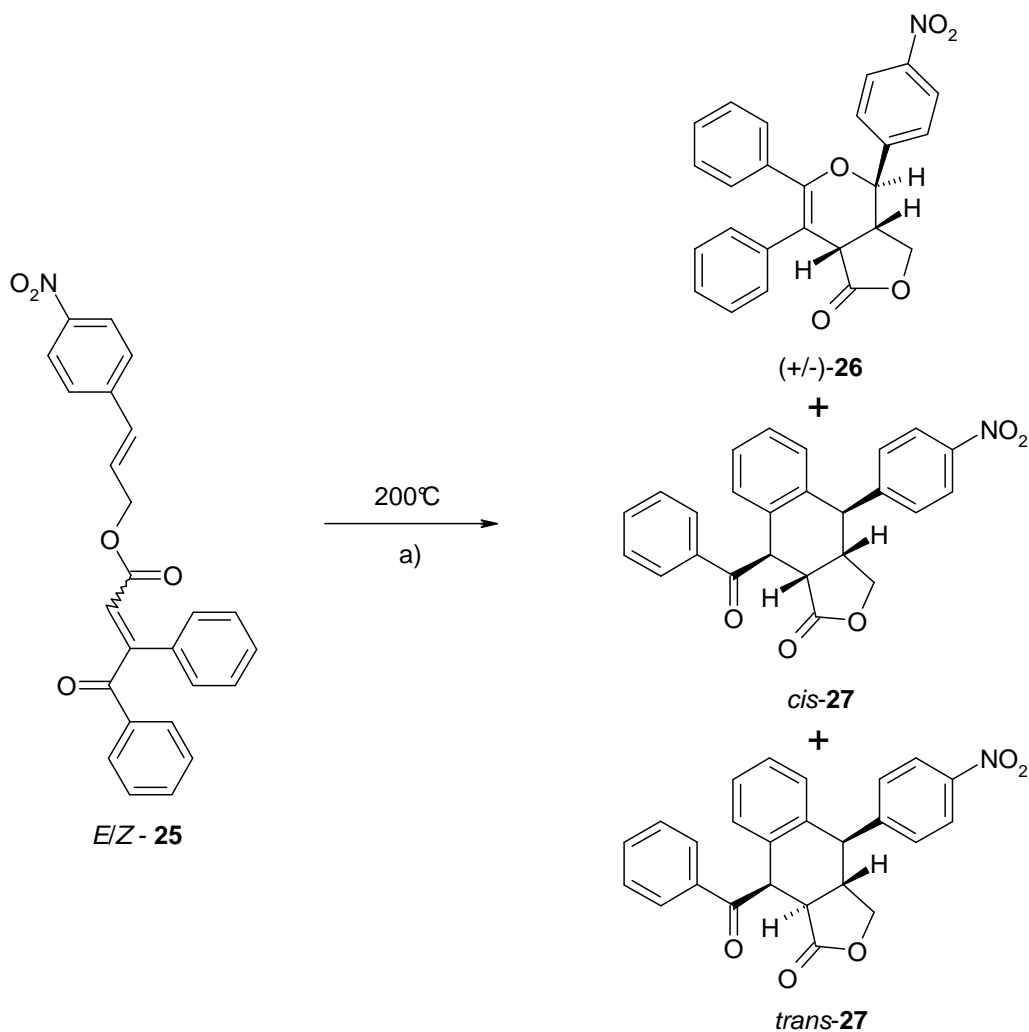
isomer. In fact the the *E*-isomer does not form the *trans*-configured tricyclic scaffold due to geometrical constraints.



**Scheme 3.21.** Stereochemical course of the intramolecular Diels-Alder reaction with a normal electron demand leading to *cis*- and *trans*-fused tricyclic scaffolds.

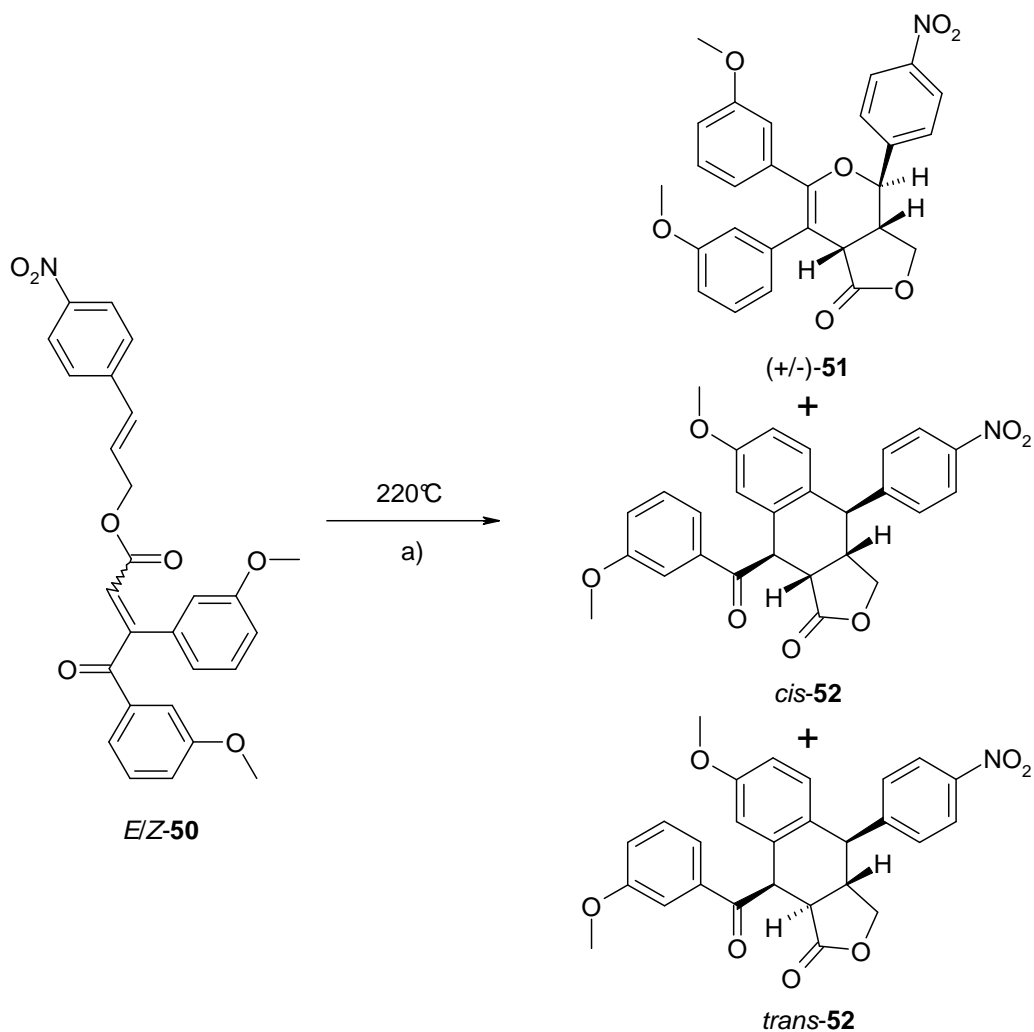
Further investigations on all the synthesised compounds confirmed that the tricyclic scaffold was only formed *via* the *Z*-isomer of the starting material, because when only the *E*-isomer was used for the thermal cyclisation reaction no tricyclic product was observed in the NMR spectra of the crude products. Due to decomposition of the starting material at higher temperatures the reactions could not be investigated at temperatures higher than 220°C.

As already mentioned in Chapter 3.3.5.1, the tricyclic product was also formed in trace amounts from ester *E/Z*-**25** containing a nitro function (see Scheme 3.22).



**Scheme 3.22.** Synthesis of furopyranone **26** and the tricyclic byproducts *cis*- and *trans*-**27**; a) autoclave, toluene, 20 h, yield for **26**: 40%.

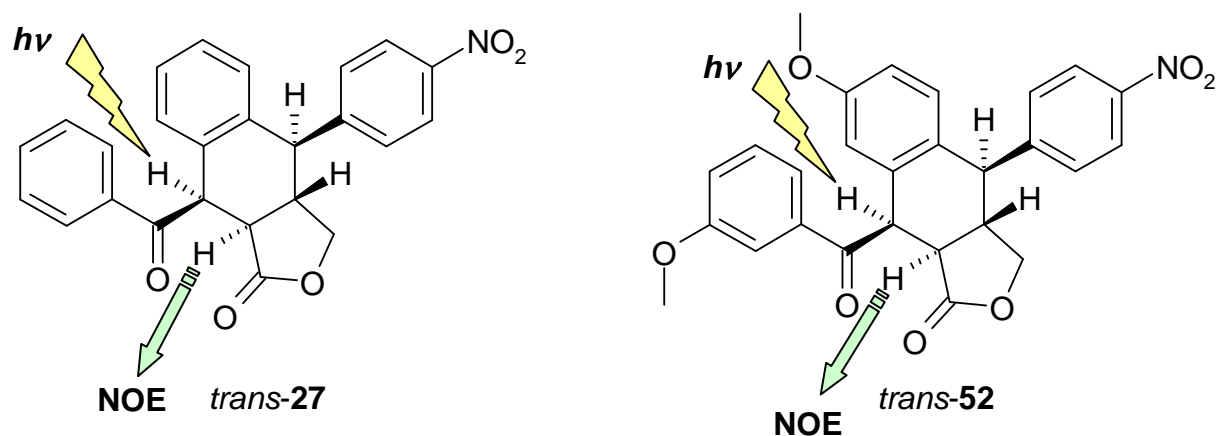
Ester **50** (yield: 69%) was synthesised at a temperature of 0°C which led to a 1:1 mixture of the isomers (*E/Z*). The thermal cyclisation reaction formed the products **51**, *cis*-**52**, *trans*-**52** in a ratio of about 18:7:5 (**51**, *cis*-**52**, *trans*-**52**, see Scheme 3.23) as determined from the crude product material. After purification furopyranone **51** (yield: 26%) and a mixture of *cis*-**52** and *trans*-**52** (yield: 5%) were isolated, but only purification of the mixture by preparative HPLC gave trace amounts of the pure products. The so obtained products were analysed by NMR including 2D-NMR ( $^1\text{H}/^1\text{H}$ -COSY) and NOE experiments to prove their configuration.



**Scheme 3.23.** Synthesis of furopyranone **51** and the tricyclic byproducts *cis*- and *trans*-**52**; a) autoclave, toluene, 24 h, yield for **51**: 26%.

NOE experiments of compounds *trans*-**27** and *trans*-**52** revealed the configuration of these scaffolds. In both cases a NOE was observed at the proton next to the lactone when the proton next to the ketone was irradiated with the corresponding frequency ( $h\nu$ ) as shown in Figure 3.11. When the proton next to the lactone was irradiated, the NOE was observed exactly the other way around. This proved the *cis*-configuration of these neighbouring protons.

These experiments demonstrated that the  $\alpha,\beta$ -unsaturated  $\gamma$ -ketoesters (e.g. **50**, see Scheme 3.23) were able to react *via* different reactions. The most favoured reaction was the *hetero* Diels-Alder reaction resulting the bicyclic furopyranones. This reaction must be energetically lower than the Diels-Alder reaction with a normal electron demand, since the tricyclic products were formed only in smaller quantities. The fact that the normal Diels-Alder reaction needs more energy is well explained with the influence of the aromatic ring involved.

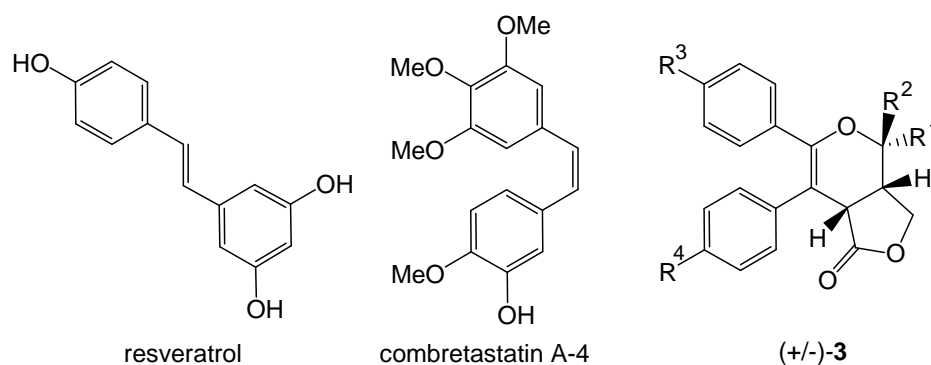


**Figure 3.11.** NOE experiments with compounds *trans-27* and *trans-52*. Irradiation of the proton next to the ketone with the corresponding frequency showed an NOE effect at the neighbouring proton next to the lactone.

There are few examples in the literature describing an intramolecular Diels-Alder reaction involving methoxy-substituted phenyl rings.<sup>21, 22, 23</sup> This reaction was investigated in the context of the synthesis of lignan lactones like podophyllotoxin.<sup>22, 23</sup> However, the strategy was seemingly not pursued further, possible due to the harsh conditions required (> 140°C).

### 3.4 Antiproliferative Properties of Natural Product-Like Furopyranones

Compounds **3** (see Figure 3.12) contain several motifs (*cis*-stilbene,  $\gamma$ -lactone, iridoid scaffold) which are common to many natural products with anticancer properties (see Chapter 1.3). In light of the clinical relevance of these classes of compounds, the effects of derivatives of type **3** on tumour cell growth were examined. The compounds were tested for their antiproliferative and apoptotic properties by Dr. Stephan Ruetz at the 'Novartis Institutes for BioMedical Research' in Basel (Switzerland).



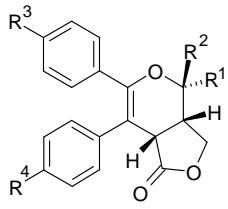
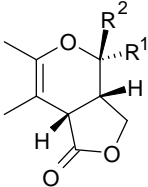
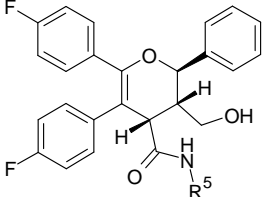
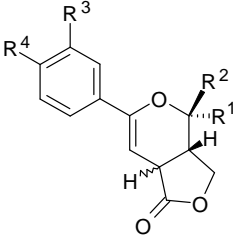
**Figure 3.12.** Structures of the naturally occurring stilbenoids resveratrol and combretastatin A-4 as well as the synthetic furopyranones of type **3**.

#### 3.4.1 *Cis*-Stilbene Derived Furopyranones and Their Antiproliferative Properties in A549 and KB31 Cells

In preliminary studies, compounds **3c**, **3d**, **3f** and **3g** showed antiproliferative activity in the human cancer cell lines KB31 (human cervix carcinoma), whereas derivatives **3a**, **3b** and **3e** lacking the *cis*-stilbene motif were inactive. Two cell lines A549 (human non-small cell lung cancer) and KB31 were chosen for further investigations.

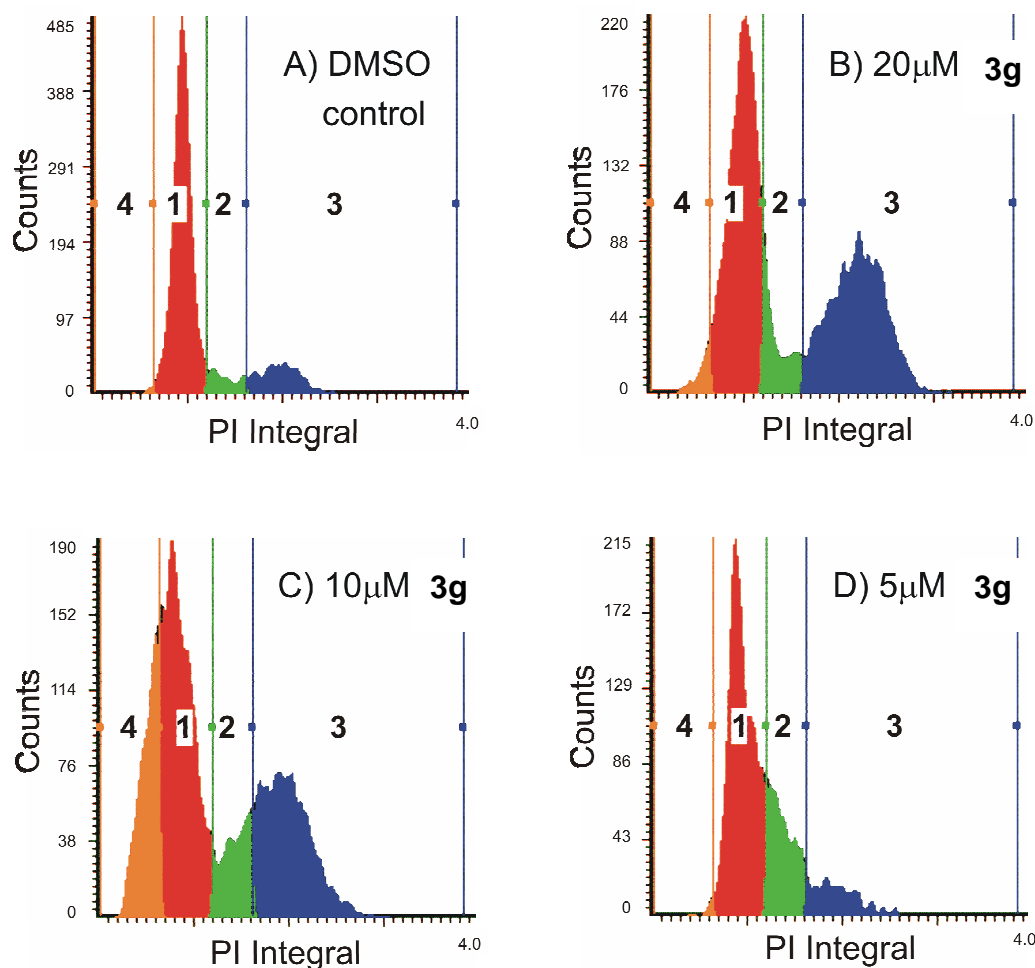
The biological activity of the compounds was determined using the YO-PRO apoptosis/viability assay.<sup>24, 25</sup> The IC<sub>50</sub> values indicating the antiproliferative activity of the synthesised compounds are shown in Table 3.3. The structure-activity profile was very similar for both cell lines. The bicyclic compounds **3c**, **3d**, **3f** and **3g** containing the *cis*-stilbene motif were active in the assay with IC<sub>50</sub> values in the range of 7 – 20  $\mu$ M. Compounds **3f** and **3g** showed the highest antiproliferative activity. Absence of one or both of the phenyl rings at the enol-ether double bond led to loss of antiproliferative activity (compounds **3b**, **3e** and **7a-f**). This clearly established the importance of the *cis*-stilbene motif. Furthermore, aminolysis of the lactone ring of the most active compound **3g** also reduced the activity partly (in the case of **8b**, **8c**, **8d** and **8e**) or completely (**8a**). This showed that the bicyclic nature of the structure also contributed to the activity.<sup>8</sup>

**Table 3.3.** Antiproliferative activity of the synthesized compounds in A549 and KB31 cell lines.

	R <sup>1</sup>	R <sup>2</sup>	R <sup>3</sup>	R <sup>4</sup>	R <sup>5</sup>	IC <sub>50</sub> (μM) <sup>[a]</sup>	
						A549	KB31
	<b>3c</b>	CH <sub>3</sub>	CH <sub>3</sub>	H	H	18.72 ± 0.89	17.69 ± 3.34
	<b>3d</b>	CH <sub>3</sub>	CH <sub>3</sub>	F	F	14.77 ± 3.26	13.18 ± 3.28
	<b>3f</b>	H	C <sub>6</sub> H <sub>5</sub>	H	H	10.67 ± 1.36	8.54 ± 1.78
	<b>3g</b>	H	C <sub>6</sub> H <sub>5</sub>	F	F	8.78 ± 2.54	7.27 ± 1.58
	<b>3b</b>	CH <sub>3</sub>	CH <sub>3</sub>			> 20	> 20
	<b>3e</b>	H	C <sub>6</sub> H <sub>5</sub>			> 20	> 20
	<b>8a</b>				benzyl	n.t. <sup>[b]</sup>	> 20
	<b>8b</b>				butyl	n.t. <sup>[b]</sup>	15.85 ± 0.30
	<b>8c</b>				isobutyl	11.76 ± 1.68	10.41 ± 0.26
	<b>8d</b>				propyl	14.73 ± 0.64	12.32 ± 0.93
	<b>8e</b>				methyl	n.t. <sup>[b]</sup>	19.87 ± 1.09
	<b>7a<sup>[d]</sup></b>	H	C <sub>6</sub> H <sub>5</sub>	H	NO <sub>2</sub>	> 20	> 20
	<b>7b<sup>[d]</sup></b>	H	C <sub>6</sub> H <sub>5</sub>	NO <sub>2</sub>	H	> 20	> 20
	<b>7c<sup>[c]</sup></b>	H	C <sub>6</sub> H <sub>5</sub>	H	H	> 20	> 20
	<b>7d<sup>[d]</sup></b>	CH <sub>3</sub>	CH <sub>3</sub>	H	NO <sub>2</sub>	> 20	> 20
	<b>7e<sup>[d]</sup></b>	CH <sub>3</sub>	CH <sub>3</sub>	NO <sub>2</sub>	H	> 20	> 20
	<b>7f<sup>[c]</sup></b>	CH <sub>3</sub>	CH <sub>3</sub>	H	H	> 20	> 20

[a] IC<sub>50</sub> values were determined as described previously.<sup>25</sup> [b] Not tested. [c] *Cis*- and *trans*-isomers were tested separately and were both found to be inactive. [d] Only the *cis*-isomer was tested.

Recent reports describe that stilbenoids show potent inhibition of cell growth in different cancer cell lines. The nature of the substituents as well as conformational aspects were shown to significantly influence the regulatory effects the compounds exert on the cell cycle. Thus, replacement of the hydroxy-groups of resveratrol by methoxy-groups greatly enhances the growth inhibitory effect on A549 cells. In addition, combretastatin and its analogues, which contain a *cis*-orientation, show a pronounced increase in activity, with an IC<sub>50</sub> value up to 100 times lower than the one of the *trans*-configured resveratrol (see Chapter 1.3.2.1).



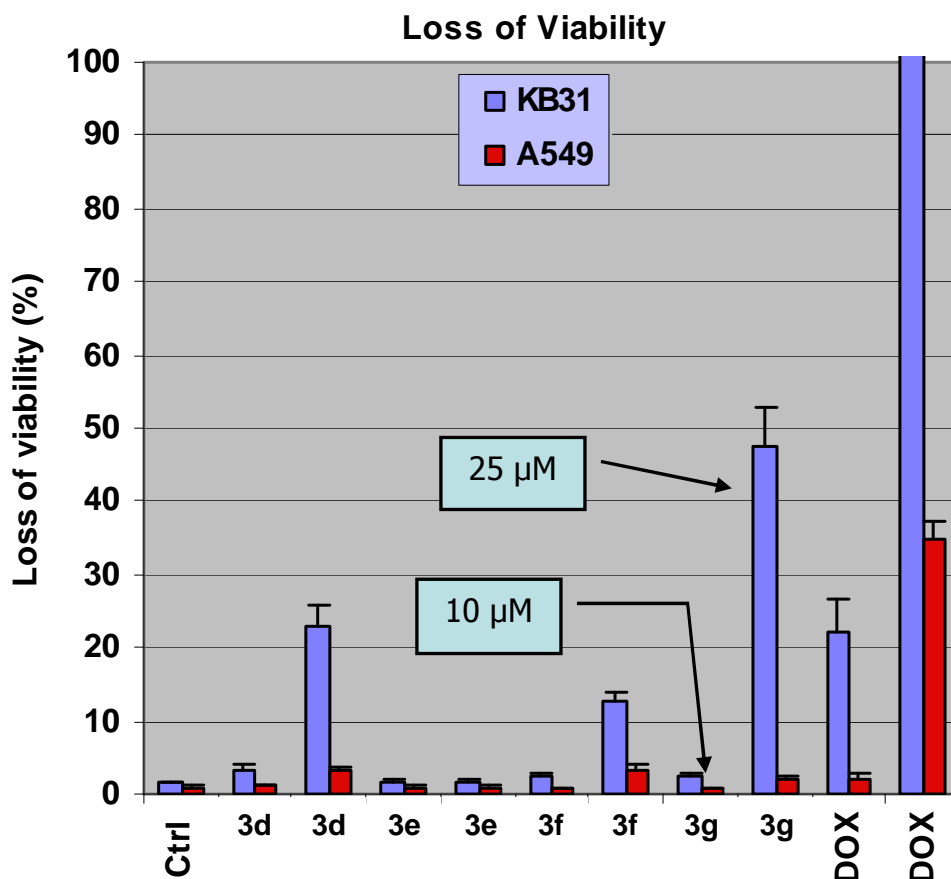
**Figure 3.13.** Cell cycle analysis (*Laser Scanning Cytometry*) after treatment of KB31 cells with compound **3g** for 24h; concentrations as indicated. A) to D) correspond with Table 3.4.

**Table 3.4.** Cell cycle distribution (KB31 cells) determined by *Laser Scanning Cytometry* after treatment with compound **3g** for 24h at different concentrations (regions 1-4 correlate with Figure 3.13).

Treatment	subG1 (Region 4)	G1 (Region 1)	S (Region 2)	G2/M (Region 3)
A) DMSO control	1.60%	71.50%	7.30%	20.00%
B) 20 $\mu$ M <b>3g</b>	3.30%	48.60%	9.10%	40.60%
C) 10 $\mu$ M <b>3g</b>	21.20%	40.30%	12.30%	29.30%
D) 5 $\mu$ M <b>3g</b>	1.60%	61.20%	22.60%	16.20%

To gain further information on the effect of the described compounds on the cell cycle progression, cell cycle analyses with the two most active compounds **3f** and **3g** (Figure 3.13 and Experimental Part) were performed. As shown in Figure 3.13 for **3g**, 24 h treatment of KB31 cells leads to a significant and dose dependent cell cycle arrest. At the highest

concentration tested (20  $\mu\text{M}$ ), the population of cells in the G2-phase increases from 20% to 40% (Table 3.4).



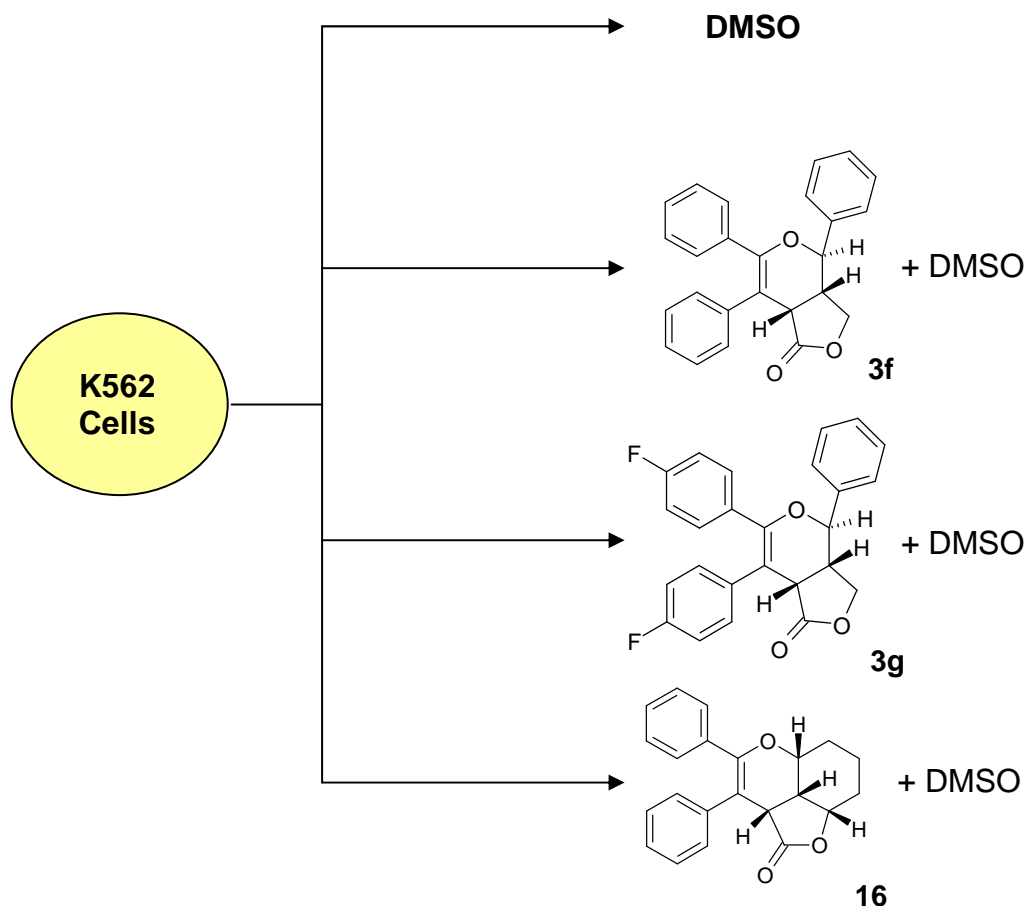
**Figure 3.14.** Viability tests of the synthesised compounds in A549 and KB31 cells. Each compound was tested at two different concentrations (10  $\mu\text{M}$  and 25  $\mu\text{M}$ ); Data represent the mean of triplicate determinations of two independent experiments. In the control sample (Ctrl) 0.1 % DMSO was present during the assay. In addition, a sample was treated with 5  $\mu\text{M}$  doxorubicin (DOX) to demonstrate induction of apoptosis and loss of viability.

Similar results were also obtained with A549 cells (see Experimental Part), suggesting a similar effect on cell cycle progression in both cell lines. These findings are in good agreement with published reports. It was shown that while resveratrol drives A549 cells to be blocked in the S phase, *cis*-configured analogs seem to have a different mode of action, leading to a G2/M arrest. Interestingly, the cell viability tests showed that both compounds, **3g** and **3f**, induced apoptosis in KB31 cells while no programmed cell death was observed in A549 cells (see Figure 3.14). It is at present unclear whether the underlying mechanism of action of these compounds is the same as the one reported for combretastatin analogues.



### 3.4.2 *Cis*-Stilbene Derived Furopyranones and Their Antiproliferative Properties in K562 Cells

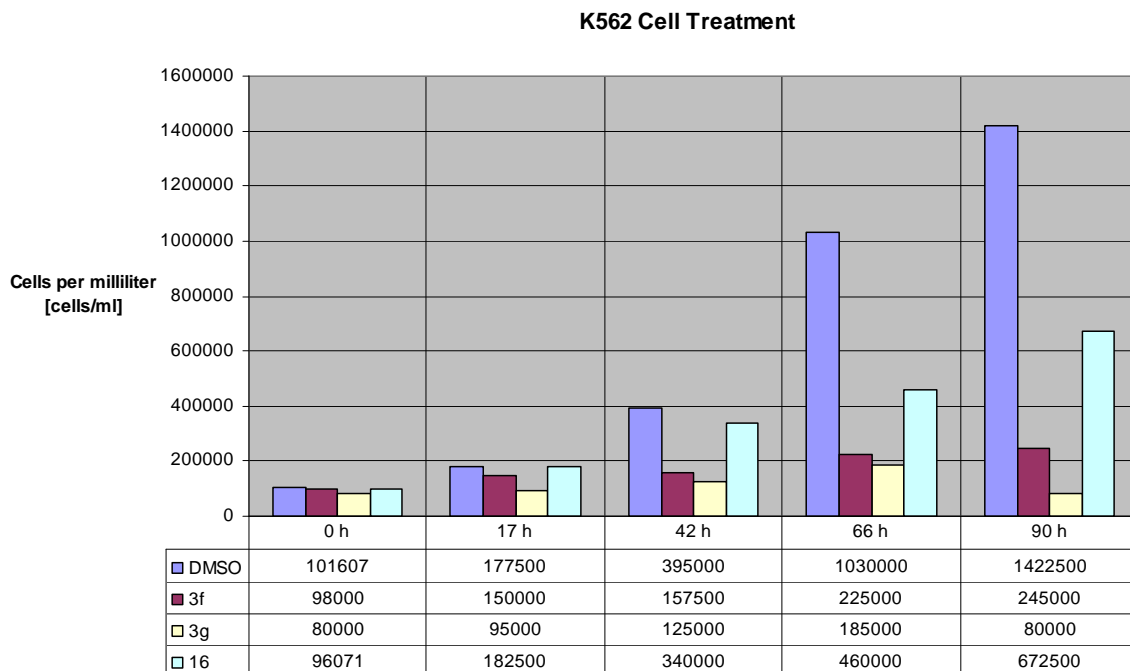
The promising results from the screening at Novartis encouraged us to perform additional cell experiments with K562 (Human Caucasian chronic myelogenous leukaemia) cells. The cells were treated with 50  $\mu$ M DMSO solutions of compounds **3f**, **3g** and **16** (see Scheme 3.24).



**Scheme 3.24.** K562 cell treatment. 50  $\mu$ M DMSO solutions were made from compounds **3f**, **3g** and **16**. As a reference one part of the K562 cells was treated only with DMSO.

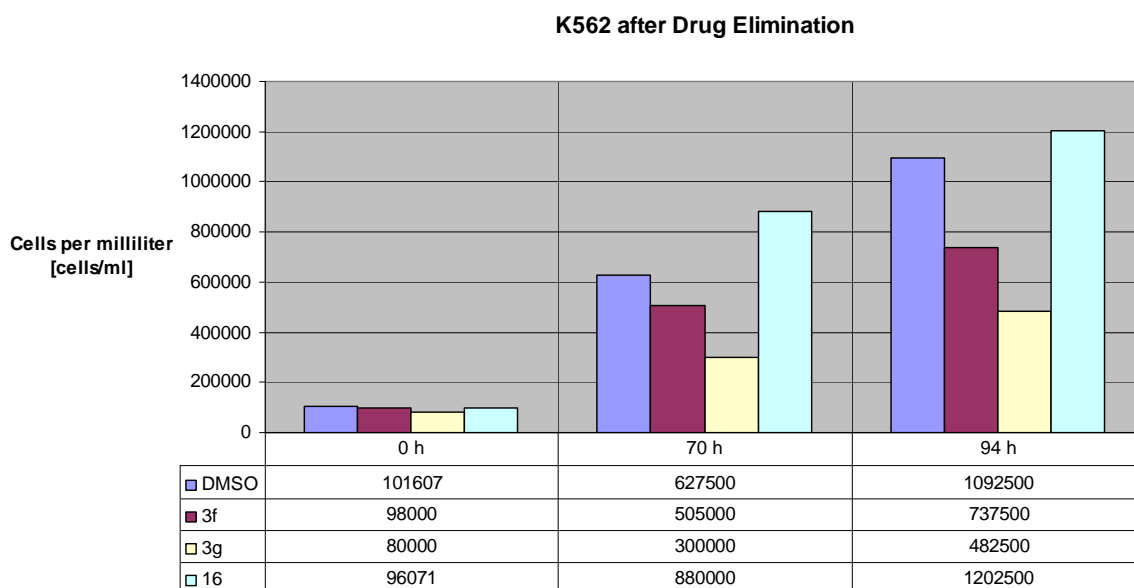
The cell proliferation was monitored with a hemacytometer up to 93 h by counting the cells per millilitre [cells/ml] under a microscope (see experimental part).

The compounds showed antiproliferative activity in the K562 cell line (see Figure 3.15) and furopyranone **3g** was the most potent compound followed by **3f**. Compound **16** showed only moderate antiproliferative activity compared to the others. In these experiments only cell proliferation was monitored and no tests for apoptosis were made. The results obtained can only give a rough picture of the antiproliferative activity in K562 cells compared to the high quality analyses at Novartis.



**Figure 3.15.** Counted cell concentration [cells/ml] of K562 cells with a hemacytometer after 0 h, 17 h, 42 h, 66 h and 90 h. The number of counted cells for compounds **3f**, **3g**, **16** and the DMSO reference is given in the table below.

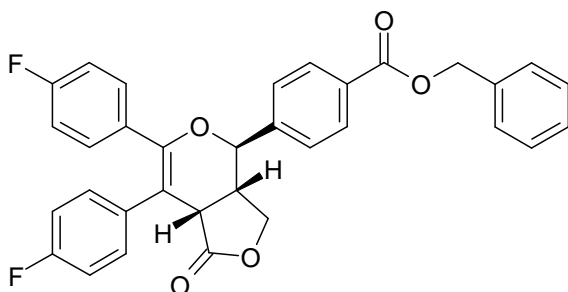
The activity of the compounds was concentration dependent and reversible. After removal of the drugs from the cells by washing and resuming in new culture medium the cells recovered and started to grow again (see Figure 3.16). In the case of compound **3f** and **3g** the cells needed a longer time period to recover because of the relatively severe antiproliferative effect. Similar effects were also observed at Novartis.



**Figure 3.16.** K562 cells recovered after drug removal and started to grow again. The number of counted cells for compounds **3f**, **3g**, **16** and the DMSO reference is given in the table below.

### 3.4.3 Further *Cis*-Stilbene Derived Furopyranones and Their Antiproliferative Properties in A549 and KB31 Cells

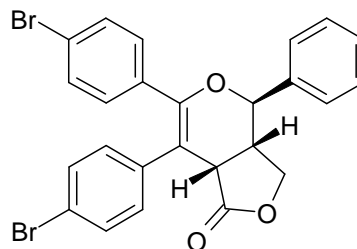
Compounds for which first results are available are presented in this chapter. For  $IC_{50}$  values higher than  $20 \mu M$  no detailed value is given; they are presented as ' $> 20 \mu M$ '.



(+/-)-37

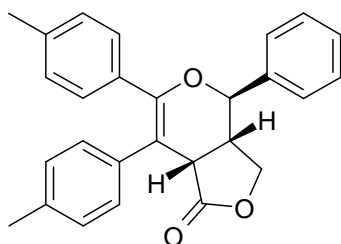
$IC_{50}$  (A549):  $8.15 \pm 1.71 \mu M$

$IC_{50}$  (KB31):  $3.35 \pm 0.54 \mu M$



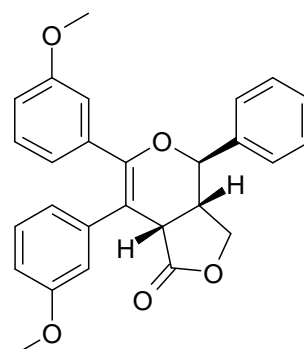
(+/-)-39

$IC_{50}$  (KB31):  $> 20 \mu M$



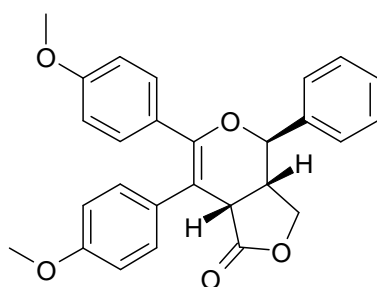
(+/-)-43

$IC_{50}$  (A549 & KB31):  $> 20 \mu M$



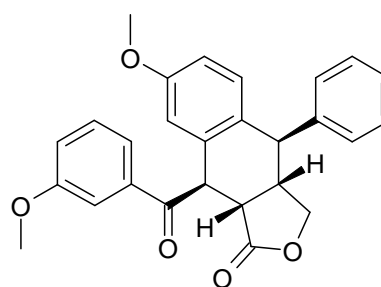
(+/-)-45

$IC_{50}$  (A549 & KB31):  $> 20 \mu M$



(+/-)-47

$IC_{50}$  (A549 & KB31):  $> 20 \mu M$



(+/-)-49

$IC_{50}$  (A549 & KB31):  $> 20 \mu M$

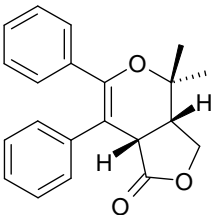
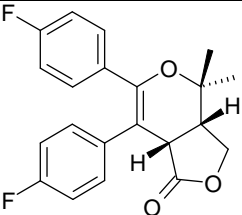
**Figure 3.17.** Further *cis*-stilbene derived furopyranones and their antiproliferative activity.

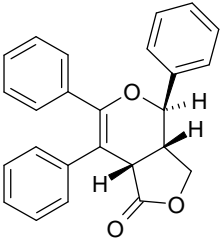
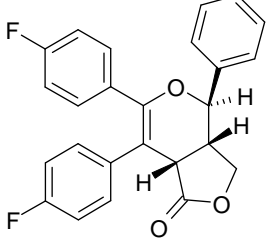
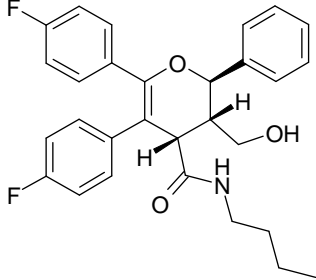
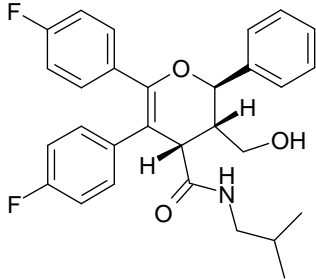
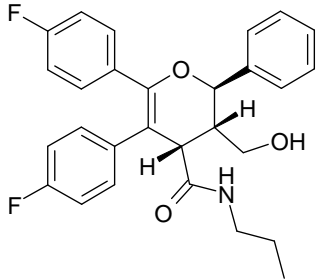
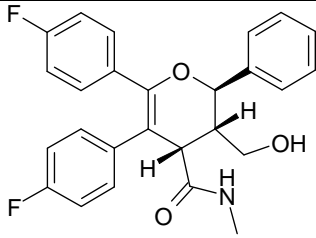
As presented in Figure 3.17 one furopyranone showed enhanced antiproliferative activity compared to the most active compound **3f**. Furopyranone **37** bears an additional benzyl ester originating from the substituted cinnamyl moiety (see Chapter 3.3.5.2). This additional group was responsible for the enhanced antiproliferative activity in the KB31 cell line while it had almost no effect on A549 cells. The other synthesised compounds (**39**, **43**, **45**, **47** and **49**), containing various substituents, showed no enhanced antiproliferative activity. These results indicated that the substitution pattern at the *cis*-stilbene moiety is critical for the anticancer properties. An identical substitution pattern to combretastatin A-4 or potent related derivatives would therefore lead to much higher activity if the present compounds act in the same way as combretastatin A-4.

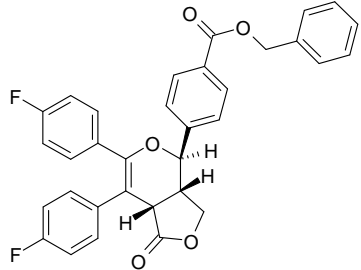
Analysis of the furopyranones in relation to Lipinski's 'Rule of Five' showed that the compounds largely obey the rule.<sup>26</sup> Only compound **37** has a molecular weight higher than 500. Possibly, this compound acts as a prodrug which is converted to the active drug in the cell, most likely by an enzymatic reaction.<sup>10</sup>

The calculated Log P values with the online available 'Actelion Property Explorer' (see Table 3.5) do not exceed 5. As a conclusion it can be stated that all the synthesised and biologically active compounds are quite lipophilic with a mean of Log P of about 4. The relatively high Log P values seem to allow the compounds to cross the cell membrane well. Further investigations would be needed to determine if these compounds display the same activity *in vivo*.

**Table 3.5.** Structures, molecular weight (MW), calculated Log P values, amount of H-acceptors/-donors and IC<sub>50</sub> values (A549 and KB31 cell lines) of furopyranones with antiproliferative activity.

Compound	MW [g/mol]	cLogP <sup>a</sup>	H - Acceptors	H - Donors	Cell Lines		
					IC <sub>50</sub> [μM] A549	IC <sub>50</sub> [μM] KB31	
	<b>3c</b>	320.39	3.07	3	0	18.72	17.69
						±	±
	<b>3d</b>	356.37	3.18	3	0	14.77	13.18
						±	±
						0.89	3.34
						3.26	3.28

	<b>3f</b>	368.44	3.76	3	0	10.67 ± 1.36	8.54 ± 1.78
	<b>3g</b>	404.42	3.87	3	0	8.78 ± 2.54	7.27 ± 1.58
	<b>8b</b>	477.56	4.66	4	2	n.t. <sup>b</sup>	15.85 ± 0.30
	<b>8c</b>	477.54	4.54	4	2	11.76 ± 1.68	10.41 ± 0.26
	<b>8d</b>	463.52	4.20	4	2	14.73 ± 0.64	12.32 ± 0.93
	<b>8e</b>	435.47	3.30	4	2	n.t. <sup>b</sup>	19.87 ± 1.09

	<b>37</b>	538.55	5.22	5	0	8.15	3.35
						±	±
						1.71	0.54

<sup>a</sup> calculated log P values with the 'Actelion Property Explorer', © 2001 by Thomas Sander, available online at <http://www.organic-chemistry.org/prog/peo/>

<sup>b</sup> not tested

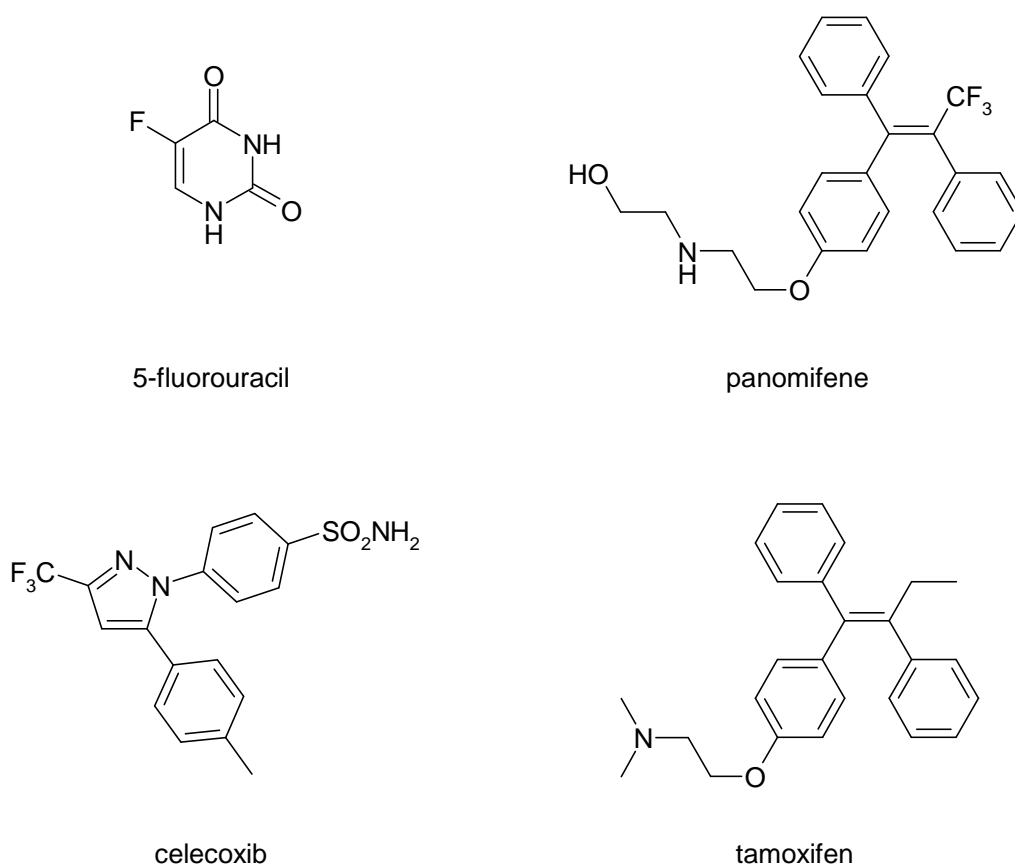
Also in the case of H-acceptors/-donors the compounds do not violate the 'Rule of Five'. The number of H-acceptors varies from three to five while the number of H-donors varies from zero to two.

As a conclusion of this part it can be stated that the furopyranones with antiproliferative activity might be suitable for oral administration according to the 'Rule of Five'.

In the SAR study the *cis*-stilbene motif was identified as a crucial part of the pharmacophore. Many alterations of the substitution pattern of the *cis*-stilbene moiety, however, did not increase the biological activity. In contrast, the compounds with other substituents than fluorine showed no activity. The fact that the fluorinated compounds had better activities than their analogues without fluorine is not surprising since the introduction of fluorine in commercial pharmaceutical compounds is a common strategy to increase activity and it is estimated that globally about 20-25% of drugs in the pharmaceutical pipeline contain at least one fluorine atom.<sup>27</sup> This is a high frequency considering that organo-fluorine compounds are virtually absent as natural products, the traditional source of bioactives.

Fluorine is a small atom with a very high electronegativity. With a van der Waals radius of 1.47 Å, covalently bound fluorine occupies a smaller volume than a methyl, amino, or hydroxyl group, but is larger than a hydrogen atom (van der Waals radius of 1.2 Å). Quite often, fluorine is introduced to improve the metabolic stability by blocking metabolically labile sites. However, fluorine can also be used to modulate the physicochemical properties, such as lipophilicity or basicity. It may exert a substantial effect on the conformation of a molecule. Additionally, fluorine is used to enhance the binding affinity to the target protein. Recent 3D-structure determinations of protein complexes with bound fluorinated ligands have led to an improved understanding of the nonbonding protein-ligand interactions that involve fluorine.<sup>28, 29</sup> In the case of the present furopyranones the fluorine seems to increase lipophilicity what should result in an enhanced ability to cross the cell membrane. Once in the cell the fluorine in *para*-position of the *cis*-stilbene moiety should have a better metabolic stability and, possibly, better interactions with the target.

There are many useful fluorinated anticancer agents like 5-fluorouracil, a thymidylase synthase inhibitor, which is an important enzyme for the synthesis of a DNA building block involved in DNA-synthesis and repair (see Figure 3.18). Another example is panomifene, a trifluoromethyl tetra-substituted alkene. This compound is a follow-up molecule to tamoxifen and is reported to exhibit anti-estrogenic activity superior to that of tamoxifen in the treatment of breast cancer. Anti-estrogens are well established in the treatment of hormone-dependent breast cancer. Celecoxib (Celebrex<sup>®</sup>, Pfizer) belongs to the group of fluorinated non-steroidal anti-inflammatory drugs and is a selective COX-2 (cyclo-oxygenase) inhibitor. The therapeutic applications of selective COX-2 inhibitors in the treatment of cancers and Alzheimer disease are under investigation.<sup>27</sup>

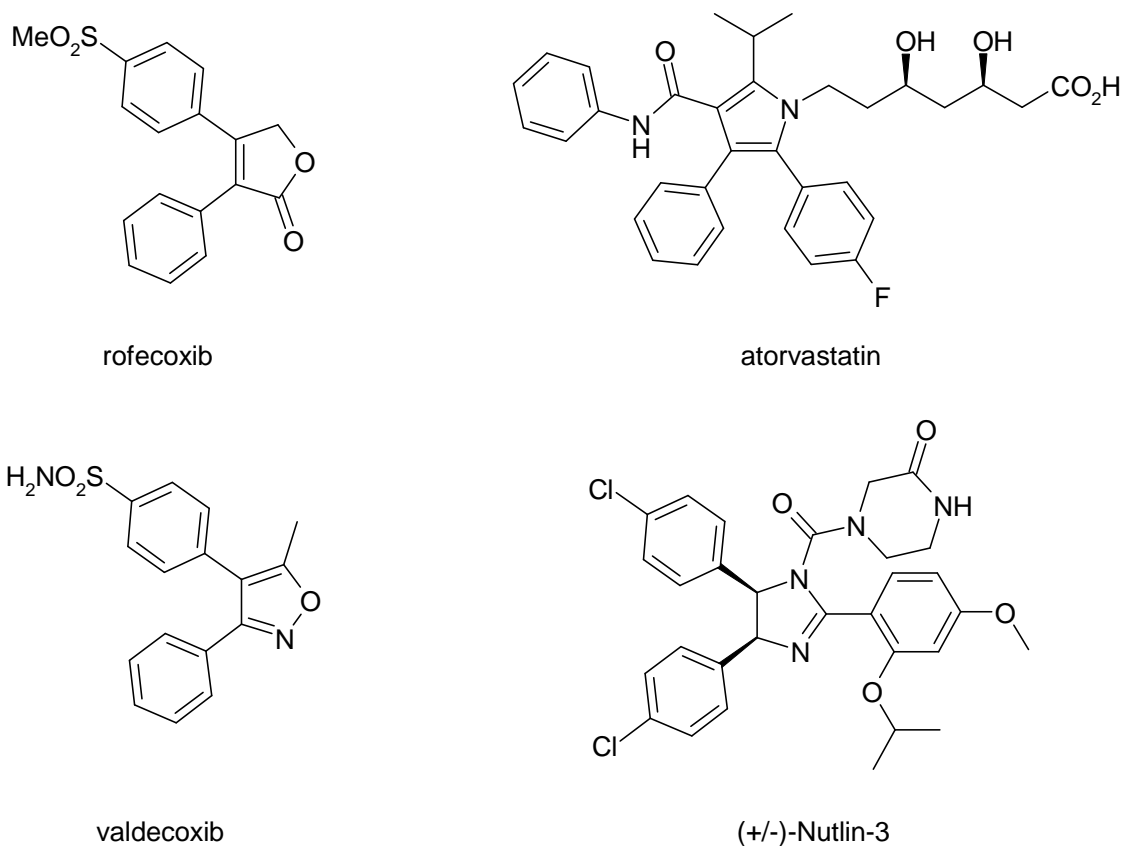


**Figure 3.18.** Structures of 5-fluorouracil, celecoxib (Celebrex<sup>®</sup>, Pfizer), panomifene and tamoxifen.

It is worth mentioning that the three drugs celecoxib, panomifene and tamoxifen contain a *cis*-stilbene moiety which is also present in the furopyranones with anticancer activity (see Table 3.5). The *cis*-stilbene motif is not only present in drugs against cancer also other agents for the treatment of different diseases contain this motif. For example the non-steroidal anti-inflammatory drugs (NSAID) like the already mentioned celecoxib (see Figure 3.18), rofecoxib (Vioxx<sup>®</sup>, Merck) and valdecoxib (Bextra<sup>®</sup>, Pfizer) are used to treat inflammatory diseases such as rheumatoid arthritis, and act by inhibiting the enzyme

cyclooxygenase (see Figure 3.19). This enzyme is involved in the biosynthesis of prostaglandins – agents which are responsible for the pain and inflammation of rheumatoid arthritis. The discovery of the two isoforms of the cyclooxygenases, COX-1 and COX-2, offered the opportunities to develop a new generation of NSAIDs with reduced side effects such as gastrointestinal damage attributed to inhibition of COX-1. In rheumatoid arthritis, the normally dormant COX-2 becomes activated and produces excess inflammatory prostaglandins. Therefore the selective inhibitors for the COX-2 isozyme like celecoxib, rofecoxib and valdecoxib have been developed. More recently, it has been discovered that Vioxx<sup>®</sup> and Bextra<sup>®</sup> are associated with increased cases of stroke and heart diseases, and in 2004 they were withdrawn from the market.<sup>10, 27</sup>

Atorvastatin (Lipitor<sup>®</sup>, Parke-Davis, see Figure 3.19) is a synthetic lipid-lowering statin for the treatment of hypercholesterolemia. The drug inhibits an enzyme involved in the cholesterol biosynthesis and so it lowers elevated low-density lipoprotein cholesterol (LDL-C) in the blood which reduces the risk for coronary artery diseases and coronary death.<sup>30</sup>



**Figure 3.19.** Structures of rofecoxib, valdecoxib and atorvastatin (Lipitor<sup>®</sup>) which contain a *cis*-stilbene moiety and the structure of *cis*-Nutlin-3 which contains a dihydro-*cis*-stilbene moiety.

The *cis*-imidazoline analogue Nutlin-3 (see Figure 3.19) is one compound of a series of different Nutlins which were investigated for the treatment of cancer. This compound is a



selective small-molecule antagonist of murine double-minute 2 (MDM2), a protein involved in the regulation process of the p53 tumor suppressor protein. The tumour suppressor p53 is a potent transcription factor that controls a major pathway protecting cells from malignant transformation and as such, it is the most frequently inactivated protein in human cancer. This protein is tightly controlled by the MDM2 protein which can inactivate p53. The *mdm2* gene has been found amplified or over-expressed in many human cancers and therefore, activation of the p53 pathway through inhibition of MDM2 has been proposed as novel therapeutic strategy. Vassilev *et al.* investigated these Nutlins as inhibitors for the p53-MDM2 binding and demonstrated the ability of these compounds for the treatment of cancer. In the case of Nutlin-3 the enantiomers were separated and tested individually. One enantiomer showed an IC<sub>50</sub> value of 13.6 μM while the other enantiomer was more potent and had an IC<sub>50</sub> value of 0.09 μM in this protein based assay. While in cancer cells with wild-type p53 the compounds were active no activity was observed in cancer cells containing mutant p53.<sup>31, 32</sup> In conclusion, the *cis*-stilbene motif, which was identified as a crucial part of the pharmacophore of the furopyranones, is found in many drugs and natural products (see Chapter 1.3.2) with potent biological activity. The increased antiproliferative and apoptotic activity after insertion of fluorine into the *cis*-stilbene motif is in good agreement with the literature since fluorine is often used to optimise the properties of a drug.<sup>27, 28, 29</sup>

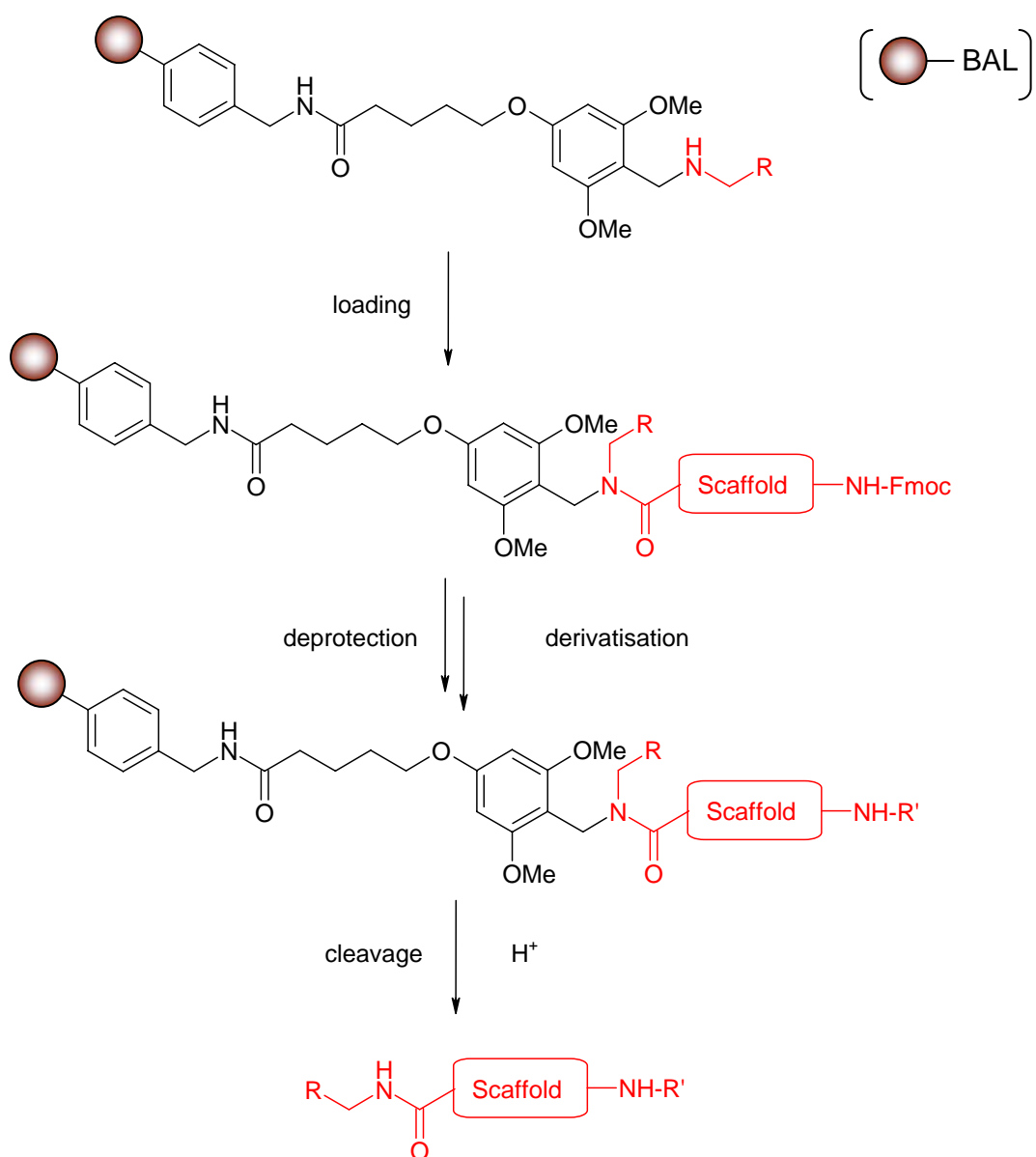
### 3.5 References for Chapter 3

- [1] R. Messer, A. Schmitz, L. Moesch, R. Häner, *J. Org. Chem.* **2004**, *69*, 8558-8560.
- [2] R. Messer, X. Pelle, A. L. Marzinzik, H. Lehmann, J. Zimmermann, R. Häner, *Synlett* **2005**, 2441-2444.
- [3] Roland Messer, *Natural Product-like Compound Libraries from D-(-) Ribose*, Dissertation **2005**, Universität Bern, Schweiz.
- [4] K. A. Jorgensen, *Angew. Chem. Int. Ed.* **2000**, *39*, 3558-3588.
- [5] a) C. A. Fuhrer, R. Messer, R. Häner, *Tetrahedron Lett.* **2004**, *45*, 4297-4300 (and references therein); b) Cyril Fuhrer, *Stereoselektive Synthese von Pyranofuranonen mittels intramolekularer hetero Diels-Alder Reaktion*, Diplomarbeit **2003**, Universität Bern, Schweiz (and references therein).
- [6] B. B. Snider, D. M. Roush, T. A. Killinger, *J. Am. Chem. Soc.* **1979**, *101*, 6023-6027.
- [7] L. F. Tietze, T. Brumby, M. Pretor, G. Remberg, *J. Org. Chem.* **1988**, *53*, 810-820.
- [8] C. A. Fuhrer, E. Grüter, S. Ruetz, R. Häner, *ChemMedChem* **2007**, *2*, 441-444 (and references therein).
- [9] D. S. Tan, M. A. Foley, B. R. Stockwell, M. D. Shair, S. L. Schreiber, *J. Am. Chem. Soc.* **1999**, *121*, 9073-9087.
- [10] G. L. Patrick, *An Introduction to Medicinal Chemistry*, Oxford University Press: UK, third edition **2005**.
- [11] A. Blond, N. Platzler, A. Guy, H. Dhotel, L. Serva, *Bull. Soc. Chim. Fr.* **1996**, *133*, 283-293.
- [12] S. F. Martin, S. R. Desai, G. W. Philips, A. C. Miller, *J. Am. Chem. Soc.* **1980**, *102*, 3294-3296.
- [13] E. Schmitz, U. Heuck, H. Preuschhof, E. Gründemann, *J. Prakt. Chem.* **1982**, *324*, 581-588.
- [14] N. Guiblin, C. A. Fuhrer, R. Häner, H. Stoeckli-Evans, K. Schenk, G. Chapuis, *Acta Cryst.* **2006**, *B62*, 506-512 (and references therein).
- [15] W. Oppolzer, *Angew. Chem.* **1977**, *89*, 10-24.
- [16] Sandro Manni, *Stereoselektive Synthese von Furo[3,4-c]pyranonen mittels intramolekularer hetero-Diels-Alder-Reaktion zur Durchführung einer Struktur-Aktivitäts-Beziehungs Studie in neoplastischen Zellen*, Bachelorarbeit **2006**, Universität Bern, Schweiz.
- [17] Y. Nagao, K. Inoue, M. Yamaki, S. Takagi, E. Fujita, *Chem. Pharm. Bull.* **1988**, *36*, 495-508.
- [18] T. W. Greene, P. G. M. Wuts, *Protective Groups in Organic Synthesis, Third Edition*; John Wiley & Sons: New York, **1999**.

- 
- [19] M. Hesse, H. Meier, B. Zeeh, *Spektroskopische Methoden in der organischen Chemie*; Georg Thieme Verlag: Stuttgart \* New York , 5. Auflage **1995**.
- [20] Florian Garo, *Trennung der Enantiomere eines biologisch aktiven Furo[3,4-c]pyranons durch die Synthese von Diastereomeren*, Bachelorarbeit **2006**, Universität Bern, Schweiz.
- [21] L. Revesz, H. Meigel, *Helv. Chim. Acta* **1988**, *71*, 1697-1703.
- [22] E. Block, R. Stevenson, *J. Org. Chem.* **1971**, *36*, 3453-3455.
- [23] L. H. Klemm, D. R. Olson, D. V. White, *J. Org. Chem.* **1971**, *36*, 3740-3743.
- [24] I. Beuvink, A. Boulay, S. Fumagalli, F. Zilbermann, S. Ruetz, T. O'Reilly, F. Natt, J. Hall, H. A. Lane, G. Thomas, *Cell* **2005**, *120*, 747-759.
- [25] T. Idziorek, J. Estaquier, F. de Bels, J. C. Ameisen, *J. Immunol. Methods* **1995**, *185*, 249-258.
- [26] C. A. Lipinski, F. Lombardo, B. W. Dominy, P. J. Feeney, *Adv. Drug Deliv. Rev.* **1997**, *23*, 3-25.
- [27] C. Isanbor, D. O'Hagan, *J. Fluor. Chem.* **2006**, *127*, 303-319.
- [28] K. L. Kirk, *J. Fluor. Chem.* **2006**, *127*, 1013-1027.
- [29] H-J. Böhm, D. Banner, S. Bendels, M. Kansy, B. Kuhn, K. Müller, U. Obst-Sander, M. Stahl, *ChemBioChem* **2004**, *5*, 637-643.
- [30] Editorial Material, *Am. J. Nurs.* **1998**, *98*, 57-59.
- [31] L. T. Vassilev, B. T. Vu, B. Graves, D. Carvajal, F. Podlaski, Z. Filipovic, N. Kong, U. Kammlott, Ch. Lukacs, Ch. Klein, N. Fotouhi, E. A. Liu, *Science* **2004**, *303*, 844-848.
- [32] M. Arkin, *Curr. Opin. Chem. Biol.* **2005**, *9*, 317-324.

## 4. Preparation of Furopyranone-Libraries

An important aspect of the whole work was the elaboration of a method for the synthesis of libraries on solid support. The scaffold should contain a suitable functional group for coupling to BAL-aminomethyl-PS solid supports (Backbone Amide Linker) which had been successfully used in previous projects.<sup>1,2</sup> The BAL-aminomethyl-PS solid support features the advantage of yielding N-substituted carboxyamides upon release from the support (see Scheme 4.1).



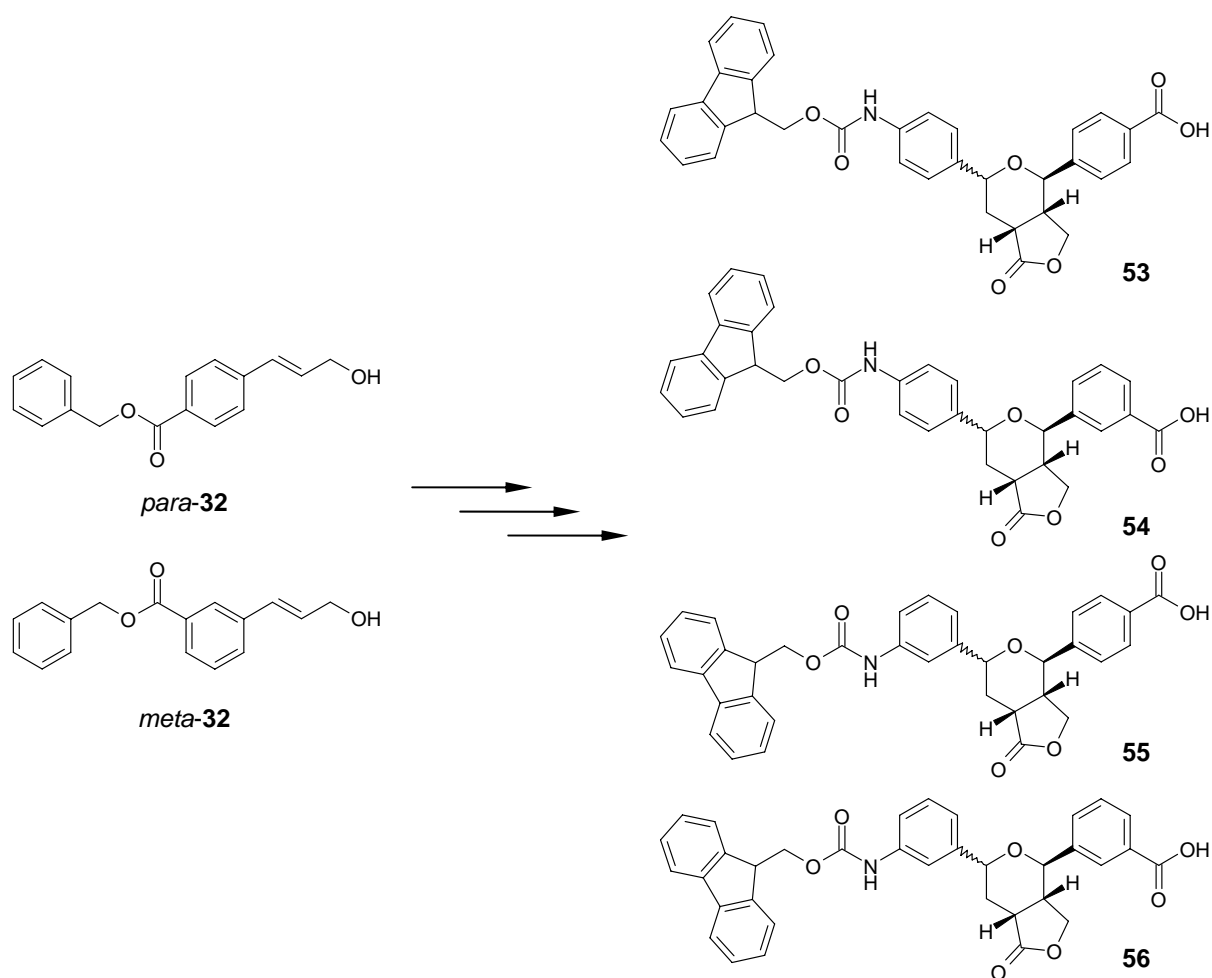
**Scheme 4.1.** Derivatisation of the scaffold using BAL-aminomethyl-PS solid support (BAL = Backbone Amide Linker).

The scaffold carries an amino functionality bearing a Fmoc-protecting group to prevent side reactions during the coupling step. After the coupling step and N-deprotection further derivatisation is accomplished. At the end of the synthesis, the scaffold is cleaved from the

support under acidic conditions. Thus, the scaffold has to be stable towards exposure to TFA (20% or 50% in CH<sub>2</sub>Cl<sub>2</sub>) at room temperature.

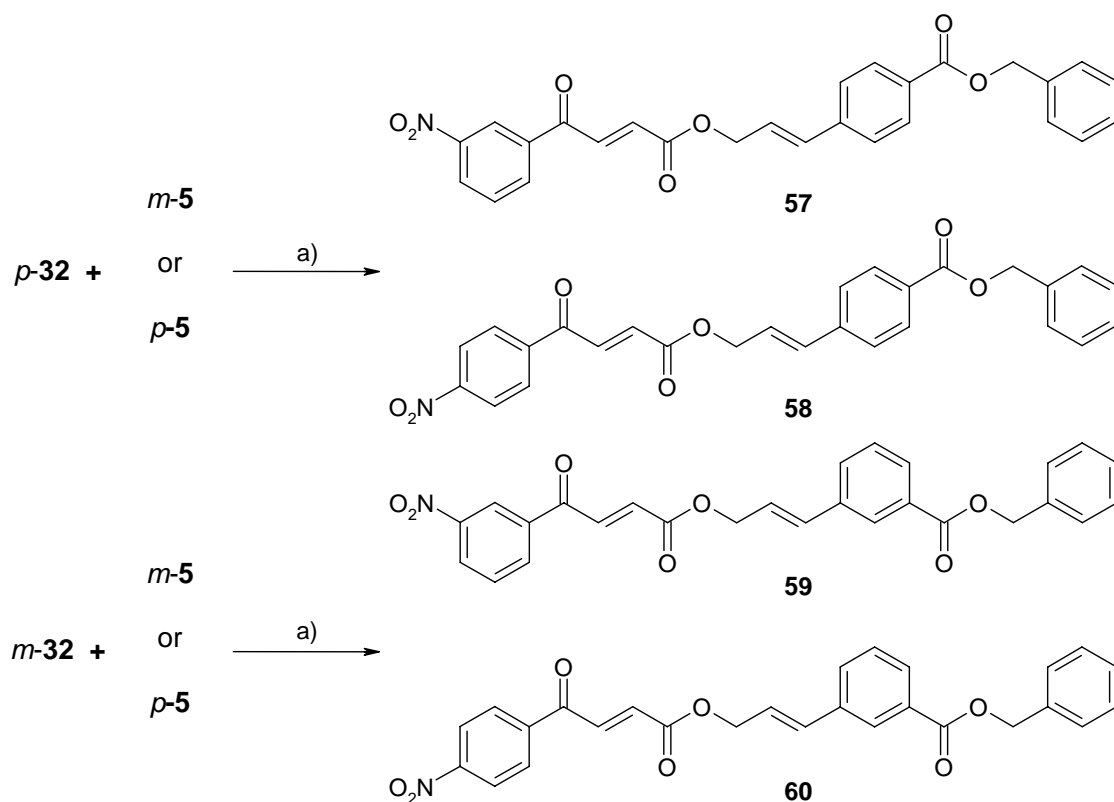
#### 4.1 Preparation of Furopyranones Containing a Linker Group and a Protected Amine Function

To have suitable scaffolds with a carboxylic acid linker in hand, different furopyranones similar to the C(7)-desphenyl derivatives (see Chapter 3.3.1) were synthesised starting from the benzyl ester cinnamyl alcohols **32** (see Scheme 4.2).



**Scheme 4.2.** Synthesis of Fmoc-protected furopyranones **53**, **54**, **55** and **56** starting from either *meta*- or *para*-**32**.

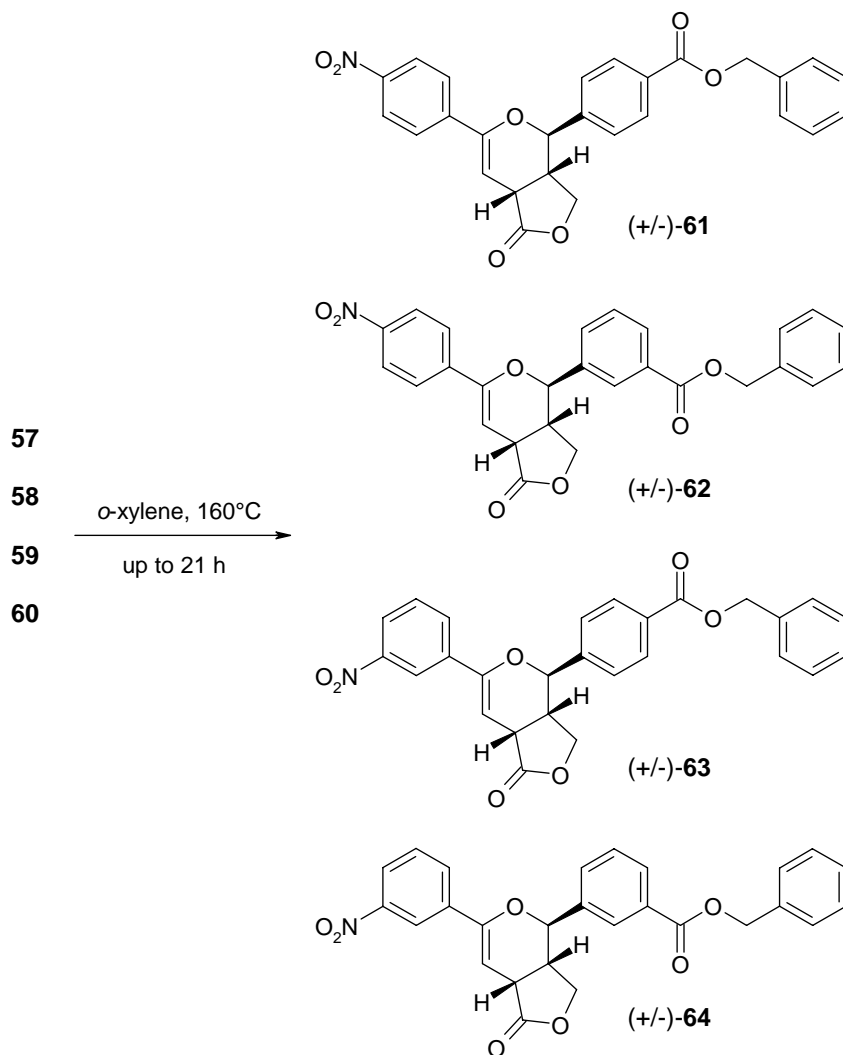
In a first step the *meta*- and *para*-alcohols **32** were esterified with the already used  $\gamma$ -oxo-butenic acids **5**. The corresponding esters **57** - **60** were prepared *via* the mixed anhydride using pivaloyl chloride as shown in Scheme 4.3.<sup>3</sup>



**Scheme 4.3.** Synthesis of esters **57** – **60** via the mixed anhydride using pivaloyl chloride; a) pivaloyl chloride, triethylamine, DMAP, 1,2-dichloroethane, 0°C, 2 h; yields: **57** (59%), **58** (59%), **59** (43%) and **60** (67%).

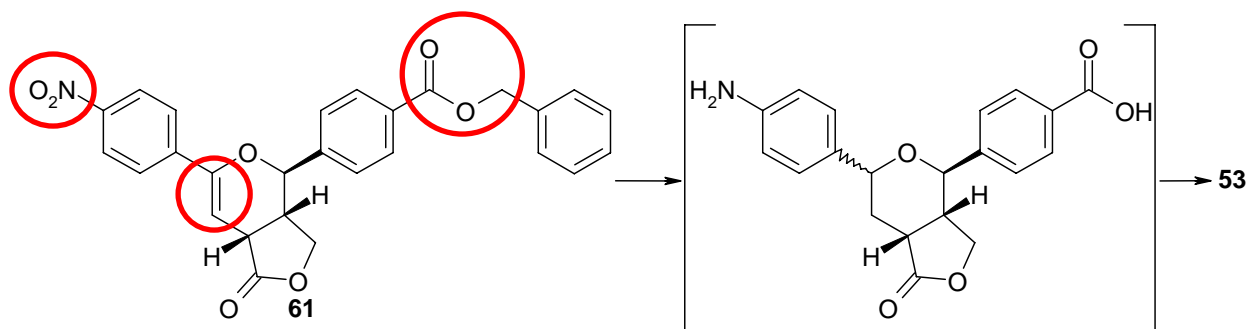
The syntheses of esters **57** – **60** via the mixed anhydride method followed the well established procedure as described in Chapter 3.3.1 and the outcome of the reactions was similar as for the previously reported esters **6a-f**.

Esters **57** – **60** were subsequently transformed into the furopyranones **61** - **64** through an intramolecular *hetero* Diels-Alder reaction. The cyclisation was carried out in refluxing *o*-xylene. Yields of isolated products varied between 42% and 67% (see Scheme 4.4), which is acceptable in view of the relatively harsh reaction conditions. In all cases the expected *cis*-fused products were isolated.



**Scheme 4.4.** Hetero Diels-Alder reaction of esters **57-60**. Yields: 56% (**61**), 53% (**62**), 42% (**63**) and 67% (**64**).

The so obtained bicyclic products **61 - 64** were converted to the Fmoc-protected furopyranones **53 - 56** via a hydrogenation reaction followed by protection of the amine using 9-fluorenylmethyloxycarbonylchloride (Fmoc-Cl, see Scheme 4.6). The hydrogenation was done according to the literature and THF served as solvent because Messer *et al.* observed *trans*-esterification if methanol was used.<sup>1, 2</sup> All the reactions worked well and the crude amino acid derivatives were directly used for the amine protection with Fmoc-Cl. The hydrogenation reaction was not as selective as reported by Messer *et al.*<sup>1,2</sup> yielding two diastereomers upon formation of the additional stereogenic center. In the hydrogenation step, several reactions took place at the same time: deprotection of the benzyl ester, hydrogenation of the enol ether double bond and reduction of the NO<sub>2</sub>-group to the corresponding amine (see Scheme 4.5). The reaction was performed at room temperature using Pd/C (10%) in a hydrogen atmosphere.

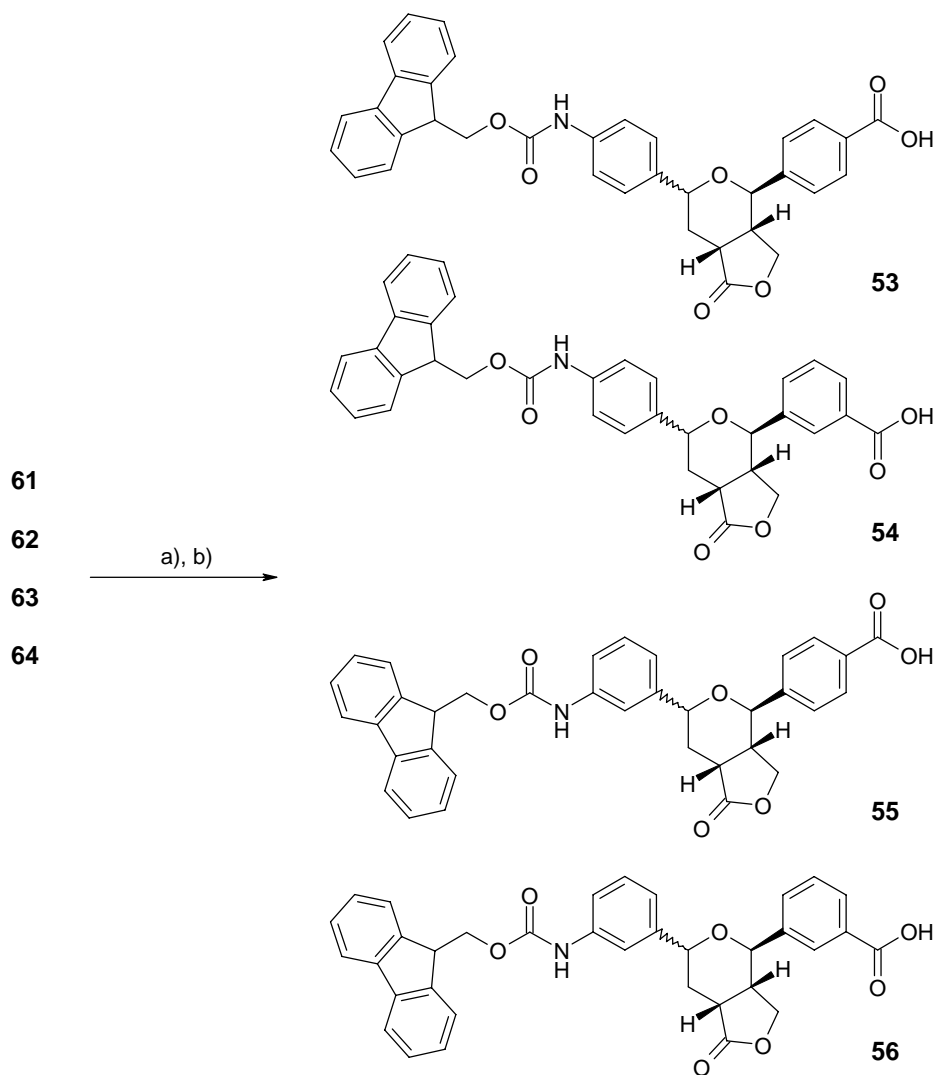


**Scheme 4.5.** Three different modifications during the hydrogenation step (example **61**): deprotection of the benzyl ester, hydrogenation of the enol ether double bond and reduction of the NO<sub>2</sub>-group to the corresponding amine. On the right the intermediate for the synthesis of **53** is shown.

For the protection of the amine Fmoc-Cl was used. The Fmoc-group is stable under acidic conditions and is readily cleaved using a mild base, such as piperidine. The Fmoc-protection worked well as monitored by TLC, but the purification process was problematic. A simple recrystallisation from a mixture of methanol and methyl *tert*-butyl ether as in the case of Messer *et al.* was not possible.<sup>1, 2</sup> Several recrystallisation methods with different solvents and solvent mixtures failed. Finally, conditions were found for purification of the Fmoc-protected amino acid derivatives **53** - **56** by chromatography (silica gel) using a solvent mixture of CH<sub>2</sub>Cl<sub>2</sub>/MeOH/HCOOH (e.g. 97:2:1). The yields for the isolated products varied from 60% to 80%.

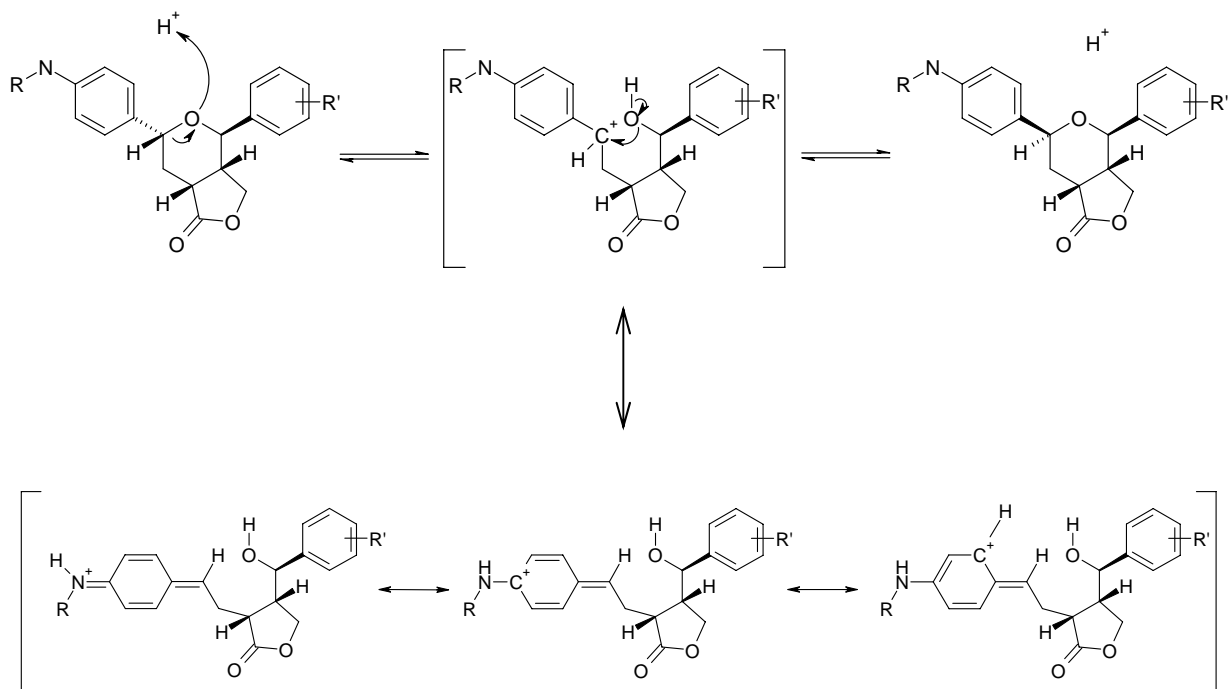
As mentioned before products **53** – **56** were obtained as diastereomeric mixtures due to the formation of an additional stereogenic center upon hydrogenation. LC/MS-analysis showed a ratio of roughly 5:1 for these diastereomeric mixtures. Analysis of the configuration for each diastereomer of **53** – **56** needed further investigations. First of all the stability of products **53** – **56** under acidic conditions was analysed using a mixture of TFA/CH<sub>2</sub>Cl<sub>2</sub> in a ratio of 1:4 or 1:1. The compounds were treated for 1 h or 18 h under these conditions. Surprisingly while products **53** and **54** epimerised nearly quantitatively to a single product, compounds **55** and **56** showed no epimerisation. This indicated that the amine group in *para*-position for **53** and **54** was responsible for the equilibration.





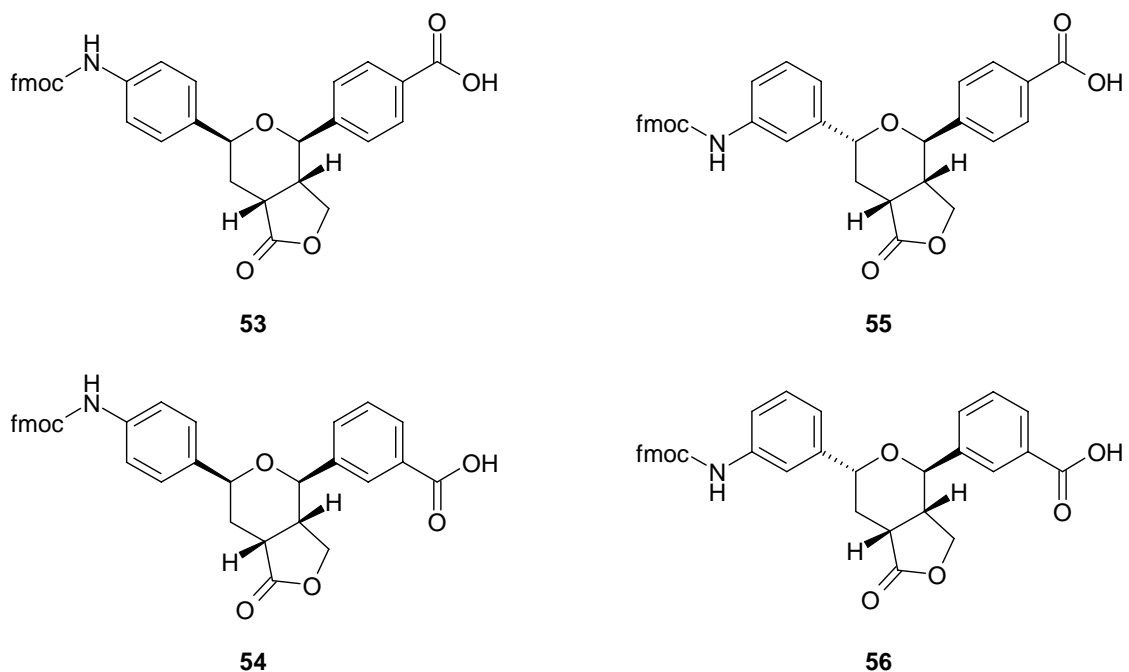
**Scheme 4.6.** Fmoc-protected diastereomeric mixtures of **53** – **56**; a) Pd/C (10%), H<sub>2</sub>, THF, 2.5 h; b) NaHCO<sub>3</sub>, Fmoc-Cl, dioxane/H<sub>2</sub>O, up to 5.5 h. Yields: 62% (**53**), 68% (**54**), 62% (**55**) and 80% (**56**).

Epimerisation of **53** and **54** most likely proceeds *via* a ring opening-closing reaction under acidic conditions, in which the oxygen of the pyran ring is protonated. The protonation leads to a ring opening and allows the change of the configuration for the neighbouring stereogenic centres. The amine in *para*-position stabilizes this charged intermediate *via* mesomeric stabilization. Ring closure follows by regeneration of the pyran ring and deprotonation (see Scheme 4.7).



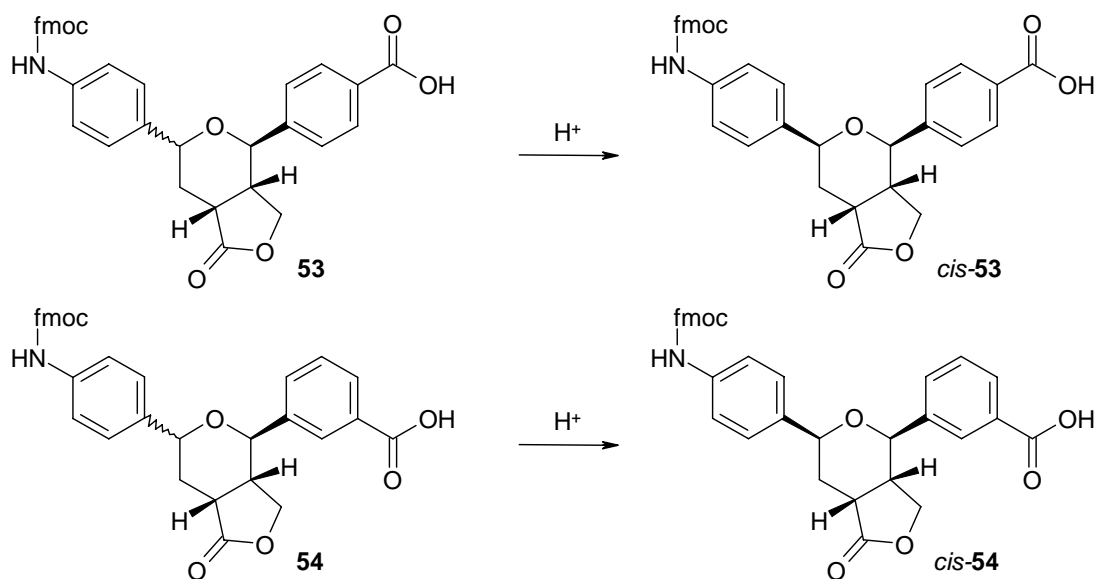
**Scheme 4.7.** Possible ring opening-closing reaction under acidic conditions and stabilisation of the charged intermediate by the amine in *para*-position.

NMR spectroscopy done at the 'Novartis Institutes for BioMedical Research' revealed the configuration of all the synthesised diastereomeric products **53** – **56** (after treatment under acidic conditions for 18 h, see Figure 4.1).



**Figure 4.1.** Analysed configurations of products **53** – **56** by NMR spectroscopy after treatment under acidic conditions for 18 h.

For compounds **53** and **54** a *cis*-configuration of the aniline moiety relative to the benzoic acid moiety was found (see Scheme 4.8) while for compound **55** and **56** the major product was the one with *trans*-configuration of the aniline to the benzoic acid moiety.



**Scheme 4.8.** Epimerisation of the diastereomeric mixtures of compounds **53** and **54** to a single product under acidic conditions.

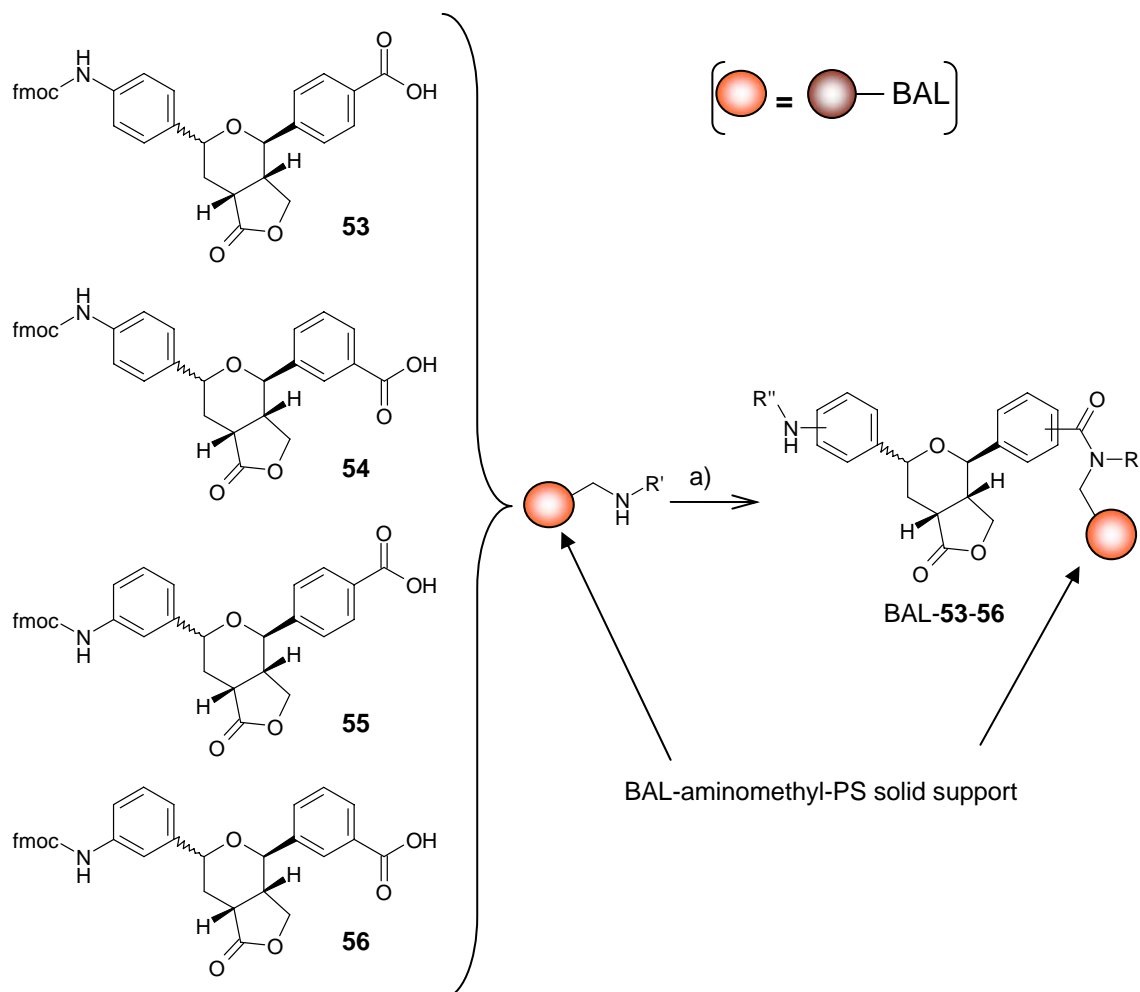
As a consequence of this finding, the solid support chemistry was performed without separation of the diastereomeric starting materials. In the case of **53** and **54** an extended cleavage time (up to 24 h) leads to a single product. In the case of **55** and **56** a standard cleaving procedure (1 h), followed by purification will lead to a mixture of diastereomers which can be separated.

## 4.2 Elaboration of Conditions for the Solid Phase Synthesis

Before the synthesis of the prototype libraries several aspects such as optimal conditions for the coupling step, determination of the loading efficiency and application of the conditions for different BAL-aminomethyl-PS solid supports had to be investigated

### 4.2.1 Conditions for the Coupling Step

For the coupling of furopyranones **53** - **56** to the solid support (BAL-aminomethyl-PS solid support) suitable conditions had to be found. The conditions previously used by Messer *et al.* were found to work extremely well (see Scheme 4.9).<sup>1,2</sup>



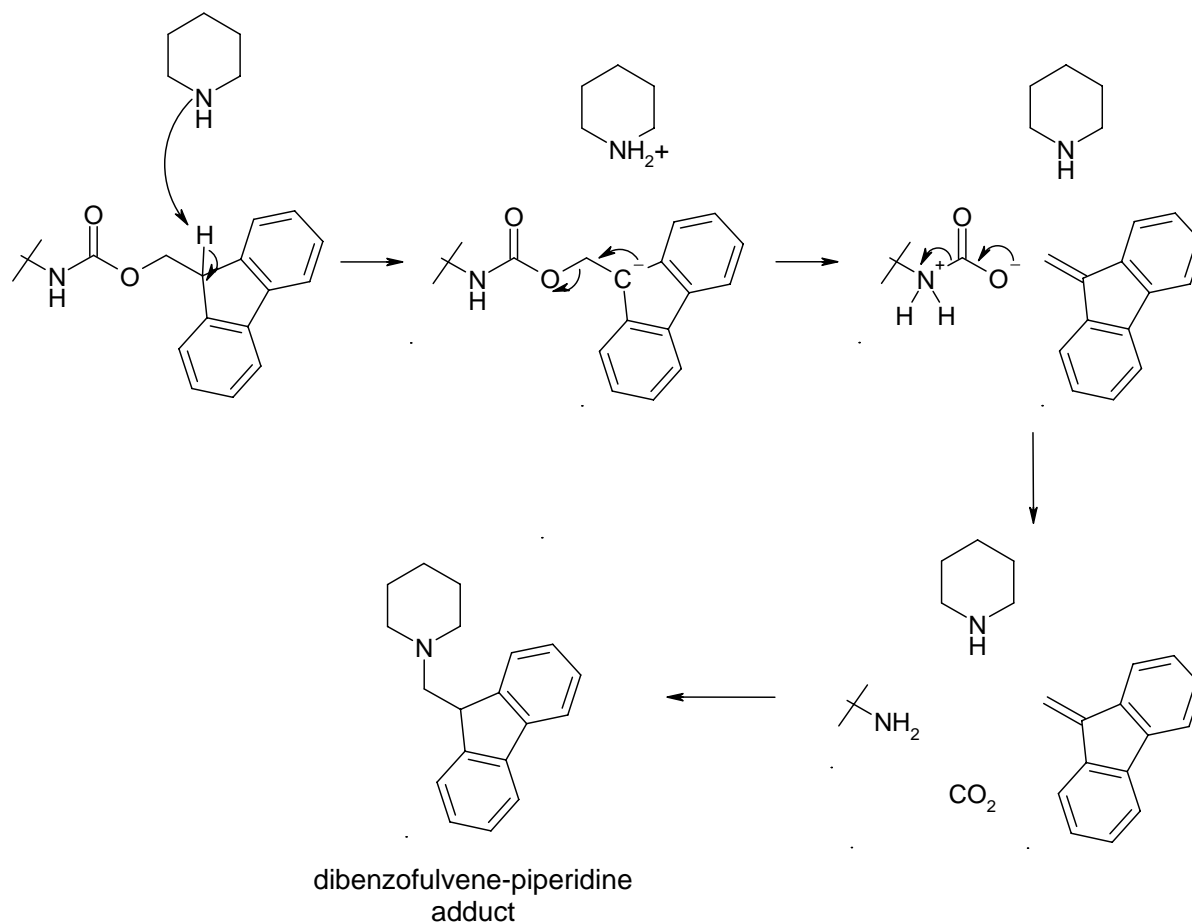
**Scheme 4.9.** Coupling step for furopyranones **53** – **56** to the BAL-aminomethyl-PS solid support; a) HCTU (3 eq.), HOBT (3 eq.), DIPEA (3 eq.), NMP, rt, over night.

The method involves the use of HCTU, HOBT (1-hydroxybenzotriazole), DIPEA (N-ethyl-diisopropylamine) and the corresponding furopyranones **53** - **56** in NMP (N-methyl pyrrolidone). After addition of the reaction mixture to the benzyl amine derived solid support, the coupling reaction was allowed to proceed at room temperature over night while the reaction vessels were gently shaken. The following washing step included the use of DMA (N,N-dimethylacetamide), MeOH, DCM and again MeOH in the order presented. This procedure had to be done after every reaction step carefully to get rid of all the reagents to avoid side reactions in the following step.

#### 4.2.2 Determination of the Loading Efficiency by UV Quantification

The loading of the support (percentage of amino groups on the solid support coupled with the scaffold) was determined using standard procedures.<sup>1, 2, 4</sup> After coupling of the furopyranones **53** and **54** on the solid support the attached compounds were deprotected using 44 ml of a piperidine/DMA-solution (1:4), forming the piperidine-dibenzofulvene adduct from the Fmoc-group

(see Scheme 4.10). The loading of the support was determined by quantitation with UV absorbance of an aliquot of the piperidine/DMA/dibenzofulvene-piperidine solution.

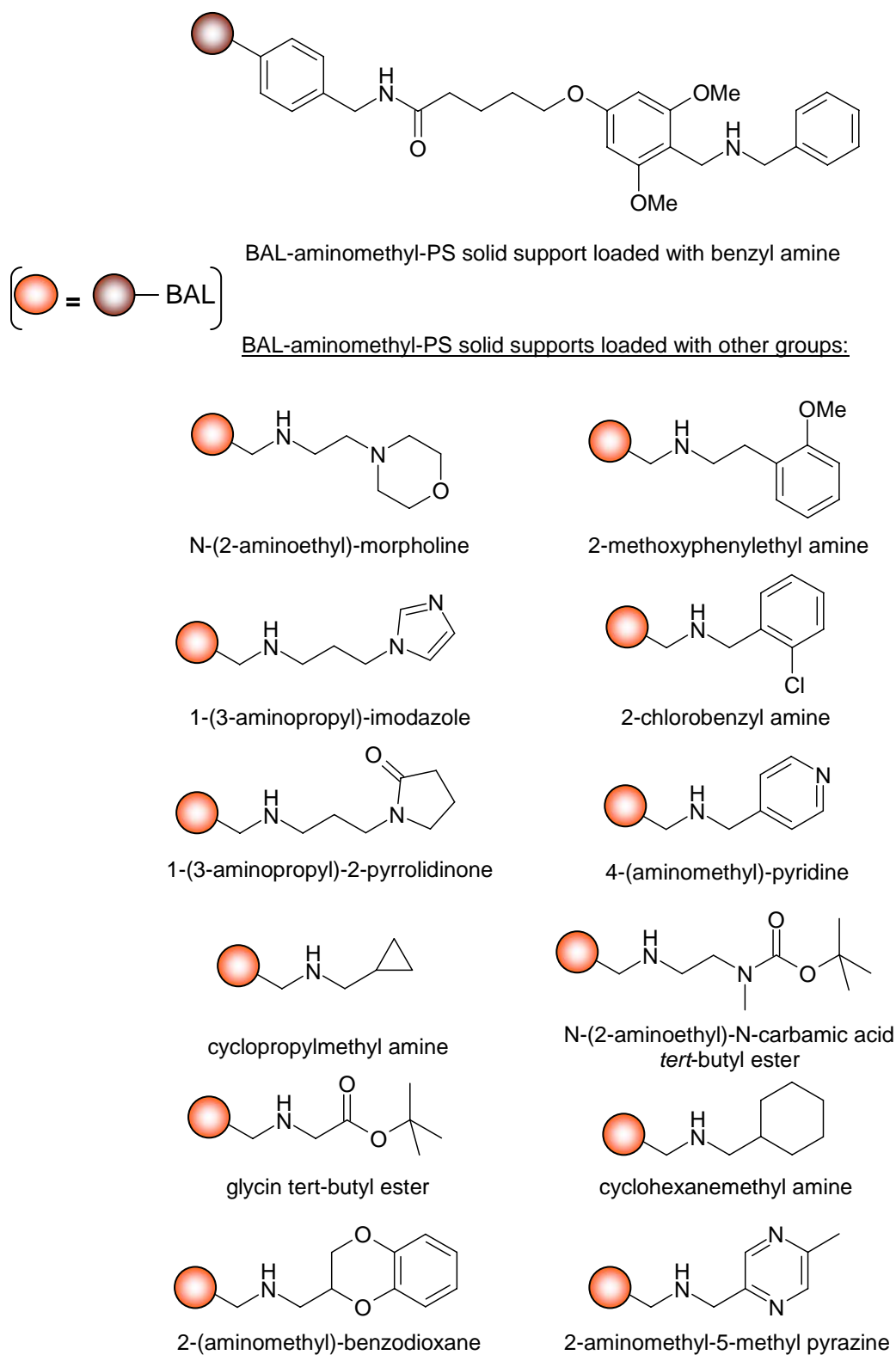


**Scheme 4.10.** Deprotection of the Fmoc-group with piperidine and the resulting dibenzofulvene-piperidine adduct.

The loading of the two furopyranones **53** and **54** was found to be over 90% (95% for **53** and 92% for **54**). The same conditions were also successfully applied to the furopyranones **55** and **56**. The position of the carboxylic acid group in either *meta*- or *para*-position had no influence on the coupling efficiency since both compounds **53** and **54** showed loadings higher than 90%.

#### 4.2.3 Application of the Conditions to Different BAL-aminomethyl-PS Solid Supports

Subsequently, several additional solid supports (see Figure 4.2) were loaded with the furopyranone **53**. Derivatisation of all the different BAL-supports shown worked very well as verified by LC-MS analysis. This verifies the broad applicability of the chosen strategy.

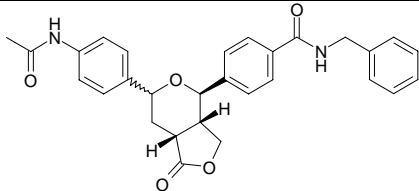
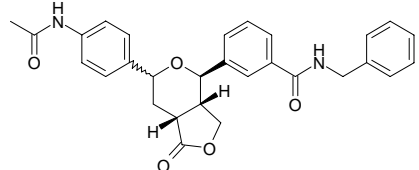
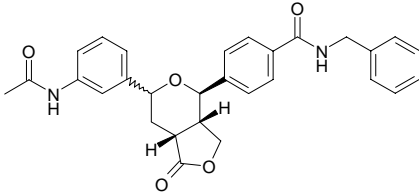
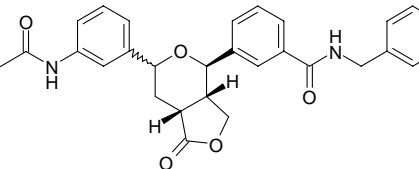


**Figure 4.2.** BAL-aminomethyl-PS solid supports tested in this work. For the first experiments the benzyl amine solid support was used.

#### 4.2.4 Configurational Stability of the Final Products Under Cleavage Conditions

In the case of the BAL-aminomethyl-PS solid support loaded with benzyl amine all different furopyranones **53** – **56** were tested for different cleavage conditions as presented in Table 4.1. One example of each compound was cleaved from the solid support under standard conditions (TFA/DCM – 1:4, 1 h) while the other examples were cleaved using longer cleaving conditions (TFA/DCM – 1:1, 18 h).

**Table 4.1.** Change of the ratio of the diastereomers with *cis*- or *trans*-configuration of the two phenyl rings after different cleaving conditions.

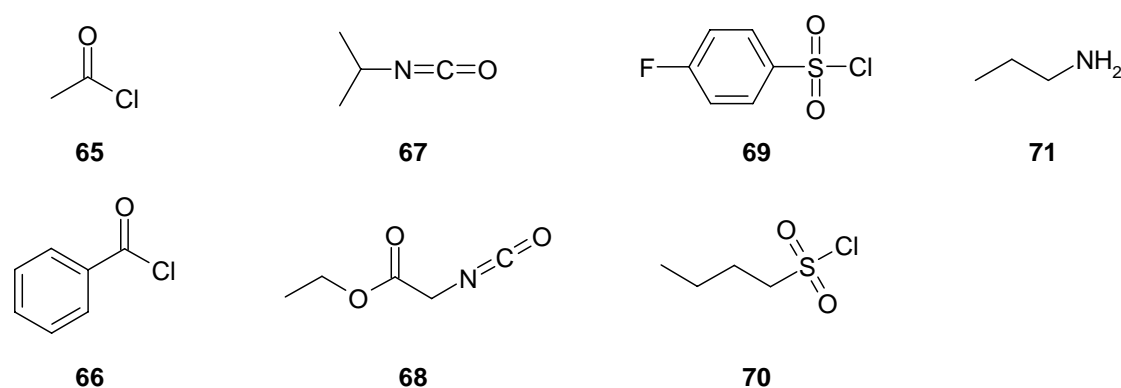
Structure of Products	Ratio of <i>cis</i> -/ <i>trans</i> -product	Ratio of <i>cis</i> -/ <i>trans</i> -product
	TFA/DCM (1:4) for 1 h	TFA/DCM (1:1) for 18 h
	2 : 7	19 : 1
	4 : 13	17 : 1
	4 : 13	4 : 13
	1 : 5	1 : 6

For these products the same results were obtained as for the starting materials **53** – **56**. In the case of the acetylated *para*-aniline derivatives almost quantitative epimerisation of the final products was observed while the acetylated *meta*-aniline derivatives showed no epimerisation under elongated cleaving conditions.

### 4.3 Synthesis of Prototypes for Each Scaffold

For demonstration of the suitability of the furopyranones **53** – **56** for solid support chemistry, different prototypes were synthesised *via* solid phase chemistry. Therefore two different resins (see Schemes 4.11 and 4.12) were chosen and a pair of two furopyranones was derivatised using the same solid support, the same reagents and conditions.

For derivatisation of the aniline part of furopyranones **53** – **56** three different reagents were chosen. In one case the acylation with different acid halides was investigated and the synthesis of urea derivatives was planned by using isocyanates. Another strategy was to synthesise sulfonic acid derivatives using sulfonic acid halides and in the case of two different furopyranones aminolysis of the lactone using propyl amine **71** was planned (see Figure 4.3).



**Figure 4.3.** Different reagents chosen for acylation, preparation of urea and sulfonic acid derivatives and aminolysis.

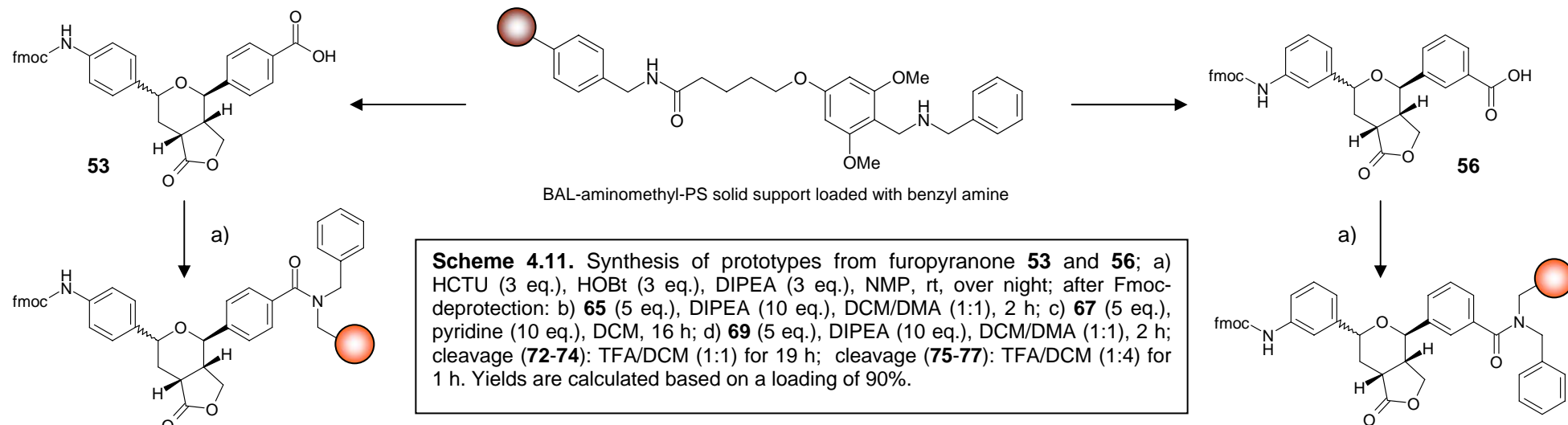
Furopyranones **53** and **56** were derivatised in the same manner using **65** as acylation reagent and **67** for making the urea derivatives. For synthesising a sulfonic ester reagent **69** was chosen and with the acetylated compounds BAL-**72** and BAL-**75** aminolysis was done with amine **71**.

In the case of furopyranone **53** the BAL-aminomethyl-PS solid support loaded with benzyl amine was used as shown in Scheme 4.11. After coupling **53** to the solid support and Fmoc-deprotection the resin was split into three equal batches and after acetylation of one batch, this batch was split again into two equal batches of which one was used for aminolysis with **71**. The prototypes were synthesised according to the conditions indicated in Scheme 4.11 and the final products **72** – **74** were isolated after an elongated cleaving procedure (TFA/DCM - 1:1 for 19 h) followed by purification *via* preparative reversed phase LC and drying (vacuum). As expected only one single product was obtained for each derivatisation step and the yields varied from 72% for **73** to 22% for **74**. The formation of the urea derivative **73** was the best reaction, followed by the acetylation reaction resulting **72**. In the case of the urea derivative **73** no further purification was possible due to insolubility of the compound under the purification conditions. In the case of

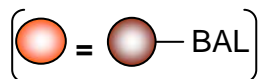
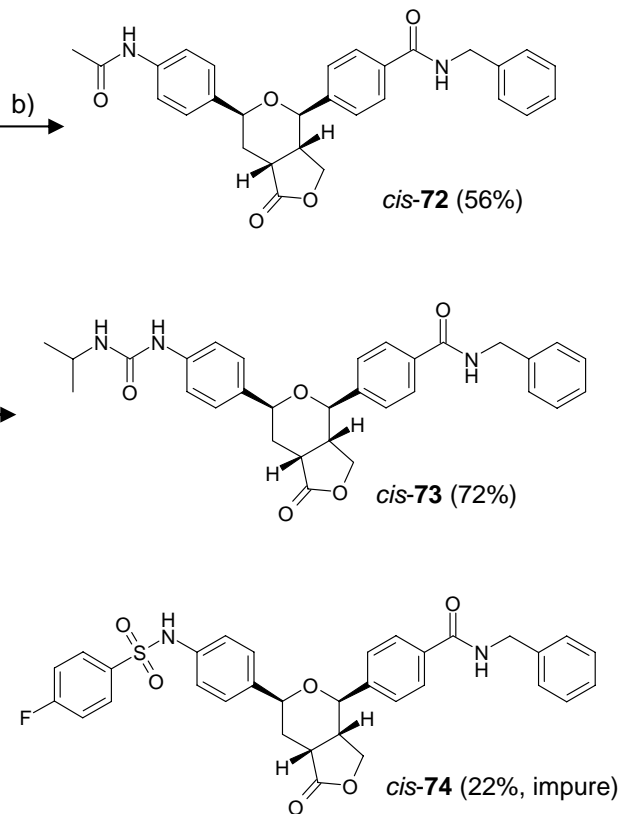


the sulfonic acid derivative **74** the reaction did not work very well and the expected product was isolated impure. Here the product was only analysed by LC-MS where the mass of **74** was detected. UV-detection and MS analysis showed the presence of impurities which could not be assigned to possible side products of the reaction (unoccupied positions on the solid support, reagents).

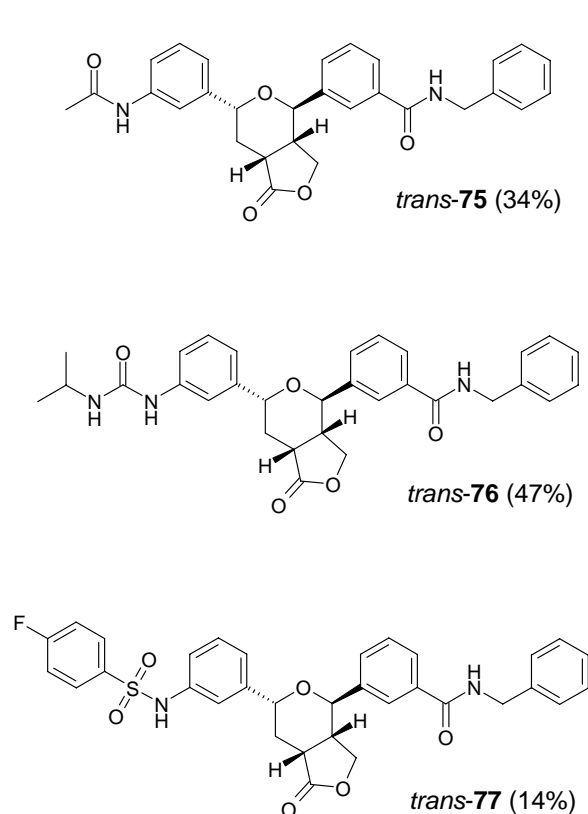
In the case of furopyranone **56** again the BAL-aminomethyl-PS solid support loaded with benzyl amine was used as shown in Scheme 4.11. After coupling **56** to the solid support and Fmoc-deprotection the resin was split into three equal batches and after acetylation of one batch, this batch was split again into two equal batches of which one was used for aminolysis with **71**. The prototypes were synthesised according to the conditions indicated in Scheme 4.11 and the final products **75** – **77** were isolated after a normal cleaving procedure (TFA/DCM - 1:4 for 1 h) followed by purification *via* preparative reversed phase LC and drying (vacuum). LC-MS analyses of the acetylation product **75** before purification showed a ratio for the two diastereomers of about 3:2 (*cis-/trans-75*) what was very surprising. The overall yield for the diastereomeric mixture was 39% and after the purification 34% of *trans-75* and a fraction of the diastereomeric mixture (5%) were isolated. In the case of the urea derivative **76** no further purification was possible due to insolubility of the compound under the purification conditions and LC-MS analyses showed a ratio for the two diastereomers of about 1:1 (*cis-/trans-76*). The overall yield for the diastereomeric mixture was 47% and *via* NMR spectroscopy *trans-76* was identified. LC-MS analyses of **77** before purification showed a ratio for the two diastereomers of about 1:3 (*cis-/trans-77*). The overall yield for the diastereomeric mixture was 16% and after the purification 14% of *trans-77* and a fraction of the diastereomeric mixture (2%) were isolated.

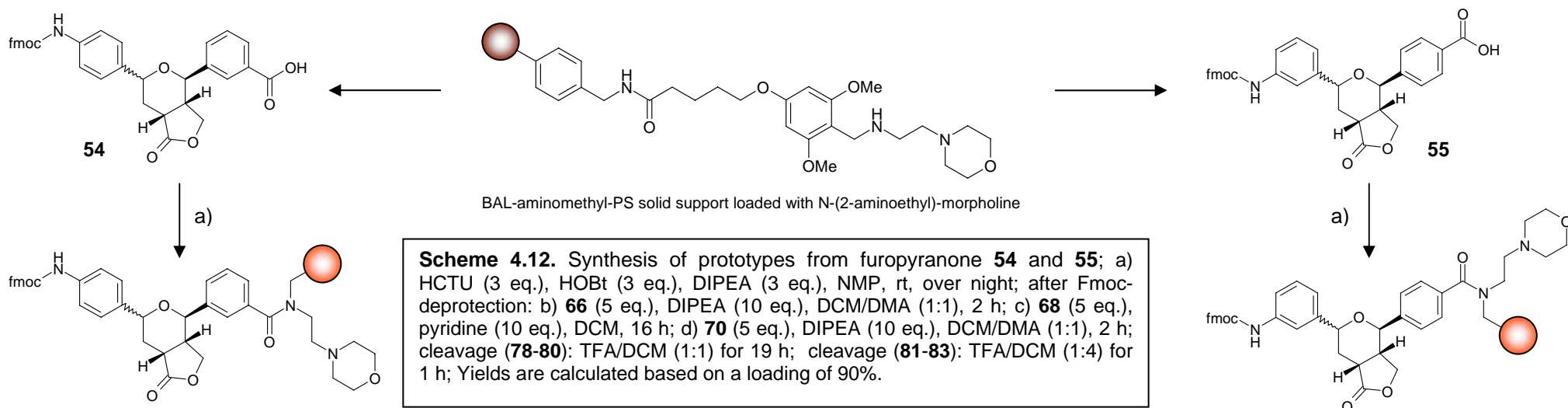


BAL-53

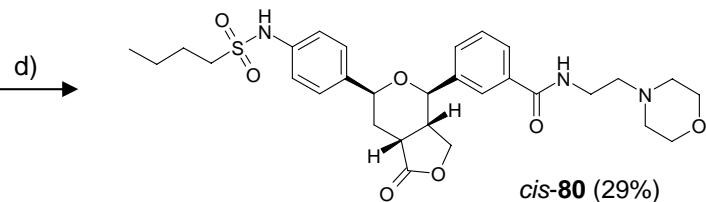
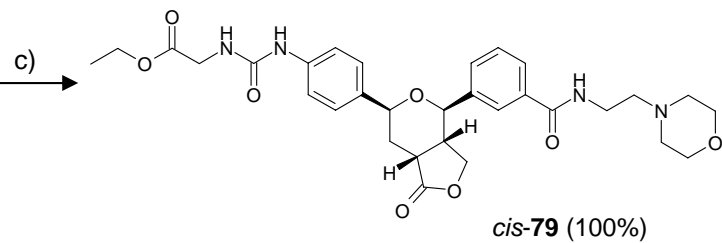
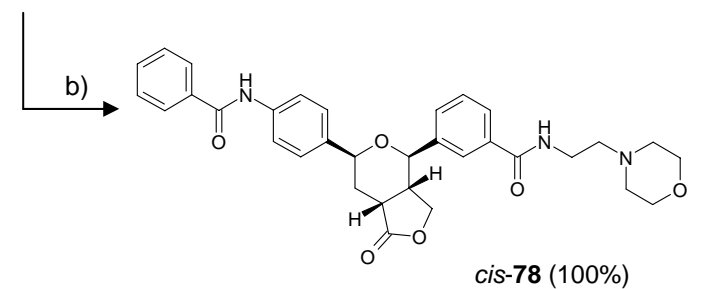


BAL-56

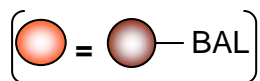
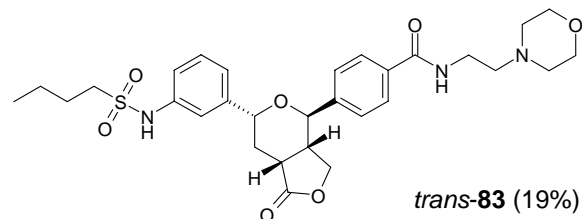
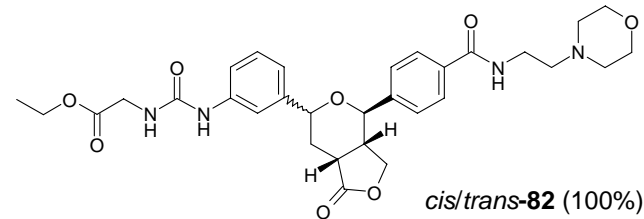
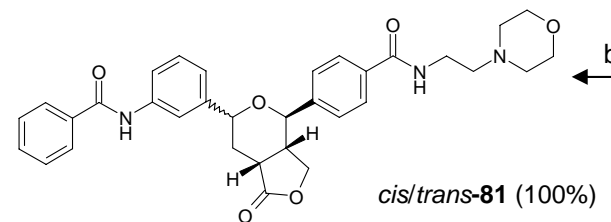




BAL-54



BAL-55



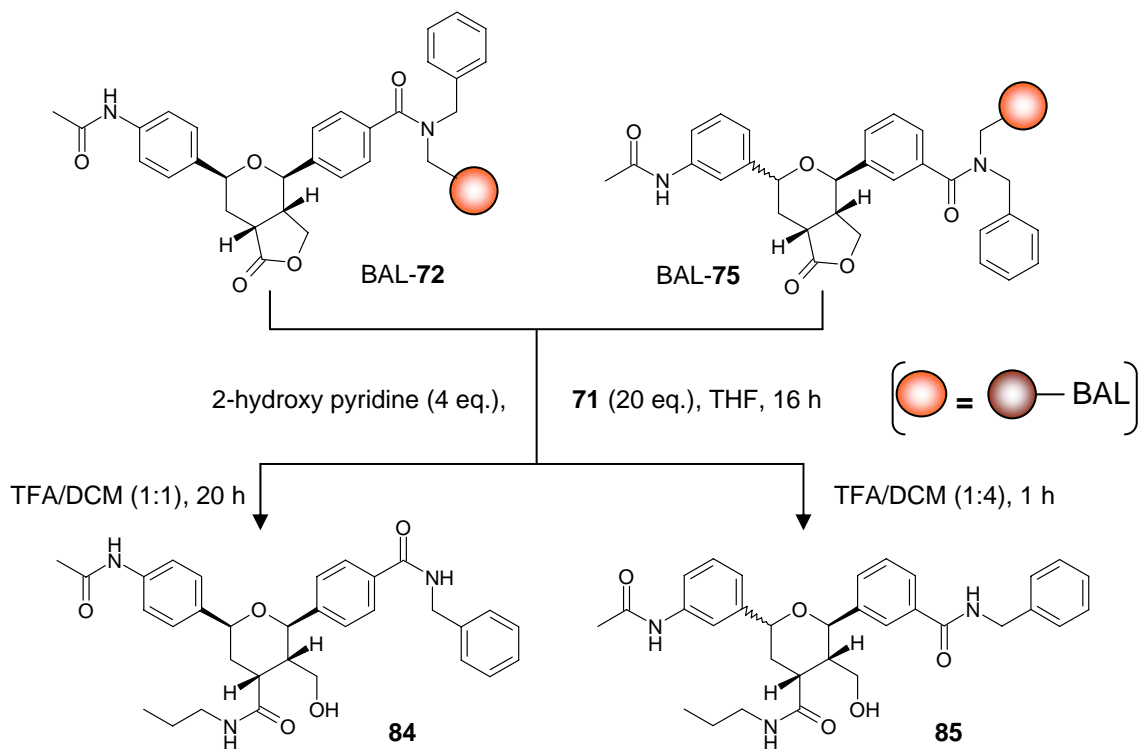
Furopyranones **54** and **55** were derivatised in the same manner using **66** as acylation reagent, **68** for making the urea derivatives and **70** was chosen for synthesising a sulfonic acid derivative.

In the case of furopyranone **54** the BAL-aminomethyl-PS solid support loaded with N-(2-aminoethyl)-morpholine was used as shown in Scheme 4.12. After coupling **54** to the solid support and Fmoc-deprotection the resin was split into three equal batches. The prototypes were synthesised according to the conditions indicated in Scheme 4.12 and the final products **78** – **80** were isolated after an elongated cleaving procedure (TFA/DCM - 1:1 for 19 h) followed by purification *via* preparative reversed phase LC and drying (vacuum). As expected only one single product was obtained for each derivation step and the yields varied from 100% for **78** and **79** to 29% for **80**. The acylation of **78** and the formation of the urea derivative **79** worked very well while the yield for **80** was low. Drying (vacuum) the compounds after purification gave yields for **78** and **79** slightly over 100% because there was still some solvent (e.g. water) inside as detected by NMR spectroscopy. Product **80** was isolated pure and was analysed by NMR spectroscopy.

In the case of furopyranone **55** again the BAL-aminomethyl-PS solid support loaded with N-(2-aminoethyl)-morpholine was used as shown in Scheme 4.12. After coupling **55** to the solid support and Fmoc-deprotection the resin was split into three equal batches. The prototypes were synthesised according to the conditions indicated in Scheme 4.12 and the final products **81** – **83** were isolated after a normal cleaving procedure (TFA/DCM - 1:4 for 1 h) followed by purification *via* preparative reversed phase LC and drying (vacuum). LC-MS analyses of the acylation product **81** before purification showed a ratio for the two diastereomers of 1:3 (*cis/trans*-**81**). The overall yield for the diastereomeric mixture was again slightly over 100% because the product still had some solvent inside as detected by NMR spectroscopy. After purification 86% of *trans*-**81**, 10% of *cis*-**81** and a fraction of the diastereomeric mixture were isolated what allowed the analysis of the single diastereomers. In the case of the urea derivative **82** LC-MS analyses before purification showed a ratio for the two diastereomers of 4:13 (*cis/trans*-**82**). The overall yield for the diastereomeric mixture was again over 100% because the product still had some water inside as detected by NMR spectroscopy. After purification 90% of *trans*-**82** and 20% of *cis*-**82** without a fraction of the diastereomeric mixture were isolated what allowed the analysis of the single diastereomers. LC-MS analyses of **83** before purification showed a ratio for the two diastereomers of about 1:4 (*cis/trans*-**83**). The overall yield for the diastereomeric mixture was 23% and after purification 19% of *trans*-**83** and a fraction of the diastereomeric mixture (4%) were isolated. Only *trans*-**83** was characterised by NMR spectroscopy.

#### 4.4 Aminolysis of the Lactone Ring

Aminolysis of the lactone ring was tested with compounds **BAL-72** and **BAL-75** as shown in Scheme 4.13. Therefore conditions from the literature were used to perform this reaction.<sup>1, 2, 5</sup>



**Scheme 4.13.** Aminolysis of **72** and **81**. The conditions as indicated were used. Compound **84** was isolated impure (yield: 9%) while in the case of compound **85** only traces of the product were detected *via* LC-MS.

Unfortunately the results from the solid phase aminolysis were disappointing. The conditions for the reaction and cleaving from the solid support were indicated in Scheme 4.13. In both cases the reaction did not work very well and bad yields as well as impure products were obtained. LC-MS analyses of product **84** before purification showed the presence of other products which could not be assigned to expected side products (unoccupied positions of the solid support, reagents). The following purification *via* preparative reversed phase LC and drying (vacuum) resulted in only impure **84** with a yield of 9%. At least the expected product **84** was detected by LC-MS. The same result was obtained analysing product **85** while in this case only traces of the product were detected.

#### 4.5 References for Chapter 4

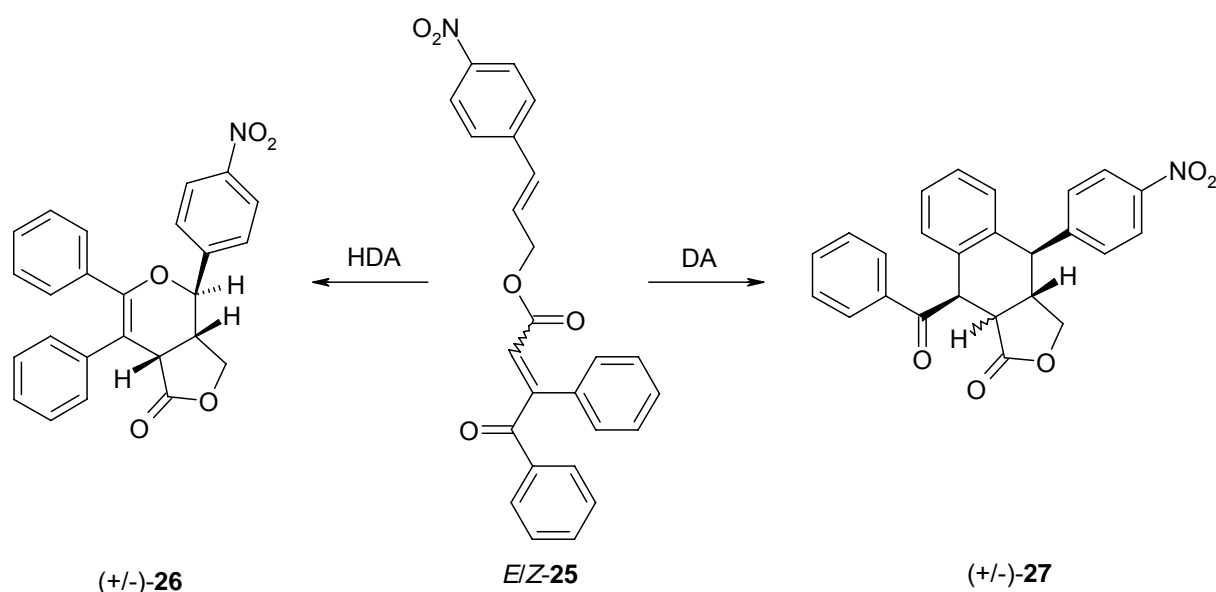
- [1] R. Messer, X. Pelle, A. L. Marzinzik, H. Lehmann, J. Zimmermann, R. Häner, *Synlett* **2005**, 2441-2444.
- [2] Roland Messer, *Natural Product-like Compound Libraries from D-(-) Ribose*, Dissertation **2005**, Universität Bern, Schweiz.
- [3] C. A. Fuhrer, E. Grüter, S. Ruetz, R. Häner, *ChemMedChem* **2007**, 2, 441-444 (and references therein).
- [4] L. A. Carpino, G. Y. Han, *J. Org. Chem.* **1972**, 37, 3404-3409.
- [5] D. S. Tan, M. A. Foley, B. R. Stockwell, M. D. Shair, S. L. Schreiber, *J. Am. Chem. Soc.* **1999**, 121, 9073-9087.

## 5. Conclusions & Outlook

### 5.1 Antiproliferative Activity of Natural Product-Like Furopyranones

A short and facile route to bicyclic, natural product-like furopyranones, which contain several structural motifs (*cis*-stilbene, iridoid-like structure,  $\gamma$ -lactone) found in natural products with anticancer properties, has been worked out. To assist the search for drugs, we focused our efforts towards the hit/lead identification process. Since natural products have been the mainstay of cancer chemotherapy for more than the past 30 years, our scaffolds are based on a natural product-like geometry.<sup>1</sup>

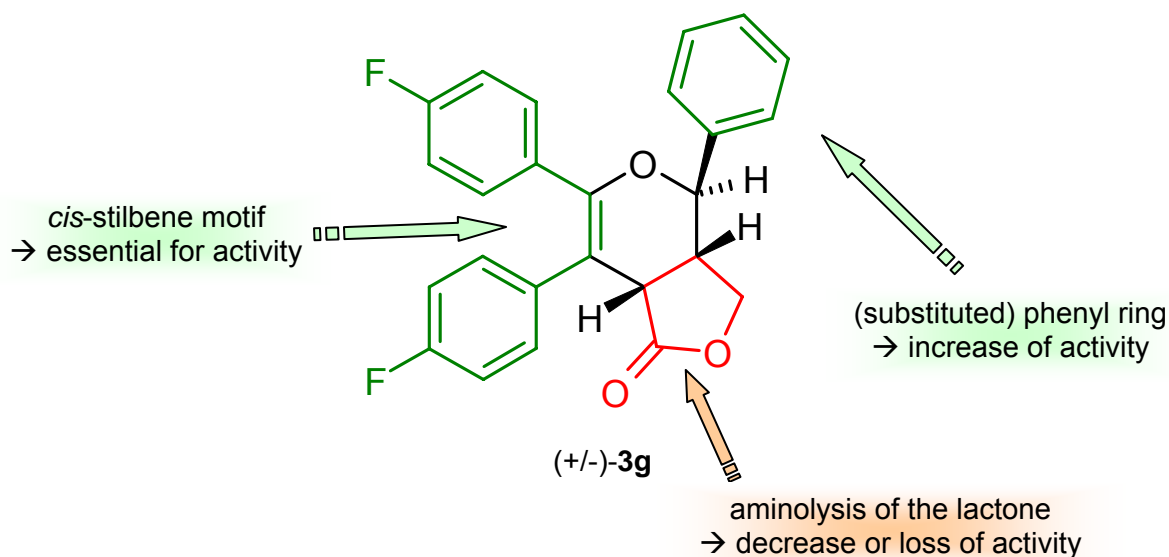
The key step of the synthesis involves an intramolecular *hetero* Diels-Alder (HDA) reaction. Depending on the substitution pattern of the diene, the reaction proceeds with high diastereoselectivity. A substituent in  $\beta$ -position of the  $\alpha,\beta$ -unsaturated  $\gamma$ -ketoesters (e.g. ester **25**, Scheme 5.1) leads to the selective formation of *cis*-fused furopyranones as shown in Figure 5.1. Without substitution in  $\beta$ -position, *cis*- and *trans*-fused products were formed during the *hetero* Diels-Alder reaction.<sup>2,3</sup> In selected cases, formation of tricyclic products like **27** via a normal Diels-Alder (DA) was observed (see Scheme 5.1). While the bicyclic furopyranones can be synthesised from the *E*- and *Z*-isomer of the corresponding precursors like **25**, the tricyclic compounds were only formed via the *Z*-isomer.



**Scheme 5.1.** Synthesis of furopyranone **26** via an intramolecular *hetero* Diels-Alder reaction and the *cis-trans*-tricyclic scaffold **27** via a normal Diels-Alder reaction.

Furopyranones synthesised in this way showed antiproliferative and apoptotic activity in several human cancer cell lines (e.g. KB31 and A549) with  $\text{IC}_{50}$  values in the low  $\mu\text{M}$  range.

Furthermore cell cycle analysis showed that the compounds led to a significant and dose dependent cell cycle arrest in the G2/M-phase. In a detailed SAR study the *cis*-stilbene moiety was identified as a significant part of the pharmacophore. In addition, a phenyl ring next to the *cis*-stilbene moiety had a positive effect on the activity, but aminolysis of the lactone decreased or eliminated the biological activity. Finally, fluorine substituents led to an increase in antiproliferative and apoptotic activity (see Figure 5.1). Since the compounds do not violate the 'Rule of Five', they can be considered as a potential class of drugs suitable for possible oral administration.<sup>4</sup>



**Figure 5.1.** Structure of furopyranone **3g** and the results of the SAR study.

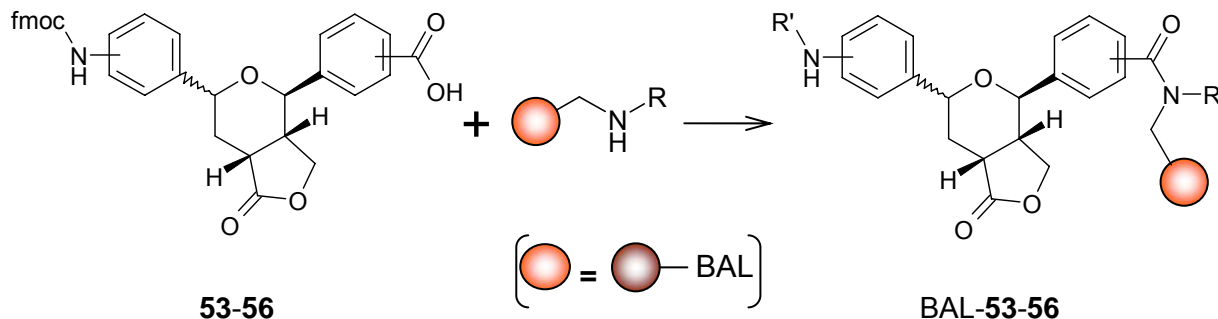
## 5.2 Solid Support Chemistry of Furopyranones

Furopyranones suitable for solid phase chemistry were synthesised from simple precursors. The key step of the synthesis is a *hetero* Diels-Alder reaction leading to the bicyclic furopyranones. After hydrogenation and Fmoc-protection of the aniline moiety the final mixture of diastereomeric compounds is linked on different BAL-aminomethyl-PS solid supports (see Scheme 5.2). These solid supports featured the advantage of yielding N-substituted carboxyamides upon release from the support.

Synthesis of prototype libraries included acylation and formation of urea and sulfonic acid derivatives as well as aminolysis of the lactone ring. The results showed that all furopyranones are suitable for solid phase chemistry. The best results were obtained with the urea derivatives followed by the acylation reactions. The synthesis of sulfonic acid derivatives was not satisfying in all cases and only few products could be isolated in a pure state. Finally, aminolysis of the lactone ring did not work.



If the amine of the aniline part was in *meta*-position, additional purification was necessary to separate the diastereomeric mixtures while an amine in *para*-position yielded a single diastereomer after epimerisation under acidic conditions.



**Scheme 5.2.** Solid support chemistry of the synthesised furopyranones **53-56**.

### 5.3 Outlook

As an outlook for the medicinal chemistry project several aspects can be addressed. The successful chemical genetic approach to find novel agents with biological activity resulted in the synthesis of different furopyranones followed by *in vitro* screening of different human cancer cell lines. The compounds showed potent antiproliferative and apoptotic activity but the mode of action of the furopyranones is still unknown. Therefore a strategy for the identification of the target(s) should be envisaged. Traditionally, the protein targets of small-molecule ligands have been identified using *in vitro* methods such as affinity chromatography and photoaffinity labelling. These methods have been integral to target identification, but they are laborious and subject to low protein expression levels, protein degradation during cell lysis or insufficient affinity for the small ligand. Another approach involves expression profiling using DNA microarrays. The DNA microarray technology allows the differential analysis of gene expression and has been used in many fields of biological and medical research in recent years. First efforts in this direction were made for the target identification of furopyranones but significant results could not be obtained. An enzyme based HT-screening of the furopyranones may also result in the target protein which interacts with the compounds.<sup>5, 6, 7</sup>

Another point is the improvement of the biological activity of the furopyranones. For this purpose new derivatives have to be synthesised to extend the SAR study and to enhance the anticancer properties. A substitution pattern similar to the one of combretastatin A-4 might well improve the biological activity. Furthermore the influence of fluorine substitution at the *cis*-stilbene moiety and the consequences on the antiproliferative and apoptotic activity

should be examined. The latter mentioned perspectives are the topic of ongoing master thesis projects.

#### 5.4 References for Chapter 5

- [1] J. Mann, *Nature Rev. Cancer* **2002**, 2, 143-148.
- [2] C. A. Fuhrer, R. Messer, R. Häner, *Tetrahedron Lett.* **2004**, 45, 4297-4300 (and references therein).
- [3] C. A. Fuhrer, E. Grüter, S. Ruetz, R. Häner, *ChemMedChem* **2007**, 2, 441-444 (and references therein).
- [4] C. A. Lipinski, F. Lombardo, B. W. Dominy, P. J. Feeney, *Adv. Drug Deliv. Rev.* **1997**, 23, 3-25.
- [5] S. Lefurgy, V. Cornish, *Chem. Biol.* **2004**, 11, 151-153.
- [6] L. Buridine, T. Kodadek, *Chem. Biol.* **2004**, 11, 593-597.
- [7] G. P. Tochtrop, R. W. King, *Comb. Chem. High Throughput Screen.* **2004**, 7, 677-688.

## 6. Experimental Part

Instrumentation and other equipments used at the 'Novartis Institutes for BioMedical Research' are not described in this chapter.

### 6.1 Instrumentation

#### 6.1.1 NMR Spectroscopy

<sup>13</sup>C- and <sup>1</sup>H-NMR spectra were recorded on the following NMR spectrometers:

- BRUKER AVANCE300 [Magnetic Field: 7.046 Tesla; Spectrometer Frequency: 300.18 MHz (1H)]
- BRUKER DRX400 [Magnetic Field: 9.395 Tesla; Spectrometer Frequency: 400.13 MHz (1H)]
- BRUKER DRX500 [Magnetic Field: 11.744 Tesla; Spectrometer Frequency: 500.13 MHz (1H)]

The spectra are reported with the chemical shift  $\delta$  (ppm) relative to the signals of the NMR-solvents.<sup>1</sup>

Solvent	<sup>1</sup> H-Signal	<sup>13</sup> C-Signal
CDCl <sub>3</sub>	7.26	77.16
DMSO-D <sub>6</sub>	2.50	39.52

<sup>31</sup>P-NMR: Bruker AVANCE 300,  $\delta$  values in ppm (external calibration done by software using an additionally measured <sup>31</sup>P spectrum of 85% H<sub>3</sub>PO<sub>4</sub> in H<sub>2</sub>O). The <sup>1</sup>H-NMR chemical shifts and coupling constants were determined assuming first-order behaviour. Multiplicities are reported using the following abbreviations: s (singlet), d (doublet), dd (doublet of doublets), dt (doublet of triplets), t (triplet), q (quartet). Where coupling behaviour of higher order has to be assumed the abbreviations m (multiplet) or br (broad) have been used. The list of coupling constants *J* [Hz] corresponds to the order of the multiplicity assignment. The NMR data was evaluated with the Bruker programs, 1D WIN-NMR and 2D WIN-NMR, version 6.0.

Special analyses were carried out by the Analytical Research and Services (ARS) of Prof. Dr. P. Bigler, Departement of Chemistry and Biochemistry, University of Bern, Switzerland (Bruker DRX400 and Bruker DRX500).

### 6.1.2 Mass Spectrometry

All mass spectrometric measurements were carried out by the Analytical Research and Services (ARS) of Dr. S. Schürch and Prof. Dr. J. Schaller, Departement of Chemistry and Biochemistry, University of Bern, Switzerland.

Electron Ionization Mass Spectrometry (EI-MS / EI-MS HR): Micromass Autospec Q (Waters / Micromass), Ionization mode: electron impact, Ionization energy: 70 eV, Sample inlet: solids probe, Acceleration voltage: 8 kV, Mass resolving power: >1000 (10% valley), Calibration: External calibration using perfluorokerosene (PFK). The mass accuracy is on the order of  $\pm 2$  ppm.

Electrospray Mass Spectrometry (ESI-MS HR): Applied Biosystems / Sciex QSTAR Pulsar (hybrid quadrupole time-of-flight mass spectrometer), Ion source: nanoelectrospray, Injection: glass needle; sample volume: 1-4  $\mu\text{l}$ ; flow rate: 10-30 nl/min, Needle potential: 700 to 900 V (both polarities), Curtain gas: nitrogen, external calibration with caesium iodide and reserpine (positive ion mode), mass accuracy is better than  $\pm 5$  ppm.

Without further information the molecular weight (MW) is given for each compound.

### 6.1.3 IR –Spectroscopy

Infrared spectra were recorded on an OMNILAB Jasco FT/IR-460 Plus spectrophotometer with a Specac MK II Golden Gate™ Single Reflection ATR System.

### 6.1.4 UV-VIS Spectroscopy

UV-VIS spectra were recorded with *UV-Visible Spectrophotometer UV-1601* of SHIMADZU. The blank, spectra of pure solvent or buffer with the same UV-cell, was subtracted from measured spectra to receive corrected spectra.

### 6.1.5 Melting Point Measurement

Melting points were determined in open capillaries using a *Büchi Melting Point B-545* apparatus and are uncorrected.

### 6.1.6 Analytical TLC and Preparative Column Chromatography

All reactions were monitored by thin layer chromatography (TLC), which was carried out on 0.25 mm Macherey-Nagel silica gel-25 UV254 precoated plates or silica-gel 60 F254 glass plates (Merck). Visualisation by UV and/or by dipping in a solution of anisaldehyde (2%) and conc. H<sub>2</sub>SO<sub>4</sub> (3%) in EtOH or a solution of vanillin (8.6 g) and conc. H<sub>2</sub>SO<sub>4</sub> (2.5 ml) in EtOH (200 ml) followed by heating. Flash column chromatography (CC): Silica 60 A 40-63 µm (SDS, France) at low pressure. Silica gel was suspended, in starting eluent, before filled into column and then covered with cristobalite (sea sand). After the dissolved crude material was added, solvent, isocratic or gradient, was pumped through the column. Collected fractions were controlled by TLC.

### 6.1.7 High Performance Liquid Chromatography (HPLC)

Bio-Tek Kontron Instruments, HPLC 545V Diode Array Detector, System 525; normal phase HPLC-Cartridge from MERCK (Germany), LiChrospher® Si 60 (10 µm), LiChroCART® 250-10; Software: Galaxie Chromatography Data System, Version 1.7.4.5, from Varian; Gradient: Ethyl acetate / hexane (40:60 → 100:0 or 50:50 → 100:0); UV detection: λ=255-320 nm.

### 6.1.8 X-Ray Crystal Structure Analyses

The X-ray crystal structure analysis was carried out by the BENEFR - Crystallography Service (Prof. Helen Stoeckli-Evans and Dr. Antonia Neels), Institute of Microtechnology, University of Neuchâtel, Switzerland.

Normally the intensity data were collected at 173K (-100°C) on a Stoe Mark II-Image Plate Diffraction System<sup>2</sup> equipped with a two-circle goniometer and using MoKα graphite monochromated radiation. Usually the structures were solved by Direct methods using the programme SHELXS.<sup>3</sup> The refinement and all further calculations were carried out using SHELXL-97.<sup>4</sup> The H-atoms were located from difference Fourier maps and refined isotropically. The non-H atoms were refined anisotropically, using weighted full-matrix least-squares on F<sup>2</sup>. The molecular structure and crystallographic numbering scheme are illustrated in the PLATON<sup>5</sup> drawing.

Supplementary data for the corresponding structures, which were not yet published, is presented in the chapter 5 (Appendix).

### 6.1.9 Autoclave

A high pressure reactor made of high-alloy, SS 316 TI stainless steel with PTFE lining by *Berghof* was used. Type: HR-100; 150 ml, 100 bar, 250°C. The autoclave is equipped with a rupture disc to reliably limit maximum pressure, clamping ring for tool-free opening and closing, thermometer, pressure gauge and sample extraction device.

Furthermore 'Parr Acid Digestion Bombs' were used as autoclave:

Bomb Part Number	4749
Size, ml	23
Maximum Charge, grams:	
• Inorganic Sample	1.0
• Organic Sample	0.1
Recommended Maximum:	
• Temperature, °C	250
• Absolute Maximum Temperature, °C	250
• Absolute Maximum pressure, psig	1800

Parr Instrument Company, 211 Fifty-Third Street, Moline, Illinois 61265 USA; <http://www.parrinst.com>

### 6.1.10 Cellular Assays and Cell Cycle Analysis (KB31 and A549 Cells)

Cellular assays and cell cycle analysis of KB31 and A549 cells were performed by Dr. Stephan Ruetz and his team at the 'Novartis Institutes for BioMedical Research' in Basel (Switzerland). Effect of inhibitors on viability and onset of apoptosis is assessed by the YO-PRO-1 assay. Cell cycle stages were analyzed by laser-scanning cytometry. For detailed information see the appendix (Chapter 7).

## 6.2 Solvents, Chemicals and Consumables

Chemicals, solvents, and reagents for reactions were from *Acros Organics*, *Sigma-Aldrich*, *Fluka* or *Alfa Aesar* and were of the highest quality available. Solvents for extraction and chromatography were of technical grade and distilled prior to use. Organic solvents used for HPLC were of HPLC quality from *Acros Organics* (Methanol, EtOAc, *n*-hexane > 95%).

Deionised water was used for synthesis work up. Deuterated solvents for NMR were from *Cambridge Isotope Laboratories Inc.*. Syringes and needles used were from *Braun AG* or *ROSE GmbH*. As protecting gas  $N_2$  45 from *Carbagas* was used.

## 6.3 Solid Support Chemistry

The whole solid support chemistry was carried out at the 'Novartis Institutes for BioMedical Research' in the laboratory of Dr. Bahaa Salem in Basel, Switzerland. Furthermore the equipment at the 'Novartis Institutes for BioMedical Research' was used (synthesis, analysis, purification).

### 6.3.1 Loading Efficiency and Loading Capacity

Each type of solid support and even each batch of a specific resin is different regarding its loading capacity. The loading capacity is the maximum amount (mmol/g) of an ideal coupling partner that can be bound onto the surface of a certain quantity of solid support. When immobilizing a substrate on a solid support only a fraction of the available functional groups get occupied, depending on the substrate and the conditions. The loading efficiency is expressed as the ratio of [bound substrate (mmol/g)/loading capacity (mmol/g)]·100%.

### 6.3.2 UV-Spectroscopic Quantification of the Loading Efficiency

In the case of immobilised substrates containing chromophoric protection groups (e.g. Fmoc) the loading efficiency can be determined accurately by UV spectroscopic quantification. In the case of an Fmoc-protecting group cleaved with piperidine, the dibenzovulvene-piperidine adduct is formed from dibenzovulvene ( $299 < \lambda < 301$  nm,  $\epsilon = 7800$  l/mol·cm).<sup>6</sup> The absorbance  $A$  of an aliquot of the cleaving solution is measured to get exact concentration of the cleaving product. The quantity of substrate bound on the support derived from this method is put into relation with the loading capacity as described above.

### 6.3.3 Absorbance and Extinction Coefficient

The absorbance  $A$  is the logarithm to base ten of the reciprocal of the spectral internal transmittance  $T$ .



$$A = -\log T = \varepsilon * c * d$$

The reading displayed by most commercially available photometers is the absorbance, because it is proportional to the concentration according to the Lambert-Beer's Law. The extinction coefficient  $\varepsilon$  (l/mol\*cm) is the constant used in the Beer-Lambert's Law which relates the concentration  $c$  (mol/l) of the substance being measured and the path length  $d$  (cm) to the absorbance of the substance in solution at a specific wavelength. Normally a cuvette where  $d = 1$  cm (width of the cuvette) is used.

$$\varepsilon = A / (c * d)$$

### 6.3.4 General Methods for the Solid Phase Chemistry

#### 6.3.4.1 Initial Tests with Compounds **53**, **54**, **55** and **56**

For the first tests of the solid support chemistry the BAL-aminomethyl-PS-solid support loaded with benzyl amine was used in combination with every compound (**53**, **54**, **55** and **56**). The following procedure was made with compounds **53**, **54**, **55** and **56**. For the loading capacity a mean of 0.6 mmol/g was used for the calculation.

##### Coupling Step:

The resin (10 mg, 0.006 mmol, 1 eq.) was put into an eppendorf vessel (0.5 ml). In a second eppendorf vessel (0.5 ml) HCTU (7.5 mg, 0.018 mmol, 3 eq.), HOBt (2.4 mg, 0.018 mmol, 3 eq.) and the corresponding furopyranone (**53**, **54**, **55** or **56**, 10.4 mg, 0.018 mmol, 3 eq.) were dissolved in NMP (60  $\mu$ l). Then DIPEA (6.2  $\mu$ l, 0.036 mmol, 6 eq.) was added and the mixture was shaken for 20 min. The solution was then added to the resin and shaken over night on the shaker. After that the resin was transferred into a syringe with filter frit (1 ml) using DCM.

##### Washing:

All the solid support was washed according to the following method (three times):

- DMA  $\rightarrow$  MeOH  $\rightarrow$  DCM  $\rightarrow$  MeOH (3x)

After the washing procedure the resin was dried (vacuum) for about 15 min.

##### Fmoc-Deprotection and Washing:

200  $\mu$ l of a piperidine/DMA-solution (1:4) were added to the resin and shaken for 0.5 h. Then the solution was sucked off (vacuum) and again the same amount of this deprotection-

solution was added and the resin was shaken for another 0.5 h. Finally the solid support was washed as described before.

#### Acetylation and Washing:

A solution for acetylation with acetic anhydride (12  $\mu$ l), DCM (120  $\mu$ l) and DIPEA (42  $\mu$ l) was prepared and a volume of 87  $\mu$ l was added to the resin. The syringe was closed and shaken for 2 h on the shaker. Then the resin was washed as already described

#### Cleavage:

In a first step the resin was split into 2 equal portions (2 eppendorf vessels). Then the final compound was cleaved using different conditions:

- Portion 1: 100  $\mu$ l TFA/DCM-solution (1:4) for 1 h
- Portion 2 : 100  $\mu$ l TFA/DCM-solution (1:4) for 24 h

During this cleaving step the resins were slightly shaken on a shaker. After that the resins were dried with an air stream and finally 500  $\mu$ l CH<sub>3</sub>CN were added and the vessels were shaken (Vortex).

#### Analysis:

Each portion was analysed by HPLC and LC-MS. For the LC-MS analysis 20  $\mu$ l from the eppendorf vessel were taken and diluted with 80  $\mu$ l CH<sub>3</sub>CN to a total volume of 100  $\mu$ l.

### **6.3.4.2 Testing of Different Solid Supports with Compound 53**

In the case of compound **53** different BAL-aminomethyl-PS-solid supports were tested for their suitability for the solid phase chemistry (see Figure 4.2). From each of these twelve different solid supports 5 mg were taken and tested.

#### Coupling Step:

From each resin 5 mg were put into an eppendorf tube (0.5 ml). For the loading capacity a mean of 0.6 mmol/g was used for the calculation. HCTU (44.7 mg, 0.11 mmol), HOBt (14.6 mg, 0.11 mmol) and **53** (62.2 mg, 0.11 mmol) were dissolved in some NMP. Then DIPEA (37.0  $\mu$ l, 0.22 mmol) was added to the mixture and additional NMP was added so that the total volume of the mixture was about 360  $\mu$ l. This solution was shaken for 20 min on the shaker. 30  $\mu$ l of this solution were added to each resin. Then the eppendorf tubes were closed and shaken over night on the shaker. Finally the resins were transferred with DCM into syringes with filter frits (1 ml).

### Washing:

All the solid supports were washed according to the following method (three times):

- DMA → MeOH → DCM → MeOH (3x)

After the washing procedure the resins were dried (vacuum) for about 15 min.

### Fmoc-Deprotection and Washing:

100 µl of a piperidine/DMA-solution (1:4) were added to each resin and shaken for 0.5 h. Then the solution was sucked off (vacuum) and again the same amount of this deprotection-solution was added and the resins were shaken for another 0.5 h. Finally the solid supports were washed as described before.

### Acetylation and Washing:

A solution for acetylation with acetic anhydride (84 µl), DCM (840 µl) and DIPEA (294 µl) was prepared and a volume of 64 µl was added to each resin. The syringes were closed and shaken for 2 h on the shaker. Then the resins were washed as already described

### Cleavage:

In a first step the resins were transferred into eppendorf vessels (0.5 ml). Then 100 µl of a TFA/DCM-solution (1:4) were added to each resin and shaken for 1 h. After that the vessels were opened and dried with an air stream. Then 500 µl CH<sub>3</sub>CN were added and the vessels were shaken (Vortex).

### Analysis:

Each resin was analysed by LC-MS. For the LC-MS analysis 20 µl from the eppendorf vessel were taken and diluted with 80 µl CH<sub>3</sub>CN to a total volume of 100 µl.

#### **6.3.4.3 Fmoc-Determination of the Loading of the Resin**

For the Fmoc-determination compounds **53** and **54** and the BAL-aminomethyl-PS solid support loaded with benzyl amine (max. loading = 0.84 mmol/g) were used. For every compound two independent experiments with 20 mg of the solid support were made. For the loading of the resin the following coupling mixture was made for 20 mg (0.012 mmol) of resin (calculated with 0.6 mmol/g loading of the solid support):

- HCTU (14.9 mg, 0.036 mmol), HOBt (4.9 mg, 0.036 mmol) and **53** or **54** (20.7 mg, 0.036 mmol) and DIPEA (12.32 µl, 0.72 mmol) were dissolved in NMP (120 µl).

After washing and drying the solid support the Fmoc-cleavage was done.

Fmoc-Cleavage: The procedure described is for a sample of 20 mg of solid support. 2 ml of a piperidine/DMA-solution (1:4) was left to run through the resin into a 100 ml volumetric flask. This action was carried out 22 times (44 ml total cleavage solution, always collecting in the same flask). 2 ml of DMA was then left to run through the resin into the same flask in order to wash out any remaining cleavage solution. The mixture was filled up to 100 ml with MeOH and mixed so it became homogenous. The UV absorbance was measured as soon as the solution was made.

UV Measurement: Neat MeOH was used as a reference for the blank. The UV absorbance of a sample of the cleavage solution was measured. The values needed from this measurement are the maximum UV absorbance and the wavelength (nm) for which this absorbance is observed. In these cases the wavelength was 300.2 nm or 300.5 nm.

Calculation of Loading: According to Beer-Lambert's Law the calculated concentration of a sample is:

$$c \text{ (mol/l)} = A / 7800 \text{ (l/mol)}$$

The amount  $n$  (mol) of dibenzovulvene-piperidine adduct can then be calculated ( $v = 0.1$  l):

$$n \text{ (mol)} = c \text{ (mol/l)} \cdot v \text{ (l)}$$

The Loading is then calculated:

$$\text{Loading (mmol/g)} = [n \text{ (mol)} \cdot 1000] / 0.02 \text{ g}$$

The loading capacity of the solid support, which was used for the calculation, was 0.84 mmol/g (=100%) as specified by the supplier.

For compound **53** absorption of 1.249 and 1.242 corresponding to **95% loading** were found.

For compound **54** absorption of 1.201 and 1.198 corresponding to **92% loading** were found.

#### 6.3.4.4 Synthesis of Prototypes Starting From Compounds 53 and 56

For these compounds the BAL-aminomethyl-PS-solid support loaded with benzyl amine was used. For the loading capacity a mean of 0.6 mmol/g was used for the calculation.

### Coupling Step:

For each compound (**53** and **56**) 480 mg (0.29 mmol, 1 eq.) of the solid support were taken (max. loading = 0.72 mmol/g). HCTU (360.0 mg, 0.87 mmol, 3 eq.), HOBt (117.6 mg, 0.87 mmol, 3 eq.) and **53** or **56** (500.8 mg, 0.87 mmol, 3 eq.) were dissolved in some NMP in a test tube. Then DIPEA (298  $\mu$ l, 1.74 mmol, 6 eq.) was added and NMP was added to the mixture until a total volume of about 2.9 ml. After that the mixture was shaken for 30 min. For each compound (**53** and **56**) the resin (480 mg, 0.29 mmol, 1 eq.) was put into a syringe with a filter frit and was treated with NMP (3 ml) for 30 min (swelling of the resin). Then NMP was sucked off and in one of the two syringes the coupling solution with **53** was added while the coupling solution with **56** was put into the other syringe. Finally the syringes were closed and shaken over night on the shaker.

### Washing:

The solid supports were washed according to the following method (three times):

- DMA  $\rightarrow$  MeOH  $\rightarrow$  DCM  $\rightarrow$  MeOH (3x)

After the washing procedure the resins were dried (vacuum) for about 1 h.

### Splitting, Fmoc-Deprotection and Washing:

Each resin was split into 3 equal portions using DCM. Then all six syringes were treated with 1.5 ml of a piperidine/DMA-solution (1:4) and were shaken for 30 min. After that the solution was replaced and the resins were shaken again for 30 min. Finally the resins were washed as described before.

### Derivatisation:

*Acetylation* (compounds **72** and **75**): each resin was treated with acetyl chloride **65** (53.3  $\mu$ l, 0.75 mmol, 5 eq.) and DIPEA (256.8  $\mu$ l, 1.5 mmol, 10 eq.) in 2.3 ml DMA/DCM-solution (1:1). The resins were shaken for 2 h on the shaker. *Urea derivatives* (compounds **73** and **76**): each resin was treated with isocyanate **67** (73.5  $\mu$ l, 0.75 mmol, 5 eq.) and pyridine (120.7  $\mu$ l, 1.50 mmol, 10 eq.) in 2.3 ml DCM. The resins were shaken for 16 h. *Sulfonic acid derivatives* (compounds **74** and **77**): each resin was treated with sulfonic acid halide **69** (146 mg, 0.75 mmol, 5 eq.) and DIPEA (256.8  $\mu$ l, 1.5 mmol, 10 eq.) in 2.3 ml DMA/DCM-solution (1:1). The resins were shaken for 2 h on the shaker.

### Washing and Splitting:

The resins were washed as described before. The two solid supports from the acetylation were split into 2 equal portions using DCM.

Aminolysis:

*Aminolysis* (compounds **84** and **85**): each resin was treated with amine **71** (115.1  $\mu$ l, 1.40 mmol, 20 eq.) and 2-hydroxypyridine (26.6 mg, 0.28 mmol, 4 eq.) in 1.5 ml THF (dry). The resins were shaken for 16 h.

Washing:

The resins were washed as described before.

Cleavage:

Procedure for compounds **72**, **73**, **74** and **84**: to each resin 4 ml TFA/DCM-solution (1:1) were added (2 ml in the case of **84**) and left for about 20 h. From time to time the resins were stirred with a spatula.

Procedure for compounds **75**, **76**, **77** and **85**: to each resin 4 ml TFA/DCM-solution (1:4) were added (2 ml in the case of **85**) and left for 1 h. From time to time the resins were stirred with a spatula.

The obtained solutions were collected in different sample flasks and dried under an air stream. Then 1 ml CH<sub>3</sub>CN was added to each vessel (except for **73** and **76** due to insolubility) and shaken (Vortex). From each vessel 10 – 20  $\mu$ l were used for LC-MS-analysis and then the samples were purified in the purification laboratory.

Analysis:

After purification each prototype was analysed by LC/MS and NMR spectroscopy.

### 6.3.4.5 Synthesis of Prototypes Starting From Compounds **54** and **55**

For these compounds the BAL-aminomethyl-PS-solid support loaded with N-(2-aminoethyl)-morpholine was used. For the loading capacity a mean of 0.6 mmol/g was used for the calculation.

Coupling Step:

For each compound (**54** and **55**) 450 mg (0.27 mmol, 1 eq.) of the solid support were taken (max. loading = 0.53 mmol/g). HCTU (335.3 mg, 0.81 mmol, 3 eq.), HOBt (109.4 mg, 0.81 mmol, 3 eq.) and **54** or **55** (466.2 mg, 0.81 mmol, 3 eq.) were dissolved in some NMP in a test tube. Then DIPEA (277.2  $\mu$ l, 1.62 mmol, 6 eq.) was added and NMP was added to the mixture until a total volume of about 2.7 ml. After that the mixture was shaken for 30 min. For each compound (**54** and **55**) the resin (450 mg, 0.27 mmol, 1 eq.) was put into a syringe with a filter frit and was treated with NMP (3 ml) for 30 min (swelling of the resin). Then NMP was

sucked off and in one of the two syringes the coupling solution with **54** was added while the coupling solution with **55** was put into the other syringe. Finally the syringes were closed and shaken over night on the shaker.

#### Washing:

The solid supports were washed according to the following method (three times):

- DMA → MeOH → DCM → MeOH (3x)

After the washing procedure the resins were dried (vacuum) for about 1 h.

#### Splitting, Fmoc-Deprotection and Washing:

Each resin was split into 3 equal portions using DCM. Then all six syringes were treated with 1.5 ml of a piperidine/DMA-solution (1:4) and were shaken for 30 min. After that the solution was replaced and the resins were shaken again for 30 min. Finally the resins were washed as described before.

#### Derivatisation & Washing:

*Acylation* (compounds **78** and **81**): each resin was treated with benzoyl chloride **66** (81.2  $\mu$ l, 0.70 mmol, 5 eq.) and DIPEA (239.7  $\mu$ l, 1.40 mmol, 10 eq.) in 2.1 ml DMA/DCM-solution (1:1). The resins were shaken for 2 h on the shaker. *Urea derivatives* (compounds **79** and **82**): each resin was treated with isocyanate **68** (69.0  $\mu$ l, 0.70 mmol, 5 eq.) and pyridine (112.7  $\mu$ l, 1.40 mmol, 10 eq.) in 2.1 ml DCM. The resins were shaken for 16 h. *Sulfonic acid derivatives* (compounds **80** and **83**): each resin was treated with sulfonic acid halide **70** (90.2  $\mu$ l, 0.70 mmol, 5 eq.) and DIPEA (239.7  $\mu$ l, 1.40 mmol, 10 eq.) in 2.1 ml DMA/DCM-solution (1:1). The resins were shaken for 2 h on the shaker.

Afterwards the resins were washed as described before.

#### Cleavage:

Procedure for compounds **78**, **79**, **80**: to each resin 4 ml TFA/DCM-solution (1:1) were added and left for about 19 h. From time to time the resins were stirred with a spatula.

Procedure for compounds **81**, **82**, **83**: to each resin 4 ml TFA/DCM-solution (1:4) were added and left for 1 h. From time to time the resins were stirred with a spatula.

The obtained solutions were collected in different sample flasks and dried under an air stream. Then 1 ml CH<sub>3</sub>CN was added to each vessel and shaken (Vortex). From each vessel 10 – 20  $\mu$ l were used for LC/MS-analysis and then the samples were purified in the purification laboratory.

Analysis: After purification each prototype was analysed by LC-MS and NMR spectroscopy.

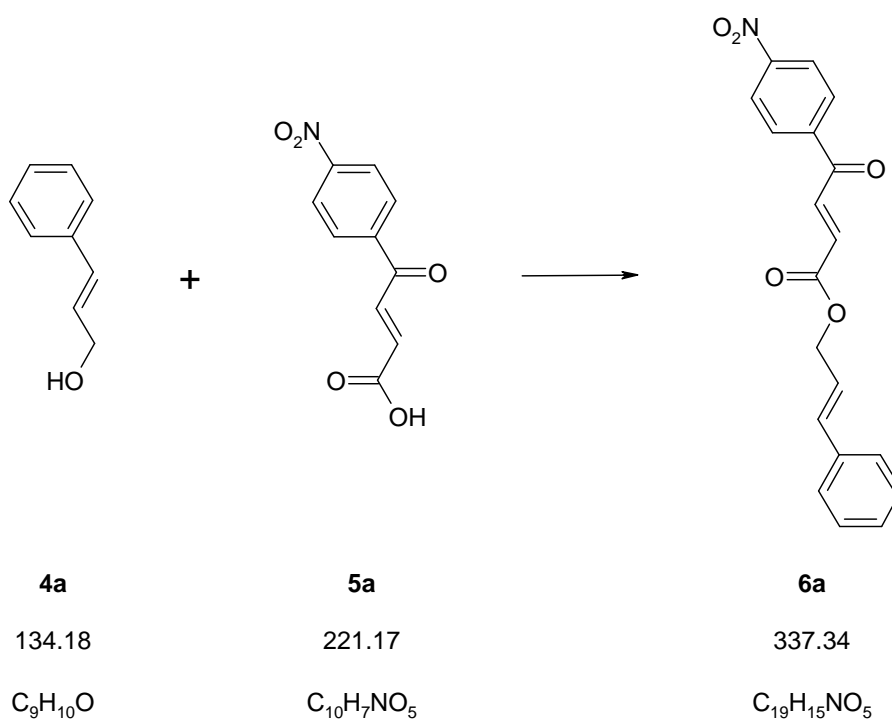
## 6.4 Experimental Procedures and Characterisation Data

Compounds **1**, **2**, **3**,<sup>7</sup> **37**,<sup>8</sup> **43**, **45**, **47** and **49**<sup>9</sup> were already described. For experimental data please see the corresponding literature.<sup>7, 8, 9</sup>

### 6.4.1 Synthesis of Esters 6a-f

**General method (6.4.1) for the esterification:** The corresponding carboxylic acids (1.5 eq.) were dissolved in 1,2-dichloroethane under an argon atmosphere. The reaction mixture was cooled to 0°C and triethylamine (1.6 eq.) was added followed by dropwise addition of pivaloyl chloride (1.5 eq.). The solution was stirred for 30 minutes. Cinnamyl alcohol (1 eq.) or 3-methyl-2-buten-1-ol (1 eq.), dissolved in 1,2-dichloroethane, was added slowly to the stirred solution followed by 4-dimethylaminopyridine (0.2 eq.). The ice bath was removed and the reaction mixture was allowed to stir for 1 - 2.5 hours. After addition of cold sat. NaHCO<sub>3</sub>-solution, the reaction mixture was extracted with diethyl ether. The organic phase was dried (Na<sub>2</sub>SO<sub>4</sub>) and filtered. After concentration, the crude product was purified by flash chromatography and dried (high vacuum).

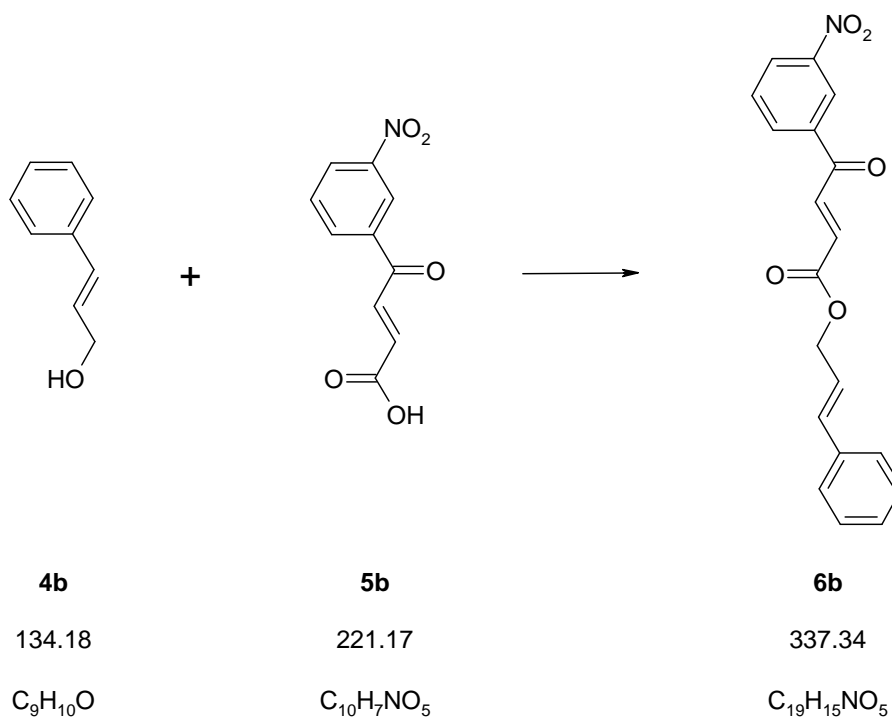
#### 4-(4-Nitro-phenyl)-4-oxo-but-2-enoic acid 3-phenyl-allyl ester (**6a**)





The product was synthesised according to the general method (6.4.1). Cinnamyl alcohol (**4a**, 404 mg, 3.01 mmol), 4-(4-nitro-phenyl)-4-oxo-but-2-enoic acid (**5a**, 1.00 g, 4.52 mmol), triethylamine (0.65 ml, 4.67 mmol), pivaloyl chloride (0.54 ml, 4.40 mmol), DMAP (63 mg, 0.51 mmol), reaction time 2 h. Flash chromatography (ethyl acetate/hexane, 1:4 → 1:2 → 1:0) gave **6a** (642 mg, 63%) as an orange amorphous solid. TLC (ethyl acetate/hexane, 1:1):  $R_f$  0.79.  $^1\text{H-NMR}$  (300 MHz,  $\text{CDCl}_3$ ):  $\delta$  4.92 (d,  $J = 6.59$  Hz, 2H), 6.34 (dt,  $J = 15.82$  Hz, 6.59 Hz, 1H), 6.73 (d,  $J = 15.82$  Hz, 1H), 6.98 (d,  $J = 15.64$  Hz, 1H), 7.28 – 7.43 (m, 5H), 7.90 (d,  $J = 15.45$  Hz, 1H), 8.15 (d,  $J = 9.04$  Hz, 2H), 8.36 (d,  $J = 9.04$  Hz, 2H).  $^{13}\text{C-NMR}$  (75 MHz,  $\text{CDCl}_3$ ):  $\delta$  66.44 (t), 122.33 (d), 124.30 (d, 2C), 126.88 (d, 2C), 128.56 (d), 128.88 (d, 2C), 130.02 (d, 2C), 134.15 (d), 135.50 (d), 135.68 (d), 136.08 (s), 141.18 (s), 150.85 (s), 165.05 (s), 188.27 (s). EI-MS  $m/z$  (%): 337 ( $[\text{C}_{19}\text{H}_{15}\text{NO}_5]^+$ , 7), 205 (40), 150 (37), 133 (100), 117 (63), 115 (82), 105 (69), 91 (39), 76 (37). IR ( $\text{cm}^{-1}$ ): 1708, 1668 (C=O), 1523 (N=O).

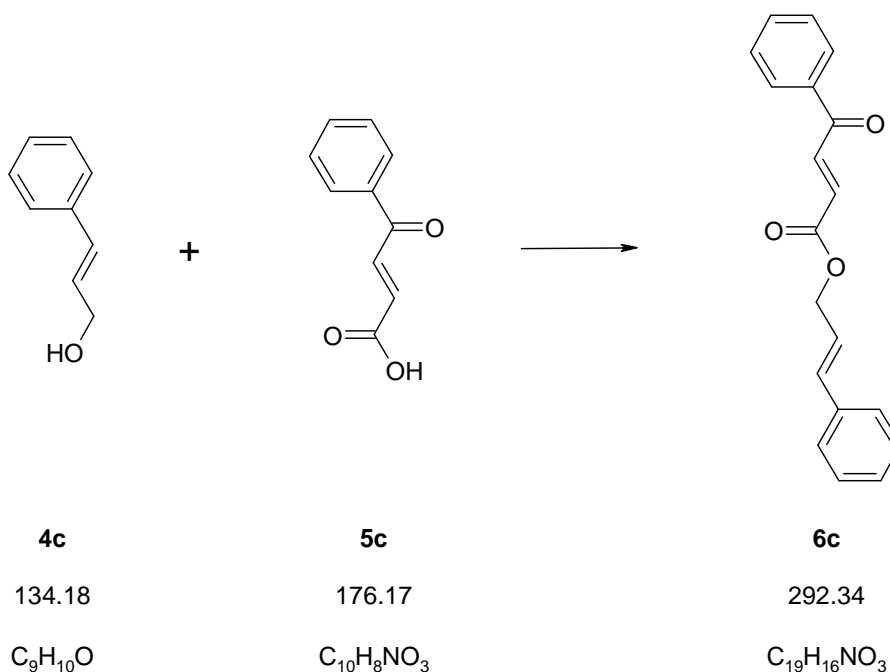
#### 4-(3-Nitro-phenyl)-4-oxo-but-2-enoic acid 3-phenyl-allyl ester (**6b**)



The product was synthesised according to the general method (6.4.1). Cinnamyl alcohol (**4b**, 202 mg, 1.51 mmol), 4-(3-nitro-phenyl)-4-oxo-but-2-enoic acid (**5b**, 500 mg, 2.26 mmol), triethylamine (0.33 ml, 2.34 mmol), pivaloyl chloride (0.27 ml, 2.20 mmol), DMAP (31 mg, 0.26 mmol) reaction time 1.5 h. Flash chromatography (ethyl acetate/hexane, 1:2) gave **6b**

(339 mg, 67%) as a yellow oil. TLC (ethyl acetate/hexane, 1:2):  $R_f$  0.50.  $^1\text{H-NMR}$  (300 MHz,  $\text{CDCl}_3$ ):  $\delta$  4.93 (d,  $J = 6.59$  Hz, 2H), 6.35 (dt,  $J = 15.82$  Hz, 6.59 Hz, 1H), 6.74 (d,  $J = 15.82$  Hz, 1H), 7.01 (d,  $J = 15.45$  Hz, 1H), 7.28 – 7.44 (m, 5H), 7.74 (t,  $J = 8.01$  Hz, 1H), 7.94 (d,  $J = 15.64$  Hz, 1H), 8.33 (d,  $J = 7.96$  Hz, 1H), 8.48 (d,  $J = 8.29$  Hz, 1H), 8.82 (s, 1H).  $^{13}\text{C-NMR}$  (75 MHz,  $\text{CDCl}_3$ ):  $\delta$  66.42 (t), 122.38 (d), 123.81 (d), 126.89 (d, 2C), 128.20 (d), 128.53 (d), 128.86 (d, 2C), 130.43 (d), 134.18 (d), 134.41 (d), 135.35 (d), 135.46 (d), 136.11 (s), 138.00 (s), 148.79 (s), 165.05 (s), 187.51 (s). EI-MS  $m/z$  (%): 337 ( $[\text{C}_{19}\text{H}_{15}\text{NO}_5]^+$ , 7), 205 (44), 150 (42), 133 (100), 117 (70), 115 (83), 105 (65), 91 (43), 76 (47). IR ( $\text{cm}^{-1}$ ): 1723, 1674 (C=O), 1529 (N=O).

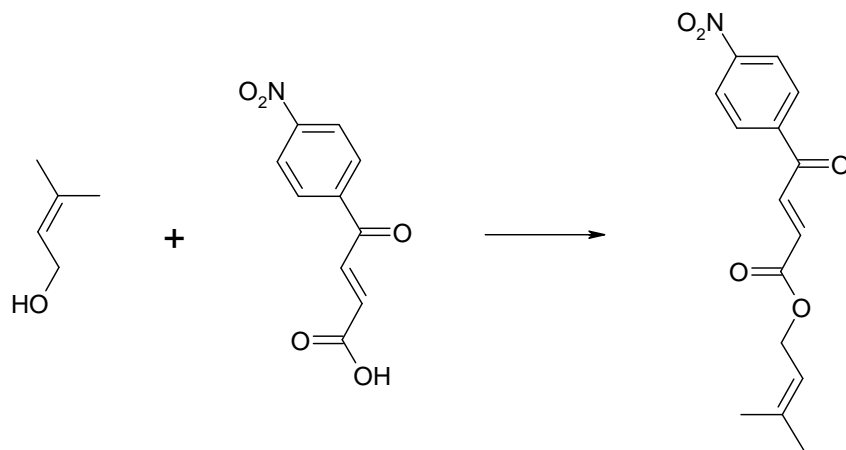
#### 4-Oxo-4-phenyl-but-2-enoic acid 3-phenyl-allyl ester (6c)



The product was synthesised according to the general method (6.4.1). Cinnamyl alcohol (**4c**, 508 mg, 3.78 mmol), 3-benzoylacrylic acid (**5c**, 1.00 g, 5.67 mmol), triethylamine (0.82 ml, 5.87 mmol), pivaloyl chloride (0.68 ml, 5.52 mmol), DMAP (79 mg, 0.64 mmol), reaction time 2 h. Flash chromatography (ethyl acetate/hexane, 1:6) gave **6c** (883 mg, 80%) as an orange oil. TLC (ethyl acetate/hexane, 1:2):  $R_f$  0.69.  $^1\text{H-NMR}$  (300 MHz,  $\text{CDCl}_3$ ):  $\delta$  4.91 (d,  $J = 6.50$  Hz, 2H), 6.34 (dt,  $J = 15.89$  Hz, 6.50 Hz, 1H), 6.73 (d,  $J = 16.01$  Hz, 1H), 6.93 (d,  $J = 15.64$  Hz, 1H), 7.28 – 7.44 (m, 5H), 7.52 (t,  $J = 7.44$  Hz, 2H), 7.63 (t,  $J = 7.35$  Hz, 1H), 7.95 (d,  $J = 15.64$  Hz, 1H), 8.01 (d,  $J = 8.38$  Hz, 2H).  $^{13}\text{C-NMR}$  (75 MHz,  $\text{CDCl}_3$ ):  $\delta$  66.14 (t), 122.63 (d), 126.87 (d, 2C), 128.44 (d, 2C), 128.84 (d), 129.07 (d, 2C), 129.08 (d, 2C), 132.45 (d), 134.06 (d), 135.13 (d), 136.19 (s), 136.76 (s), 136.95 (d), 165.54 (s), 189.65 (s). EI-MS  $m/z$  (%): 292

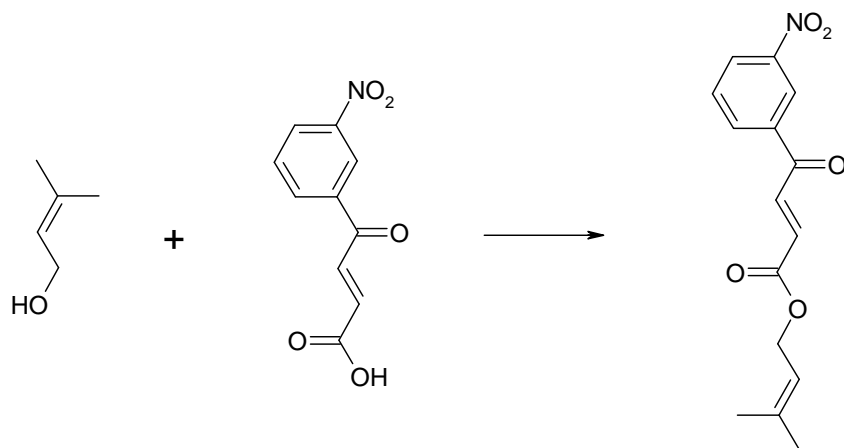
( $[\text{C}_{19}\text{H}_{16}\text{O}_3]^+$ , 79), 160 (100), 131 (54), 115 (61), 105 (97), 77 (64). IR ( $\text{cm}^{-1}$ ): 1709, 1672 (C=O).

#### 4-(4-Nitro-phenyl)-4-oxo-but-2-enoic acid 3-methyl-but-2-enyl ester (**6d**)



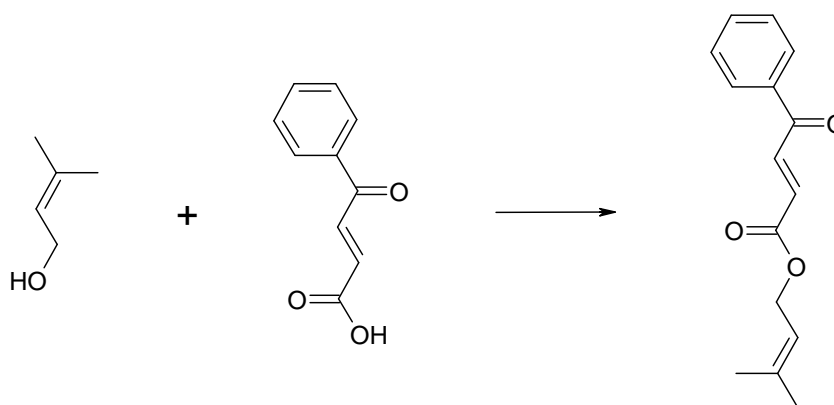
<b>4d</b>	<b>5d</b>	<b>6d</b>
86.13	221.17	289.29
$\text{C}_5\text{H}_{10}\text{O}$	$\text{C}_{10}\text{H}_7\text{NO}_5$	$\text{C}_{15}\text{H}_{15}\text{NO}_5$

The product was synthesised according to the general method (6.4.1). 3-Methyl-2-buten-1-ol (**4d**, 0.30 ml, 3.01 mmol), 4-(4-nitro-phenyl)-4-oxo-but-2-enoic acid (**5d**, 1.00 g, 4.52 mmol), triethylamine (0.65 ml, 4.67 mmol), pivaloyl chloride (0.54 ml, 4.40 mmol), DMAP (63 mg, 0.51 mmol), reaction time 1 h. Flash chromatography (ethyl acetate/hexane, 1:4 → 1:3) gave **6d** (509 mg, 58%) as a yellow amorphous solid. TLC (ethyl acetate/hexane, 1:2):  $R_f$  0.71.  $^1\text{H-NMR}$  (300 MHz,  $\text{CDCl}_3$ ):  $\delta$  1.76 (s, 3H), 1.79 (s, 3H), 4.75 (d,  $J = 7.35$  Hz, 2H), 5.41 (t,  $J = 7.35$  Hz, 1H), 6.93 (d,  $J = 15.64$  Hz, 1H), 7.85 (d,  $J = 15.64$  Hz, 1H), 8.14 (d,  $J = 8.85$  Hz, 2H), 8.36 (d,  $J = 9.04$  Hz, 2H).  $^{13}\text{C-NMR}$  (75 MHz,  $\text{CDCl}_3$ ):  $\delta$  18.27 (q), 25.98 (q), 62.71 (t), 118.00 (d), 124.26 (d, 2C), 129.99 (d, 2C), 134.51 (d), 135.38 (d), 140.48 (s), 141.26 (s), 150.82 (s), 165.28 (s), 188.39 (s). EI-MS  $m/z$  (%): 289 ( $[\text{C}_{15}\text{H}_{15}\text{NO}_5]^+$ , 2), 205 (78), 150 (66), 104 (61), 85 (100), 76 (67), 69 (81), 53 (57), 41 (90). IR ( $\text{cm}^{-1}$ ): 1721, 1665 (C=O), 1525 (N=O).

**4-(3-Nitro-phenyl)-4-oxo-but-2-enoic acid 3-methyl-but-2-enyl ester (6e)**

<b>4e</b>	<b>5e</b>	<b>6e</b>
86.13	221.17	289.29
$C_5H_{10}O$	$C_{10}H_7NO_5$	$C_{15}H_{15}NO_5$

The product was synthesised according to the general method (6.4.1). 3-Methyl-2-buten-1-ol (**4e**, 0.12 ml, 1.21 mmol), 4-(3-nitro-phenyl)-4-oxo-but-2-enoic acid (**5e**, 400 mg, 1.81 mmol), triethylamine (0.26 ml, 1.87 mmol), pivaloyl chloride (0.22 ml, 1.76 mmol), DMAP (25 mg, 0.20 mmol), reaction time 2 h. Flash chromatography (ethyl acetate/hexane, 1:2) gave **6e** (241 mg, 69%) as a yellow oil. TLC (ethyl acetate/hexane, 1:2):  $R_f$  0.60.  $^1H$ -NMR (300 MHz,  $CDCl_3$ ):  $\delta$  1.76 (s, 3H), 1.79 (s, 3H), 4.76 (d,  $J = 7.35$  Hz, 2H), 5.41 (t,  $J = 7.35$  Hz, 1H), 6.96 (d,  $J = 15.64$  Hz, 1H), 7.74 (t,  $J = 8.01$  Hz, 1H), 7.89 (d,  $J = 15.45$  Hz, 1H), 8.32 (d,  $J = 8.01$  Hz, 1H), 8.48 (d,  $J = 8.20$  Hz, 1H), 8.81 (s, 1H).  $^{13}C$ -NMR (75 MHz,  $CDCl_3$ ):  $\delta$  18.28 (q), 25.98 (q), 62.71 (t), 118.02 (d), 123.80 (d), 128.14 (d), 130.40 (d), 134.40 (d), 134.55 (d), 135.02 (d), 138.06 (s), 140.45 (s), 148.79 (s), 165.28 (s), 187.63 (s). EI-MS  $m/z$  (%): 289 ( $[C_{15}H_{15}NO_5]^+$ , 2), 205 (78), 150 (81), 104 (58), 85 (100), 76 (78), 69 (82), 53 (61), 41 (91). IR ( $cm^{-1}$ ): 1712 (C=O), 1674 (C=O), 1532 (N=O).

**4-Oxo-4-phenyl-but-2-enoic acid 3-methyl-but-2-enyl ester (6f)**

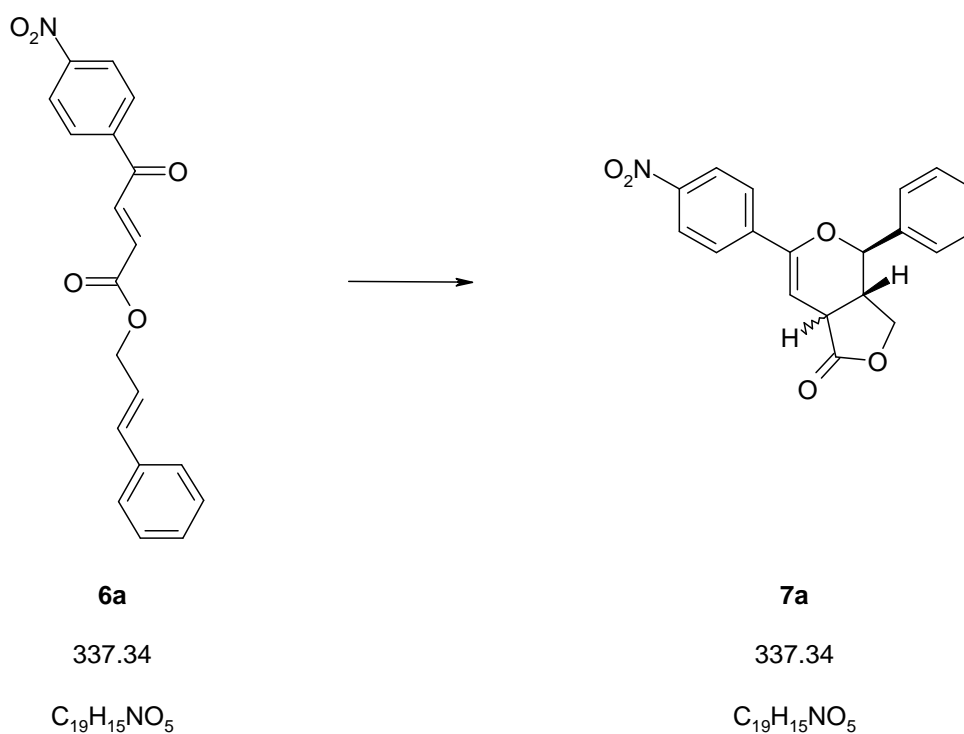
<b>4f</b>	<b>5f</b>	<b>6f</b>
86.13	176.17	244.29
C <sub>5</sub> H <sub>10</sub> O	C <sub>10</sub> H <sub>8</sub> NO <sub>3</sub>	C <sub>15</sub> H <sub>16</sub> NO <sub>3</sub>

The product was synthesised according to the general method (6.4.1). 3-Methyl-2-buten-1-ol (**4f**, 0.38 ml, 3.78 mmol), 3-benzoylacrylic acid (**5f**, 1.00 g, 5.67 mmol), triethylamine (0.82 ml, 5.87 mmol), pivaloyl chloride (0.68 ml, 5.52 mmol), DMAP (79 mg, 0.64 mmol), reaction time 1.5 h Flash chromatography (ethyl acetate/hexane, 1:7) gave **6f** (849 mg, 92%) as an orange oil. TLC (ethyl acetate/hexane, 1:2):  $R_f$  0.67. <sup>1</sup>H-NMR (300 MHz, CDCl<sub>3</sub>): δ 1.75 (s, 3H), 1.79 (s, 3H), 4.74 (d,  $J = 7.35$  Hz, 2H), 5.41 (t,  $J = 7.35$  Hz, 1H), 6.88 (d,  $J = 15.64$  Hz, 1H), 7.51 (t,  $J = 7.63$  Hz, 2H), 7.62 (t,  $J = 7.35$  Hz, 1H), 7.90 (d,  $J = 15.45$  Hz, 1H), 7.99 (d,  $J = 6.97$  Hz, 2H). <sup>13</sup>C-NMR (75 MHz, CDCl<sub>3</sub>): δ 189.77 (s), 165.79 (s), 140.14 (s), 136.81 (s), 136.61 (d), 133.99 (d), 132.80 (d), 129.04 (d, 4C), 118.20 (d), 62.43 (t), 25.97 (q), 18.27 (q). EI-MS  $m/z$  (%): 244 ([C<sub>15</sub>H<sub>16</sub>O<sub>3</sub>]<sup>+</sup>, 4), 160 (69), 105 (36), 68 (45), 44 (100), 41 (38). IR (cm<sup>-1</sup>): 1718, 1671 (C=O).

### 6.4.2 Synthesis of Furopyranones 7a-f

**General method (6.4.2) for the *hetero Diels-Alder* reaction:** The corresponding  $\alpha,\beta$ -unsaturated  $\gamma$ -ketoesters were dissolved in *o*-xylene and refluxed for the indicated time. The solution was poured on saturated aqueous  $\text{NaHCO}_3$ -solution, extracted with ethyl acetate and washed with brine. The organic phase was dried ( $\text{Na}_2\text{SO}_4$ ) and filtered. After concentration, the crude product was purified by flash chromatography and dried (high vacuum). Where possible, the obtained compounds were further recrystallised from the indicated solvents. The ratio of the *cis/trans*-isomers was determined by  $^1\text{H-NMR}$ .

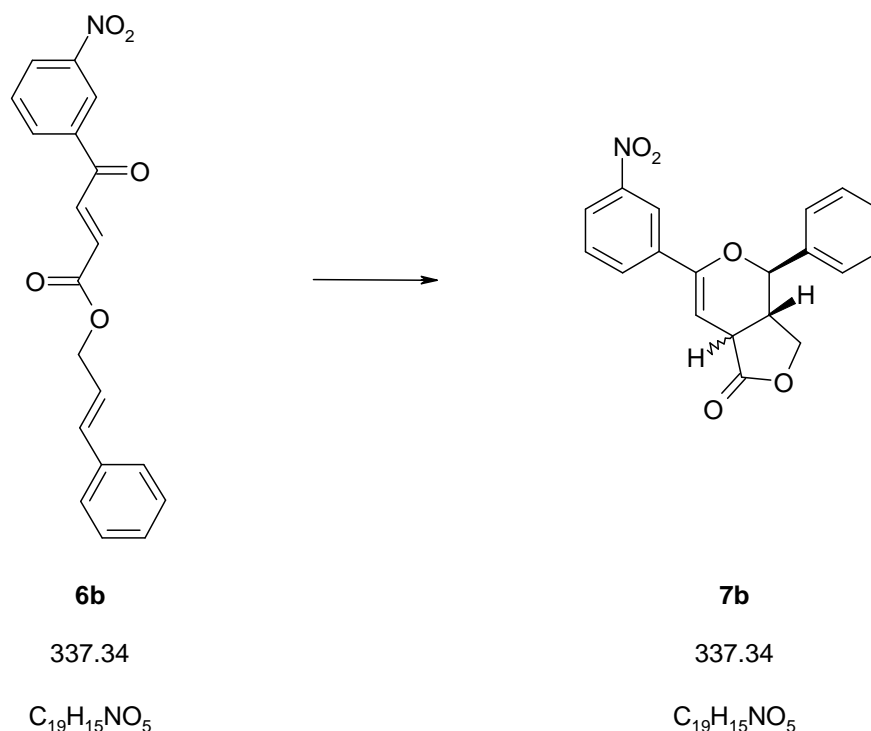
#### 6-(4-Nitro-phenyl)-4-phenyl-3a,7a-dihydro-3H,4H-furo[3,4-c]pyran-1-one (7a)



Ester **6a** (600 mg, 1.78 mmol) was treated according to the general method (6.4.2) in *o*-xylene (30 ml) for 22 h. Ratio of *cis/trans-7a* from NMR of raw product was 92:8. Flash chromatography ( $\text{CHCl}_3/\text{Et}_2\text{O}/\text{hexane}$  1:1:1) yielded **7a** (330 mg, 55%) as a yellow amorphous solid. Pure *cis-7a* (yield = 54%): TLC ( $\text{CHCl}_3/\text{ethyl acetate}/\text{hexane}$ , 1:1:1):  $R_f$  0.30.  $^1\text{H-NMR}$  (300 MHz,  $\text{CDCl}_3$ ):  $\delta$  2.95 (m, 1H), 3.52 (dd,  $J = 7.72$  Hz, 5.09 Hz, 1H), 4.14 (dd,  $J = 10.17$  Hz, 0.94 Hz, 1H), 4.35 (dd,  $J = 10.17$  Hz, 6.41 Hz, 1H), 4.56 (d,  $J = 10.93$  Hz, 1H), 6.02 (d,  $J = 4.90$  Hz, 1H), 7.42 – 7.52 (m, 5H), 7.76 (d,  $J = 9.04$  Hz, 2H), 8.17 (d,  $J = 9.04$  Hz, 2H).  $^{13}\text{C-NMR}$  (75 MHz,  $\text{CDCl}_3$ ):  $\delta$  175.76 (s), 152.70 (s), 148.04 (s), 140.19 (s),

137.62 (s), 129.58 (d), 129.26 (d, 2C), 127.90 (d, 2C), 125.74 (d, 2C), 123.79 (d, 2C), 96.52 (d), 78.59 (d), 67.98 (t), 39.92 (d), 38.64 (d). EI-MS  $m/z$  (%): 337 ( $[\text{C}_{19}\text{H}_{15}\text{NO}_5]^+$ , 15), 150 (79), 143 (100), 142 (57), 128 (57), 115 (65), 105 (46), 91 (49), 77 (39). IR ( $\text{cm}^{-1}$ ): 1770 (C=O); 1514, 1342 (N=O). Mp (MeOH): 149°C. ESI-MSHR positive mode: Calc. mass  $m/z$  (*cis*- $\text{C}_{19}\text{H}_{16}\text{NO}_5$ ) = 338.1028, found: 338.1022. HPLC purity: 97.1%.

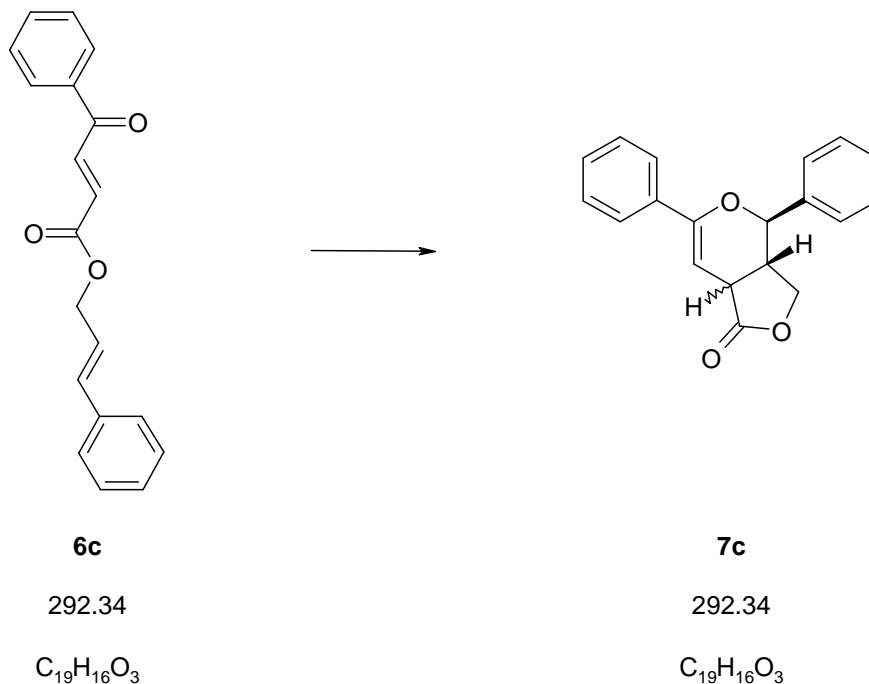
### 6-(3-Nitro-phenyl)-4-phenyl-3a,7a-dihydro-3H,4H-furo[3,4-c]pyran-1-one (7b)



Ester **6b** (149 mg, 0.44 mmol) was treated according to the general method (6.4.2) in *o*-xylene (15 ml) for 24 h. Ratio of *cis/trans*-**7b** from NMR of raw product was 42:58. Flash chromatography (ethyl acetate/hexane, 1:3 → 1:2 → 1:0) yielded **7b** (69 mg 46%) as an amorphous solid. Pure *cis*-**7b** (yield = 35%) was separated by flash chromatography ( $\text{CHCl}_3$ /ethyl acetate/hexane, 1:1:1): TLC (ethyl acetate/hexane, 1:2):  $R_f$  0.30.  $^1\text{H-NMR}$  (300 MHz,  $\text{CDCl}_3$ ):  $\delta$  2.95 (m, 1H), 3.51 (dd,  $J = 7.72$  Hz, 4.90 Hz, 1H), 4.14 (dd,  $J = 10.17$  Hz, 1.13 Hz, 1H), 4.35 (dd,  $J = 10.08$  Hz, 6.31 Hz, 1H), 4.57 (d,  $J = 10.93$  Hz, 1H), 5.97 (d,  $J = 4.90$  Hz, 1H), 7.43 – 7.53 (m, 6H), 7.92 (d,  $J = 8.10$  Hz, 1H), 8.17 (d,  $J = 8.23$  Hz, 1H), 8.44 (s, 1H).  $^{13}\text{C-NMR}$  (75 MHz,  $\text{CDCl}_3$ ):  $\delta$  175.91 (s), 152.55 (s), 148.60 (s), 137.63 (s), 136.07 (s), 130.85 (d), 129.55 (d), 129.49 (d), 129.27 (d, 2C), 127.92 (d, 2C), 123.70 (d), 120.12 (d), 94.99 (d), 78.61 (d), 68.00 (t), 39.03 (d), 38.50 (d). EI-MS  $m/z$  (%): 337 ( $[\text{C}_{19}\text{H}_{15}\text{NO}_5]^+$ , 13), 150 (97), 143 (100), 142 (92), 133 (45), 128 (61), 115 (74), 105 (47), 104 (38), 91 (42), 76

(46). IR ( $\text{cm}^{-1}$ ): 1770 (C=O); 1525, 1346 (N=O). Mp (MeOH): 126°C. ESI-MSHR positive mode: Calc. mass  $m/z$  (*cis*- $\text{C}_{19}\text{H}_{16}\text{NO}_5$ ) = 338.1028, found: 338.1018.

#### 4,6-Diphenyl-3a,7a-dihydro-3H,4H-furo[3,4-c]pyran-1-one (7c)

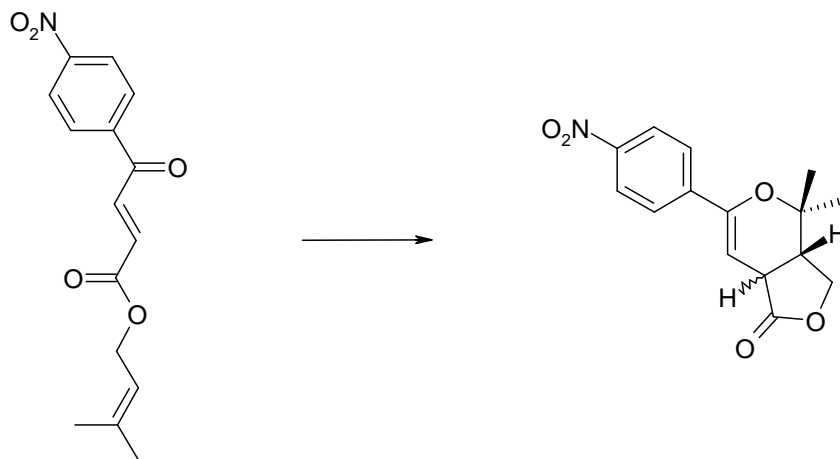


Ester **6c** (785 mg, 2.69 mmol) was treated according to the general method (6.4.2) in *o*-xylene (45 ml) for 46 h. Ratio of *cis/trans*-**7c** from NMR of raw product was 37:63. Flash chromatography (toluene/ $\text{Et}_2\text{O}$ /hexane, 8:1:3) yielded *cis*-**7c** and *trans*-**7c** (307 mg 39%) as a light yellow solid. Pure *cis*-**7c** (yield = 15%) was separated by flash chromatography (toluene/ethyl acetate/hexane, 8:1:3): TLC (*cis*, toluene/ $\text{Et}_2\text{O}$ /hexane, 8:1:3):  $R_f$  0.30.  $^1\text{H}$ -NMR (*cis*, 300 MHz,  $\text{CDCl}_3$ ):  $\delta$  2.91 (m, 1H), 3.45 (dd,  $J = 7.72$  Hz, 4.78 Hz, 1H), 4.13 (dd,  $J = 10.11$  Hz, 1.29 Hz, 1H), 4.32 (dd,  $J = 9.93$  Hz, 6.25 Hz, 1H), 4.56 (d,  $J = 10.66$  Hz, 1H), 5.81 (d,  $J = 4.78$  Hz, 1H), 7.30 – 7.35 (m, 3H), 7.43 – 7.47 (m, 5H), 7.59 – 7.63 (m, 2H).  $^{13}\text{C}$ -NMR (75 MHz,  $\text{CDCl}_3$ ):  $\delta$  176.50 (s), 154.58 (s), 138.29 (s), 134.32 (s), 129.22 (d), 129.09 (d, 3C), 128.43 (d, 2C), 127.88 (d, 2C), 125.12 (d, 2C), 92.32 (d), 78.11 (d), 68.01 (t), 39.17 (d), 38.42 (d). EI-MS  $m/z$  (%): 292 ( $[\text{C}_{19}\text{H}_{16}\text{O}_3]^+$ , 13), 244 (30), 115 (31), 105 (100), 77 (67). IR ( $\text{cm}^{-1}$ ): 1761 (C=O). Mp (*cis*, MeOH): 147°C. EI-MSHR: Calc. mass (*cis*- $\text{C}_{19}\text{H}_{16}\text{O}_3$ ) = 292.109945, found: 292.109950. HPLC purity (*cis*-**7c**): 96.0%. Pure *trans*-**7c** (yield = 11%) was separated by flash chromatography ( $\text{CHCl}_3$ /ethyl acetate/hexane, 1:1:3): TLC (*trans*,  $\text{CHCl}_3$ / $\text{Et}_2\text{O}$ /hexane, 1:1:3):  $R_f$  0.22.  $^1\text{H}$ -NMR (*trans*, 300 MHz,  $\text{CDCl}_3$ ):  $\delta$  2.84 (m, 1H), 3.41



(dd,  $J = 13.56$  Hz, 2.26 Hz, 1H), 4.16 (m, 2H), 5.39 (d,  $J = 10.55$  Hz, 1H), 5.81 (d,  $J = 2.26$  Hz, 1H), 7.32 – 7.46 (m, 8H), 7.62 – 7.66 (m, 2H).

#### 4,4-Dimethyl-6-(4-nitro-phenyl)-3a,7a-dihydro-3H,4H-furo[3,4-c]pyran-1-one (7d)

**6d**

289.29

 $C_{15}H_{15}NO_5$ **7d**

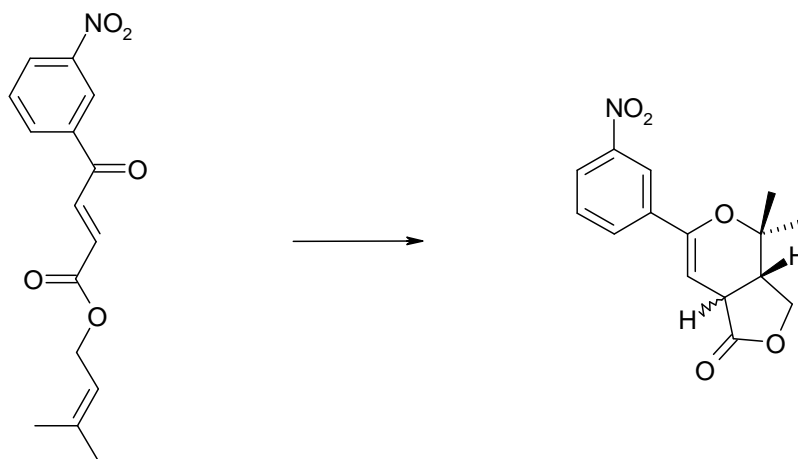
289.29

 $C_{15}H_{15}NO_5$ 

Ester **6d** (437 mg, 1.51 mmol) was treated according to the general method (6.4.2) in *o*-xylene (25 ml) for 22 h. Flash chromatography ( $CHCl_3/Et_2O$ /hexane, 1:1:2) yielded **7d** (289 mg, 66%) as a yellow amorphous solid [ratio of *cis/trans* (36:64)]. Pure *cis*-**7d** (yield = 20%) was separated by flash chromatography (toluene/hexane/ethyl acetate, 8:2:1): TLC (toluene/hexane/ $Et_2O$ , 8:2:1):  $R_f$  (*cis*) 0.40.  $^1H$ -NMR (*cis*, 300 MHz,  $CDCl_3$ ):  $\delta$  1.37 (s, 3H), 1.40 (s, 3H), 2.85 (q,  $J = 8.58$  Hz, 1H), 3.37 (dd,  $J = 8.27$  Hz, 3.49 Hz, 1H), 4.22 (t,  $J = 9.19$  Hz, 1H), 4.46 (t,  $J = 8.64$  Hz, 1H), 5.61 (d,  $J = 3.68$  Hz, 1H), 7.73 (d,  $J = 9.19$  Hz, 2H), 8.19 (d,  $J = 8.82$  Hz, 2H).  $^{13}C$ -NMR (75 MHz,  $CDCl_3$ ):  $\delta$  175.84 (s), 150.01 (s), 147.97 (s), 141.00 (s), 125.73 (d, 2C), 123.74 (d, 2C), 94.26 (d), 74.39 (s), 68.11 (t), 43.12 (d), 37.68 (d), 25.25 (q), 24.61 (q). EI-MS  $m/z$  (%): 289 ( $[C_{15}H_{15}NO_5]^+$ , 60), 245 (100), 230 (41), 216 (54), 202 (71), 150 (66), 120 (69), 95 (73), 76 (40), 44 (52), 41 (62). IR ( $cm^{-1}$ ): 1760 (C=O); 1508, 1350 (N=O). Mp (*cis*, MeOH): 132°C. ESI-MSHR positive mode: Calc. mass  $m/z$  (*cis*- $C_{15}H_{16}NO_5$ ) = 290.1028, found: 290.1025. HPLC purity (*cis*-**7d**): 98.1%. Impure *trans*-**7d** [yield = 10%  $\rightarrow$  ratio of *cis/trans* (34:66)]. TLC (toluene/hexane/ $Et_2O$ , 8:2:1):  $R_f$  (*trans*) 0.47.  $^1H$ -NMR (*trans*, 300 MHz,  $CDCl_3$ ):  $\delta$  1.38 (s, 3H), 1.55 (s, 3H), 2.61 (m, 1H), 3.15 (dd,  $J = 14.13$  Hz, 2.26 Hz,

1H), 4.05 (dd,  $J = 11.68$  Hz, 8.29 Hz, 1H), 4.43 (dd,  $J = 8.29$  Hz, 6.41 Hz, 1H), 5.82 (d,  $J = 2.26$  Hz, 1H), 7.74 (d,  $J = 9.04$  Hz, 2H), 8.19 (d,  $J = 9.04$  Hz, 2H).

#### 4,4-Dimethyl-6-(3-nitro-phenyl)-3a,7a-dihydro-3H,4H-furo[3,4-c]pyran-1-one (7e)

**6e**

289.29

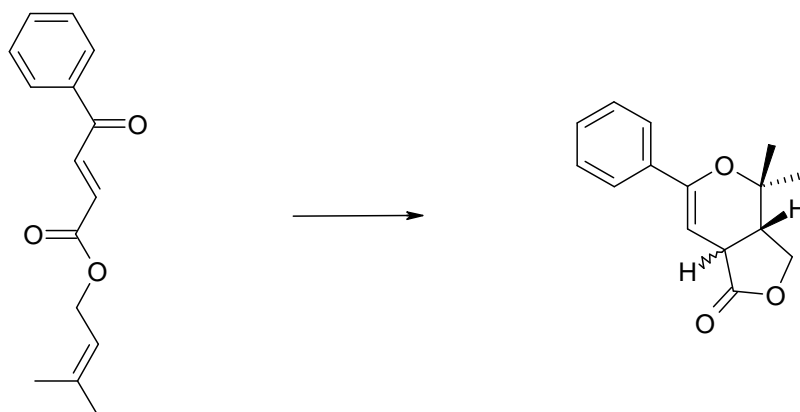
 $C_{15}H_{15}NO_5$ **7e**

289.29

 $C_{15}H_{15}NO_5$ 

Ester **6e** (183 mg, 0.63 mmol) was treated according to the general method (6.4.2) in *o*-xylene (18 ml) for 18 h. Flash chromatography (ethyl acetate/hexane, 1:3 → 1:0) yielded **7e** (80 mg, 44%) as a light yellow foam [ratio of *cis/trans* (97:3)]. Pure *cis*-**7e** (yield = 43%): TLC (ethyl acetate/hexane, 1:2):  $R_f$  0.30.  $^1H$ -NMR (300 MHz,  $CDCl_3$ ):  $\delta$  1.39 (s, 3H), 1.41 (s, 3H), 2.85 (m, 1H), 3.37 (dd,  $J = 8.48$  Hz, 3.58 Hz, 1H), 4.23 (t,  $J = 9.23$  Hz, 1H), 4.46 (dd,  $J = 9.23$  Hz, 8.10 Hz, 1H), 5.56 (d,  $J = 3.58$  Hz, 1H), 7.52 (t,  $J = 8.10$  Hz, 1H), 7.89 (d,  $J = 8.15$  Hz, 1H), 8.18 (d,  $J = 8.15$  Hz, 1H), 8.42 (s, 1H).  $^{13}C$ -NMR (75 MHz,  $CDCl_3$ ):  $\delta$  175.98 (s), 149.83 (s), 148.62 (s), 136.82 (s), 130.79 (d), 129.45 (d), 123.67 (d), 120.08 (d), 92.70 (d), 74.45 (s), 68.11 (t), 43.28 (d), 37.57 (d), 25.27 (q), 24.71 (q). EI-MS  $m/z$  (%): 289 ( $[C_{15}H_{15}NO_5]^+$ , 59), 245 (78), 216 (48), 202 (55), 150 (100), 104 (42), 95 (49), 76 (55), 68 (42), 41 (55). IR ( $cm^{-1}$ ): 1767 (C=O); 1526, 1338 (N=O). Mp (MeOH): 156°C. EI-MSHR: Calc. mass (*cis*- $C_{15}H_{15}NO_5$ ) = 289.095023, found: 289.095000. HPLC purity: 92.6%.

## 4,4-Dimethyl-6-phenyl-3a,7a-dihydro-3H,4H-furo[3,4-c]pyran-1-one (7f)

**6f**

244.29

C<sub>15</sub>H<sub>16</sub>O<sub>3</sub>**7f**

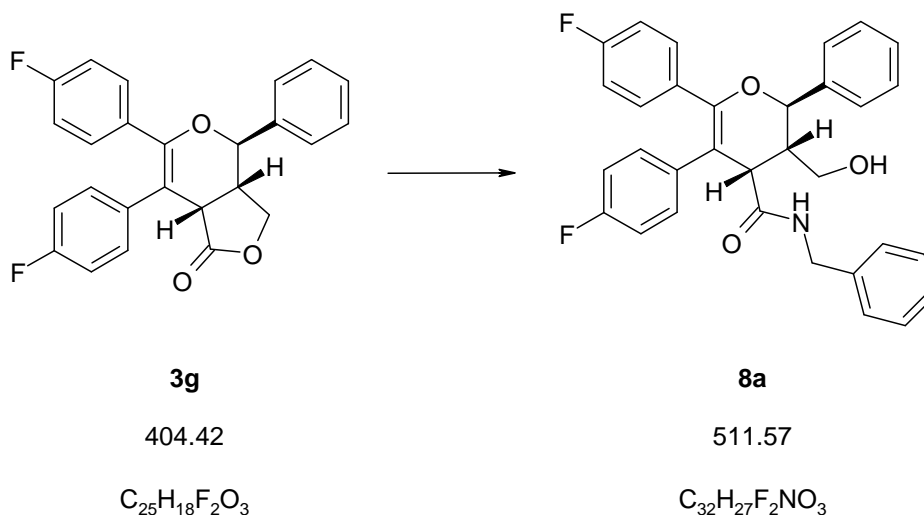
244.29

C<sub>15</sub>H<sub>16</sub>O<sub>3</sub>

Ester **6f** (767 mg, 3.14 mmol) was treated according to the general method (6.4.2) in *o*-xylene (44 ml) for 28.5 h. Ratio of *cis/trans*-**7f** from NMR of raw product was 34:66. Flash chromatography (toluene/Et<sub>2</sub>O/hexane, 8:1:3) yielded *cis*-**7f** and *trans*-**7f** (562 mg, 73%) as an amorphous solid. Pure *cis*-**7f** (yield = 7%) was separated by flash chromatography (CHCl<sub>3</sub>/ethyl acetate/hexane, 1:1:3): TLC (*cis*, CHCl<sub>3</sub>/Et<sub>2</sub>O/hexane, 1:1:3): *R<sub>f</sub>* 0.18. <sup>1</sup>H-NMR (*cis*, 300 MHz, CDCl<sub>3</sub>): δ 1.35 (s, 3H), 1.39 (s, 3H), 2.81 (q, *J* = 8.58 Hz, 1H), 3.32 (dd, *J* = 8.27 Hz, 3.49 Hz, 1H), 4.25 (t, *J* = 9.19 Hz, 1H), 4.42 (t, *J* = 8.46 Hz, 1H), 5.38 (d, *J* = 2.94 Hz, 1H), 7.33 – 7.37 (m, 3H), 7.56 – 7.59 (m, 2H). <sup>13</sup>C-NMR (75 MHz, CDCl<sub>3</sub>): δ 176.70 (s), 151.99 (s), 135.20 (s), 129.08 (d), 128.46 (d, 2C), 125.16 (d, 2C), 90.20 (d), 73.59 (s), 68.19 (t), 43.52 (d), 37.66 (d), 25.11 (q), 25.04 (q). EI-MS *m/z* (%): 244 ([C<sub>15</sub>H<sub>16</sub>O<sub>3</sub>]<sup>+</sup>, 40), 105 (91), 77 (45), 44 (85), 40 (100). IR (cm<sup>-1</sup>): 1759 (C=O). Mp (*cis*, MeOH): 96°C. EI-MSHR: Calc. mass (*cis*-C<sub>15</sub>H<sub>16</sub>O<sub>3</sub>) = 244.109945, found: 244.110090. HPLC purity (*cis*-**7f**): 94.3%. Pure *trans*-**7f** (yield = 28%) was separated by flash chromatography (toluene/hexane/ethyl acetate, 8:3:1): TLC (*trans*, toluene / hexane/Et<sub>2</sub>O, 8:3:1): *R<sub>f</sub>* 0.28. <sup>1</sup>H-NMR (*trans*, 300 MHz, CDCl<sub>3</sub>): δ 1.35 (s, 3H), 1.52 (s, 3H), 2.55 – 2.65 (m, 1H), 3.12 (dd, *J* = 14.22 Hz, 2.17 Hz, 1H), 4.03 (dd, *J* = 11.68 Hz, 8.29 Hz, 1H), 4.40 (dd, *J* = 8.20 Hz, 6.69 Hz, 1H), 5.61 (d, *J* = 1.88 Hz, 1H), 7.30 – 7.37 (m, 3H), 7.57 – 7.60 (m, 2H). EI-MSHR: Calc. mass (*trans*-C<sub>15</sub>H<sub>16</sub>O<sub>3</sub>) = 244.109945, found: 244.109920. HPLC purity (*trans*-**7f**): 87.1% (major impurity is *cis*-**7f**, 8.2%).

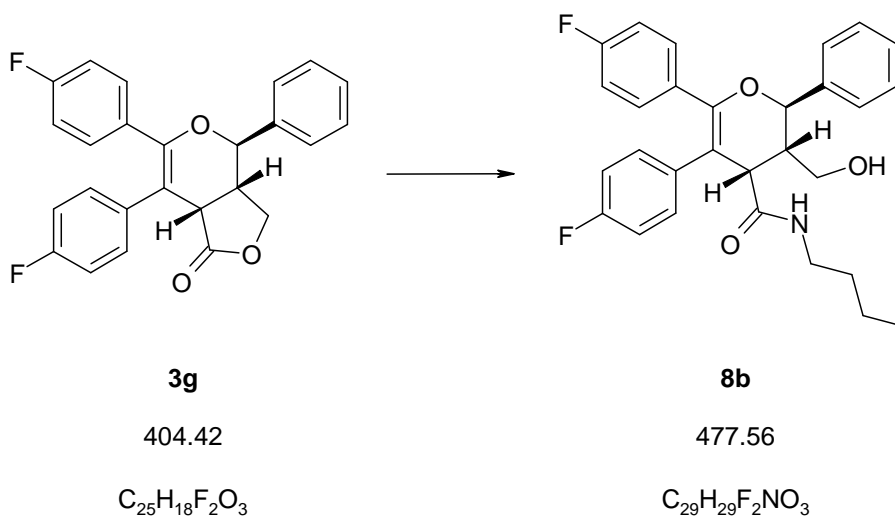
### 6.4.3 Aminolysis of Furopyranone **3g** (**8a-e**)

#### 5,6-Bis-(4-fluoro-phenyl)-3-hydroxymethyl-2-phenyl-3,4-dihydro-2H-pyran-4-carboxylic acid benzylamide (**8a**)



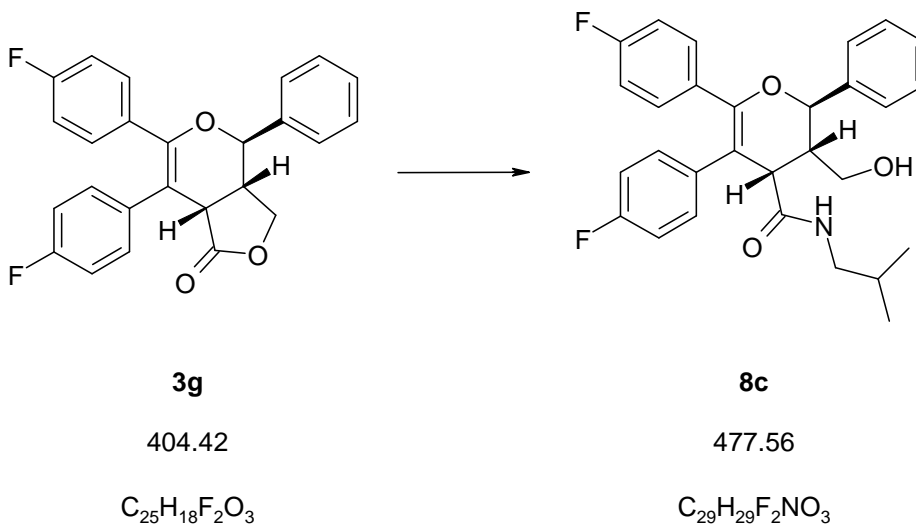
2-Hydroxypyridine (28.5 mg, 0.30 mmol) and benzylamine (0.16 ml, 1.50 mmol) were added to a suspension of **3g** (60 mg, 0.15 mmol) in toluene (2.5 ml). The mixture was stirred and refluxed over night. At room temperature the yellow solution was poured onto a saturated  $NH_4Cl$ -solution and extracted with ethyl acetate. The combined organic phases were dried ( $Na_2SO_4$ ) and concentrated. Flash chromatography (ethyl acetate/hexane, 2:3) gave **8a** (36 mg, 47%) as a white solid. For X-ray analysis the compound was recrystallised in MeOH. Mp (MeOH): 207°C. TLC (ethyl acetate/hexane, 2:3):  $R_f$  0.24.  $^1H$ -NMR (300 MHz, DMSO):  $\delta$  2.42 (m, 1H), 3.02 (m, 1H), 3.17 (m, 1H), 3.89 (d,  $J = 5.46$  Hz, 1H), 3.95 (dd,  $J = 5.46$  Hz, 15.64 Hz, 1H), 4.36 (dd,  $J = 6.78$  Hz, 15.64 Hz, 1H), 4.47 (t,  $J = 4.62$  Hz, 1H), 5.54 (d,  $J = 10.36$  Hz, 1H), 6.72-6.75 (m, 2H), 6.94-7.18 (m, 11H), 7.33-7.43 (m, 5H), 8.34 (t,  $J = 5.75$  Hz, 1H). EI-MS  $m/z$  (%): 511 ( $[C_{32}H_{27}F_2NO_3]^+$ , 15), 493 (46), 123 (96), 117 (100), 91 (97). EI-MSHR: Calc. mass ( $C_{32}H_{27}F_2NO_3$ ) = 511.195901, found: 511.195280.

**5,6-Bis-(4-fluoro-phenyl)-3-hydroxymethyl-2-phenyl-3,4-dihydro-2H-pyran-4-carboxylic acid butylamide (8b)**



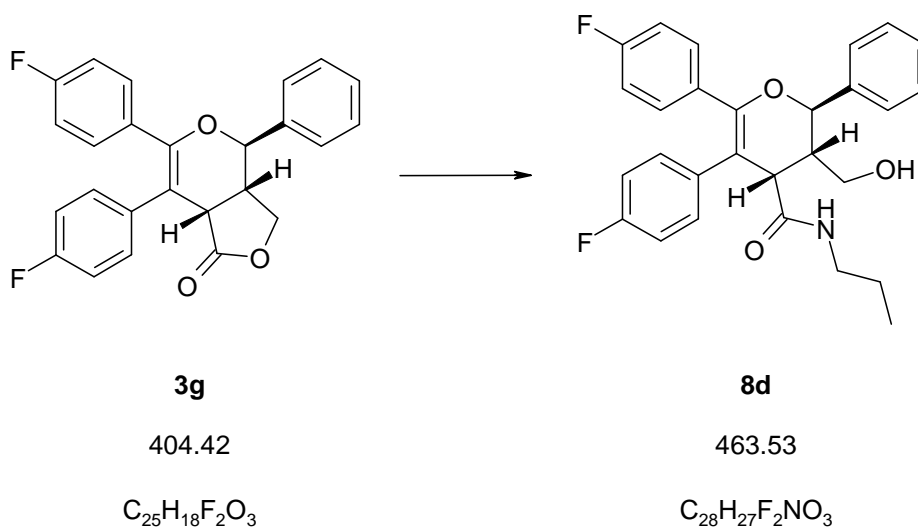
2-Hydroxypyridine (18.3 mg, 0.19 mmol) and *n*-butylamine (0.10 ml, 0.96 mmol) were added to a suspension of **3g** (39 mg, 0.10 mmol) in toluene (1.5 ml). The mixture was stirred and refluxed over night. At room temperature the yellow solution was poured onto a saturated  $NH_4Cl$ -solution and extracted with ethyl acetate. The combined organic phases were dried ( $Na_2SO_4$ ) and concentrated. Flash chromatography (ethyl acetate/hexane, 2:3) gave **8b** (36 mg, 48%) as a white solid. TLC (ethyl acetate/hexane, 2:3):  $R_f$  0.22.  $^1H$ -NMR (300 MHz, DMSO):  $\delta$  0.68 (t,  $J = 7.25$  Hz, 3H), 0.84-0.97 (m, 2H), 1.04-1.13 (m, 2H), 2.39 (m, 1H), 2.77 (m, 1H), 2.95-3.18 (m, 3H), 3.74 (d,  $J = 5.46$  Hz, 1H), 4.41 (t,  $J = 4.71$  Hz, 1H), 5.51 (d,  $J = 10.36$  Hz, 1H), 6.93-7.02 (m, 4H), 7.04-7.17 (m, 4H), 7.33-7.42 (m, 5H), 7.72 (t,  $J = 5.93$  Hz, 1H). EI-MS  $m/z$  (%): 477 ( $[C_{29}H_{29}F_2NO_3]^+$ , 18), 459 (74), 123 (100), 117 (100), 95 (57), 91 (52). EI-MSHR: Calc. mass ( $C_{29}H_{29}F_2NO_3$ ) = 477.211551, found: 477.211360.

**5,6-Bis-(4-fluoro-phenyl)-3-hydroxymethyl-2-phenyl-3,4-dihydro-2H-pyran-4-carboxylic acid isobutylamide (8c)**



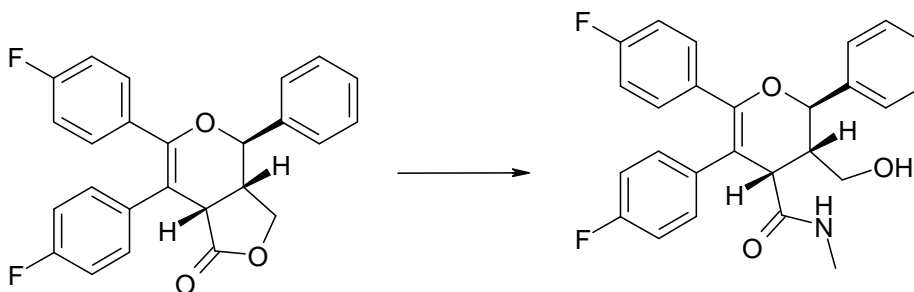
2-Hydroxypyridine (50 mg, 0.53 mmol) and isobutylamine (0.25 ml, 2.5 mmol) were added to a suspension of **3g** (102 mg, 0.25 mmol) in toluene (3 ml). The mixture was stirred and refluxed for 3 h. At room temperature the yellow solution was poured onto a saturated  $NH_4Cl$ -solution and extracted with ethyl acetate. The combined organic phases were dried ( $Na_2SO_4$ ) and concentrated. Flash chromatography (ethyl acetate/hexane, 2:3) gave **8c** (60 mg, 52%) as a white foam. TLC (ethyl acetate/hexane, 2:3):  $R_f$  0.21.  $^1H$ -NMR (300 MHz,  $CDCl_3$ ):  $\delta$  7.40-7.33 (m, 5H), 7.23-7.16 (m, 2H), 7.10-7.03 (m, 2H), 6.93-6.78 (m, 4H), 6.10 (t,  $J = 6.03$  Hz, 1H), 5.08 (d,  $J = 10.74$  Hz, 1H), 3.88 (d,  $J = 5.84$  Hz, 1H), 3.38-3.24 (m, 2H), 3.11-2.97 (m, 3H), 2.65 (m, 1H), 1.60 (m, 1H), 0.75 (d,  $J = 6.78$  Hz, 3H), 0.70 (d,  $J = 6.78$  Hz, 3H).  $^{13}C$ -NMR (75 MHz,  $CDCl_3$ ): 172.1, 162.6 (d, 1C,  $^1J_{CF}=249.00$  Hz), 161.6 (d, 1C,  $^1J_{CF}=247.14$  Hz), 152.2, 138.4, 135.5 (d, 1C,  $^4J_{CF}=3.12$  Hz), 131.8 (d, 2C,  $^3J_{CF}=8.11$  Hz), 131.3 (d, 2C,  $^3J_{CF}=7.49$  Hz), 128.9, 128.8, 127.3, 115.7 (d, 2C,  $^2J_{CF}=21.22$  Hz), 114.9 (d, 2C,  $^2J_{CF}=21.85$  Hz), 107.6, 77.7, 61.4, 47.8, 47.3, 44.7, 29.8, 28.6, 20.0, 19.9. EI-MS  $m/z$  (%): 477 ( $[C_{29}H_{29}F_2NO_3]^+$ , 33), 459 (57), 269 (40), 123 (95), 117 (100), 105 (67), 91 (60), 57 (29).

**5,6-Bis-(4-fluoro-phenyl)-3-hydroxymethyl-2-phenyl-3,4-dihydro-2H-pyran-4-carboxylic acid propylamide (8d)**



2-Hydroxypyridine (50 mg, 0.53 mmol) and propylamine (0.21 ml, 2.5 mmol) were added to a suspension of **3g** (99 mg, 0.25 mmol) in toluene (3 ml). The mixture was stirred and refluxed for 5 h. At room temperature the yellow solution was poured onto a saturated  $NH_4Cl$ -solution and extracted with ethyl acetate. The combined organic phases were dried ( $Na_2SO_4$ ) and concentrated. Flash chromatography (ethyl acetate/hexane, 2:3) gave **8d** (98 mg, 84%) as white foam. TLC (ethyl acetate/hexane, 2:3):  $R_f$  0.30.  $^1H$ -NMR (300 MHz, DMSO):  $\delta$  7.74 (t,  $J$  = 5.75 Hz, 1H), 7.43-7.33 (m, 5H), 7.15-7.05 (m, 4H), 7.01-6.93 (m, 4H), 5.50 (d,  $J$  = 10.36 Hz, 1H), 4.43 (t,  $J$  = 4.71 Hz, 1H), 3.74 (d,  $J$  = 5.46 Hz, 1H), 3.18-3.10 (m, 1H), 3.01-2.90 (m, 2H), 2.83-2.72 (m, 1H), 2.45-2.34 (m, 1H), 1.14 (m, 2H), 0.56 (t,  $J$  = 7.44 Hz, 3H).  $^{13}C$ -NMR (75 MHz, DMSO): 170.9, 161.4 (d, 1C,  $^1J_{CF}$ =245.89 Hz), 160.65 (d, 1C,  $^1J_{CF}$ =242.77 Hz), 149.4, 139.6, 135.9 (d, 1C,  $^4J_{CF}$ =3.12 Hz), 132.3 (d, 1C,  $^4J_{CF}$ =3.12 Hz), 131.9 (d, 2C,  $^3J_{CF}$ =7.49 Hz), 131.4 (d, 2C,  $^3J_{CF}$ = 8.11 Hz), 128.4, 128.2, 127.3, 114.6 (d, 2C,  $^2J_{CF}$ = 21.22 Hz), 114.4 (d, 2C,  $^2J_{CF}$ = 21.84 Hz), 109.8, 76.5, 59.5, 45.9, 44.3, 40.3, 22.0, 11.0. ESI-MS positive mode:  $m/z$  [ $C_{28}H_{27}F_2NO_3 + H$ ] $^+$  = 464.4.

**5,6-Bis-(4-fluoro-phenyl)-3-hydroxymethyl-2-phenyl-3,4-dihydro-2H-pyran-4-carboxylic acid methylamide (8e)**

**3g**

404.42

 $C_{25}H_{18}F_2O_3$ **8e**

435.47

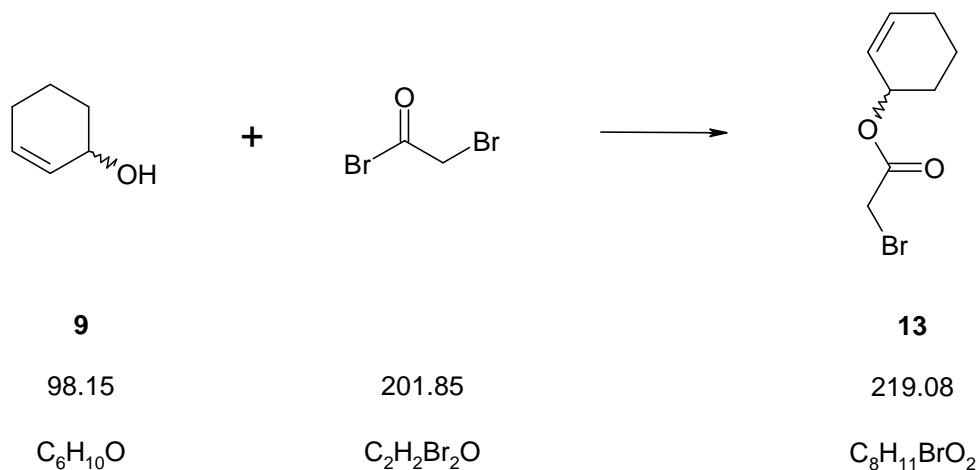
 $C_{26}H_{23}F_2NO_3$ 

2-Hydroxypyridine (33 mg, 0.35 mmol) and methylamine (0.22 ml, 1.73 mmol) were added to a suspension of **3g** (70 mg, 0.17 mmol) in toluene (1 ml). The mixture was stirred and refluxed for 24 h. At room temperature the yellow solution was poured onto a saturated  $NH_4Cl$ -solution and extracted with ethyl acetate. The combined organic phases were dried ( $Na_2SO_4$ ) and concentrated. Flash chromatography (ethyl acetate/hexane, 1:1) gave **8e** (20 mg, 27%) as white foam. The starting material **3g** (39 mg, 57%) was isolated as well.  $R_f$  (ethyl acetate/hexane, 2:3): 0.30.  $^1H$ -NMR (300 MHz, DMSO):  $\delta$  2.35-2.44 (m, 4H), 2.98 (m, 1H), 3.09 (m, 1H), 3.69 (d,  $J = 5.46$  Hz, 1H), 4.46 (t,  $J = 4.71$  Hz, 1H), 5.47 (d,  $J = 10.36$  Hz, 1H), 6.93-7.16 (m, 8H), 7.33-7.43 (m, 5H), 7.69 (q,  $J = 4.58$  Hz, 1H). EI-MS  $m/z$  (%): 435 ( $[C_{26}H_{23}F_2NO_3]^+$ , 15), 417 (69), 123 (100), 117 (99), 95 (52), 91 (55). EI-MSHR: Calc. Mass ( $C_{26}H_{23}F_2NO_3$ ) = 435.164600, found: 435.164550.

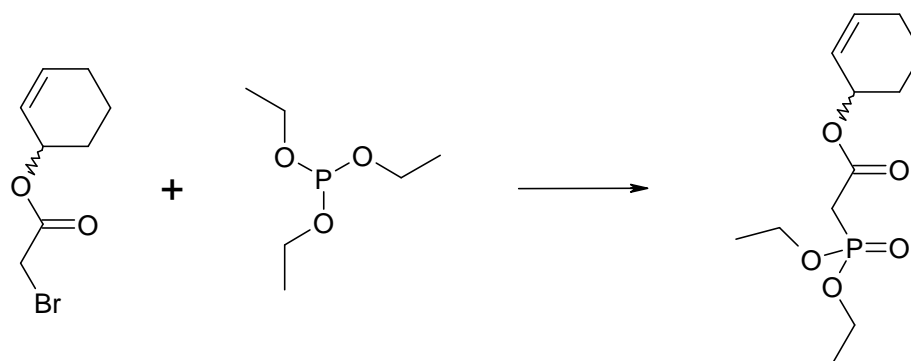


### 6.4.4 Synthesis of the Tricyclic Scaffold 16

#### Bromoacetic acid cyclohex-2-enyl ester (**13**)



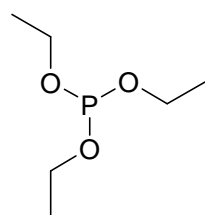
A solution of bromoacetyl bromide (0.44 ml, 5.1 mmol) in CH<sub>2</sub>Cl<sub>2</sub> (1 ml) was added dropwise to a stirred solution of racemic 2-cyclohexen-1-ol (**9**, 0.50 ml, 5.1 mmol) and pyridine (0.45 ml, 5.6 mmol) in CH<sub>2</sub>Cl<sub>2</sub> (5 ml) at 0°C under a nitrogen atmosphere. Directly after the addition of bromoacetyl bromide the colour changed to white later yellow and formation of a solid was visible. The obtained suspension was allowed to warm to room temperature during one hour. The mixture was poured onto saturated aqueous ammonium chloride and extracted three times with CH<sub>2</sub>Cl<sub>2</sub>. The combined organic phases were dried (Na<sub>2</sub>SO<sub>4</sub>) and concentrated. The liquid product was separated from a small amount of brown residue by removal with a pipette. The obtained bromoacetic acid cyclohex-2-enyl ester (**13**, 0.865 g, 78%) was used without further purification. TLC (EtOAc/hexane, 1:8): *R<sub>f</sub>* 0.68. <sup>1</sup>H-NMR (300 MHz, CDCl<sub>3</sub>): δ 6.00 (m, 1H), 5.71 (m, 1H), 5.30 (m, 1H), 3.82 (s, 2H), 2.16-1.57 (m, 6H). <sup>13</sup>C-NMR (75 MHz, CDCl<sub>3</sub>): δ 167.0 (s), 133.8 (d), 124.8 (d), 70.3 (d), 28.1 (t), 26.5 (t), 24.9 (t), 18.7 (t). EI-MS *m/z* (%): 220 ([C<sub>8</sub>H<sub>11</sub>O<sub>2</sub><sup>81</sup>Br]<sup>+</sup>, weak), 218 ([C<sub>8</sub>H<sub>11</sub>O<sub>2</sub><sup>79</sup>Br]<sup>+</sup>, weak), 139 (84), 98 (83), 97 (89), 81 (94), 80 (90), 79 (100), 70 (84), 41 (97), 39 (83). IR (cm<sup>-1</sup>): 1726, 1273.

**(Diethoxy-phosphoryl)-acetic acid cyclohex-2-enyl ester (14)****13**

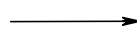
219.08

 $C_8H_{11}BrO_2$ 

+



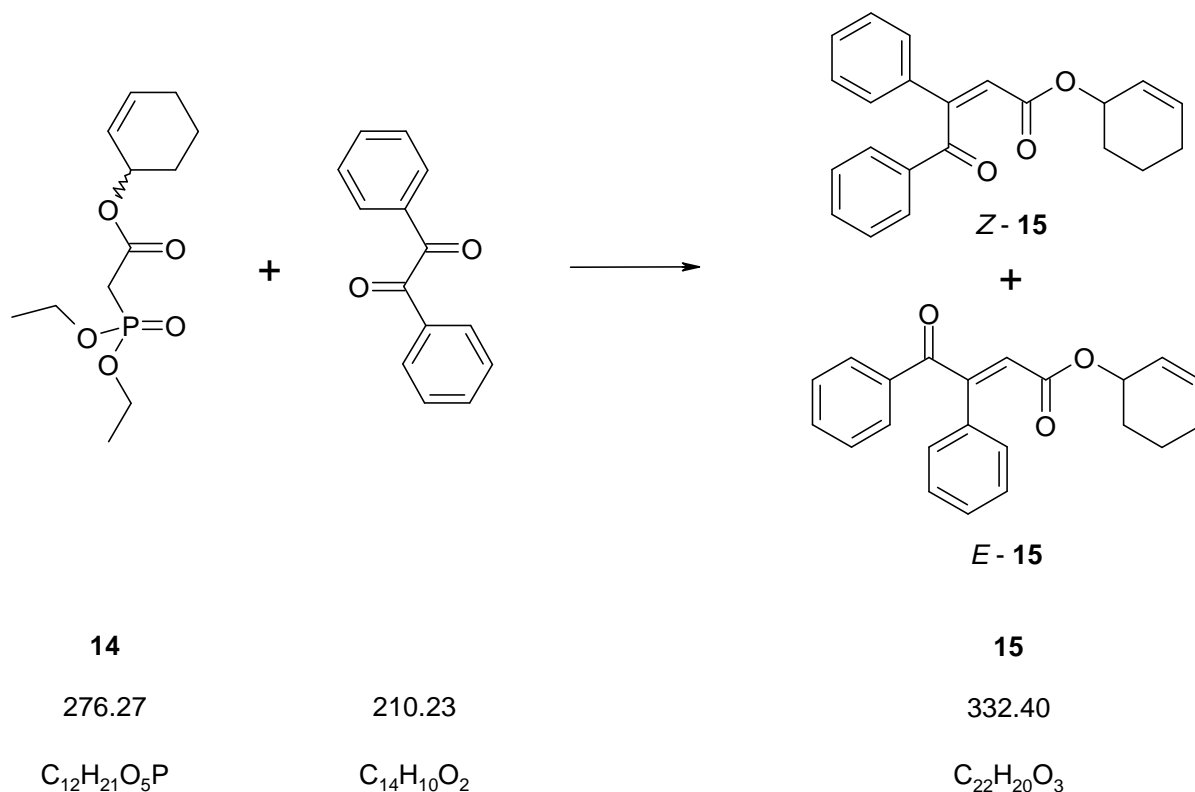
166.16

 $C_6H_{15}O_3P$ **14**

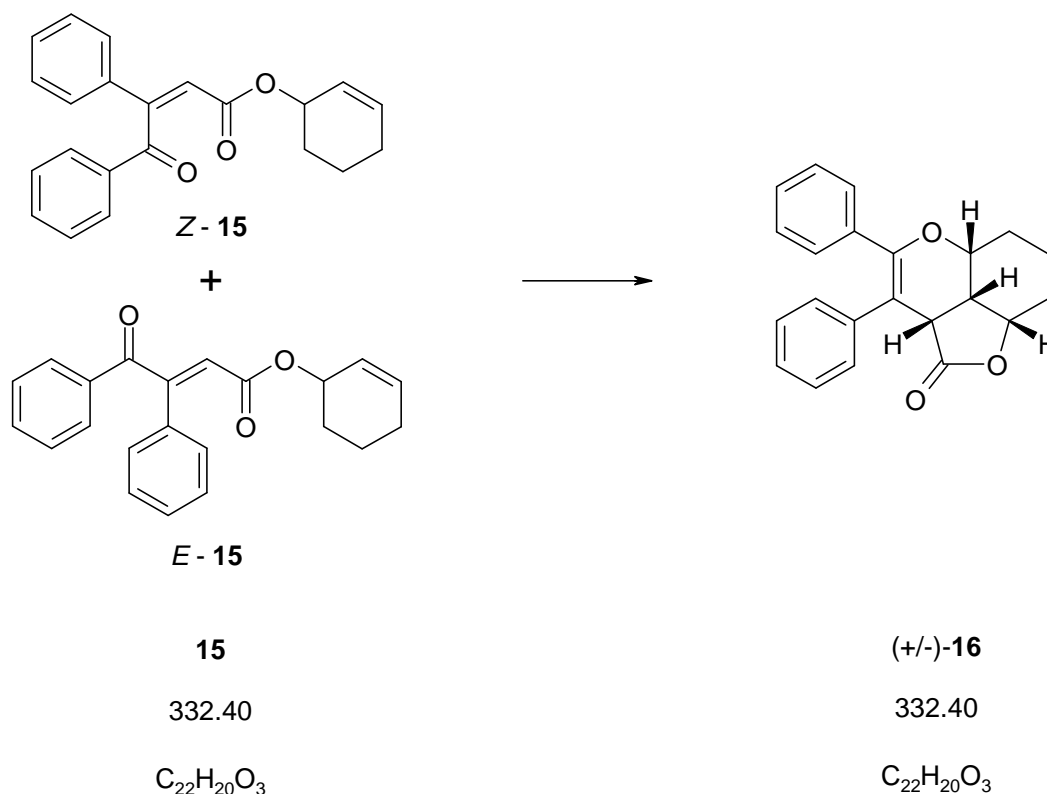
276.27

 $C_{12}H_{21}O_5P$ 

Triethyl phosphite (0.48 ml, 2.8 mmol) was added to a solution of bromoacetic acid cyclohex-2-enyl ester (**13**, 0.40 g, 1.83 mmol) in dry THF (3.5 ml) under a nitrogen atmosphere. The light brown solution was stirred and refluxed for 19 h. Then THF and triethyl phosphite were removed in vacuo. (Diethoxy-phosphoryl)-acetic acid cyclohex-2-enyl ester (**14**, 0.417 g, 83%) was isolated and used without further purification.  $^1H$ -NMR (300 MHz,  $CDCl_3$ ):  $\delta$  5.93 (m, 1H), 5.68 (m, 1H), 5.27 (m, 1H), 4.14 (m, 4H), 2.93 (d, 2H,  $^2J_{HP}=21.5$  Hz), 2.12-1.52 (m, 6H), 1.31 (t, 6H,  $J=7.1$  Hz).  $^{13}C$ -NMR (75 MHz,  $CDCl_3$ ):  $\delta$  165.6 [s (d, 1C,  $^2J_{CP}=6.2$  Hz)], 133.2 (d), 125.2 (d), 69.4 (d), 62.7 [t (d, 2C,  $^2J_{CP}=6.2$  Hz)], 34.7 [t (d, 1C,  $^1J_{CP}=133.6$  Hz)], 28.2 (t), 24.9 (t), 18.8 (t), 16.4 [q (d, 2C,  $^3J_{CP}=6.2$  Hz)].  $^{31}P$ -NMR (121 MHz,  $CDCl_3$ ):  $\delta$  20.0 (s, 1P). EI-MS  $m/z$  (%): 276 ( $[C_{12}H_{21}PO_5]^+$ , 7), 197 (58), 179 (68), 169 (58), 152 (82), 151 (75), 125 (71), 123 (86), 81 (61), 79 (100). IR ( $cm^{-1}$ ): 1726, 1259, 1047, 1018, 962, 912.

**(E/Z)-4-Oxo-3,4-diphenyl-but-2-enoic acid cyclohex-2-enyl ester (15)**

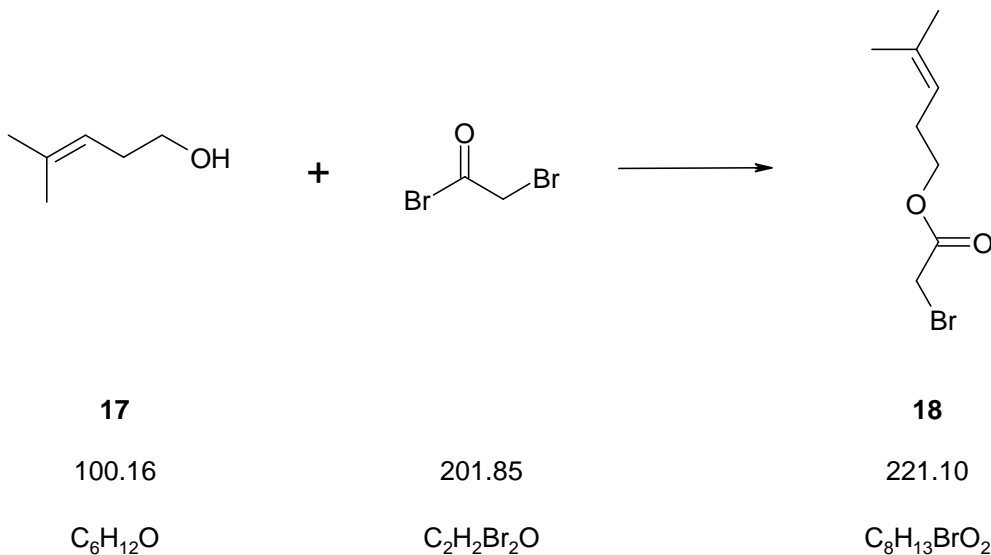
HMDS (0.18 ml, 0.87 mmol) was added slowly to a stirred solution of *n*-butyllithium (0.5 ml, 0.80 mmol, 1.6 M solution in hexane) in dry THF (2.5 ml) at 0°C under a nitrogen atmosphere. After half an hour, (diethoxy-phosphoryl)-acetic acid cyclohex-2-enyl ester (**14**, 0.200 g, 0.72 mmol) dissolved in dry THF (1 ml) was added to the solution. Then the solution was cooled down to -78°C and benzil (0.167 g, 0.80 mmol) dissolved in dry THF (1 ml) was added slowly. For the final half hour the cooling bath was removed. After 3 hours, the solution was poured onto saturated aqueous ammonium chloride and extracted three times with EtOAc. The combined organic phases were dried ( $\text{Na}_2\text{SO}_4$ ) and concentrated. The crude product was purified by column chromatography (EtOAc/hexane, 1:10) and (*E/Z*)-4-oxo-3,4-diphenyl-but-2-enoic acid cyclohex-2-enyl ester (**15**, 0.180 g, 90%) was isolated as a yellow oily liquid. The ratio of the *E*- and *Z*-isomer was 35:65 (as determined by NMR). TLC (EtOAc/Hexane, 1:10):  $R_f$  0.36 (both *E*- and *Z*-isomer).  $^1\text{H-NMR}$  (300 MHz,  $\text{CDCl}_3$ , mixture of isomers):  $\delta$  7.98-7.90 (m, 4H), 7.60-7.32 (m, 16H), 6.52 (s, 1H, *E*), 6.28 (s, 1H, *Z*), 5.94-5.83 (m, 2H), 5.66-5.52 (m, 2H), 5.25-5.18 (m, 2H), 2.03-1.43 (m, 12H). EI-MS  $m/z$  (%): 332 ( $[\text{C}_{22}\text{H}_{20}\text{O}_3]^+$ , 19), 105 (99), 77 (100), 51 (96).

**3,4-Diphenyl-2a,5a,6,7,8,8a,8b-heptahydro-furo[4,3,2-de]chromen-2-one (16)**

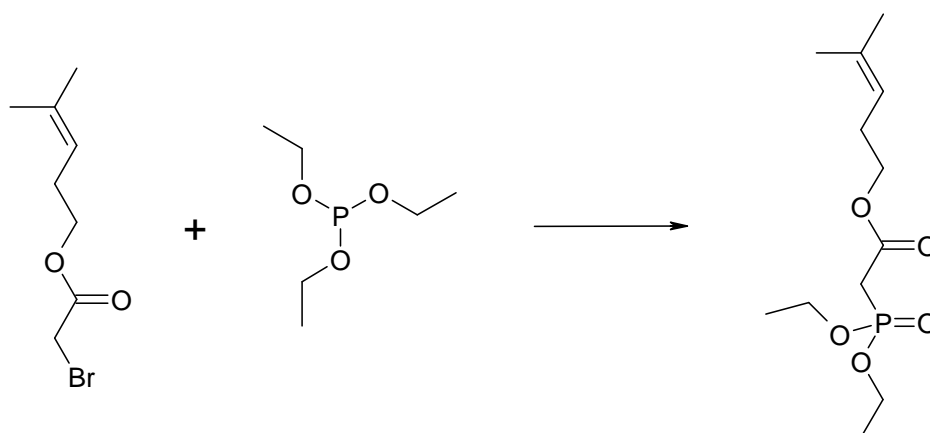
The reaction was carried out in an autoclave. (*E/Z*)-4-Oxo-3,4-diphenyl-but-2-enoic acid cyclohex-2-enyl ester (**15**, 171 mg, 0.51 mmol) was dissolved in dry toluene (17 ml) and placed in a Teflon<sup>®</sup> reaction chamber inside a sealed steel autoclave. The autoclave was heated in an oil bath and kept at an inside temperature of 184-187°C for 17 h. The solvent was removed in vacuo and the product was purified by column chromatography (EtOAc/hexane, 1:4). 3,4-Diphenyl-2a,5a,6,7,8,8a,8b-heptahydro-furo[4,3,2-de]chromen-2-one (**16**, 69 mg, 41%) was isolated as a white solid. For X-ray analysis the compound was recrystallised from EtOH. Besides the product, unreacted *E*-4-oxo-3,4-diphenyl-but-2-enoic acid cyclohex-2-enyl ester (*E*-**15**, 67 mg, 39%) was also isolated. TLC (EtOAc/Hexane, 1:4):  $R_f$  0.24. <sup>1</sup>H-NMR (300 MHz, DMSO):  $\delta$  7.27-7.16 (m, 10H), 4.75 (m, 1H), 3.98 (d, 1H,  $J=9.0$  Hz), 3.90 (m, 1H), 3.11 (m, 1H), 2.27-2.12 (m, 2H), 1.77-1.45 (m, 4H). <sup>13</sup>C-NMR (75 MHz, CDCl<sub>3</sub>):  $\delta$  178.2 (s), 156.2 (s), 139.6 (s), 134.4 (s), 129.2 (d), 129.1 (d), 128.7 (d), 128.5 (d), 128.0 (d), 126.8 (d), 116.9 (s), 76.2 (d), 74.9 (d), 47.1 (d), 44.1 (d), 28.8 (t), 27.4 (t), 13.2 (t). EI-MS  $m/z$  (%): 332 ([C<sub>22</sub>H<sub>20</sub>O<sub>3</sub>]<sup>+</sup>, 74), 105 (100), 77 (66). IR (cm<sup>-1</sup>): 1755, 1168, 1055, 980, 743, 693, 667; mp (EtOH): 185°C.

### 6.4.5 Attempted Synthesis of Pyranopyranone 21

#### Bromo-acetic acid 4-methyl-pent-3-enyl ester (**18**)



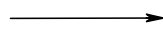
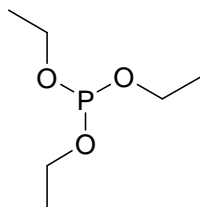
A solution of bromoacetyl bromide (303 mg, 1.50 mmol) in CH<sub>2</sub>Cl<sub>2</sub> (1 ml) was added dropwise to a stirred solution of alcohol **17** (150 mg, 1.50 mmol) and pyridine (89 μl, 1.65 mmol) in CH<sub>2</sub>Cl<sub>2</sub> (3 ml) at 0°C under a nitrogen atmosphere. Directly after the addition of bromoacetyl bromide the colour changed to white later yellow and formation of a solid was visible. The obtained suspension was allowed to warm to room temperature during one hour. The mixture was poured onto saturated aqueous ammonium chloride and extracted three times with CH<sub>2</sub>Cl<sub>2</sub>. The combined organic phases were dried (Na<sub>2</sub>SO<sub>4</sub>) and concentrated. The liquid product was separated from a small amount of brown residue by removal with a pipette. The obtained ester **18** (330 mg, 99%) was used without further purification. TLC (EtOAc/hexane, 1:10): *R<sub>f</sub>* 0.49. <sup>1</sup>H-NMR (300 MHz, CDCl<sub>3</sub>): δ 5.10 (m, 1H), 4.14 (t, *J*=7.06 Hz, 2H), 3.83 (s, 2H), 2.36 (q, *J*=7.10 Hz, 2H), 1.71 (s, 3H), 1.64 (s, 3H). EI-MS *m/z* (%): 223 ([C<sub>8</sub>H<sub>13</sub>O<sub>2</sub><sup>81</sup>Br]<sup>+</sup>, weak), 221 ([C<sub>8</sub>H<sub>13</sub>O<sub>2</sub><sup>79</sup>Br]<sup>+</sup>, weak), 82 (100), 69 (34), 67 (43), 41 (33).

**(Diethoxy-phosphoryl)-acetic acid 4-methyl-pent-3-enyl ester (19)****18**

221.10

 $C_8H_{13}BrO_2$ 

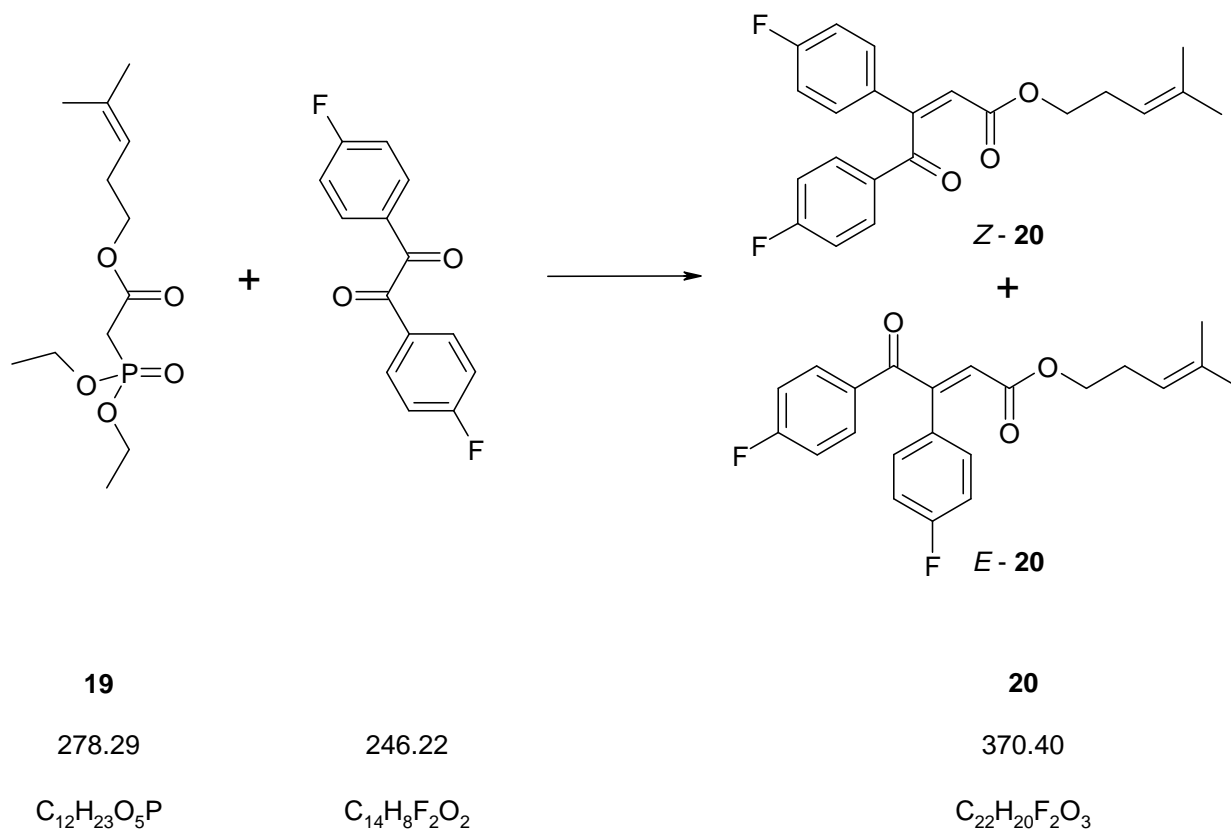
+

**19**

278.29

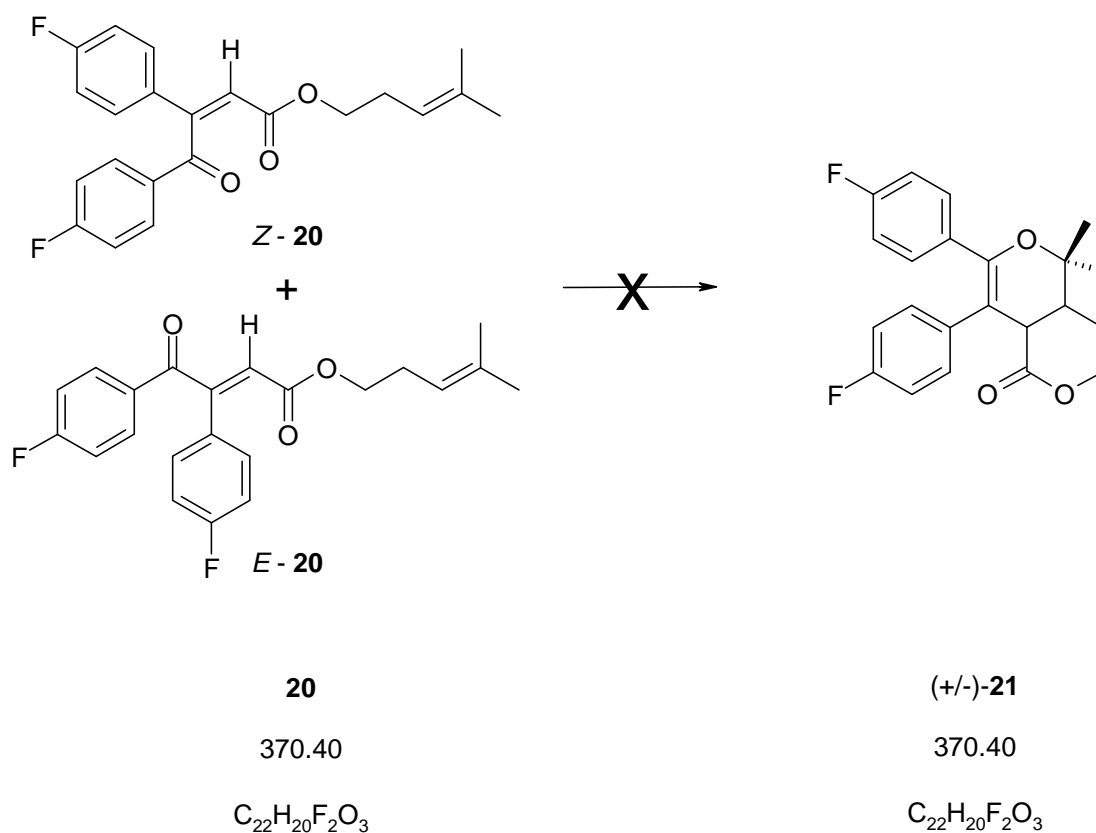
 $C_{12}H_{23}O_5P$ 

Triethyl phosphite (0.56 ml, 3.2 mmol) was added to a solution of ester **18** (352 mg, 1.6 mmol) in dry THF (7 ml) under a nitrogen atmosphere. The light brown solution was stirred and refluxed for 22 h. Then THF and triethyl phosphite were removed in vacuo. The phosphonate **19** (0.445 g, 99%) was isolated and used without further purification.  $^1H$ -NMR (300 MHz,  $CDCl_3$ ):  $\delta$  5.10 (m, 1H), 4.15 (m, 6H), 2.96 (d,  $^2J_{HP}=21.66$  Hz, 2H), 2.34 (q,  $J=7.16$  Hz, 2H), 1.70 (s, 3H), 1.62 (s, 3H), 1.34 (t,  $J=6.78$  Hz, 6H).  $^{13}C$ -NMR (75 MHz,  $CDCl_3$ ):  $\delta$  166.0 [s (d, 1C,  $^2J_{CP}=6.24$  Hz)], 134.9 (s), 119.0 (d), 65.4 (t), 62.8 [t (d, 2C,  $^2J_{CP}=6.24$  Hz)], 34.5 [t (d, 1C,  $^1J_{CP}=134.2$  Hz)], 27.6 (t), 25.8 (q), 17.9 (q), 16.5 [q (d, 2C,  $^3J_{CP}=6.2$  Hz)].  $^{31}P$ -NMR (121 MHz,  $CDCl_3$ ):  $\delta$  19.9 (s, 1P). EI-MS  $m/z$  (%): 279 [ $[C_{12}H_{23}PO_5]^+$ , weak], 197 (97), 179 (89), 151 (66), 123 (66), 82 (100), 67 (97), 41 (73).

**(E/Z)-3,4-Bis-(4-fluoro-phenyl)-4-oxo-but-2-enoic acid 4-methyl-pent-3-enyl ester (20)**

HMDS (0.18 ml, 0.87 mmol) was added slowly to a stirred solution of *n*-butyllithium (0.5 ml, 0.80 mmol, 1.6 M solution in hexane) in dry THF (2.5 ml) at 0°C under a nitrogen atmosphere. After half an hour, phosphonate **19** (200 mg, 0.72 mmol) dissolved in dry THF (1 ml) was added to the solution. Then 4,4'-difluorobenzil (195 mg, 0.80 mmol) dissolved in dry THF (1 ml) was added slowly. After 2 hours the cooling bath was removed. After 5.5 hours, the solution was poured onto saturated aqueous ammonium chloride and extracted three times with EtOAc. The combined organic phases were dried (Na<sub>2</sub>SO<sub>4</sub>) and concentrated. The crude product was purified by column chromatography (EtOAc/hexane, 1:9) and ester **20** (159 mg, 60%) was isolated as a yellow oily liquid. The ratio of the *E*- and *Z*-isomer was about 1:1 (as determined by NMR). TLC (EtOAc/hexane, 1:9): *R<sub>f</sub>* 0.42 (both *E*- and *Z*-isomer). <sup>1</sup>H-NMR (300 MHz, CDCl<sub>3</sub>, mixture of isomers): δ 8.05-7.90 (m, 4H), 7.51-7.36 (m, 4H), 7.24-7.02 (m, 8H), 6.45 (s, 1H, *E*), 6.24 (s, 1H, *Z*), 5.01-4.92 (m, 2H), 4.07-3.97 (m, 4H), 2.21 (m, 4H), 1.68 (s, 6H), 1.58 (s, 6H). EI-MS *m/z* (%): 370 ([C<sub>22</sub>H<sub>20</sub>F<sub>2</sub>O<sub>3</sub>]<sup>+</sup>, 6), 123 (100), 95, (73), 82 (52).

**7,8-Bis-(4-fluoro-phenyl)-5,5-dimethyl-3,4,4a,8a-tetrahydro-5H-pyrano[4,3-c]pyran-1-one (21)**

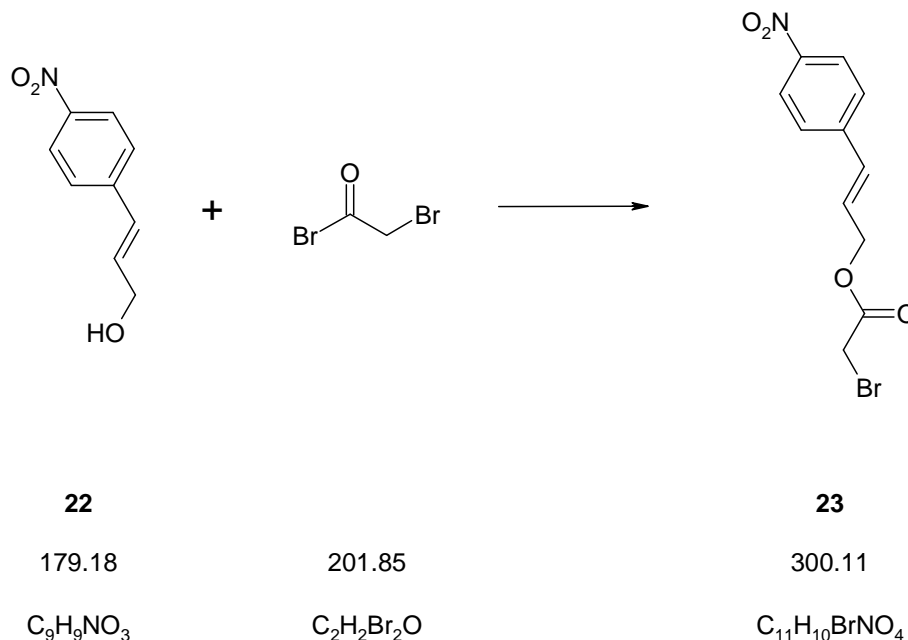


The reaction was carried out in an autoclave. Ester **20** (156 mg, 0.42 mmol) was dissolved in dry toluene (20 ml) and placed in a Teflon<sup>®</sup> reaction chamber inside a sealed steel autoclave. The autoclave was heated in an oil bath and kept at an inside temperature of 190°C for 22 h (temperature oil bath: 200°C). Then the solvent was removed in vacuo and the crude material was analysed by NMR spectroscopy. No expected product **21** was identified in the crude NMR spectrum. Only isomerisation of **Z-20** to **E-20** was observed. The ratio of **E-20** to **Z-20** changed from 1:1 before heating to about 4:1 after heating as determined by the NMR signals of the protons drawn above.

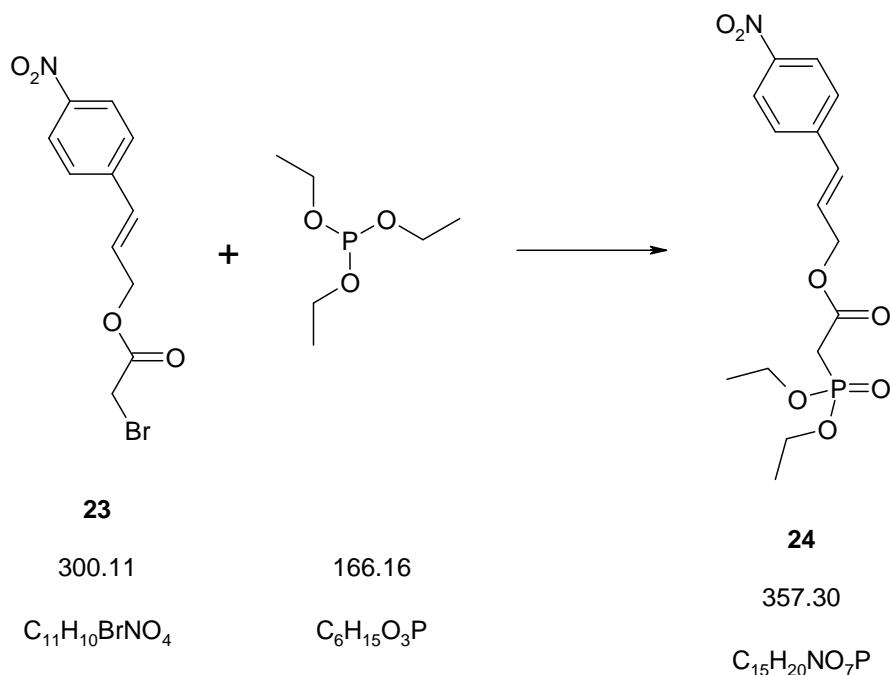


### 6.4.6 Synthesis of Furopyranone 26 and the Tricyclic Scaffold 27

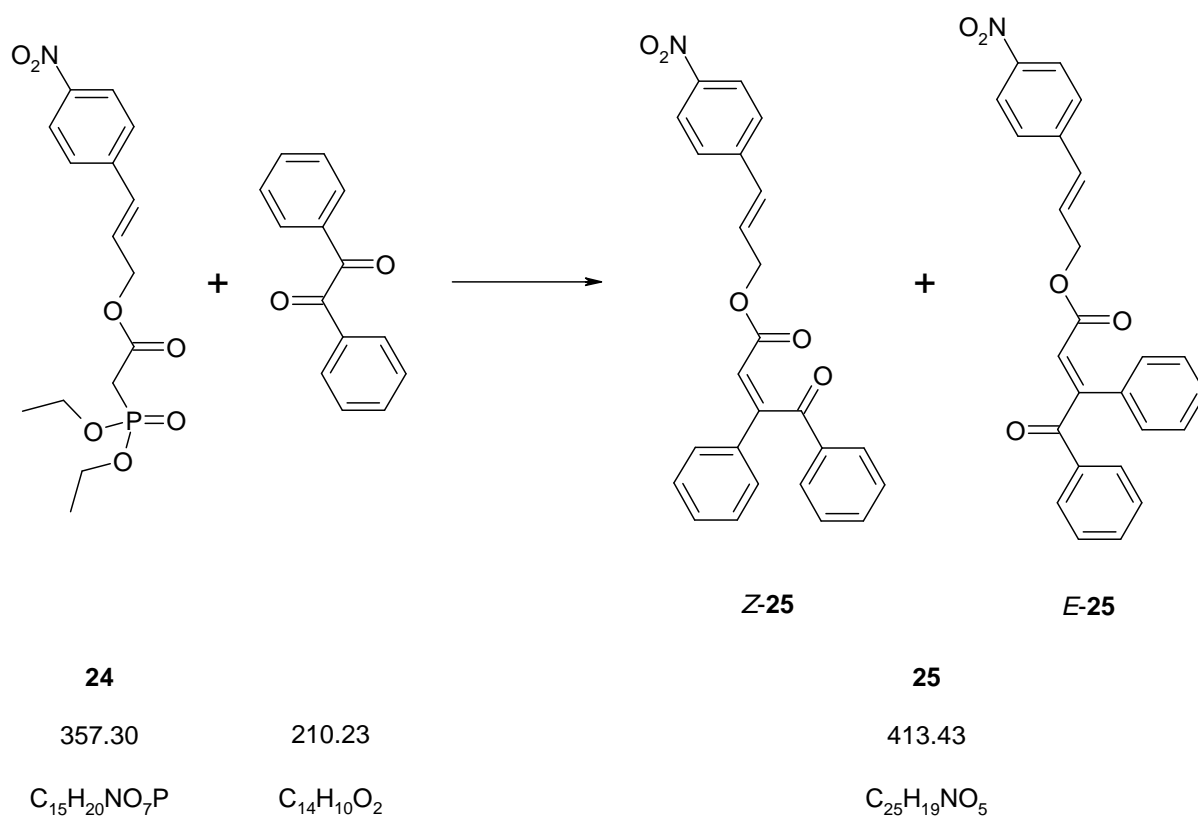
#### Bromo-acetic acid 3-(4-nitro-phenyl)-allyl ester (23)



The reaction was carried out at 0°C and in a nitrogen atmosphere. The nitro-cinnamyl alcohol **22** (2 g, 11.16 mmol) was dissolved in CH<sub>2</sub>Cl<sub>2</sub> (~ 15 ml) and pyridine (1 ml, 12.28 mmol) was added. Bromoacetyl bromide (0.97 ml, 11.16 mmol) was slowly added to the cooled reaction mixture. After 2.5 h the reaction mixture was poured onto a saturated aqueous NH<sub>4</sub>Cl-solution and extracted with CH<sub>2</sub>Cl<sub>2</sub>. The organic phase was dried (Na<sub>2</sub>SO<sub>4</sub>), filtered, concentrated and dried (high vacuum). Ester **23** (3.31 g, 99 %) was isolated as a brown-yellow solid and used without further purification. TLC (EtOAc/hexane, 1:2): *R<sub>f</sub>* 0.52. <sup>1</sup>H-NMR (300 MHz, CDCl<sub>3</sub>): δ 8.19 (d, *J* = 8.85 Hz, 2H), 7.53 (d, *J* = 8.85 Hz, 2H), 6.76 (d, *J* = 15.82 Hz, 1H), 6.45 (m, 1H), 4.87 (d, *J* = 6.03 Hz, 2H), 3.90 (s, 2H). <sup>13</sup>C-NMR (75 MHz, CDCl<sub>3</sub>): δ 167.0 (s), 147.5 (s), 142.5 (s), 132.3 (d), 127.4 (d, 2C), 127.2 (d), 124.2 (d, 2C), 66.0 (t), 25.7 (t). EI-MS *m/z* (%): 301 ([C<sub>11</sub>H<sub>10</sub>N<sup>81</sup>BrO<sub>4</sub>]<sup>+</sup>, 22), 299 ([C<sub>11</sub>H<sub>10</sub>N<sup>79</sup>BrO<sub>4</sub>]<sup>+</sup>, 23), 220 (88), 179 (90), 116 (92), 115 (100).

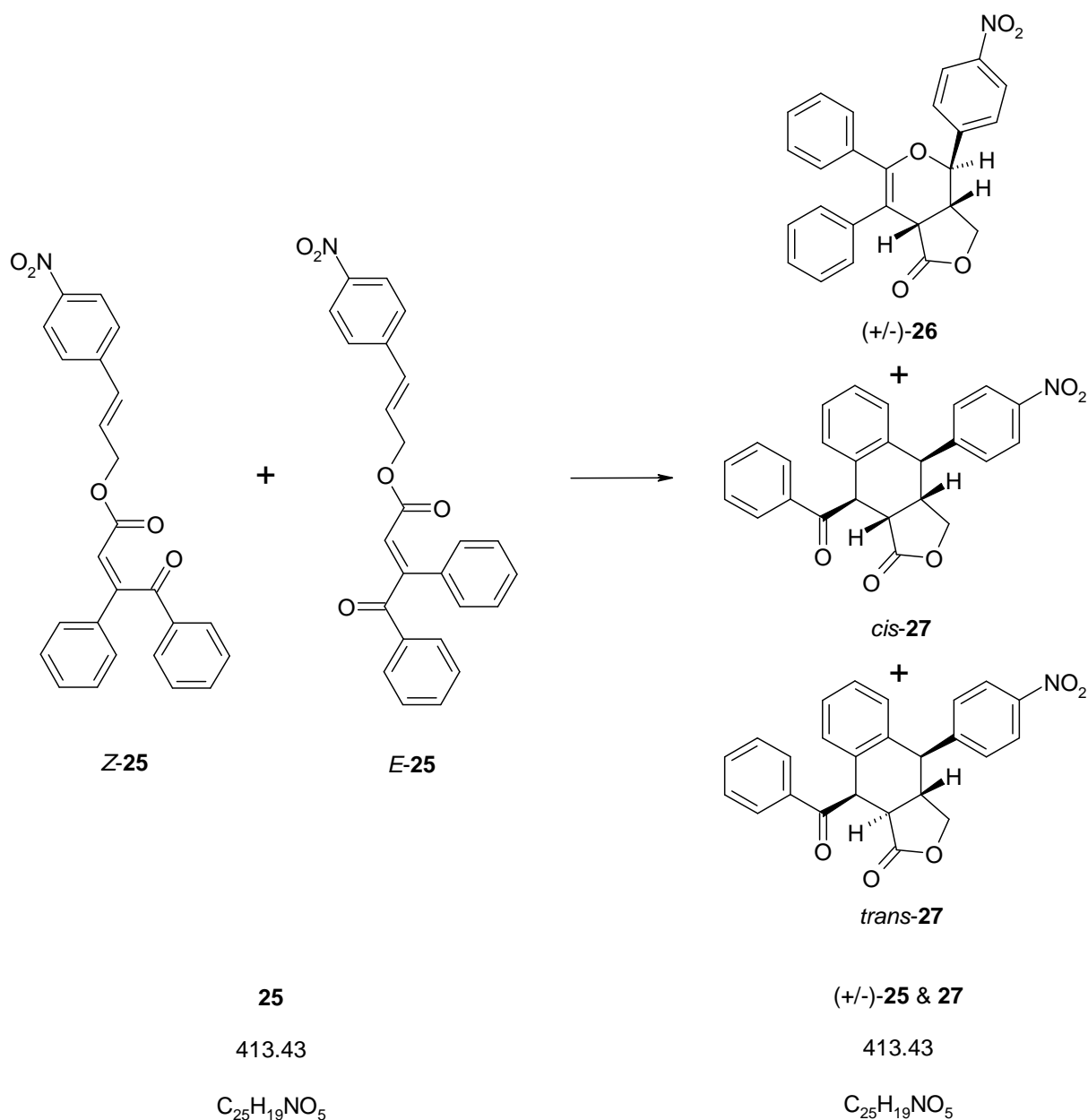
**(Diethoxy-phosphoryl)-acetic acid 3-(4-nitro-phenyl)-allyl ester (24)**

The bromoacetate **23** (1.5 g, 5 mmol) was dissolved in THF (~ 20 ml). Triethyl phosphite (1.7 ml, 10 mmol) was added and the stirred solution was refluxed for 24 h (temperature oil bath: ~ 70 °C). Then the reaction mixture was allowed to cool down to room temperature. After this the reaction mixture was concentrated and dried at the high vacuum by heating with a water bath up to 40°C. The phosphonate **24** (1.7 g, 96 %) was isolated as a brown and oily liquid.  $^1\text{H-NMR}$  (300 MHz,  $\text{CDCl}_3$ ):  $\delta$  8.14 (d,  $J = 8.85$  Hz, 2H), 7.48 (d,  $J = 8.67$  Hz, 2H), 6.74 (d, ), 6.41 (m, 1H), 4.81 (d,  $J = 5.84$  Hz, 2H), 4.14 (m, 4H), 3.00 (d,  $^2J_{\text{HP}} = 21.48$  Hz, 2H), 1.30 (t,  $J = 7.06$  Hz, 6H).  $^{13}\text{C-NMR}$  (75 MHz,  $\text{CDCl}_3$ ):  $\delta$  165.5 [s (d,  $^2J_{\text{CP}} = 6.24$  Hz, 1C)], 147.3 (s), 142.6 (s), 131.5 (d), 127.6 (d), 127.2 (d, 2C), 124.1 (d, 2C), 65.2 (t), 62.8 [t (d,  $^2J_{\text{CP}} = 6.24$  Hz, 2C)], 34.4 [t (d,  $^1J_{\text{CP}} = 134.18$  Hz, 1C)], 16.4 [q (d,  $^3J_{\text{CP}} = 6.24$  Hz, 2C)].  $^{31}\text{P-NMR}$  (121 MHz,  $\text{CDCl}_3$ ): 19.47 (s, 1P). EI-MS  $m/z$  (%): 357 ( $[\text{C}_{15}\text{H}_{20}\text{NO}_7\text{P}]^+$ , < 1, not visible), 205 (44), 155 (73), 127 (60), 99 (100), 81 (55).

**(E/Z)-4-Oxo-3,4-diphenyl-but-2-enoic acid 3-(4-nitro-phenyl)-allyl ester (25)**

HMDS (0.35 ml, 1.68 mmol) was added slowly to a stirred solution of *n*-butyllithium (1 ml, 1.54 mmol, 1.6 M solution in hexane) in dry THF (5 ml) at 0°C under a nitrogen atmosphere. After half an hour, phosphonate **24** (500 mg, 1.40 mmol) dissolved in dry THF (1 ml) was added to the solution. Then benzil (324 mg, 1.54 mmol) dissolved in dry THF (1 ml) was added slowly. After 2 hours the cooling bath was removed. After 3.5 hours, the solution was poured onto saturated aqueous ammonium chloride and extracted three times with EtOAc. The combined organic phases were dried ( $Na_2SO_4$ ) and concentrated. The crude product was purified by column chromatography (EtOAc/hexane, 1:3) and ester **25** (338 mg, 59%) was isolated as a yellow oily liquid. The ratio of the *E*- and *Z*-isomer was about 1:1 (as determined by NMR). TLC (EtOAc/hexane, 1:3):  $R_f$  0.32 (both *E*- and *Z*-isomer).  $^1H$ -NMR (300 MHz,  $CDCl_3$ , mixture of isomers):  $\delta$  8.21-8.15 (m, 4H), 7.97-7.91 (m, 4H), 7.61-7.34 (m, 20H), 6.62-6.49 (m, 3H), 6.33-6.21 (m, 3H), 4.78-4.71 (m, 4H). Signal at 6.56 (s, 1H, *E*), 6.30 (s, 1H, *Z*). EI-MS  $m/z$  (%): 413 ( $[C_{25}H_{19}NO_5]^+$ , 5), 236 (44), 105 (100), 77 (82).

**4-(4-Nitro-phenyl)-6,7-diphenyl-3a,7a-dihydro-3H,4H-furo[3,4-c]pyran-1-one (26) and 9-Benzoyl-4-(4-nitro-phenyl)-3a,4,9,9a-tetrahydro-3H-naphtho[2,3-c]furan-1-one (27)**



The reaction was carried out in a Parr-autoclave. (*E/Z*)-ester **25** (200 mg, 0.48 mmol) was dissolved in dry toluene (10 ml) and placed in a Teflon<sup>®</sup> reaction chamber inside a sealed steel autoclave. The Parr-autoclave was heated in an oven up to 184°C for 21 h. The solvent was removed in vacuo and the products were purified by column chromatography (EtOAc/hexane, 1:3 → 1:2 → 1:1). Furopyranone **26** (119 mg, 60%) and a mixture of *cis*/*trans*-**27** (21 mg, 11%) were isolated. After NP-HPLC up to 3 mg of pure *cis*-**27** and pure *trans*-**27** were isolated. The ratio of 5:2:1 (**26**:*cis*-**27**:*trans*-**27**) was determined by NMR spectroscopy of the crude reaction mixture.

Analysis of Product **26**:

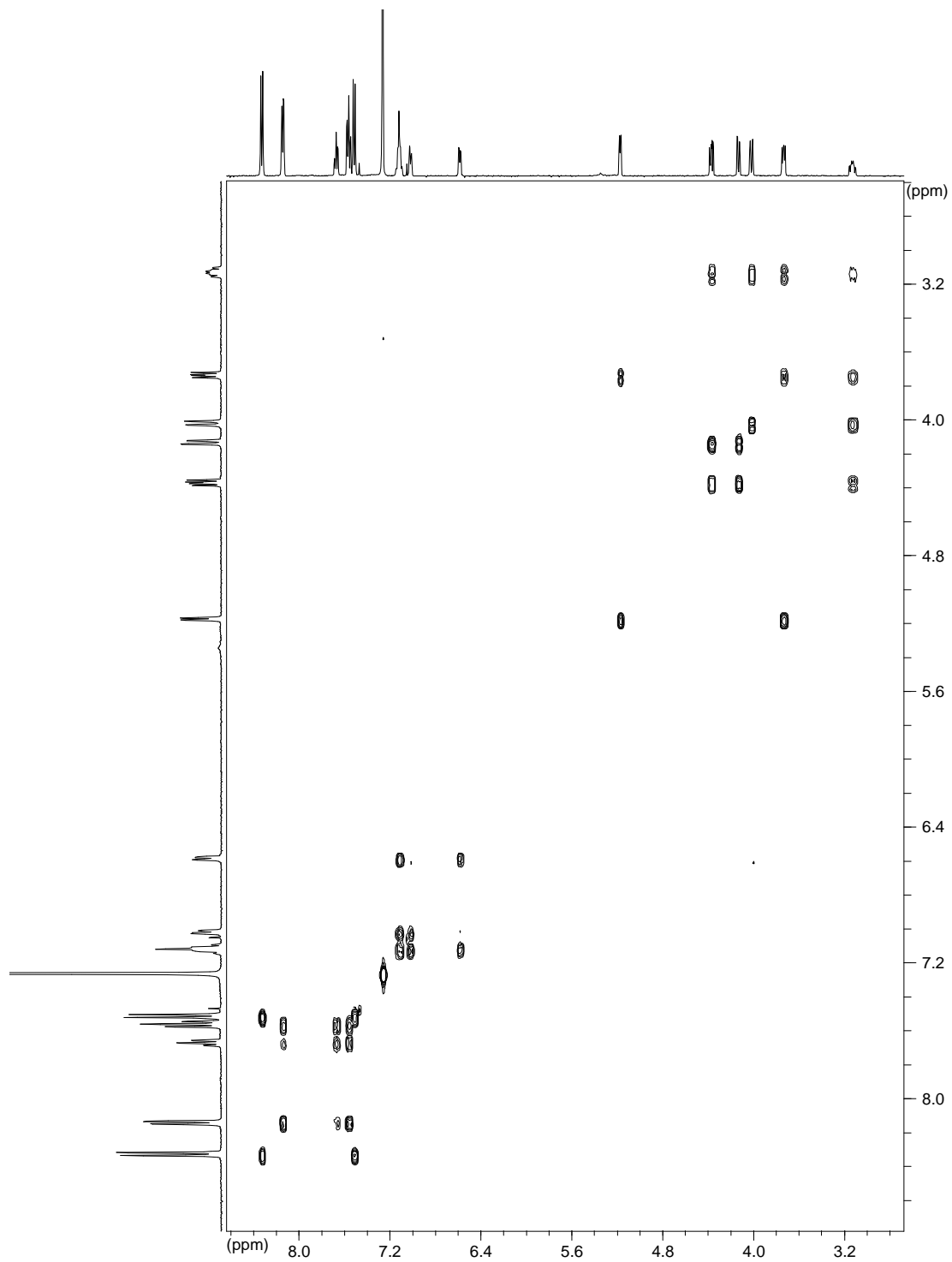
TLC (EtOAc/hexane, 1:2):  $R_f$  0.35.  $^1\text{H-NMR}$  (300 MHz,  $\text{CDCl}_3$ ):  $\delta$  8.32 (m, 2H), 7.67 (m, 2H), 7.24-7.10 (m, 10H), 4.85 (d,  $J = 11.11$  Hz, 1H), 4.33 (dd,  $J = 10.17$  Hz,  $J = 5.65$  Hz, 1H), 4.09 (d,  $J = 10.17$  Hz, 1H), 3.98 (d,  $J = 6.97$  Hz, 1H), 2.95 (m, 1H).  $^{13}\text{C-NMR}$  (75 MHz,  $\text{CDCl}_3$ ):  $\delta$  174.1 (s), 151.7 (s), 148.6 (s), 145.1 (s), 138.1 (s), 134.5 (s), 130.0 (d, 2C), 129.8 (d, 2C), 128.9 (d, 2C), 128.7 (d), 128.5 (d, 2C), 127.9 (d, 2C), 127.0 (d), 124.3 (d, 2C), 107.6 (s), 76.6 (d), 66.3 (t), 42.4 (d), 40.2 (d). EI-MS  $m/z$  (%): 413 ( $[\text{C}_{25}\text{H}_{19}\text{NO}_5]^+$ , 8), 70 (38), 61 (40), 45 (41), 43 (100).

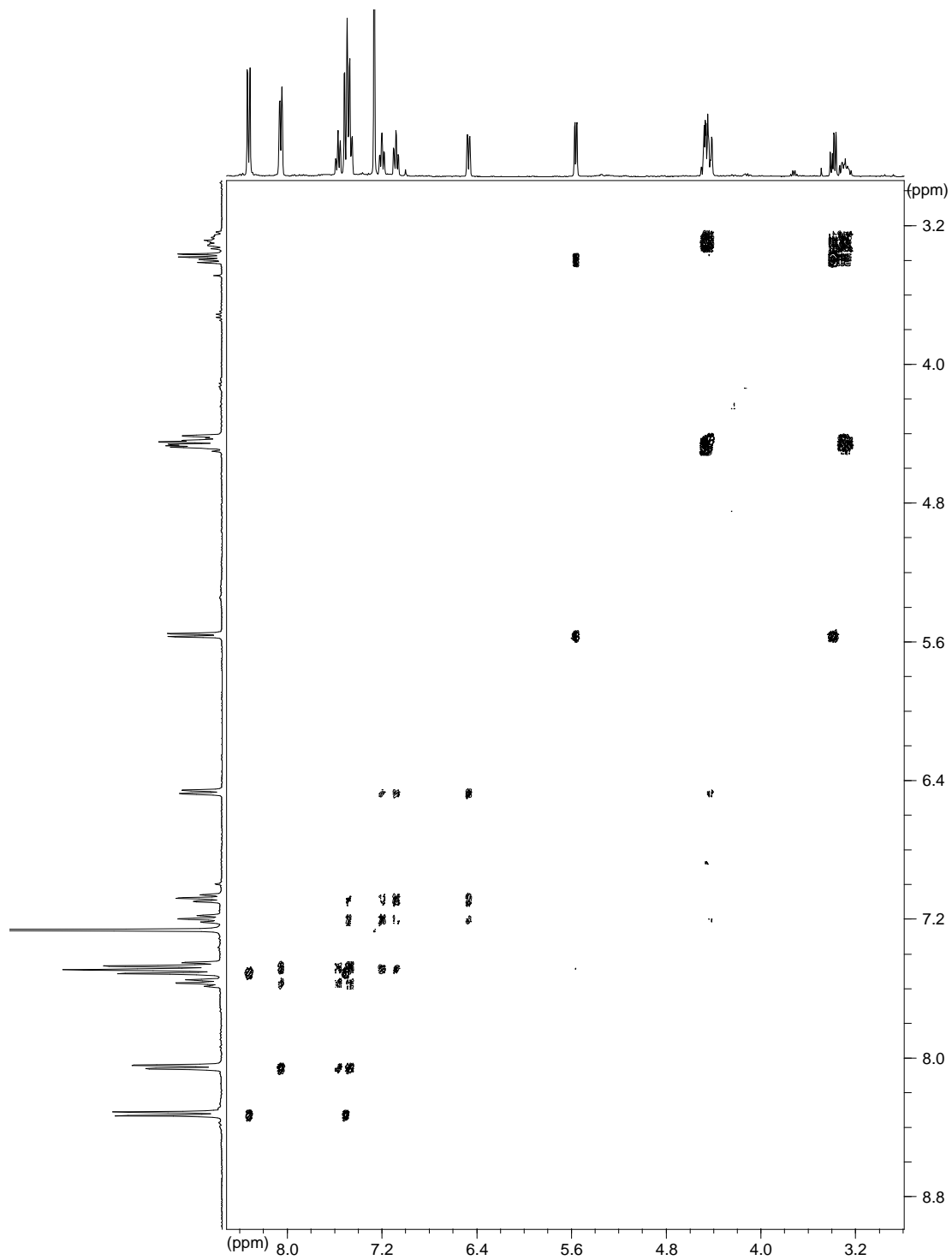
Analysis of Product *cis*-**27**:

$^1\text{H-NMR}$  (300 MHz,  $\text{CDCl}_3$ ):  $\delta$  8.32 (m, 2H), 8.14 (m, 2H), 7.67 (m, 1H), 7.58-7.49 (m, 4H), 7.13-7.10 (m, 2H), 7.02 (m, 1H), 6.58 (m, 1H), 5.17 (d,  $J = 5.65$  Hz, 1H), 4.37 (m, 1H), 4.06 (m, 1H), 4.02 (m, 1H), 3.74 (m, 1H), 3.13 (m, 1H). EI-MS  $m/z$  (%): 413 ( $[\text{C}_{25}\text{H}_{19}\text{NO}_5]^+$ , 3), 105 (100), 77 (49). NP-HPLC: Gradient (2 ml/min): ethyl acetate/hexane 50:50 (2 min)  $\rightarrow$  100:0 (14 min); Retention Time: 10.40 min; Detection  $\lambda$ : 220 – 340 nm.

Analysis of Product *trans*-**27**:

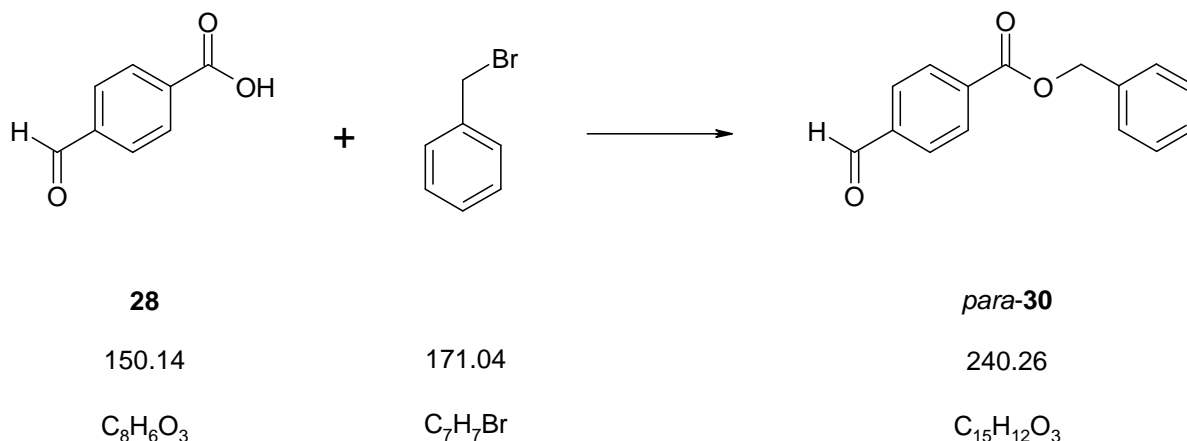
$^1\text{H-NMR}$  (300 MHz,  $\text{CDCl}_3$ ):  $\delta$  8.32 (m, 2H), 8.05 (m, 2H), 7.60-7.42 (m, 6H), 7.20 (m, 1H), 7.08 (m, 1H), 6.47 (d,  $J = 7.72$  Hz, 1H), 5.56 (d,  $J = 6.78$  Hz, 1H), 4.49-4.41 (m, 3H), 3.43-3.22 (m, 2H). EI-MS  $m/z$  (%): 413 ( $[\text{C}_{25}\text{H}_{19}\text{NO}_5]^+$ , 3), 105 (100), 77 (59). NP-HPLC: Gradient (2 ml/min): ethyl acetate/hexane 50:50 (2 min)  $\rightarrow$  100:0 (14 min); Retention Time: 15.04 min; Detection  $\lambda$ : 220 – 340 nm.

2D-NMR Spectrum ( $^1\text{H}/^1\text{H}$ -COSY) of Product *cis*-27:

2D-NMR Spectrum ( $^1\text{H}/^1\text{H}$ -COSY) of Product *trans*-27:

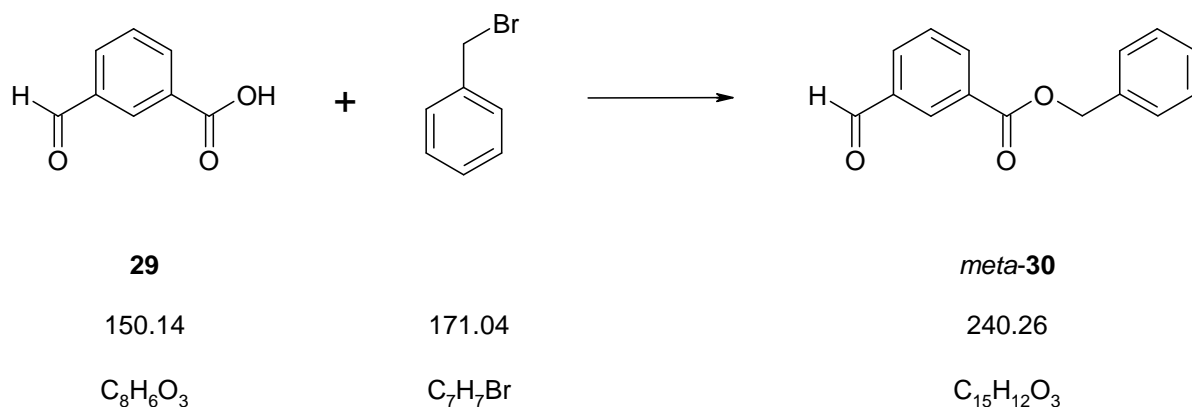
### 6.4.7 Synthesis of Cinnamyl Alcohol Derivatives *meta*-32 and *para*-32

#### 4-Formyl-benzoic acid benzyl ester (*para*-30)



4-Carboxybenzaldehyde **28** (2.3 g, 15.3 mmol), cesium carbonate (7.45 g, 22.9 mmol) and benzylbromide (2.1 ml, 18.3 mmol) were dissolved in  $\text{CH}_3\text{CN}$  (20 ml) and stirred over night. Then the reaction mixture was poured onto a saturated  $\text{NaHCO}_3$ -solution and extracted with EtOAc. The organic phase was washed with a saturated aqueous  $\text{NaCl}$ -solution, dried ( $\text{Na}_2\text{SO}_4$ ), filtered and concentrated. Ester *para*-**30** (3.7 g, 100 %) was isolated as a white solid. The product was used without further purification. TLC (EtOAc/Hexane, 1:2):  $R_f$  0.49.  $^1\text{H-NMR}$  (300 MHz,  $\text{CDCl}_3$ ):  $\delta$  10.10 (s, 1H), 8.23 (d,  $J = 8.10$  Hz, 2H), 7.95 (d,  $J = 8.48$  Hz, 2H), 7.48-7.34 (m, 5H), 5.40 (s, 2H).  $^{13}\text{C-NMR}$  (75 MHz,  $\text{CDCl}_3$ ):  $\delta$  191.7, 165.6, 139.4, 135.7, 135.3, 130.5, 129.7, 128.8, 128.7, 128.5, 67.5. EI-MS  $m/z$  (%): 240 ( $[\text{C}_{15}\text{H}_{12}\text{O}_3]^+$ , 14), 133 (38), 91 (100), 65 (26).

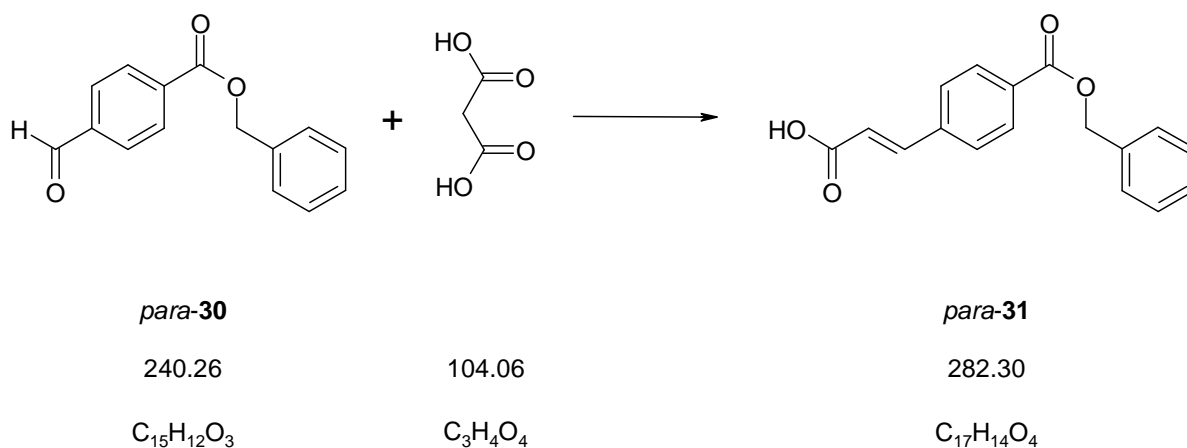
#### 3-Formyl-benzoic acid benzyl ester (*meta*-30)



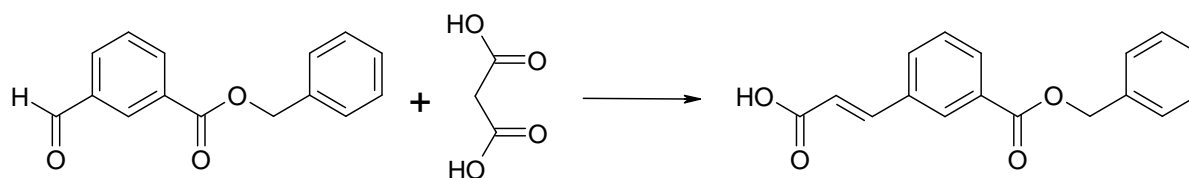


3-Carboxybenzaldehyde **29** (2.41 g, 16.01 mmol), cesium carbonate (7.77 g, 23.88 mmol) and benzylbromide (2.2 ml, 19.08 mmol) were dissolved in CH<sub>3</sub>CN (20 ml) and stirred over night. Then the reaction mixture was poured onto a saturated aqueous NaHCO<sub>3</sub>-solution and extracted with EtOAc. The organic phase was washed with a saturated aqueous NaCl-solution, dried (MgSO<sub>4</sub>), filtered and concentrated. Ester *meta*-**30** (3.95 g, 99 %) was isolated as a white solid. The product was used without further purification. TLC (EtOAc/hexane, 1:4): R<sub>f</sub> 0.65. <sup>1</sup>H-NMR (300 MHz, CDCl<sub>3</sub>): δ 10.07 (s, 1H), 8.56 (s, 1H), 8.33 (d, J = 7.72 Hz, 1H), 8.09 (d, J = 7.72 Hz, 1H), 7.62 (t, J = 7.72 Hz, 1H), 7.50 – 7.29 (m, 5H), 5.41 (s, 2H). <sup>13</sup>C-NMR (300 MHz, CDCl<sub>3</sub>): δ 191.4, 165.4, 136.7, 135.7, 135.3, 133.2, 131.4, 131.4, 129.4, 129.1, 128.9, 128.8, 128.6, 128.5, 67.3. EI-MS m/z (%): 240 ([C<sub>15</sub>H<sub>12</sub>O<sub>3</sub>]<sup>+</sup>, 3), 170 (5), 133 (6), 91 (100), 65 (15), 51 (6), 39 (8).

#### 4-(2-Carboxy-vinyl)-benzoic acid benzyl ester (*para*-**31**)



A mixture of *para*-**30** (3.7 g, 15.3 mmol), malonic acid (4.3 g, 41.2 mmol), pyridine (13.7 ml) and piperidine (1.4 ml) was heated at 60°C for 1 h and then at 100°C for 2 h with stirring. After being acidified with 5% HCl (or 10%), the precipitate was filtered off and washed with some water. Then the product was dissolved in hot methanol, cooled and precipitated with water. The white solid was dried (high vacuum) and carboxylic acid *para*-**31** (3.6 g, 84%) was isolated. <sup>1</sup>H-NMR (300 MHz, DMSO): δ 12.62 (s, 1H), 7.99 (d, J = 8.45 Hz, 2H), 7.82 (d, J = 8.29 Hz, 2H), 7.64 (d, J = 16.01 Hz, 1H), 7.48-7.32 (m, 5H), 6.66 (d, J = 16.01 Hz, 1H), 5.35 (s, 1H). <sup>13</sup>C-NMR (75 MHz, DMSO): δ 167.2, 165.1, 142.4, 138.9, 136.0, 130.5, 129.7, 128.5, 128.4, 128.1, 128.0, 122.0, 66.3. EI-MS m/z (%): 282 ([C<sub>17</sub>H<sub>14</sub>O<sub>4</sub>]<sup>+</sup>, 46), 175 (94), 91 (100), 65 (54). Mp (MeOH/H<sub>2</sub>O): 210°C.

**3-(2-Carboxy-vinyl)-benzoic acid benzyl ester (*meta*-31)***meta*-30

240.26

C<sub>15</sub>H<sub>12</sub>O<sub>3</sub>

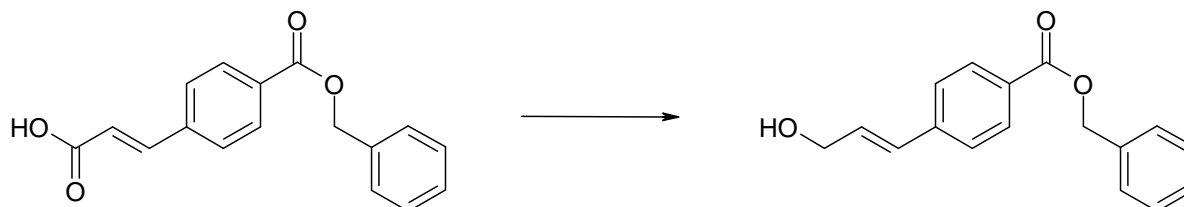
104.06

C<sub>3</sub>H<sub>4</sub>O<sub>4</sub>*meta*-31

282.30

C<sub>17</sub>H<sub>14</sub>O<sub>4</sub>

A mixture of ester *meta*-30 (8.33 g, 34.60 mmol), malonic acid (9.92 g, 95.30 mmol), pyridine (30.5 ml) and piperidine (3.2 ml) was heated at 60°C for 1 h and then at 100°C for 2 h with stirring. After being acidified with 5% HCl (or 10%), the precipitate was filtered off and washed with some water. Then the product was dissolved in hot methanol (~ 30 ml), cooled and precipitated. The white solid was dried (high vacuum) and carboxylic acid *meta*-31 (7.92 g, 81 %) was isolated. TLC (EtOAc/hexane, 1:4): R<sub>f</sub> 0.47. <sup>1</sup>H-NMR (300 MHz, DMSO): δ 8.33 (s, 1H), 8.13 (d, J = 7.91 Hz, 1H), 7.80 (d, J = 16.01 Hz, 1H), 7.70 (t, J = 7.82 Hz, 1H), 7.61 (d, J = 7.91 Hz, 1H), 7.56 – 7.45 (m, 5H), 6.73 (d, J = 16.01 Hz, 1H), 5.50 (s, 2H). <sup>13</sup>C-NMR (300 MHz, DMSO): δ 167.0, 164.9, 142.4, 135.8, 134.7, 132.1, 130.4, 130.1, 129.2, 128.7, 128.3, 127.9, 127.7, 120.5, 66.1. EI-MS m/z (%): 282 ([C<sub>17</sub>H<sub>14</sub>O<sub>4</sub>]<sup>+</sup>, 24), 264 (7), 240 (14), 175 (74), 149 (10), 133 (29), 105 (16), 95 (11), 91 (89), 77 (22), 65 (100), 55 (22), 51 (56), 44 (20), 39 (24). Mp (MeOH): 122.3 °C.

**4-(3-Hydroxy-propenyl)-benzoic acid benzyl ester (*para*-32)***para*-31

282.30

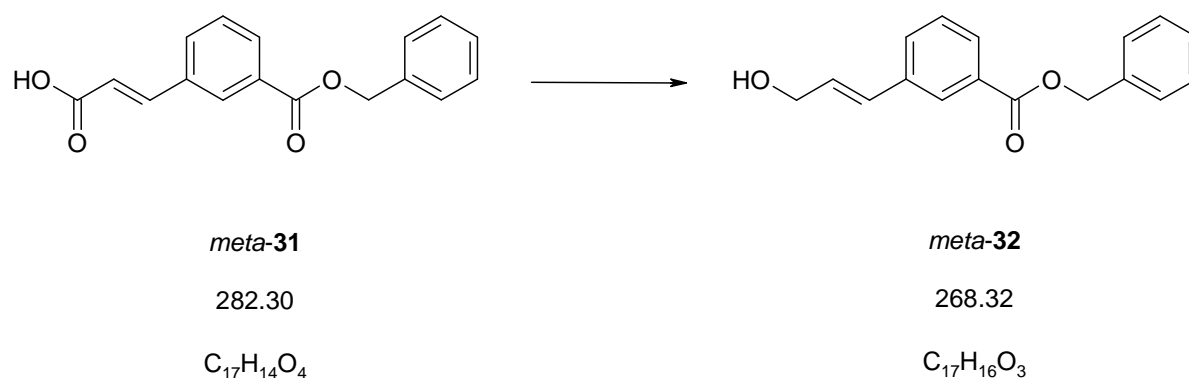
C<sub>17</sub>H<sub>14</sub>O<sub>4</sub>*para*-32

268.32

C<sub>17</sub>H<sub>16</sub>O<sub>3</sub>

A mixture of a solution of *para*-**31** (1.0 g, 3.5 mmol) in THF (30 ml), Et<sub>3</sub>N (1 ml, 7.1 mmol) and diethyl chlorophosphate (1 ml, 7.1 mmol), was stirred at room temperature for 3 h. The precipitate was filtered off. After evaporation of the filtrate, the residue was dissolved in THF (~10 ml). This solution was cooled with an ice bath and reacted with a solution of NaBH<sub>4</sub> (0.3 g, 7.1 mmol) in aqueous THF solution (~10 ml, H<sub>2</sub>O/THF (1:4), drop wise addition). Then the ice bath was removed and the reaction mixture was stirred for 2 h at room temperature. After that the mixture was poured onto a saturated NaHCO<sub>3</sub>-solution and extracted with EtOAc. The organic phase was dried (Na<sub>2</sub>SO<sub>4</sub>), filtered, concentrated and directly purified by flash chromatography (EtOAc/hexane, 2:3). The alcohol *para*-**32** (0.6 g, 62%) was isolated as a white solid. TLC (EtOAc/hexane, 2:3): R<sub>f</sub> 0.32. <sup>1</sup>H-NMR (300 MHz, CDCl<sub>3</sub>): δ 8.03 (d, *J* = 8.45 Hz, 2H), 7.47-7.34 (m, 7H), 6.67 (d, *J* = 16.01 Hz, 1H), 6.47 (m, 1H), 5.36 (s, 2H), 4.36 (dd, *J* = 1.51 Hz, 5.28 Hz, 2H). <sup>13</sup>C-NMR (75 MHz, CDCl<sub>3</sub>): δ 166.3, 141.5, 136.2, 131.5, 130.2, 129.9, 129.2, 128.8, 128.4, 128.3, 126.5, 66.8, 63.6. EI-MS *m/z* (%): 268 ([C<sub>17</sub>H<sub>16</sub>O<sub>3</sub>]<sup>+</sup>, 25), 161 (88), 91 (100), 77 (44).

### 3-(3-Hydroxy-propenyl)-benzoic acid benzyl ester (*meta*-**32**)

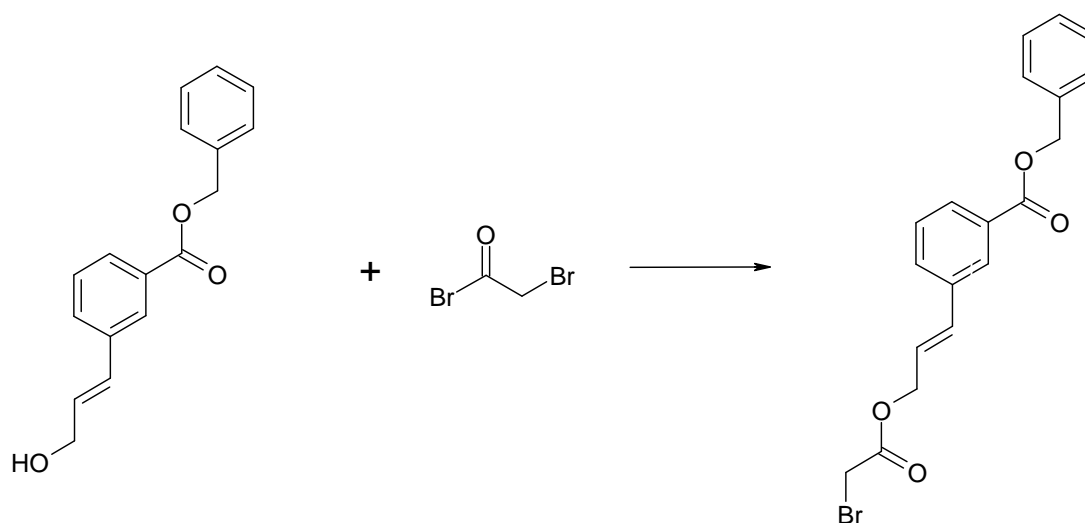


A mixture of a solution of *meta*-**31** (5.0 g, 17.7 mmol) in THF (150 ml), Et<sub>3</sub>N (4.9 ml, 35.4 mmol) and diethyl chlorophosphate (5 ml, 35.4 mmol), was stirred at room temperature for 3 h. The precipitate was filtered off. After evaporation of the filtrate, the residue was dissolved in THF (~50 ml). This solution was cooled with an ice bath and NaBH<sub>4</sub> (1.3 g, 35.4 mmol) was slowly added. Then the ice bath was removed and the reaction mixture was stirred for 2 h at room temperature. After that the mixture was poured onto a saturated NaHCO<sub>3</sub>-solution and extracted with EtOAc. The organic phase was dried (Na<sub>2</sub>SO<sub>4</sub>), filtered, concentrated and directly purified by flash chromatography (EtOAc/hexane, 2:3). The alcohol *meta*-**32** (2.93 g, 62%) was isolated as a colourless liquid. TLC (EtOAc/Hexan, 2:3): R<sub>f</sub> 0.43. <sup>1</sup>H-NMR (300 MHz, CDCl<sub>3</sub>): δ 8.09 (s, 1H), 7.95 (d, *J* = 7.72 Hz, 1H), 7.57 (d, *J* = 7.72 Hz, 1H), 7.47 – 7.32

(m, 6H), 6.66 (d,  $J = 16.01$  Hz, 1H), 6.43 (dt,  $J_1 = 16.01$  Hz,  $J_2 = 5.46$  Hz, 1H), 5.37 (s, 2H), 4.35 (d,  $J = 5.46$  Hz, 2H).  $^{13}\text{C-NMR}$  (300 MHz,  $\text{CDCl}_3$ ):  $\delta$  166.5, 137.2, 136.1, 130.9, 130.1, 129.9, 128.9, 128.8, 128.8, 128.4, 128.4, 127.8, 66.9, 63.6, 62.2. EI-MS  $m/z$  (%): 268 ( $[\text{C}_{17}\text{H}_{16}\text{O}_3]^+$ , 6), 252 (5), 240 (7), 224 (25), 179 (6), 161 (46), 145 (20), 133 (15), 115 (14), 107 (13), 91 (100), 77 (25), 65 (27), 51 (12), 44 (7), 39 (11).

#### 6.4.8 Synthesis of Fuopyranone 36

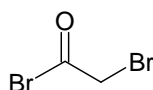
##### 3-[3-(2-Bromo-acetoxy)-propenyl]-benzoic acid benzyl ester (*meta*-33)

*meta*-32

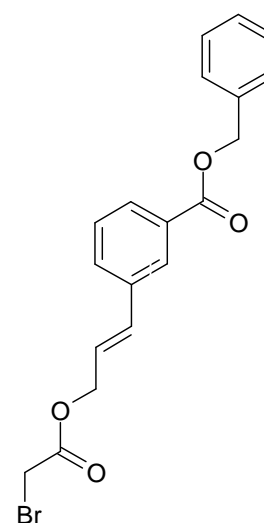
268.32

 $\text{C}_{17}\text{H}_{16}\text{O}_3$ 

+



201.85

 $\text{C}_2\text{H}_2\text{Br}_2\text{O}$ *meta*-33

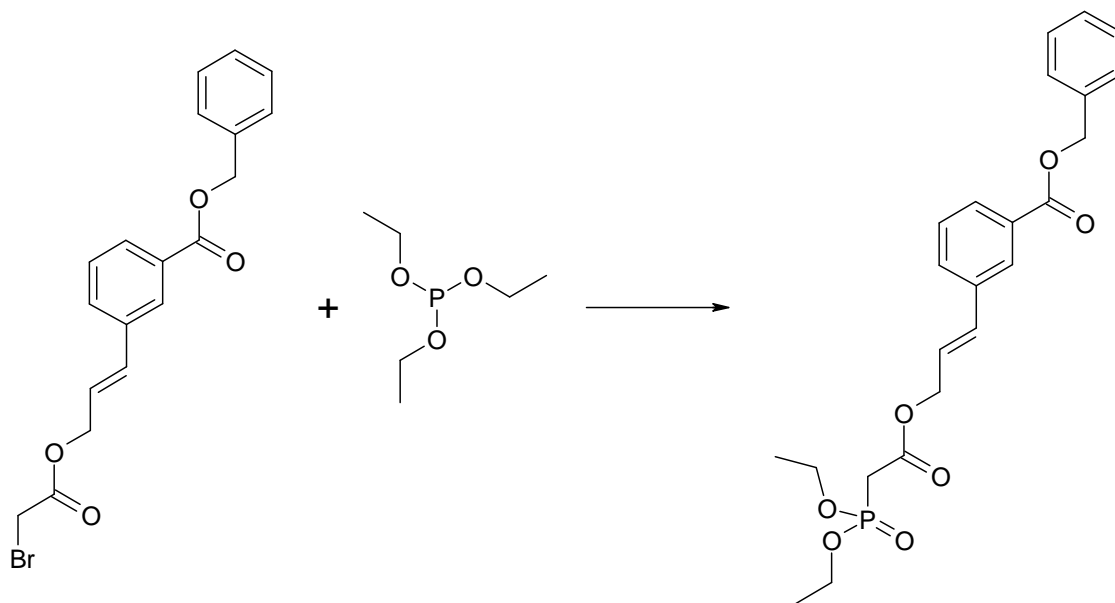
389.25

 $\text{C}_{19}\text{H}_{17}\text{BrO}_4$ 

A solution of bromoacetyl bromide (122  $\mu\text{l}$ , 1.39 mmol) in  $\text{CH}_2\text{Cl}_2$  (1 ml) was added dropwise to a stirred solution of alcohol *meta*-32 (373 mg, 1.39 mmol) and pyridine (124  $\mu\text{l}$ , 1.53 mmol) in  $\text{CH}_2\text{Cl}_2$  (3 ml) at  $0^\circ\text{C}$  under a nitrogen atmosphere. Directly after the addition of bromoacetyl bromide the colour changed to white, later yellow and formation of a solid was visible. The obtained suspension was allowed to warm to room temperature during one hour. The mixture was poured onto saturated aqueous ammonium chloride and extracted three times with  $\text{CH}_2\text{Cl}_2$ . The combined organic phases were dried ( $\text{Na}_2\text{SO}_4$ ), concentrated and directly purified by flash chromatography (EtOAc/hexane, 1:4) Ester *meta*-33 (400 mg, 74%) was obtained as colourless oily liquid. TLC (EtOAc/hexane, 2:3):  $R_f$  0.77.  $^1\text{H-NMR}$  (300 MHz,  $\text{CDCl}_3$ ):  $\delta$  8.10 (s, 1H), 7.98 (m, 1H), 7.58 (m, 1H), 7.48-7.35 (m, 6H), 6.73 (d,  $J=15.82$  Hz,

1H), 6.35 (m, 1H), 5.38 (s, 2H), 4.84 (m, 2H), 3.89 (s, 2H).  $^{13}\text{C}$ -NMR (300 MHz,  $\text{CDCl}_3$ ):  $\delta$  167.1, 166.3, 136.5, 136.1, 134.0, 131.2, 130.8, 129.5, 128.8, 128.4, 128.0, 123.7, 67.0, 66.5, 25.8. EI-MS  $m/z$  (%): 390 ( $[\text{C}_{19}\text{H}_{17}\text{O}_4^{81}\text{Br}]^+$ , 2), 388 ( $[\text{C}_{19}\text{H}_{17}\text{O}_4^{79}\text{Br}]^+$ , 2), 283 (42), 159 (66), 144 (78), 91 (100).

### 3-{3-[2-(Diethoxy-phosphoryl)-acetoxy]-propenyl}-benzoic acid benzyl ester (*meta*-34)



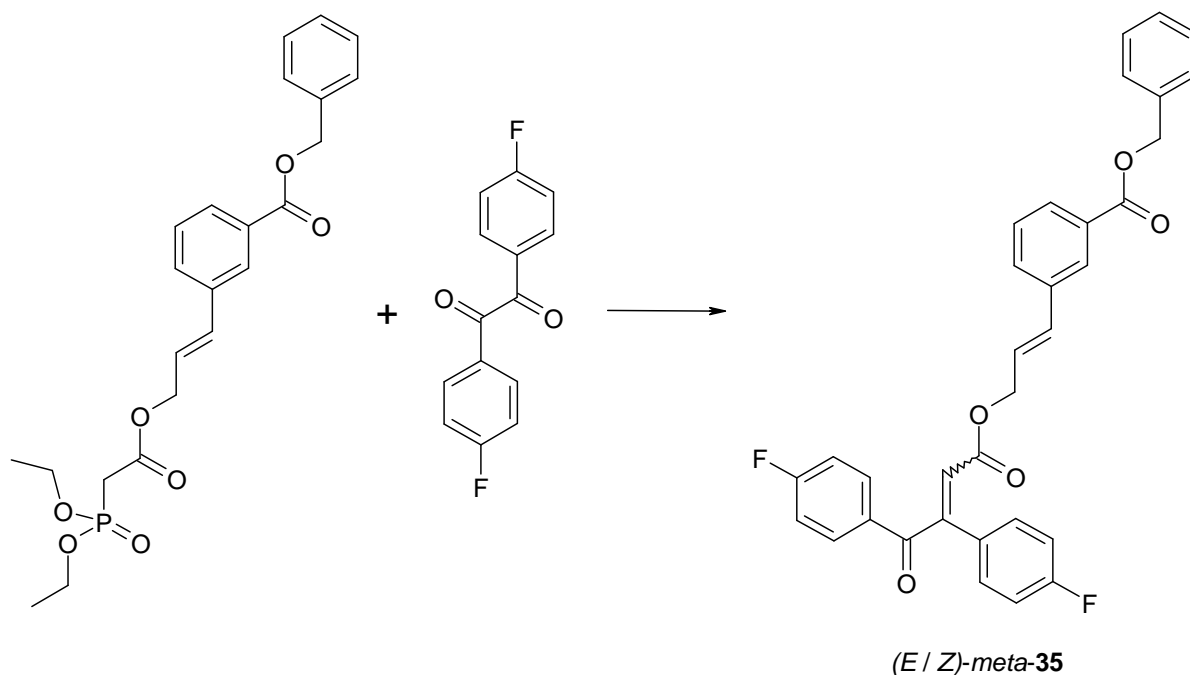
*meta*-33  
389.25  
 $\text{C}_{19}\text{H}_{17}\text{BrO}_4$

166.16  
 $\text{C}_6\text{H}_{15}\text{O}_3\text{P}$

*meta*-34  
446.44  
 $\text{C}_{23}\text{H}_{27}\text{O}_7\text{P}$

The bromoacetate *meta*-33 (500 mg, 1.28 mmol) was dissolved in THF (~ 20 ml). Triethyl phosphite (1 ml, 5.88 mmol) was added and the stirred solution was refluxed for 20 h. Then the reaction mixture was allowed to cool down to room temperature. After this the reaction mixture was concentrated and dried (high vacuum) by heating with a water bath up to 40°C. The phosphonate *meta*-34 (578 mg, 92 %) was isolated as a brown and oily liquid.  $^1\text{H}$ -NMR (300 MHz,  $\text{CDCl}_3$ ):  $\delta$  8.08 (s, 1H), 7.97 (m, 1H), 7.57 (m, 1H), 7.50-7.35 (m, 6H), 6.72 (d,  $J = 16.01$  Hz, 1H), 6.34 (m, 1H), 5.37 (s, 2H), 4.81 (m, 2H), 4.17 (m, 4H), 3.02 (d,  $^2J_{\text{HP}} = 21.66$  Hz, 2H), 1.33 (t,  $J = 7.06$  Hz, 6H).  $^{31}\text{P}$ -NMR (121 MHz,  $\text{CDCl}_3$ ): 19.58 (s, 1P). EI-MS  $m/z$  (%): 446 ( $[\text{C}_{23}\text{H}_{27}\text{O}_7\text{P}]^+$ , 7), 179 (99), 151 (66), 123 (61), 91 (100).

**3-{3-[3,4-Bis-(4-fluoro-phenyl)-4-oxo-but-2-enoyloxy]-propenyl}-benzoic acid benzyl ester (*meta*-35)**



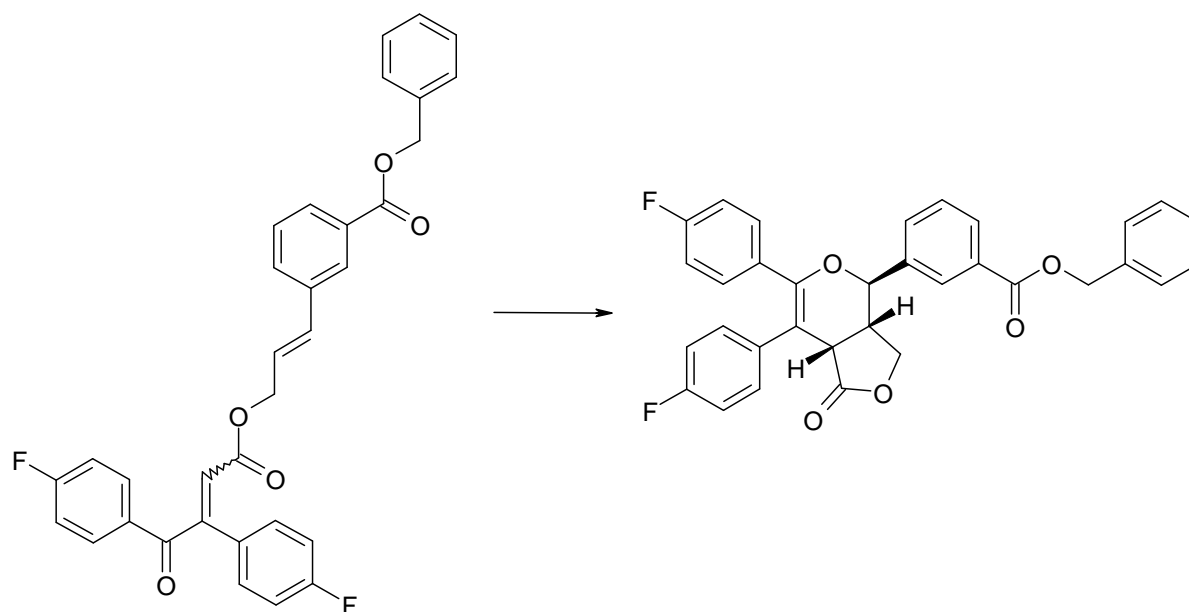
*meta*-34  
446.44  
C<sub>23</sub>H<sub>27</sub>O<sub>7</sub>P

246.22  
C<sub>14</sub>H<sub>8</sub>F<sub>2</sub>O<sub>2</sub>

*meta*-35  
538.55  
C<sub>33</sub>H<sub>24</sub>F<sub>2</sub>O<sub>5</sub>

HMDS (0.30 ml, 1.40 mmol) was added slowly to a stirred solution of *n*-butyllithium (0.80 ml, 1.30 mmol, 1.6 M solution in hexane) in dry THF (5 ml) at 0°C under a nitrogen atmosphere. After half an hour, phosphonate *meta*-34 (456 mg, 1.02 mmol) dissolved in dry THF (1 ml) was added to the solution. Then 4,4'-difluorobenzil (195 mg, 0.80 mmol) dissolved in dry THF (1 ml) was added slowly. After 1 hour the cooling bath was removed. After 2 hours, the solution was poured onto saturated aqueous ammonium chloride and extracted with EtOAc. The combined organic phases were dried (Na<sub>2</sub>SO<sub>4</sub>) and concentrated. The crude product was purified by column chromatography (EtOAc/hexane, 1:5) and ester *meta*-35 (272 mg, 50%) was isolated as a yellow oily liquid. The ratio of the *E*- and *Z*-isomer was about 1:1 (as determined by NMR). TLC (EtOAc/hexane, 1:5): *R<sub>f</sub>* 0.33 (both *E*- and *Z*-isomer). <sup>1</sup>H-NMR (300 MHz, CDCl<sub>3</sub>, mixture of isomers): δ 8.05-8.02 (m, 2H), 8.00-7.92 (m, 6H), 7.54-7.32 (m, 18H), 7.17-7.00 (m, 8H), 6.61-6.49 (m, 3H), 6.28-6.13 (m, 3H), 5.38 (s, 4H), 4.76-4.68 (m, 4H). EI-MS *m/z* (%): 538 ([C<sub>33</sub>H<sub>24</sub>F<sub>2</sub>O<sub>5</sub>]<sup>+</sup>, 14), 272 (61), 123 (100), 91 (73).

**3-[6,7-Bis-(4-fluoro-phenyl)-1-oxo-1,3a,4,7a-tetrahydro-3H-furo[3,4-c]pyran-4-yl]-benzoic acid benzyl ester (36)**



*(E/Z)*-**meta-35**

*meta-35*

538.55

$C_{33}H_{24}F_2O_5$

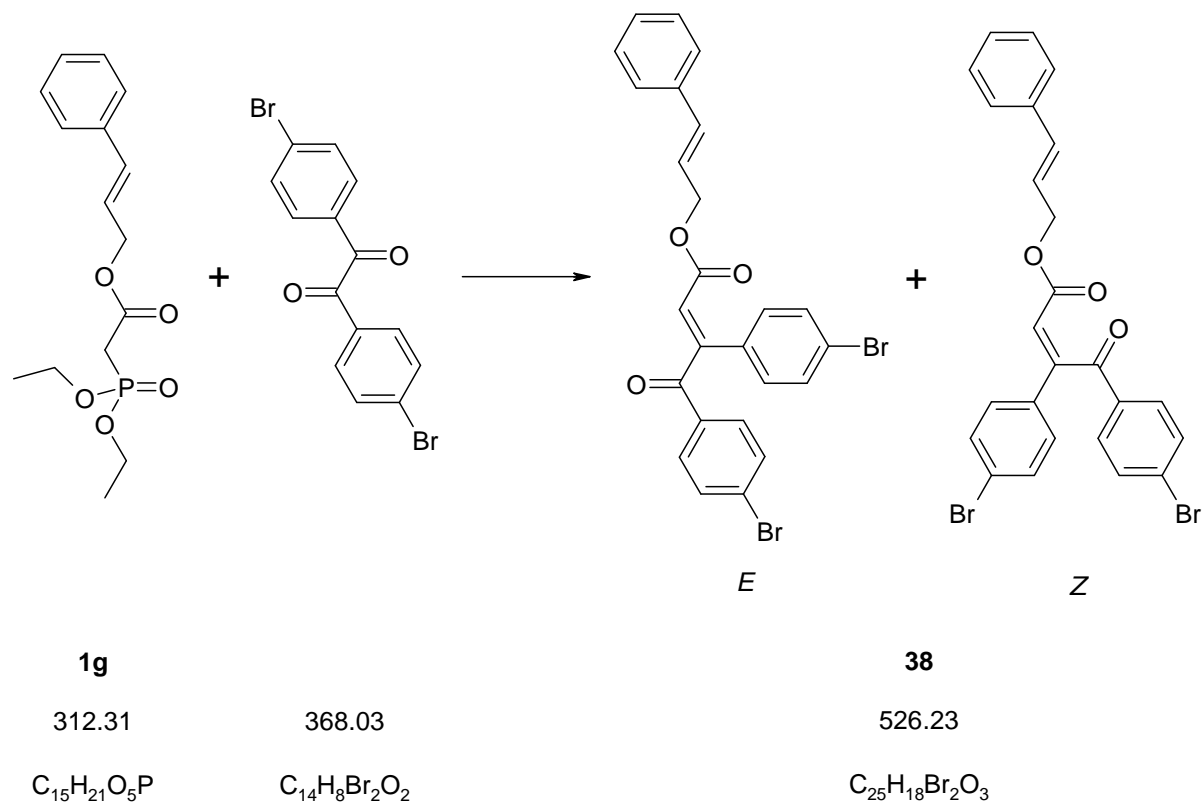
*(+/-)*-**36**

538.55

$C_{33}H_{24}F_2O_5$

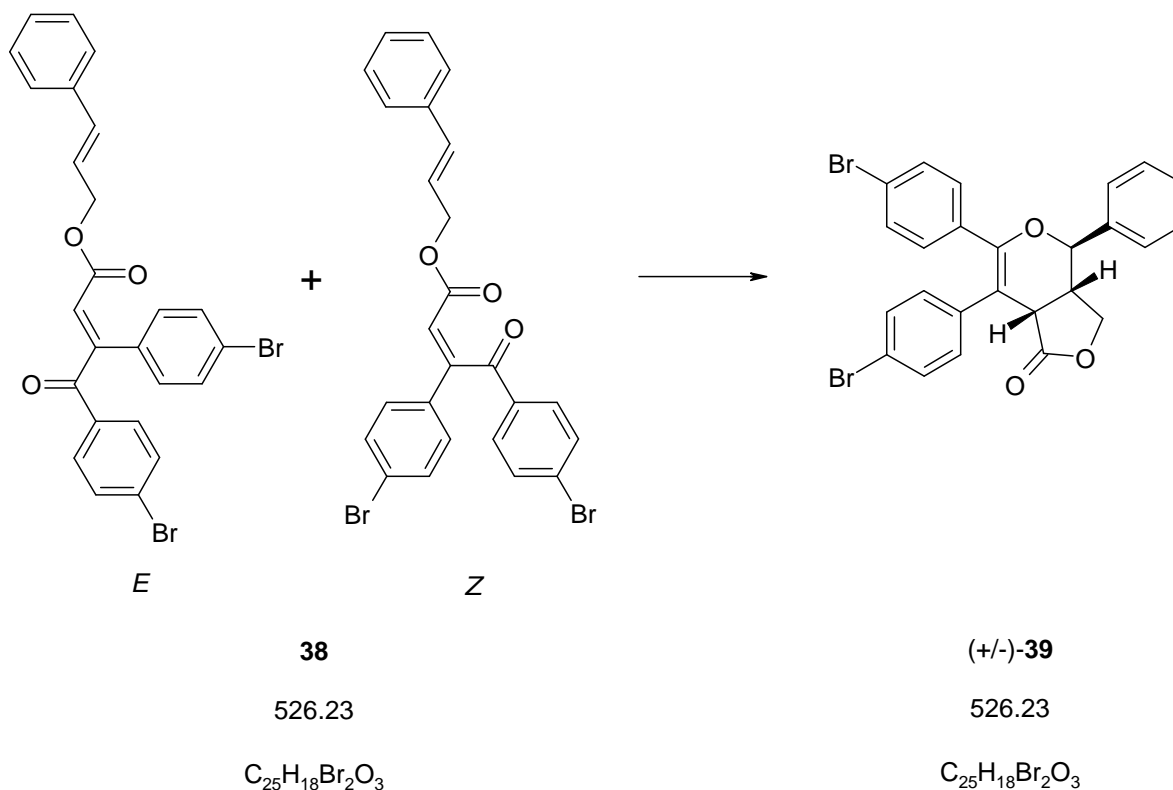
The reaction was carried out in an autoclave. Ester *meta-35* (258 mg, 0.48 mmol) was dissolved in dry toluene (20 ml) and placed in a Teflon<sup>®</sup> reaction chamber inside a sealed steel autoclave. The autoclave was heated and kept at an inside temperature of 170-175°C for 23 h. Then the solvent was removed (vacuum). The crude product was directly recrystallised in MeOH (~100 ml) and after filtration pure **36** (66 mg, 25%) was isolated. TLC (EtOAc/Hexane, 1:2):  $R_f$  0.41. <sup>1</sup>H-NMR (300 MHz, CDCl<sub>3</sub>): δ 8.16-8.12 (m, 2H), 7.65 (d,  $J$  = 7.72 Hz, 1H), 7.54 (t,  $J$  = 7.54 Hz, 1H), 7.48-7.36 (m, 5 H), 7.17-7.10 (m, 4H), 6.95 (m, 2H), 6.81 (m, 2H), 5.39 (d,  $J$  = 5.84 Hz, 2H), 4.75 (d,  $J$  = 11.11 Hz, 1H), 4.30 (m, 1H), 4.05 (d,  $J$  = 10.17 Hz, 1H), 3.88 (d,  $J$  = 7.16 Hz, 1H), 3.01 (m, 1H). EI-MS  $m/z$  (%): 538 ( $[C_{33}H_{24}F_2O_5]^+$ , 48), 272 (66), 123 (100), 91 (77).

## 6.4.9 Synthesis of Furopyranone 39

**(E/Z)-3,4-Bis-(4-bromo-phenyl)-4-oxo-but-2-enoic acid 3-phenyl-allyl ester (38)**

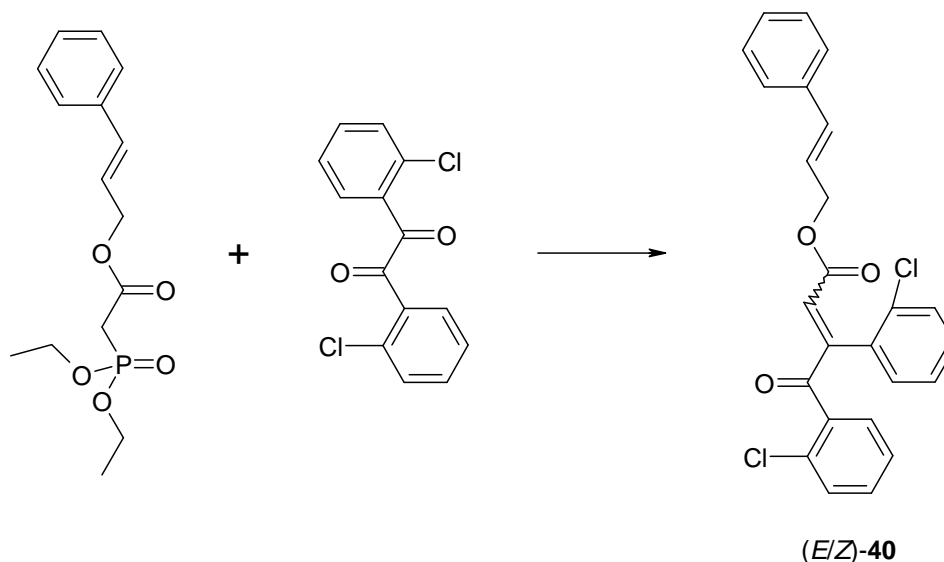
HMDS (4 ml, 19.2 mmol) was added slowly to a stirred solution of *n*-butyllithium (11 ml, 17.6 mmol, 1.6 M solution in hexane) in dry THF (40 ml) at 0°C under a nitrogen atmosphere. After half an hour, phosphonate **1g** (5 g, 16.0 mmol) dissolved in dry THF (10 ml) was added to the solution. The reaction mixture was cooled to -78°C. Then 4,4'-dibromobenzil (6.48 g, 17.6 mmol) dissolved in dry THF (22 ml) was added slowly. After 4 hours, the solution was poured onto saturated aqueous ammonium chloride and extracted with CH<sub>2</sub>Cl<sub>2</sub>. The combined organic phases were dried (Na<sub>2</sub>SO<sub>4</sub>) and concentrated. The crude product was purified by column chromatography (EtOAc/hexane, 1:7) and ester **38** (3.2 g, 47%) was isolated as a yellow oily liquid. The ratio of the *E*- and *Z*-isomer was about 3:1 (as determined by NMR). TLC (EtOAc/hexane, 1:4): *R<sub>f</sub>* 0.66 (both *E*- and *Z*-isomer). <sup>1</sup>H-NMR (300 MHz, CDCl<sub>3</sub>, mixture of isomers): δ 7.79-7.41 (m, 15H), 7.29-7.19 (m, 11H), 6.54-6.47 (m, 3H), 6.26 (s, 1H, *Z*-isomer), 6.12-5.99 (m, 2H), 4.69-4.61 (m, 4H). EI-MS *m/z* (%): 526 ([C<sub>25</sub>H<sub>18</sub>Br<sub>2</sub>O<sub>3</sub>]<sup>+</sup>, 25), 394 (80), 183 (100), 117 (97), 115 (90).



**6,7-Bis-(4-bromo-phenyl)-4-phenyl-3a,7a-dihydro-3H,4H-furo[3,4-c]pyran-1-one (39)**


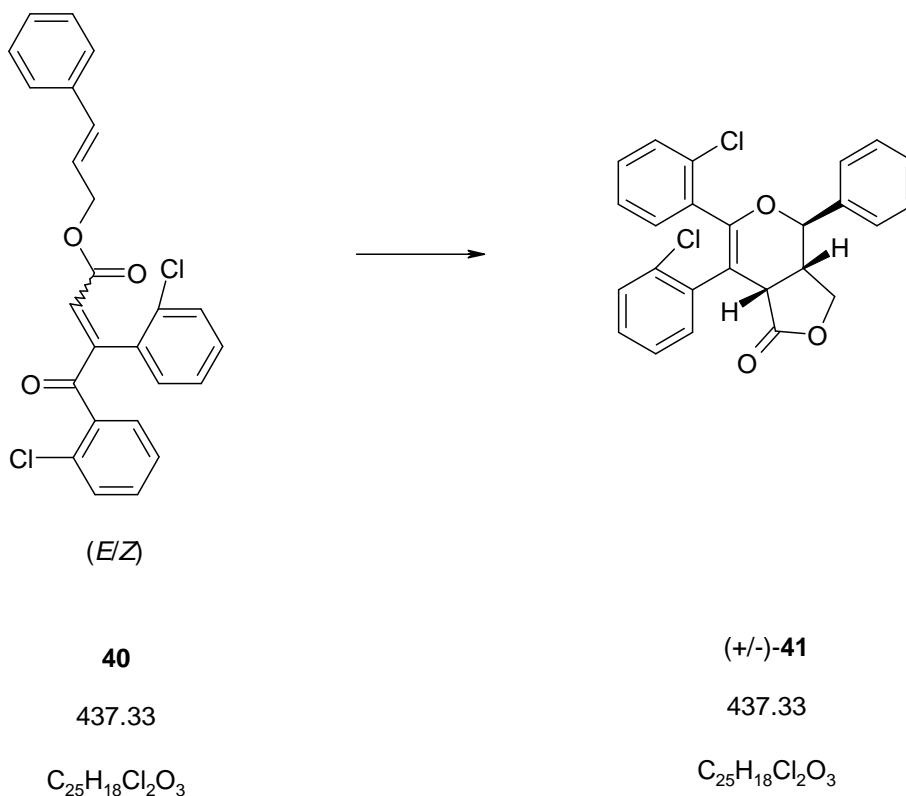
The reaction was carried out in an autoclave. Ester (*E/Z*)-**38** (314 mg, 0.60 mmol) was dissolved in dry toluene (25 ml) and placed in a Teflon<sup>®</sup> reaction chamber inside a sealed steel autoclave. The autoclave was heated and kept at an inside temperature of 185°C for 20 h. Then the solvent was removed (vacuum). The crude product was purified by column chromatography (EtOAc/hexane, 1:4) and ester **39** (85 mg, 27%) was isolated as a white solid. TLC (EtOAc/Hexane, 1:4):  $R_f$  0.32. <sup>1</sup>H-NMR (300 MHz, CDCl<sub>3</sub>): δ 7.44 (m, 5H), 7.37 (m, 2H), 7.27 (m, 2H), 7.05 (m, 4H), 4.68 (d,  $J = 11.11$  Hz, 1H), 4.30 (m, 1H), 4.11 (d,  $J = 10.17$  Hz, 1H), 3.88 (d, 7.16 Hz, 1H), 2.96 (m, 1H). <sup>13</sup>C-NMR (300 MHz, CDCl<sub>3</sub>): δ 174.4, 151.7, 137.6, 137.4, 133.5, 131.8, 131.6, 131.5, 131.2, 129.5, 129.2, 128.0, 123.0, 121.1, 106.8, 77.9, 66.9, 42.4, 39.8. EI-MS  $m/z$  (%): 526 ([C<sub>25</sub>H<sub>18</sub>Br<sub>2</sub>O<sub>3</sub>]<sup>+</sup>, 27), 134 (52), 115 (55), 91 (100), 77 (79), 51 (57).

## 6.4.10 Synthesis of Furopyranone 41

**(E/Z)-3,4-Bis-(2-chloro-phenyl)-4-oxo-but-2-enoic acid (E)-3-phenyl-allyl ester (40)**

<b>1g</b>		<b>40</b>
312.31	279.12	437.33
$C_{15}H_{21}O_5P$	$C_{14}H_8Cl_2O_2$	$C_{25}H_{18}Cl_2O_3$

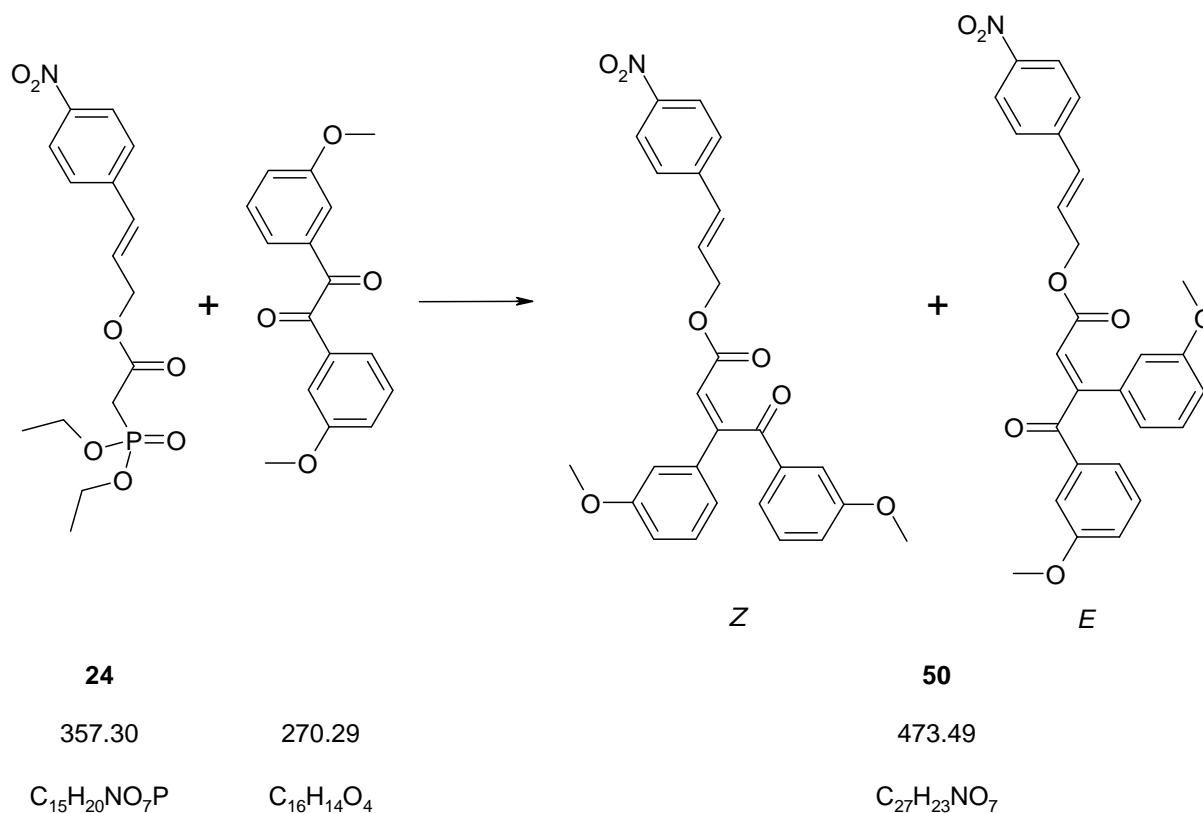
HMDS (0.8 ml, 3.85 mmol) was added slowly to a stirred solution of *n*-butyllithium (2.2 ml, 3.53 mmol, 1.6 M solution in hexane) in dry THF (5 ml) at 0°C under a nitrogen atmosphere. After half an hour, phosphonate **1g** (1 g, 3.21 mmol) dissolved in dry THF (1 ml) was added to the solution. Then 2,2'-dichlorobenzil (984 mg, 3.53 mmol) dissolved in dry THF (1 ml) was added slowly. After 4 hours, the solution was poured onto saturated aqueous ammonium chloride and extracted with  $CH_2Cl_2$ . The combined organic phases were dried ( $Na_2SO_4$ ) and concentrated. The crude product was purified by column chromatography (EtOAc/hexane, 1:8  $\rightarrow$  1:7) and ester **40** (330 mg, 24%) was isolated as a yellow oily liquid. Only *E*-**40** was isolated. TLC (EtOAc/hexane, 1:7):  $R_f$  0.31 (*E*-isomer).  $^1H$ -NMR (300 MHz,  $CDCl_3$ , *E*-isomer):  $\delta$  7.55-7.28 (m, 13H), 6.63 (s, 1H), 6.49 (m, 1H), 6.04 (m, 1H), 4.66 (m, 2H). EI-MS  $m/z$  (%): 438 ( $[C_{25}H_{18}^{37}ClO_3]^+$ , 7), 436 ( $[C_{25}H_{18}^{35}ClO_3]^+$ , 11), 139 (100), 117 (77).

**6,7-Bis-(2-chloro-phenyl)-4-phenyl-3a,7a-dihydro-3H,4H-furo[3,4-c]pyran-1-one (41)**

The reaction was carried out in an autoclave. *E*-**40** (211 mg, 0.48 mmol) was dissolved in dry toluene (25 ml) and placed in a Teflon<sup>®</sup> reaction chamber inside a sealed steel autoclave. The autoclave was heated and kept at an inside temperature of 190°C for 20 h (temperature oil bath: 200°C). The solution was poured onto saturated aqueous NaHCO<sub>3</sub>-solution and extracted with EtOAc. The combined organic phases were dried (Na<sub>2</sub>SO<sub>4</sub>), filtered and concentrated (vacuum). The crude product was purified by column chromatography (EtOAc/hexane, 1:4) and **41** (76 mg, 36%) was isolated as a white solid. For x-ray analysis the compound was recrystallised from MeOH. TLC (EtOAc/Hexane, 1:4): *R<sub>f</sub>* 0.33. <sup>1</sup>H-NMR (300 MHz, CDCl<sub>3</sub>): δ 7.51-6.94 (m, 13H), 4.82 (d, *J* = 11.11 Hz, 1H), 4.34 (m, 1H), 4.10 (m, 2H), 3.15 (m, 1H). EI-MS *m/z* (%): 438 ([C<sub>25</sub>H<sub>18</sub><sup>37</sup>ClO<sub>3</sub>]<sup>+</sup>, 28), 436 ([C<sub>25</sub>H<sub>18</sub><sup>35</sup>ClO<sub>3</sub>]<sup>+</sup>, 43), 139 (100), 117 (42).

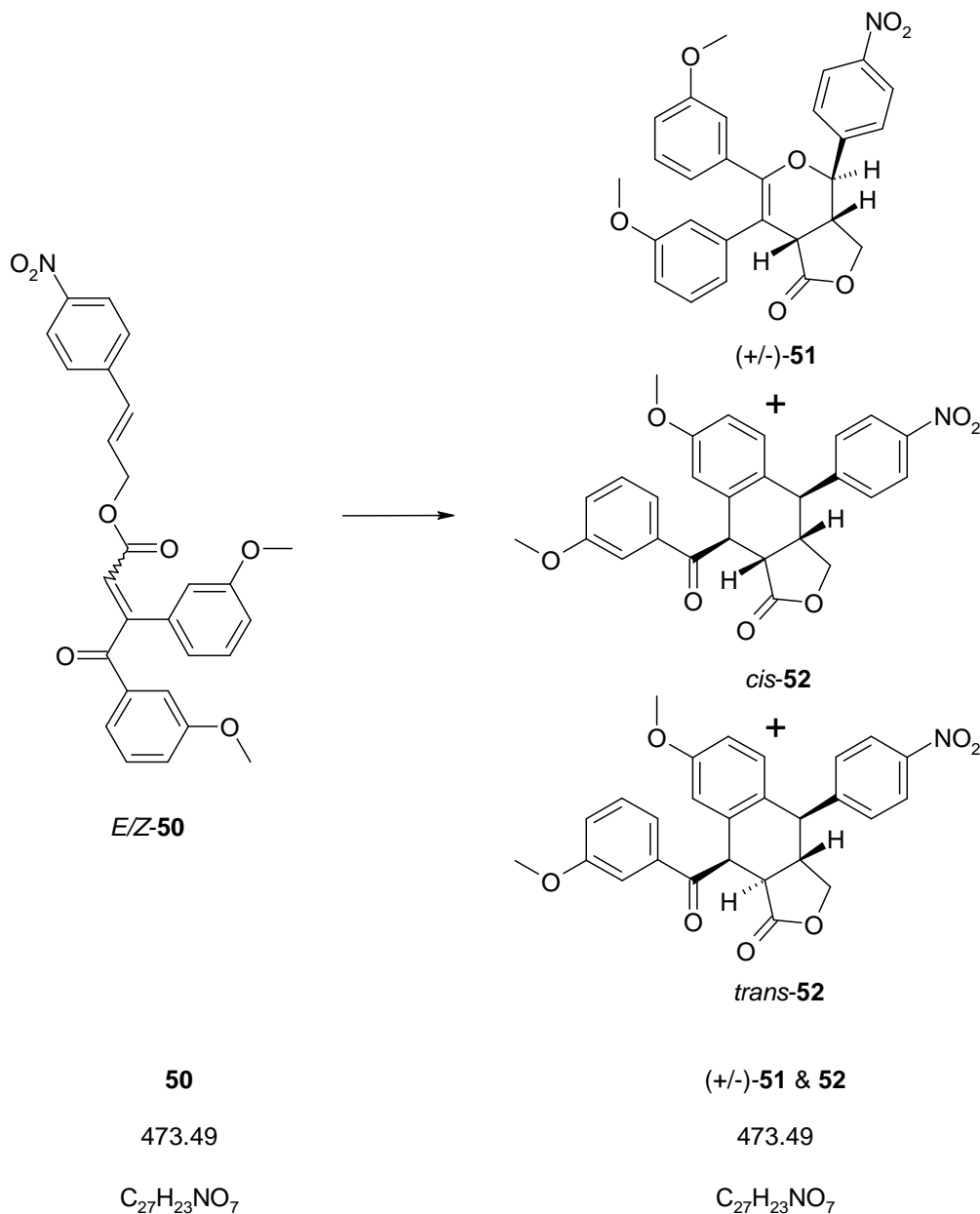
6.4.11 Synthesis of Furopyranone **51** and the Tricyclic Scaffold **52**

(*E/Z*)-3,4-Bis-(3-methoxy-phenyl)-4-oxo-but-2-enoic acid (E)-3-(4-nitro-phenyl)-allyl ester (**50**)



HMDS (0.35 ml, 1.68 mmol) was added slowly to a stirred solution of *n*-butyllithium (0.96 ml, 1.54 mmol, 1.6 M solution in hexane) in dry THF (5 ml) at 0°C under a nitrogen atmosphere. After half an hour, phosphonate **24** (500 mg, 1.40 mmol) dissolved in dry THF (1 ml) was added to the solution. Then 3,3'-dimethoxybenzil (420 mg, 1.54 mmol) dissolved in dry THF (1 ml) was added slowly. After 2.5 hours, the solution was poured onto saturated aqueous ammonium chloride and extracted with EtOAc. The combined organic phases were dried ( $Na_2SO_4$ ) and concentrated (vacuum). The crude product was purified by column chromatography (EtOAc/hexane, 1:5) and ester **50** (460 mg, 69%) was isolated as a yellow oily liquid. The ratio of the *E*- and *Z*-isomer was about 1:1 (as determined by NMR). TLC (EtOAc/hexane, 1:5):  $R_f$  0.25.  $^1H$ -NMR (300 MHz,  $CDCl_3$ , mixture of isomers):  $\delta$  8.20-8.16 (m, 4H), 7.56-6.84 (m, 20H), 6.62-6.49 (m, 3H), 6.33-6.22 (m, 3H), 4.78-4.71 (m, 4H), 3.83-3.74 (4s, 12H). EI-MS  $m/z$  (%): 473 ( $[C_{27}H_{23}NO_7]^+$ , 12), 135 (100).

**6,7-Bis-(3-methoxy-phenyl)-4-(4-nitro-phenyl)-3a,7a-dihydro-3H,4H-furo[3,4-c]pyran-1-one (51) and 7-Methoxy-9-(3-methoxy-benzoyl)-4-(4-nitro-phenyl)-3a,4,9,9a-tetrahydro-3H-naphtho[2,3-c]furan-1-one (52)**



The reaction was carried out in an autoclave. (*E/Z*)-ester **50** (202 mg, 0.43 mmol) was dissolved in dry toluene (25 ml) and placed in a Teflon<sup>®</sup> reaction chamber inside a sealed steel autoclave. The autoclave was heated up to 220°C for 24 h (inside temperature: 176°C). The solvent was removed in vacuo and the products were purified by column chromatography (EtOAc/hexane,1:2). Furopyranone **51** (52 mg, 26%) and a mixture of *cis*-/*trans*-**52** (10 mg, 5%) were isolated. After NP-HPLC up to 3 mg of pure *cis*-**52** and pure

*trans*-**52** were isolated. The ratio of 18:7:5 (**51**:*cis*-**52**:*trans*-**52**) was determined by NMR spectroscopy of the crude reaction mixture.

Analysis of Product **51**:

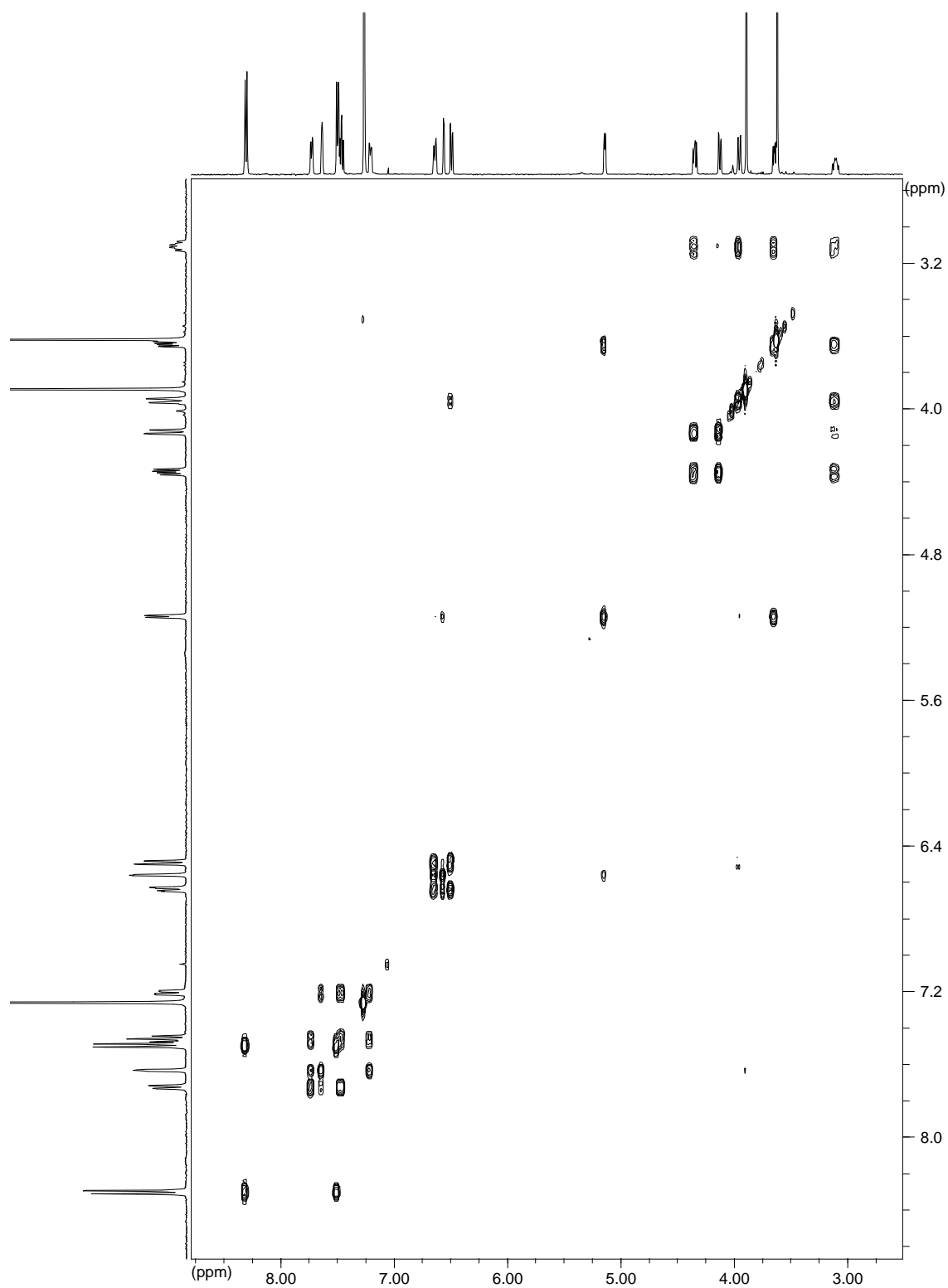
TLC (EtOAc/hexane, 1:2):  $R_f$  0.33.  $^1\text{H-NMR}$  (300 MHz,  $\text{CDCl}_3$ ):  $\delta$  8.30 (m, 2H), 7.65 (m, 2H), 7.16 (m, 1H), 7.05 (m, 1H), 6.83-6.71 (m, 6H), 4.82 (d,  $J = 10.93$  Hz, 1H), 4.31 (m, 1H), 4.06 (d,  $J = 10.17$  Hz, 1H), 3.96 (d,  $J = 7.16$  Hz, 1H), 3.66 (s, 3H), 3.55 (s, 3H), 2.93 (m, 1H). EI-MS  $m/z$  (%): 473 ( $[\text{C}_{27}\text{H}_{23}\text{NO}_7]^+$ , 40), 135 (100), 59 (80).

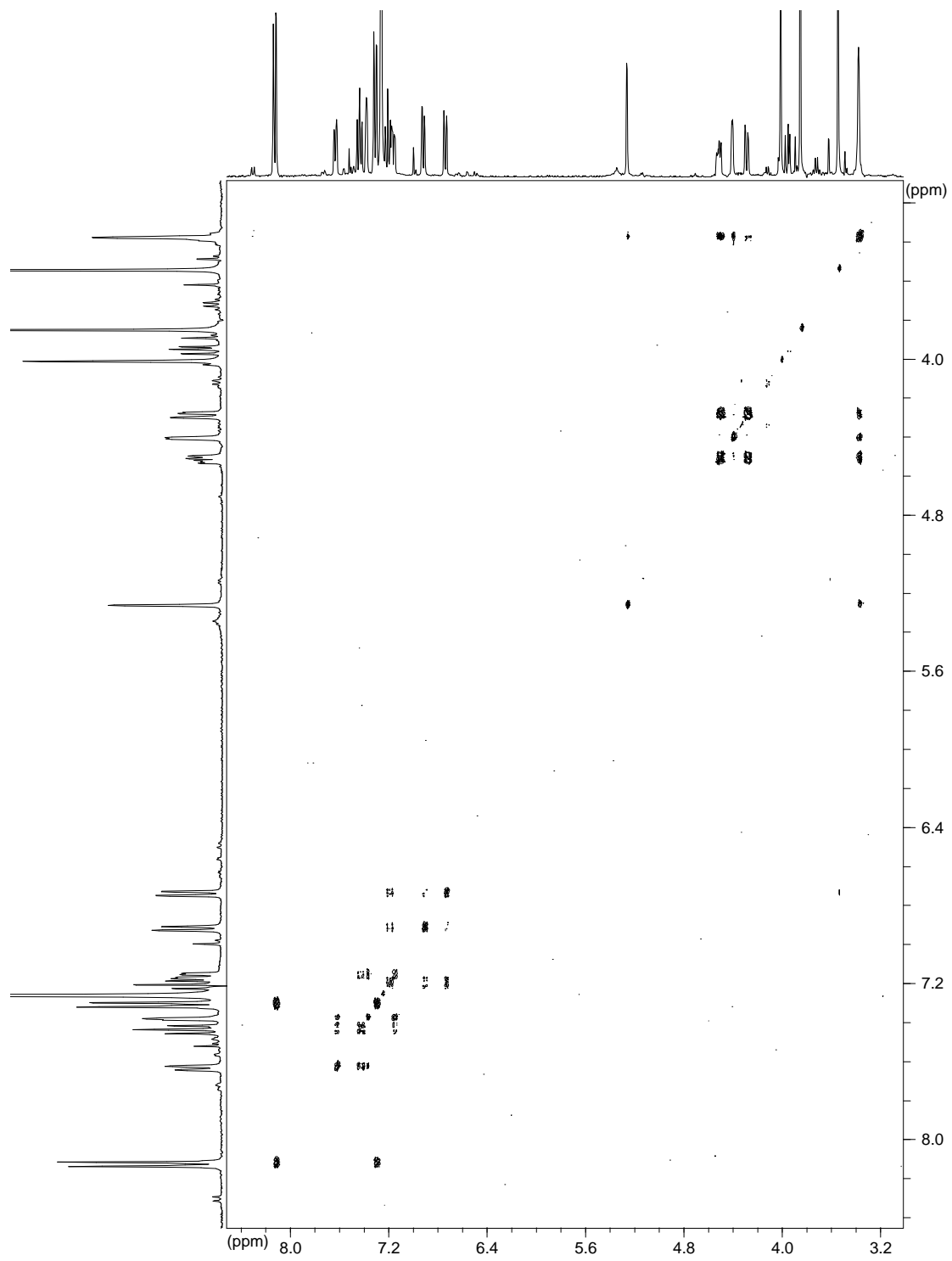
Analysis of Product *cis*-**52**:

$^1\text{H-NMR}$  (300 MHz,  $\text{CDCl}_3$ ):  $\delta$  8.30 (m, 2H), 7.72 (d,  $J = 7.72$  Hz, 1H), 7.63 (m, 1H), 7.52-7.43 (m, 3H), 7.21 (m, 1H), 6.64 (m, 1H), 6.56 (d,  $J = 2.45$  Hz, 1H), 6.49 (d,  $J = 8.48$  Hz, 1H), 5.14 (d,  $J = 5.09$  Hz, 1H), 4.35 (m, 1H), 4.13 (d,  $J = 10.93$  Hz, 1H), 3.96 (d,  $J = 10.55$  Hz, 1H), 3.89 (s, 3H), 3.67-3.62 (m, 4H), 3.11 (m, 1H). EI-MS  $m/z$  (%): 473 ( $[\text{C}_{27}\text{H}_{23}\text{NO}_7]^+$ , 4), 135 (100). NP-HPLC: Gradient (2 ml/min): ethyl acetate/hexane 50:50 (2 min)  $\rightarrow$  100:0 (14 min); Retention Time: 7.96 min; Detection  $\lambda$ : 220 – 340 nm.

Analysis of Product *trans*-**52**:

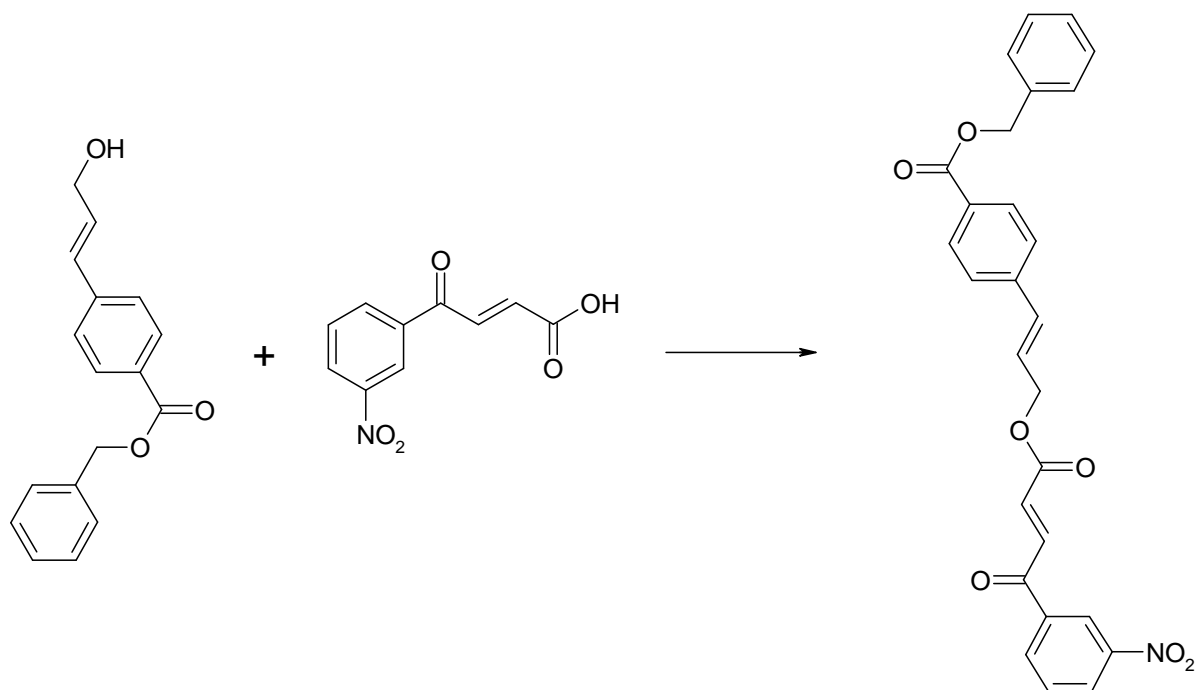
$^1\text{H-NMR}$  (300 MHz,  $\text{CDCl}_3$ ):  $\delta$  8.12 (m, 2H), 7.63 (m, 1H), 7.46-7.14 (m, 6H), 6.92 (d,  $J = 7.54$  Hz, 1H), 6.74 (m, 1H), 5.26 (s, 1H), 4.52 (m, 1H), 4.41 (d,  $J = 3.01$  Hz, 1H), 4.29 (m, 1H), 3.85 (s, 3H), 3.55 (s, 3H), 3.38 (m, 2H). EI-MS  $m/z$  (%): 473 ( $[\text{C}_{27}\text{H}_{23}\text{NO}_7]^+$ , 3), 135 (67) 86 (100). NP-HPLC: Gradient (2 ml/min): ethyl acetate/hexane 50:50 (2 min)  $\rightarrow$  100:0 (14 min); Retention Time: 8.91 min; Detection  $\lambda$ : 220 – 340 nm.

2D-NMR Spectrum ( $^1\text{H}/^1\text{H}$ -COSY) of Product *cis*-52:

2D-NMR Spectrum ( $^1\text{H}/^1\text{H}$ -COSY) of Product *trans*-52:



## 6.4.12 Synthesis of Furopyranones 53-56 for Solid Phase Chemistry

4-{3-[4-(3-Nitro-phenyl)-4-oxo-but-2-enoyloxy]-propenyl}-benzoic acid benzyl ester (**57**)*para-32**meta-5***57**

268.32

221.17

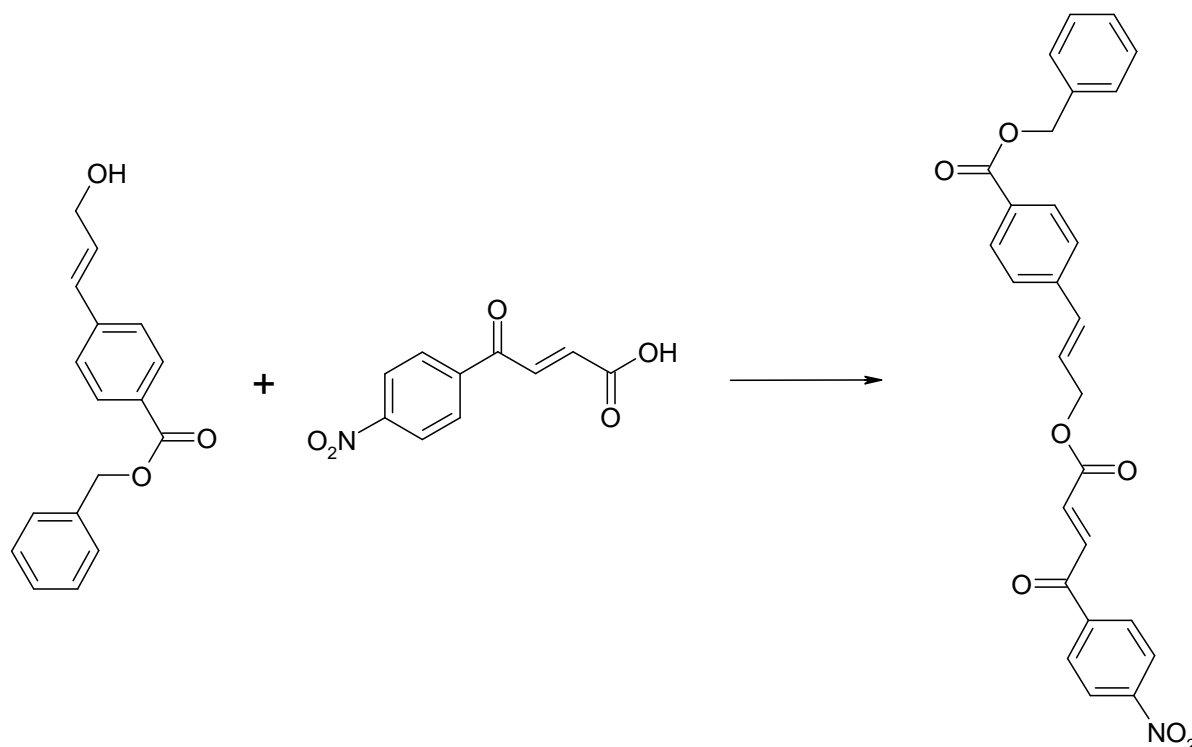
471.47

C<sub>17</sub>H<sub>16</sub>O<sub>3</sub>C<sub>10</sub>H<sub>7</sub>NO<sub>5</sub>C<sub>27</sub>H<sub>21</sub>NO<sub>7</sub>

Under an argon atmosphere the carboxylic acid **5** (3.71 g, 16.77 mmol) was dissolved in 1,2-dichloroethane (48 ml). The mixture was cooled in an ice bath (~1°C), Et<sub>3</sub>N (2.3 ml, 16.77 mmol) was added and the reaction mixture was stirred for 5 minutes. Then pivaloyl chloride (2.0 ml, 16.77 mmol) was added slowly during 10 minutes and the reaction mixture was stirred for 30 minutes. The alcohol **32** (3.0 g, 11.18 mmol) was dissolved in 1,2-dichloroethane (9 ml) and added to the reaction mixture. Finally DMAP (273 mg, 2.33 mmol) was added. Then the ice bath was removed and the reaction mixture was allowed to warm up to room temperature. The reaction mixture was poured onto saturated NaHCO<sub>3</sub>-solution and was extracted with diethyl ether. The organic phase was dried over Na<sub>2</sub>SO<sub>4</sub>, filtered and concentrated. The crude product was purified by flash chromatography (ethyl acetate/hexane, 1:4 → 1:3) and the pure ester **57** (2.49 g, 48%) was isolated. TLC (EtOAc/hexane, 2:3): R<sub>f</sub> 0.47. <sup>1</sup>H-NMR (300 MHz, CDCl<sub>3</sub>): δ 8.81 (m, 1H), 8.47 (m, 1H), 8.32 (m, 1H), 8.04 (d, *J* = 8.29 Hz, 2H), 7.95 (d, *J* = 15.64 Hz, 1H), 7.73 (dd, *J* = 8.10 Hz, 1H), 7.48-7.34 (m, 7H), 7.01 (d, *J* = 15.45 Hz, 1H), 6.76 (d, *J* = 16.01 Hz, 1H), 6.45 (m, 1H), 5.36

(s, 2H), 4.95 (m, 2H).  $^{13}\text{C-NMR}$  (75 MHz,  $\text{CDCl}_3$ ):  $\delta$  187.4, 166.13, 164.9, 148.7, 140.6, 137.9, 136.1, 135.5, 134.3, 133.9, 130.4, 130.3, 129.8, 128.7, 128.4, 128.3, 128.2, 126.7, 125.2, 123.7, 66.9, 65.9. EI-MS  $m/z$  (%): 471 ( $[\text{C}_{27}\text{H}_{21}\text{NO}_7]^+$ , <1), 130 (65), 129 (67), 102 (47), 91 (92), 86 (66), 84 (100), 57 (61), 44 (83).

**4-{3-[4-(4-Nitro-phenyl)-4-oxo-but-2-enyloxy]-propenyl}-benzoic acid benzyl ester (58)**



*para-32*

268.32

$\text{C}_{17}\text{H}_{16}\text{O}_3$

*para-5*

221.17

$\text{C}_{10}\text{H}_7\text{NO}_5$

**58**

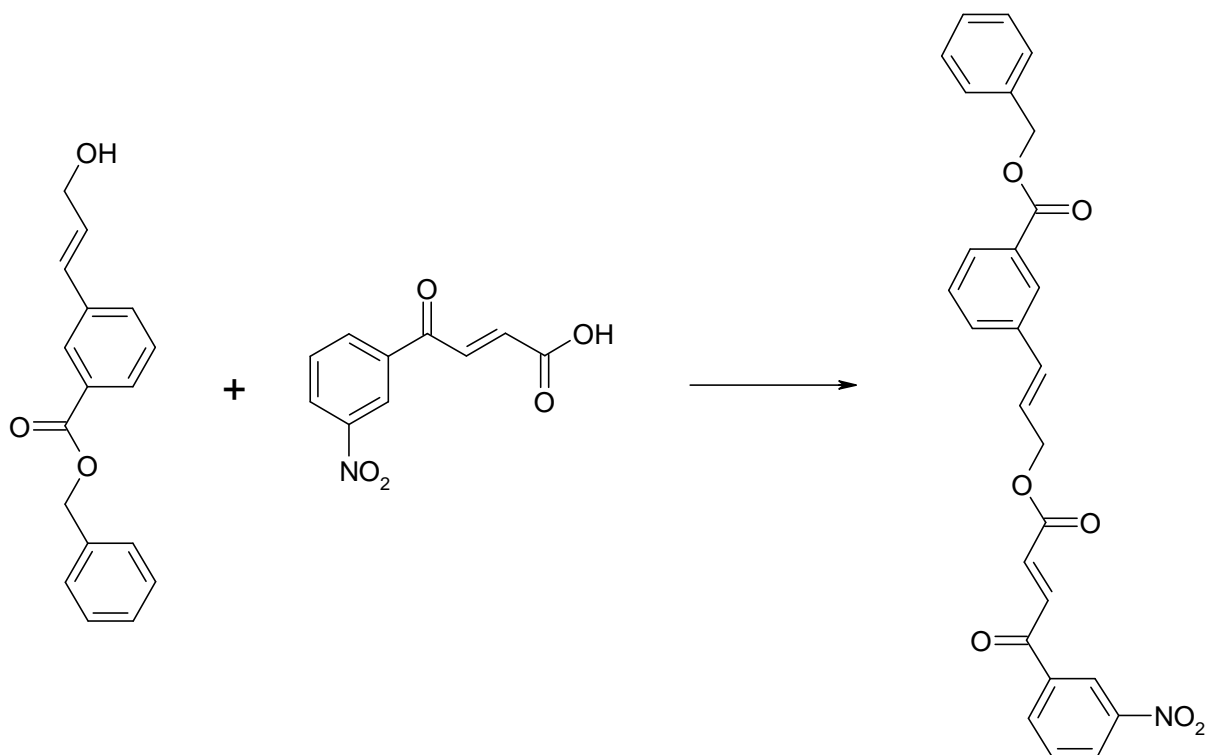
471.47

$\text{C}_{27}\text{H}_{21}\text{NO}_7$

Under an argon atmosphere the carboxylic acid **5** (1.25 g, 5.65 mmol) was dissolved in 1,2-dichloroethane (16 ml). The mixture was cooled in an ice bath ( $\sim 1^\circ\text{C}$ ),  $\text{Et}_3\text{N}$  (0.79 ml, 5.65 mmol) was added and the reaction mixture was stirred for 5 minutes. Then pivaloyl chloride (0.69 ml, 5.65 mmol) was added slowly during 10 minutes and the reaction mixture was stirred for 30 minutes. The alcohol **32** (1.01 g, 3.76 mmol) was dissolved in 1,2-dichloroethane (3 ml) and added to the reaction mixture. Finally DMAP (92 mg, 0.75 mmol) was added. Then the ice bath was removed and the reaction mixture was allowed to warm up to room temperature. The reaction mixture was poured onto saturated  $\text{NaHCO}_3$ -solution and was extracted with diethyl ether. The organic phase was dried ( $\text{Na}_2\text{SO}_4$ ), filtered and concentrated. The crude product was purified by flash chromatography (ethyl

acetate/hexane, 1:4 → 1:3 → 1:0) and the pure ester **58** (1.04 g, 59%) was isolated. TLC (EtOAc/hexane, 2:3):  $R_f$  0.63.  $^1\text{H-NMR}$  (300 MHz,  $\text{CDCl}_3$ ):  $\delta$  8.36 (m, 2H), 8.15 (m, 2H), 8.04 (m, 2H), 7.91 (d,  $J = 15.64$  Hz, 1H), 7.48-7.34 (m, 7H), 6.99 (d,  $J = 15.64$ , 1H), 6.75 (d,  $J = 16.01$ , 1H), 6.44 (m, 1H), 5.36 (s, 2H), 4.94 (m, 2H).  $^{13}\text{C-NMR}$  (75 MHz,  $\text{CDCl}_3$ ):  $\delta$  188.1, 166.2, 164.9, 150.9, 141.1, 140.6, 136.2, 135.8, 134.0, 133.9, 130.3, 130.0, 128.8, 128.4 (2C), 126.7, 125.1, 124.3, 66.9, 65.9. EI-MS  $m/z$  (%): 471 ( $[\text{C}_{27}\text{H}_{21}\text{NO}_7]^+$ , 27), 364 (49), 304 (51), 214 (51), 118 (73), 91 (100), 65 (54).

### 3-{3-[4-(3-Nitro-phenyl)-4-oxo-but-2-enoyloxy]-propenyl}-benzoic acid benzyl ester (**59**)

*meta-32*

268.32

 $\text{C}_{17}\text{H}_{16}\text{O}_3$ *meta-5*

221.17

 $\text{C}_{10}\text{H}_7\text{NO}_5$ **59**

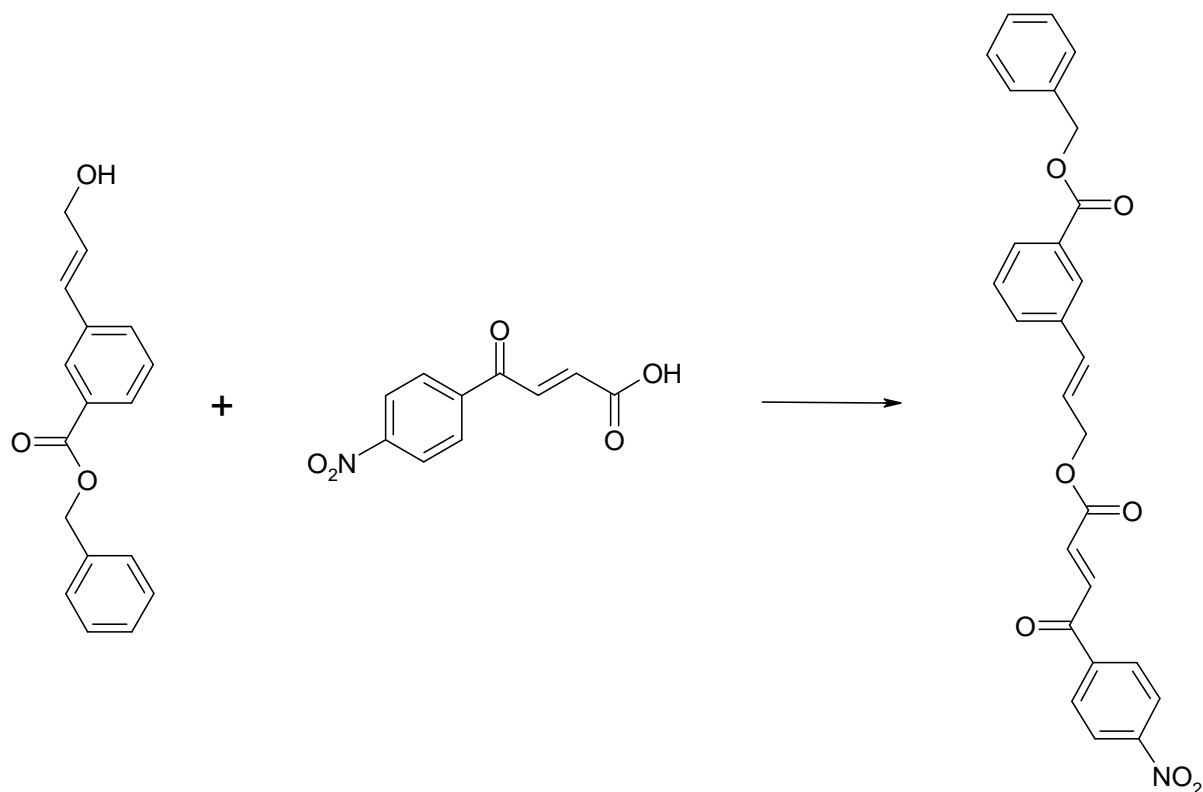
471.47

 $\text{C}_{27}\text{H}_{21}\text{NO}_7$ 

The carboxylic acid (2.1 g, 9.50 mmol) was dissolved in ethylene chloride (27 ml). At a temperature of about 10°C  $\text{Et}_3\text{N}$  (1.3 ml, 9.50 mmol) was added. The reaction mixture was stirred for 10 min at 0-5°C. Then pivaloyl chloride (1.2 ml, 9.50 mmol) was added slowly during 5 min and the reaction mixture was stirred for 30 min at 0°C. The alcohol (1.7 g, 6.33 mmol) was dissolved in ethylene chloride (5 ml) and added to the reaction mixture. After that DMAP (155 mg, 1.27 mmol) was added and the reaction mixture was stirred for 2 h and

allowed to warm up to room temperature. The reaction mixture was poured onto saturated NaHCO<sub>3</sub>-solution and extracted with diethyl ether. The organic phase was washed with saturated NaCl-solution, dried (Na<sub>2</sub>SO<sub>4</sub>), filtered and concentrated. After purification by flash chromatography (silicagel, EtOAc/hexane 1:4 → 1:3 → 1:0) the pure ester (1.46 g, 49 %) was isolated as an orange liquid. TLC (EtOAc/hexane, 1:3): R<sub>f</sub> = 0.26. <sup>1</sup>H-NMR (300 MHz, CDCl<sub>3</sub>): δ 8.82 (m, 1H), 8.48 (m, 1H), 8.33 (m, 1H), 8.11 (s, 1H), 8.00-7.92 (m, 2H), 7.74 (dd, J = 8.01 Hz, 1H), 7.60 (d, J = 7.91 Hz, 1H), 7.47-7.32 (m, 6H), 7.01 (d, J = 15.45 Hz, 1H), 6.76 (d, J = 16.01 Hz, 1H), 6.41 (m, 1H), 5.37 (s, 2H), 4.94 (m, 2H). <sup>13</sup>C-NMR (75 MHz, CDCl<sub>3</sub>): δ 187.4, 166.3, 164.9, 148.8, 138.0, 136.5, 136.1, 135.4, 134.3, 134.1, 134.0, 131.2, 130.8, 130.4, 129.5, 128.9, 128.8, 128.5, 128.4, 128.1, 128.0, 123.8 (2C), 67.0, 66.0. ESI-MS *m/z* (positive ion mode): [C<sub>27</sub>H<sub>21</sub>NO<sub>7</sub> + Na]<sup>+</sup> = 494.4.

### 3-{3-[4-(4-Nitro-phenyl)-4-oxo-but-2-enyloxy]-propenyl}-benzoic acid benzyl ester (60)

*meta*-32*para*-5

60

268.32

221.17

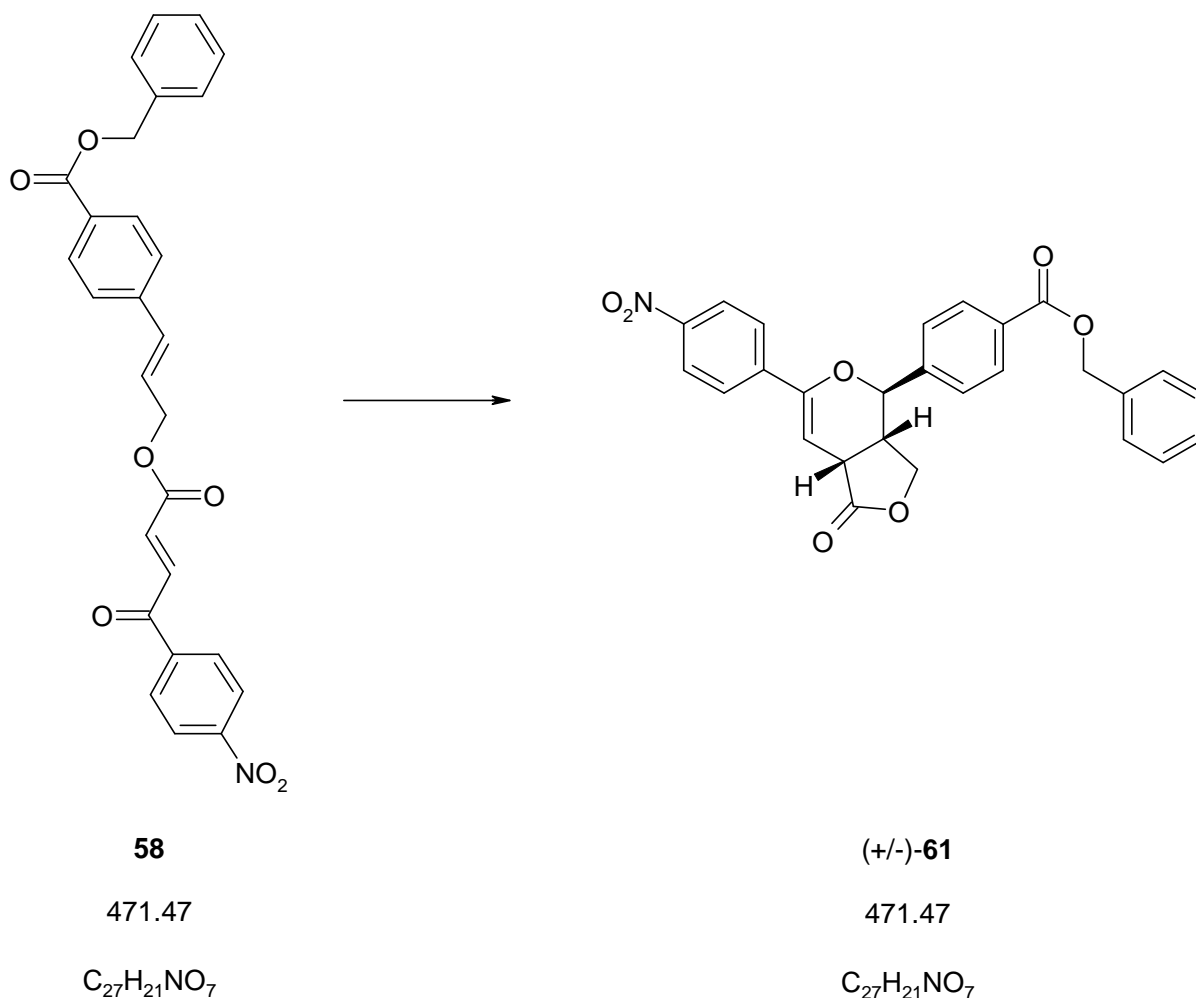
471.47

C<sub>17</sub>H<sub>16</sub>O<sub>3</sub>C<sub>10</sub>H<sub>7</sub>NO<sub>5</sub>C<sub>27</sub>H<sub>21</sub>NO<sub>7</sub>

Under an argon atmosphere the carboxylic acid **5** (1.11 g, 5.03 mmol) was dissolved in 1,2-dichloroethane (16 ml). The mixture was cooled in an ice bath (~1°C), Et<sub>3</sub>N (0.79 ml, 5.67

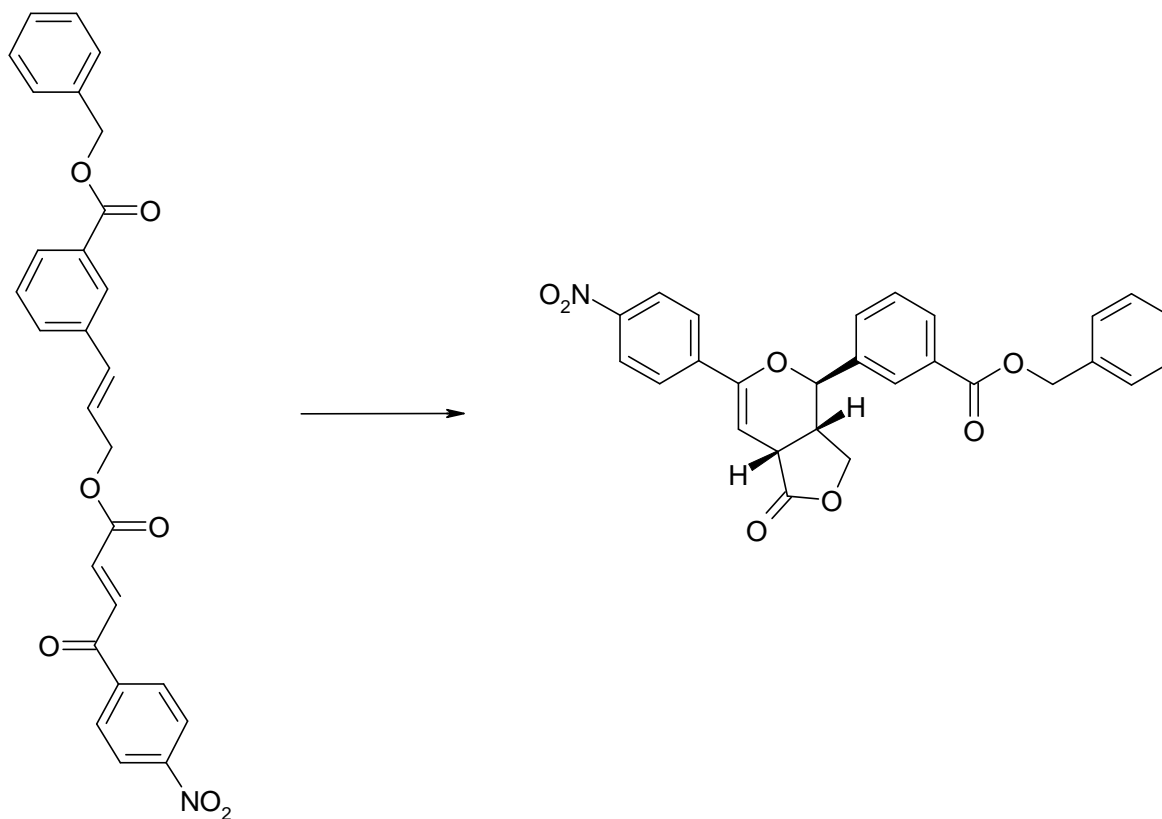
mmol) was added and the reaction mixture was stirred for 5 minutes. Then pivaloyl chloride (0.69 ml, 5.02 mmol) was added slowly during 10 minutes and the reaction mixture was stirred for 30 minutes. The alcohol **32** (0.90 g, 3.35 mmol) was dissolved in 1,2-dichloroethane (3 ml) and added to the reaction mixture. Finally DMAP (0.95 mg, 0.75 mmol) was added. Then the ice bath was removed and the reaction mixture was allowed to warm up to room temperature. The reaction mixture was poured onto saturated NaHCO<sub>3</sub>-solution and was extracted with diethyl ether. The organic phase was dried over Na<sub>2</sub>SO<sub>4</sub>, filtered and concentrated. The crude product was purified by flash chromatography (ethyl acetate/hexane, 1:4) and the pure ester **60** (869 mg, 55%) was isolated. TLC (EtOAc/hexane, 1:4): R<sub>f</sub> 0.47. <sup>1</sup>H-NMR (300 MHz, CDCl<sub>3</sub>): δ 8.36 (m, 2H), 8.17 – 8.06 (m, 4H), 7.91 (d, J = 15.64 Hz, 1H), 7.47 – 7.32 (m, 7H), 6.98 (d, J = 15.45 Hz, 1H), 6.75 (d, J = 16.01 Hz, 1H), 6.41 (m, 1H), 5.38 (s, 2H), 4.93 (m, 2H). <sup>13</sup>C-NMR (75 MHz, CDCl<sub>3</sub>): δ 188.2, 166.3, 164.9, 150.8, 141.1, 136.4, 136.1, 135.8, 134.1, 133.9, 131.1, 130.8, 129.9, 129.5, 128.9, 128.8, 128.5, 128.4, 128.0, 124.2, 123.8, 67.0, 66.0. EI-MS m/z (%): 471 ([C<sub>27</sub>H<sub>21</sub>NO<sub>7</sub>]<sup>+</sup>, 1), 380 (8), 252 (10), 232 (7), 204 (34), 189 (9), 177 (21), 159 (48), 150 (57), 145 (47), 131 (45), 115 (56), 104 (56), 91 (100), 77 (48), 65 (49), 57 (29), 51 (20), 44 (21).

**4-[6-(4-Nitro-phenyl)-1-oxo-1,3a,4,7a-tetrahydro-3H-furo[3,4-c]pyran-4-yl]-benzoic acid benzyl ester (61)**



Ester **58** (1.2 g, 2.54 mmol) was dissolved in *o*-xylene (100 ml) and refluxed for 21 h. The reaction mixture was allowed to cool down to room temperature and then the solution was poured onto saturated  $NaHCO_3$ -solution and was extracted with ethyl acetate. The organic phase was washed with brine, dried ( $Na_2SO_4$ ), filtered and concentrated. The crude product was purified by flash chromatography (ethyl acetate/hexane, 1:2) and the pure furopyranone **61** (665 mg, 55%) was isolated as an orange solid. TLC (EtOAc/hexane, 1:2):  $R_f$  0.33.  $^1H$ -NMR (300 MHz,  $CDCl_3$ ):  $\delta$  8.19-8.15 (m, 4H), 7.74 (m, 2H), 7.53 (m, 2H), 7.47-7.36 (m, 5H), 6.03 (d,  $J=5.09$  Hz, 1H), 5.39 (s, 2H), 4.62 (d,  $J=10.93$  Hz, 1H), 4.35 (m, 1H), 4.11 (d,  $J=10.17$  Hz, 1H), 3.53 (m, 1H), 2.93 (m, 1H).  $^{13}C$ -NMR (75 MHz,  $CDCl_3$ ):  $\delta$  175.4, 165.8, 162.3, 152.4, 148.1, 142.5, 139.9, 135.9, 131.3, 130.6, 130.2, 128.8, 128.5, 128.3 (2C), 127.8, 126.4, 125.6, 123.8, 96.6, 77.9, 67.6, 67.1, 38.9, 38.4. EI-MS  $m/z$  (%): 471 ( $[C_{27}H_{21}NO_7]^+$ , 53), 364 (54), 304 (66), 214 (71), 169 (63), 150 (77), 91 (100), 65 (68).

**3-[6-(4-Nitro-phenyl)-1-oxo-1,3a,4,7a-tetrahydro-3H-furo[3,4-c]pyran-4-yl]-benzoic acid benzyl ester (62)**

**60**

471.47

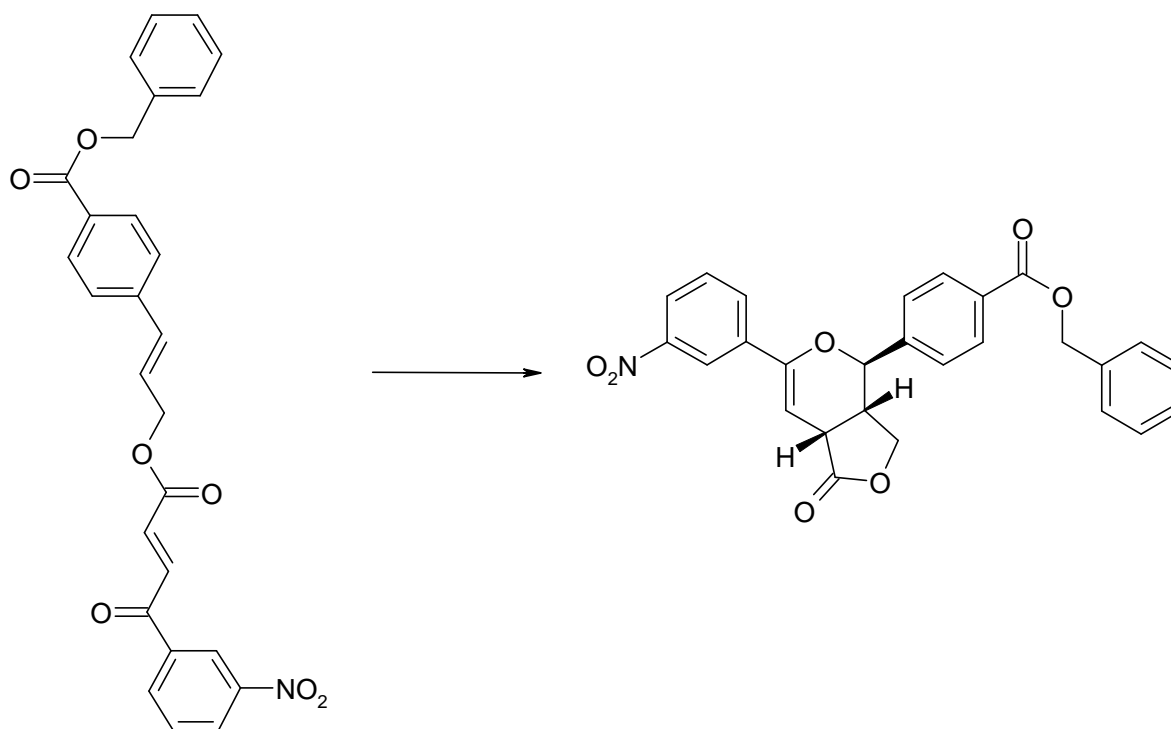
 $C_{27}H_{21}NO_7$ **(+/-)-62**

471.47

 $C_{27}H_{21}NO_7$ 

Ester **60** (869 mg, 1.84 mmol) was dissolved in *o*-xylene (80 ml) and refluxed for 21 h. The reaction mixture was allowed to cool down to room temperature and then the solution was poured onto saturated  $\text{NaHCO}_3$ -solution and was extracted with ethyl acetate. The organic phase was washed with brine, dried over  $\text{Na}_2\text{SO}_4$ , filtered and concentrated. The crude product was purified by flash chromatography (ethyl acetate/hexane, 1:2) and the pure furopyranone **62** (274 mg, 32%) was isolated as a reddish solid. TLC (EtOAc/hexane, 1:2):  $R_f$  0.24.  $^1\text{H-NMR}$  (300 MHz,  $\text{CDCl}_3$ ):  $\delta$  8.20 – 8.15 (m, 4H), 7.74 (m, 2H), 7.65 (m, 1H), 7.58 (m, 1H), 7.48 – 7.35 (m, 5H), 6.03 (d,  $J = 5.09$  Hz, 1H), 5.39 (m, 2H), 4.62 (d,  $J = 10.93$  Hz, 1H), 4.35 (m, 1H), 4.10 (m, 1H), 3.53 (m, 1H), 2.98 (m, 1H).  $^{13}\text{C-NMR}$  (75 MHz,  $\text{CDCl}_3$ ):  $\delta$  175.4, 165.6, 152.0, 147.6, 139.7, 138.0, 135.7, 132.3, 130.9, 130.4, 129.1, 128.8, 128.5, 128.3, 128.2, 125.4, 123.4, 96.6, 77.7, 67.5, 66.9, 38.4, 38.2. EI-MS  $m/z$  (%): 471 ( $[\text{C}_{27}\text{H}_{21}\text{NO}_7]^+$ , 2), 380 (14), 363 (7), 304 (8), 214 (13), 150 (19), 91 (100), 65 (7).

**4-[6-(3-Nitro-phenyl)-1-oxo-1,3a,4,7a-tetrahydro-3H-furo[3,4-c]pyran-4-yl]-benzoic acid benzyl ester (63)**

**57**

471.47

 $C_{27}H_{21}NO_7$ **(+/-)-63**

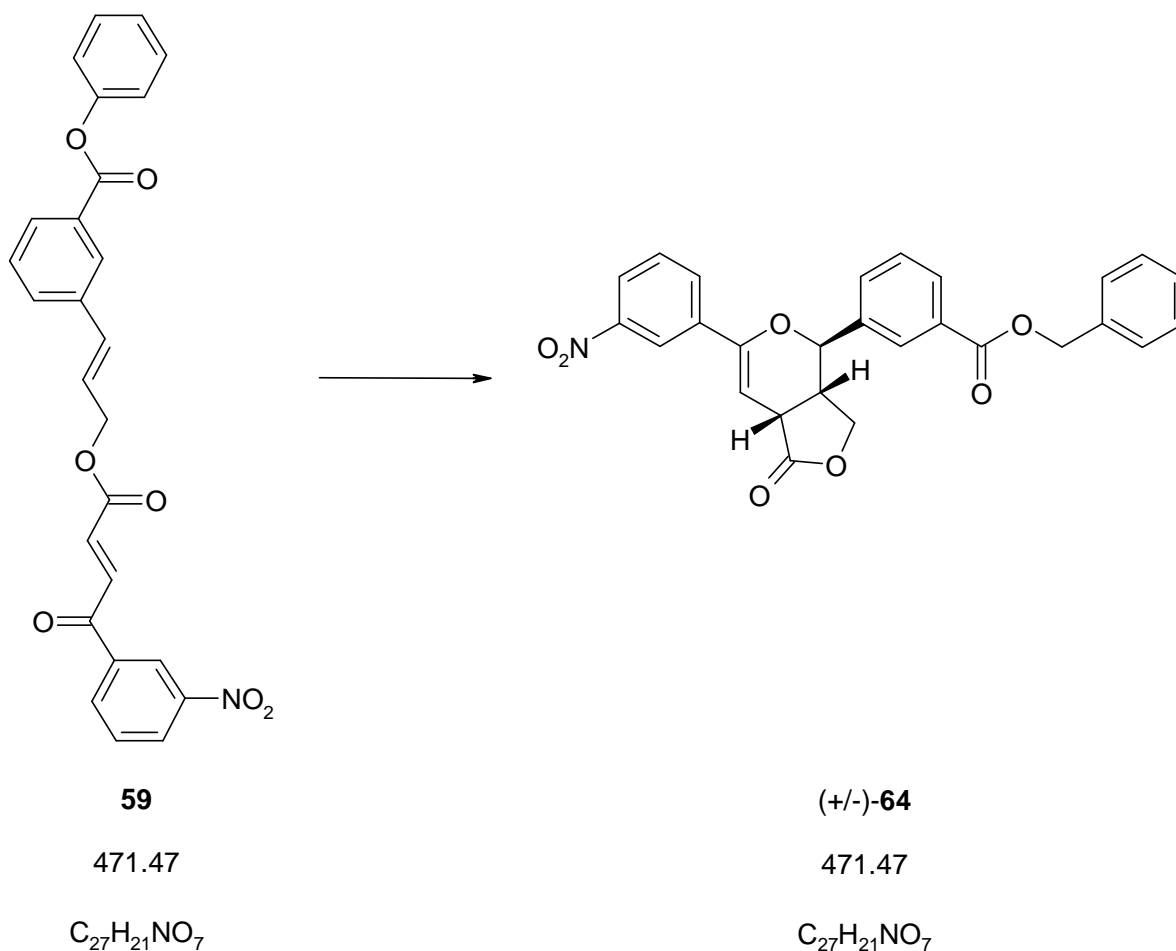
471.47

 $C_{27}H_{21}NO_7$ 

Ester **57** (1.77 g, 3.75 mmol) was dissolved in *o*-xylene (150 ml) and refluxed for 21 h (Temperature oil bath: 160°C, Temperature inside: 142°C). The reaction mixture was allowed to cool down to room temperature and then the solution was poured onto saturated  $\text{NaHCO}_3$ -solution and extracted with ethyl acetate. The organic phase was washed with brine, dried over  $\text{Na}_2\text{SO}_4$ , filtered and concentrated. The crude product was purified by flash chromatography (ethyl acetate/hexane, 1:4  $\rightarrow$  1:3  $\rightarrow$  1:0) and the pure furopyranone **63** (1.17 g, 66%) was isolated as a yellow amorphous solid. TLC (EtOAc/hexane, 1:2):  $R_f$  0.22.  $^1\text{H-NMR}$  (300 MHz,  $\text{CDCl}_3$ ):  $\delta$  8.43 (m, 1H), 8.19 (m, 3H), 7.91 (m, 1H), 7.55-7.35 (m, 8H), 5.99 (d,  $J=5.09$  Hz, 1H), 5.40 (s, 2H), 4.64 (d,  $J=10.74$  Hz, 1H), 4.35 (m, 1H), 4.12 (m, 1H), 3.51 (m, 1H), 2.93 (m, 1H).  $^{13}\text{C-NMR}$  (75 MHz,  $\text{CDCl}_3$ ):  $\delta$  175.5, 165.8, 152.2, 148.6, 142.5, 136.0, 135.8, 131.3, 130.7, 130.6, 129.5, 128.8, 128.5, 128.3, 127.8, 123.7, 120.0, 95.1, 77.9, 67.6, 67.1, 39.0, 38.3. EI-MS  $m/z$  (%): 471 ( $[\text{C}_{27}\text{H}_{21}\text{NO}_7]^+$ , 49), 364 (56), 304 (78), 214 (83), 169 (76), 150 (96), 91 (100), 65 (85).

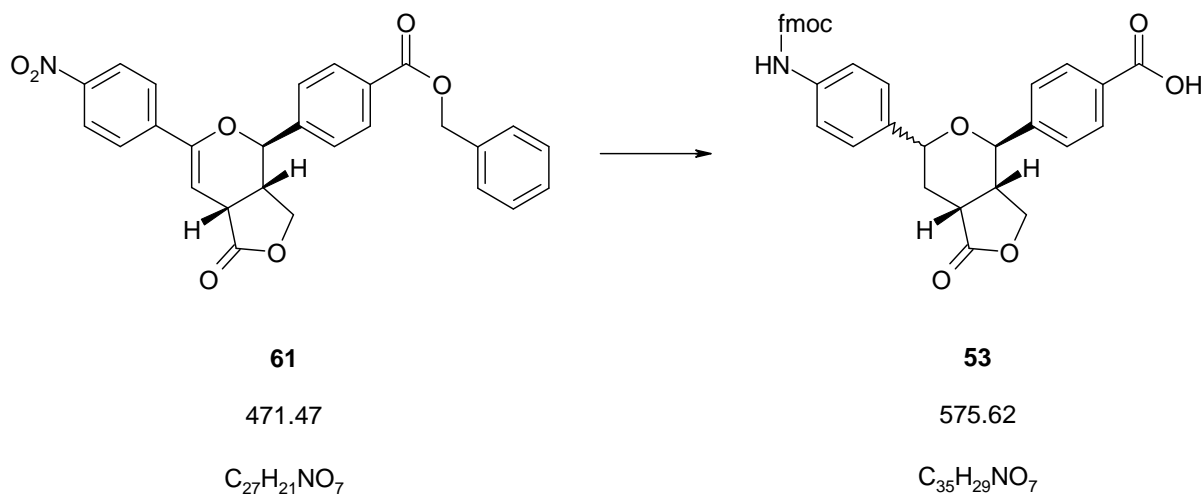


**3-[6-(3-Nitro-phenyl)-1-oxo-1,3a,4,7a-tetrahydro-3H-furo[3,4-c]pyran-4-yl]-benzoic acid benzyl ester (64)**



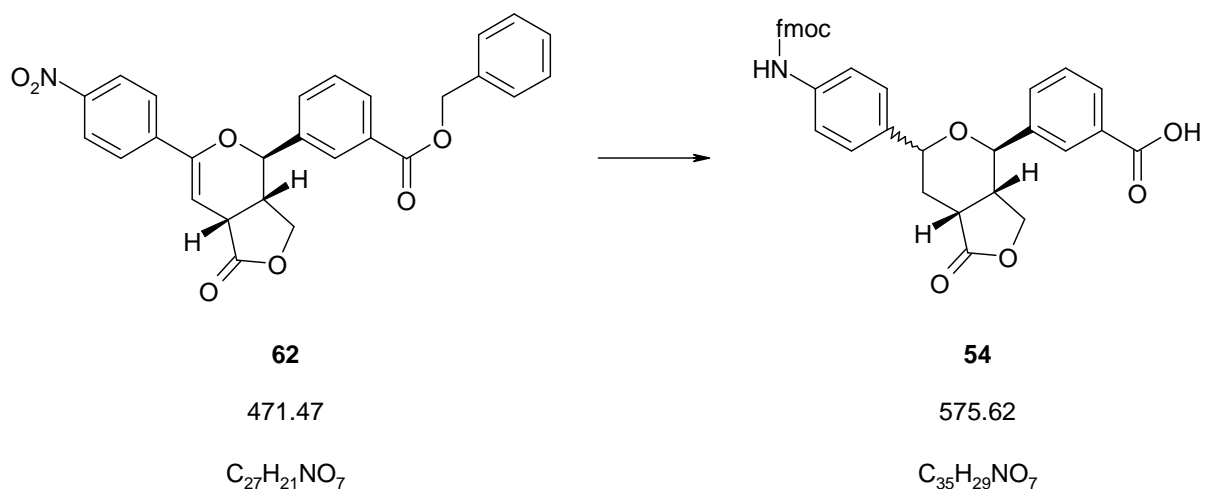
Ester **59** (1.1 g, 2.33 mmol) was dissolved in *o*-xylene (90 ml), stirred and refluxed for 24 h (temperature oil bath: 160°C). The solution was allowed to cool to room temperature. Then the solution was poured on saturated  $NaHCO_3$ -solution and extracted with EtOAc. The organic phase was washed with brine, dried ( $Na_2SO_4$ ), filtered and concentrated. After purification by flash chromatography (silicagel, EtOAc/ hexane 1:2) the pure product **64** (940 mg, 86 %) was isolated as a light yellow solid. TLC (EtOAc/hexane, 1:2):  $R_f = 0.31$ .  $^1H$ -NMR (300 MHz,  $CDCl_3$ ):  $\delta$  8.41 (m, 1H), 8.18-8.15 (m, 3H), 7.90 (m, 1H), 7.66 (m, 1H), 7.59-7.35 (m, 7 H), 5.98 (d,  $J = 4.90$  Hz, 1H), 5.39 (m, 2H), 4.63 (d,  $J = 10.93$  Hz, 1H), 4.35 (m, 1H), 4.10 (m, 1H), 3.52 (m, 1H), 2.98 (m, 1H).  $^{13}C$ -NMR (75 MHz,  $CDCl_3$ ):  $\delta$  175.5, 165.9, 162.4, 152.4, 148.6, 138.1, 135.9 (2C), 132.5, 131.3, 130.8 (2C), 129.5, 129.4, 129.1, 128.8, 128.6, 128.5, 123.7, 120.1, 95.2, 78.1, 67.7, 67.3, 38.9, 38.3. EI-MS  $m/z$  (%): 471 ( $[C_{27}H_{21}NO_7]^+$ , <1), 441 (18), 91 (27), 88 (29), 86 (91), 84 (100), 49 (39), 47 (49).

**4-{6-[4-(9H-Fluoren-9-ylmethoxycarbonylamino)-phenyl]-1-oxo-hexahydro-furo[3,4-c]pyran-4-yl}-benzoic acid (**53**)**



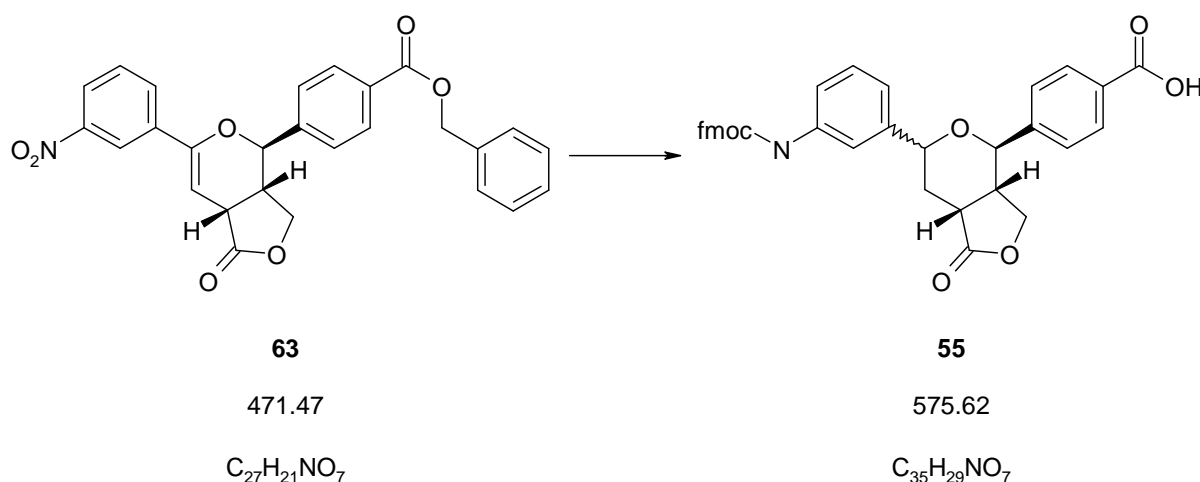
Furopyranone **61** (1.45 g, 3.08 mmol) was dissolved in dry THF (100 ml) under an argon atmosphere and stirred. Then Pd/C 10 % (725 mg) was added to the solution. The vessel was evacuated four times and filled with H<sub>2</sub>. The reaction mixture was stirred at room temperature for 2.5 h. Then the vessel was evacuated and filled with argon and the reaction mixture was filtered through THF-soaked celite. The celite was washed twice more with THF. The solution was then concentrated and dried under vacuum. The crude product obtained as a yellow foam was used without further purification. The crude material (1.17 g, 3.31 mmol) was dissolved in dioxane/H<sub>2</sub>O (70 ml / 0.91 ml). NaHCO<sub>3</sub> (0.28 g, 3.31 mmol), was dissolved in H<sub>2</sub>O (3.1 ml) and added to the solution. Fmoc-Cl (0.86 g, 3.31 mmol) was dissolved in dioxane (30 ml) and added to the reaction mixture. The reaction mixture was stirred for 5.5 h at room temperature. Then the reaction mixture was poured onto saturated NaHCO<sub>3</sub>-solution and was extracted with ethyl acetate. The organic phase was dried (Na<sub>2</sub>SO<sub>4</sub>), filtered and concentrated. The crude product was purified by flash chromatography (CH<sub>2</sub>Cl<sub>2</sub>/MeOH/HCOOH, 97:2:1) and the diastereomeric mixture of Fmoc-protected furopyranones **53** (1.18 g, 62%) was isolated as a yellow foam. TLC (EtOAc/MeOH, 2:1): R<sub>f</sub> 0.69. <sup>1</sup>H-NMR (500 MHz, DMSO, only *cis*-isomer): δ 12.85 (s, 1H, -COOH), 9.68 (s, 1H, -NH), 7.96-7.23 (m, 16H), 4.48-4.18 (m, 6H), 3.92 (m, 1H), 3.32 (m, 1H), 2.73 (m, 1H), 2.18-1.93 (m, 2H). ESI-MS *m/z* (Positive ion mode): [C<sub>35</sub>H<sub>29</sub>NO<sub>7</sub> + Na]<sup>+</sup> = 598.2.

**3-{6-[4-(9H-Fluoren-9-ylmethoxycarbonylamino)-phenyl]-1-oxo-hexahydro-furo[3,4-c]pyran-4-yl}-benzoic acid (**54**)**



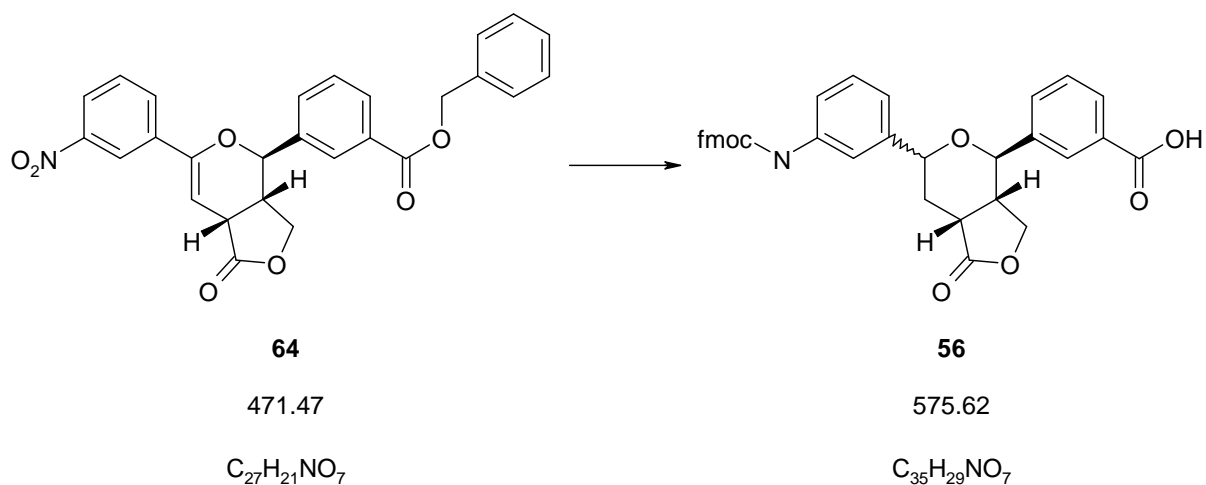
Furo-pyranone **62** (473 mg, 1.0 mmol) was dissolved in dry THF (36 ml) under a nitrogen atmosphere and stirred. Then Pd/C 10 % (240 mg) was added to the solution. The vessel was evacuated four times and filled with H<sub>2</sub>. The reaction mixture was stirred at room temperature for 2 h. Then the vessel was evacuated and filled with nitrogen and the reaction mixture was filtered through THF-soaked celite. The celite was washed twice more with THF. The solution was then concentrated and dried under vacuum. The crude product obtained as a yellow foam was used without further purification. The crude material (353 mg, 1.0 mmol) was dissolved in dioxane/H<sub>2</sub>O (25 ml / 0.28 ml). NaHCO<sub>3</sub> (87 mg, 1.0 mmol), was dissolved in H<sub>2</sub>O (1 ml) and added to the solution. Fmoc-Cl (273 mg, 1.0 mmol) was dissolved in dioxane (12 ml) and added to the reaction mixture. The reaction mixture was stirred for 2.5 h at room temperature. Then the reaction mixture was poured onto saturated NH<sub>4</sub>Cl-solution and was extracted with ethyl acetate. The organic phase was dried (Na<sub>2</sub>SO<sub>4</sub>), filtered and concentrated. The crude product was purified by flash chromatography (CH<sub>2</sub>Cl<sub>2</sub>/MeOH/HCOOH, 97:2:1) and the diastereomeric mixture of Fmoc-protected furo-pyranones **54** (404 mg, 68%) was isolated as a yellow amorphous solid. TLC (CH<sub>2</sub>Cl<sub>2</sub>/MeOH/HCOOH, 97:2:1): R<sub>f</sub> 0.21. <sup>1</sup>H-NMR (500 MHz, DMSO, only *cis*-isomer): δ 12.85 (s, 1H, -COOH), 9.68 (s, 1H, -NH), 8.02-7.22 (m, 16H), 4.48-4.19 (m, 6H), 3.88 (m, 1H), 3.32 (m, 1H), 2.78 (m, 1H), 2.18-1.96 (m, 2H). ESI-MS *m/z* (positive ion mode): [C<sub>35</sub>H<sub>29</sub>NO<sub>7</sub> + H]<sup>+</sup> = 576.2.

**4-{6-[3-(9H-Fluoren-9-ylmethoxycarbonylamino)-phenyl]-1-oxo-hexahydro-furo[3,4-c]pyran-4-yl}-benzoic acid (**55**)**



Furo-pyranone **63** (1.1 g, 2.33 mmol) was dissolved in dry THF (100 ml) under an argon atmosphere and stirred. Then Pd/C 10 % (0.55 g) was added to the solution. The vessel was evacuated four times and filled with H<sub>2</sub>. The reaction mixture was stirred at room temperature for 2.5 h. Then the vessel was evacuated and filled with argon and the reaction mixture was filtered through THF-soaked celite. The celite was washed twice more with THF. The solution was then concentrated and dried under vacuum. The crude product obtained as a yellow foam was used without further purification. The crude material (825 mg, 2.33 mmol) was dissolved in dioxane/H<sub>2</sub>O (80 ml / 0.64 ml). NaHCO<sub>3</sub> (196 mg, 2.33 mmol), was dissolved in H<sub>2</sub>O (2.2 ml) and added to the solution. Fmoc-Cl (604 mg, 2.33 mmol) was added to the reaction mixture and the reaction mixture was stirred for 2.5 h at room temperature. Then the reaction mixture was concentrated. The crude product was purified by flash chromatography (CH<sub>2</sub>Cl<sub>2</sub>/HCOOH, 99:1 → CH<sub>2</sub>Cl<sub>2</sub>/HCOOH/MeOH, 99:1:0.5) and the diastereomeric mixture of Fmoc-protected furo-pyranones **55** (823 mg, 62%) was isolated as a yellow amorphous solid. TLC (EtOAc/MeOH, 2:1): R<sub>f</sub> 0.69. <sup>1</sup>H-NMR (500 MHz, DMSO, only *trans*-isomer): δ 12.98 (s, 1H, -COOH), 9.67 (s, 1H, -NH), 7.97-6.95 (m, 16H), 4.99-4.15 (m, 7H), 3.20 (m, 2H), 2.20-1.85 (m, 2H). ESI-MS *m/z* (positive ion mode): [C<sub>35</sub>H<sub>29</sub>NO<sub>7</sub> + H]<sup>+</sup> = 576.2.

**3-{6-[3-(9H-Fluoren-9-ylmethoxycarbonylamino)-phenyl]-1-oxo-hexahydro-furo[3,4-c]pyran-4-yl}-benzoic acid (**56**)**

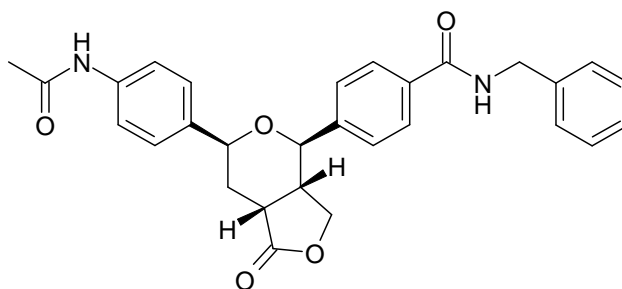


Furopyranone **64** (0.94 g, 1.99 mmol) was dissolved in dry THF (70 ml) under a nitrogen atmosphere and stirred. Then Pd/C 10 % (0.48 g) was added to the solution. The vessel was evacuated four times and filled with  $H_2$ . The reaction mixture was stirred at room temperature for 2.5 h. Then the vessel was evacuated and filled with nitrogen and the reaction mixture was filtered through THF-soaked celite. The celite was washed twice more with THF. The solution was then concentrated and dried under vacuum. The crude product obtained as a yellow foam was used without further purification. The crude material (0.68 mg, 1.92 mmol) was dissolved in dioxane/ $H_2O$  (40 ml / 0.53 ml).  $NaHCO_3$  (162 mg, 1.92 mmol), was dissolved in  $H_2O$  (1.8 ml) and added to the solution. Fmoc-Cl (498 mg, 1.92 mmol) was dissolved in dioxane (17 ml) and added to the reaction mixture. The reaction mixture was stirred for 5.5 h at room temperature. Then the reaction mixture was poured onto saturated  $NH_4Cl$ -solution and was extracted with ethyl acetate. The organic phase was dried ( $Na_2SO_4$ ), filtered and concentrated. The crude product was purified by flash chromatography ( $CH_2Cl_2/HCOOH/MeOH$ , 98:1:1) and the diastereomeric mixture of Fmoc-protected furopyranones **56** (920 mg, 80%) was isolated as a yellow amorphous solid. TLC (EtOAc/MeOH, 2:1):  $R_f$  0.75.  $^1H$ -NMR (500 MHz, DMSO, only *trans*-isomer):  $\delta$  13.09 (s, 1H, -COOH), 9.67 (s, 1H, -NH), 8.00-6.96 (m, 16H), 5.00-4.10 (m, 7H), 3.21 (m, 2H), 2.22-1.85 (m, 2H). ESI-MS  $m/z$  (Positive ion mode):  $[C_{35}H_{29}NO_7 + H]^+ = 576.2$ .

### 6.4.13 Products 72-85 obtained by Solid Phase Chemistry

The procedures for the synthesis of the prototypes are described in Chapter 6.3.4.

#### 4-[6-(4-Acetylamino-phenyl)-1-oxo-hexahydro-furo[3,4-c]pyran-4-yl]-N-benzyl-benzamide (72)



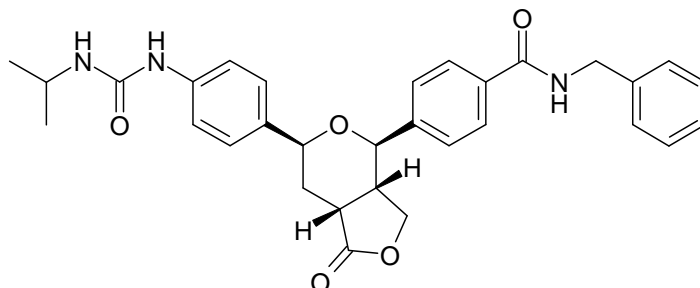
*cis*-72

484.56

C<sub>29</sub>H<sub>28</sub>N<sub>2</sub>O<sub>5</sub>

Yield of *cis*-72: 14 mg (56 %, based on 90% loading). RP-HPLC (acetonitrile/H<sub>2</sub>O, 4 min, λ=214 nm): t<sub>R</sub> = 2.71 min. <sup>1</sup>H-NMR (300 MHz, DMSO): δ 9.94 (s, 1H), 9.07 (t, J = 6.03 Hz, 1H), 7.92 (d, J = 8.48 Hz, 2H), 7.60-7.53 (m, 4H), 7.35-7.20 (m, 7H), 4.48 (d, J = 6.03 Hz, 2H), 4.41-4.32 (m, 2H), 4.22 (m, 1H), 3.91 (d, J = 9.61 Hz, 1H), 3.32 (m, 1H), 2.75 (m, 1H), 2.17-1.93 (m, 5H). ESI-MS *m/z* (positive ion mode): [C<sub>29</sub>H<sub>28</sub>N<sub>2</sub>O<sub>5</sub> + H]<sup>+</sup> = 485.22.

#### N-Benzyl-4-{6-[4-(3-isopropyl-ureido)-phenyl]-1-oxo-hexahydro-furo[3,4-c]pyran-4-yl}-benzamide (73)



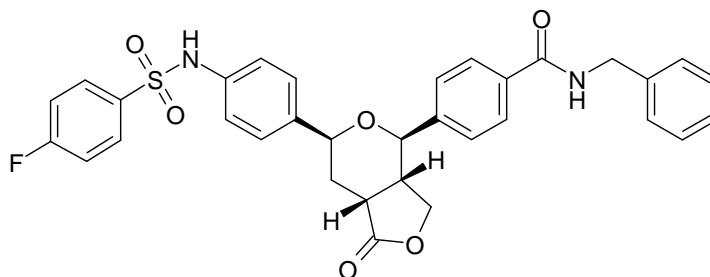
*cis*-73

527.63

C<sub>31</sub>H<sub>33</sub>N<sub>3</sub>O<sub>5</sub>

Yield of *cis*-**73**: 39 mg (72 %, based on 90% loading). RP-HPLC (acetonitrile/H<sub>2</sub>O, 8 min,  $\lambda=210$  nm):  $t_R = 5.43$  min. <sup>1</sup>H-NMR (300 MHz, DMSO):  $\delta$  9.06 (t,  $J = 6.03$  Hz, 1H), 8.28 (s, 1H), 7.91 (d,  $J = 8.23$  Hz, 2H), 7.58 (d,  $J = 8.48$  Hz, 2H), 7.35-7.20 (m, 9H), 5.95 (d,  $J = 7.54$  Hz, 1H), 4.48 (d,  $J = 6.03$  Hz, 2H), 4.39-4.19 (m, 3H), 3.91 (d,  $J = 9.61$  Hz, 1H), 3.73 (m, 1H), 3.30 (m, 1H), 2.74 (m, 1H), 2.15-1.91 (m, 2H), 1.08 (d,  $J = 6.59$  Hz, 6H). ESI-MS  $m/z$  (positive ion mode):  $[C_{31}H_{33}N_3O_5 + H]^+ = 528.30$ .

**N-Benzyl-4-{6-[4-(4-fluoro-benzenesulfonylamino)-phenyl]-1-oxo-hexahydro-furo[3,4-c]pyran-4-yl}-benzamide (74)**



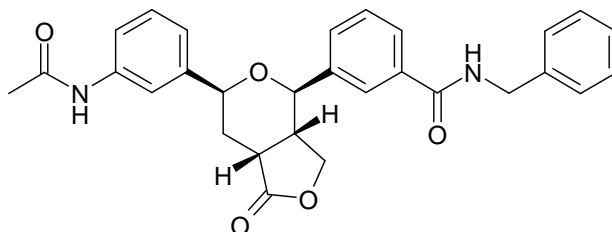
*cis*-**74**

600.67

$C_{33}H_{29}FN_2O_6S$

The reaction was bad and product *cis*-**74** was only detected by LC/MS. RP-HPLC (acetonitrile/H<sub>2</sub>O, 8 min,  $\lambda=210$  nm):  $t_R = 5.86$  min. ESI-MS  $m/z$  (positive ion mode):  $[C_{33}H_{29}N_2FO_6S + H]^+ = 601.30$ .

**3-[6-(3-Acetylamino-phenyl)-1-oxo-hexahydro-furo[3,4-c]pyran-4-yl]-N-benzylbenzamide (75)**

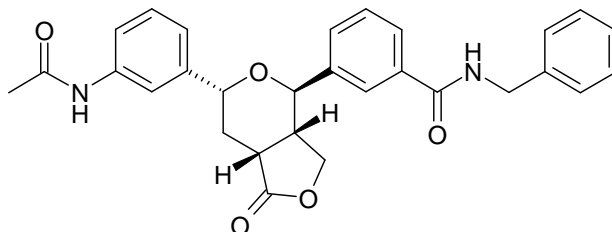


*cis*-**75**

484.56

$C_{29}H_{28}N_2O_5$

No pure *cis*-**75** could be isolated. Only a mixture of *cis*-/*trans*-**75** was isolated. Yield: 1.4 mg (5%, based on 90% loading). RP-HPLC (acetonitrile/H<sub>2</sub>O, 4min,  $\lambda=214$  nm):  $t_R = 2.81$  min. ESI-MS  $m/z$  (Positive ion mode):  $[C_{29}H_{28}N_2O_5 + H]^+ = 485.24$ .

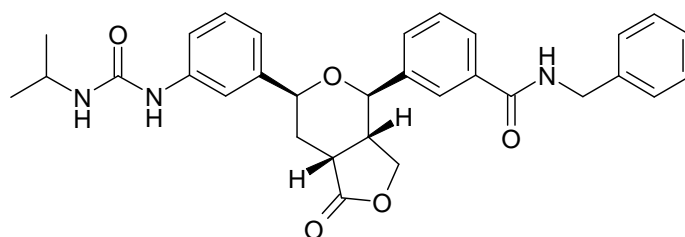
*trans*-**75**

484.56

 $C_{29}H_{28}N_2O_5$ 

Yield of *trans*-**75**: 8.5 mg (34%, based on 90% loading). RP-HPLC (acetonitrile/H<sub>2</sub>O, 4min,  $\lambda=214$  nm):  $t_R = 2.75$  min. <sup>1</sup>H-NMR (300 MHz, DMSO):  $\delta$  9.93 (s, 1H), 9.10 (t,  $J = 5.93$  Hz, 1H), 7.98 (s, 1H), 7.87 (d,  $J = 7.72$  Hz, 1H), 7.63 (d,  $J = 7.72$  Hz, 1H), 7.53-7.48 (m, 3H), 7.33-7.21 (m, 6H), 7.02 (d,  $J = 7.72$  Hz, 1H), 4.94 (d,  $J = 6.22$  Hz, 1H), 4.70 (m, 1H), 4.50 (d,  $J = 6.97$  Hz, 2H), 4.38 (m, 1H), 4.15 (m, 1H), 3.23 (m, 2H), 2.19 (m, 1H), 2.00-1.88 (m, 4H). ESI-MS  $m/z$  (positive ion mode):  $[C_{29}H_{28}N_2O_5 + H]^+ = 485.23$ .

**N-Benzyl-3-{6-[3-(3-isopropyl-ureido)-phenyl]-1-oxo-hexahydro-furo[3,4-c]pyran-4-yl}-benzamide (76)**

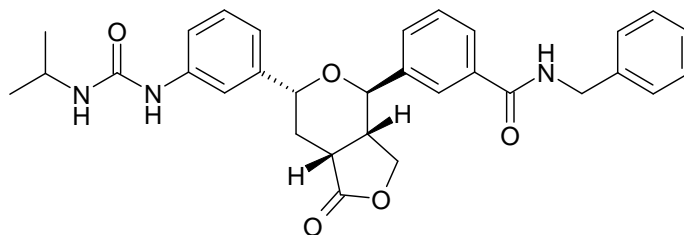
*cis*-**76**

527.63

 $C_{31}H_{33}N_3O_5$ 

No pure *cis*-**76** could be isolated. RP-HPLC (acetonitrile/H<sub>2</sub>O, 8 min,  $\lambda=210$  nm):  $t_R = 5.59$  min. ESI-MS  $m/z$  (positive ion mode):  $[C_{31}H_{33}N_3O_5 + H]^+ = 528.29$ .



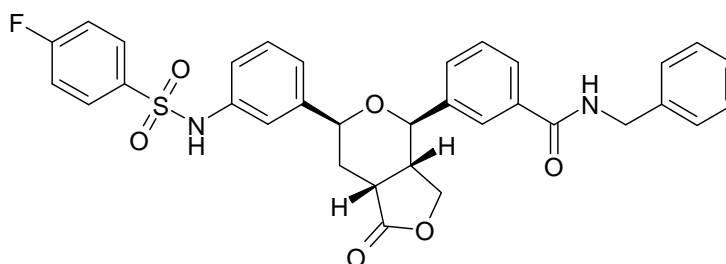
*trans*-**76**

527.63

 $C_{31}H_{33}N_3O_5$ 

Yield of *trans*-**76**: 25.8 mg (47%, based on 90% loading). RP-HPLC (acetonitrile/ $H_2O$ , 8 min,  $\lambda=210$  nm):  $t_R = 5.52$  min.  $^1H$ -NMR (300 MHz, DMSO):  $\delta$  9.09 (t,  $J = 5.93$  Hz, 1H), 8.27 (s, 1H), 7.97 (s, 1H), 7.87 (d,  $J = 7.72$  Hz, 1H), 7.63 (d,  $J = 7.72$  Hz, 1H), 7.50 (t,  $J = 7.63$  Hz, 1H), 7.33-7.13 (m, 8H), 6.88 (d,  $J = 7.72$  Hz, 1H), 5.93 (d,  $J = 7.54$  Hz, 1H), 4.93 (d,  $J = 6.41$  Hz, 1H), 4.67 (m, 1H), 4.50 (d,  $J = 7.16$  Hz, 2H), 4.38 (m, 1H), 4.16 (m, 1H), 3.72 (m, 1H), 3.21 (m, 2H), 2.17 (m, 1H), 1.94 (m, 1H), 1.07 (t,  $J = 6.59$  Hz, 6H). ESI-MS  $m/z$  (positive ion mode):  $[C_{31}H_{33}N_3O_5 + H]^+ = 528.29$ .

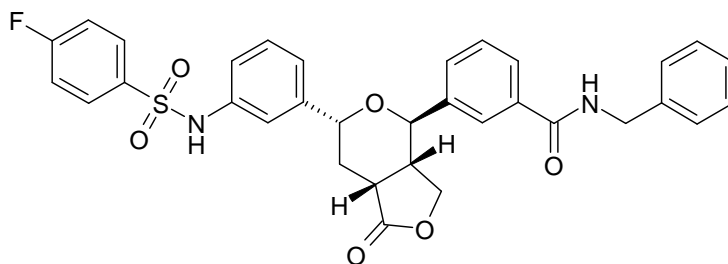
**N-Benzyl-3-{6-[3-(4-fluoro-benzenesulfonylamino)-phenyl]-1-oxo-hexahydro-furo[3,4-c]pyran-4-yl}-benzamide (**77**)**

*cis*-**77**

600.67

 $C_{33}H_{29}N_2O_6F$ 

No pure *cis*-**77** could be isolated. Only a mixture of *cis*-/*trans*-**77** was isolated. Yield: 1.5 mg (2%, based on 90% loading). RP-HPLC (acetonitrile/ $H_2O$ , 4 min,  $\lambda=214$  nm):  $t_R = 3.35$  min. ESI-MS  $m/z$  (positive ion mode):  $[C_{33}H_{29}N_2O_6F + H]^+ = 601.23$ .

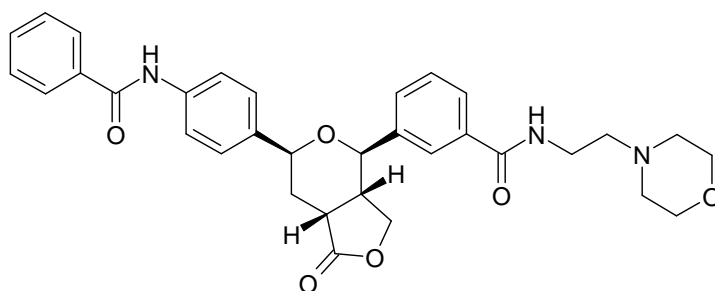
*trans-77*

600.67

 $C_{33}H_{29}N_2O_6F$ 

Yield of *trans-77*: 8.9 mg (14%, based on 90% loading). RP-HPLC (acetonitrile/H<sub>2</sub>O, 4 min,  $\lambda=214$  nm):  $t_R = 3.29$  min. <sup>1</sup>H-NMR (300 MHz, DMSO):  $\delta$  10.29 (s, 1H), 9.09 (t,  $J = 6.22$  Hz, 1H), 7.95-7.74 (m, 4H), 7.60-7.48 (m, 2H), 7.35-7.16 (m, 8H), 7.07-6.87 (m, 3H), 4.89 (d,  $J = 6.59$  Hz, 1H), 4.65 (m, 1H), 4.50 (d,  $J = 7.54$  Hz, 2H), 4.36 (m, 1H), 4.12 (m, 1H), 3.21 (m, 2H), 2.14 (m, 1H), 1.84 (m, 1H). ESI-MS  $m/z$  (positive ion mode):  $[C_{33}H_{29}N_2O_6F + H]^+ = 601.25$ .

### 3-[6-(4-Benzoylamino-phenyl)-1-oxo-hexahydro-furo[3,4-c]pyran-4-yl]-N-(2-morpholin-4-yl-ethyl)-benzamide (78)

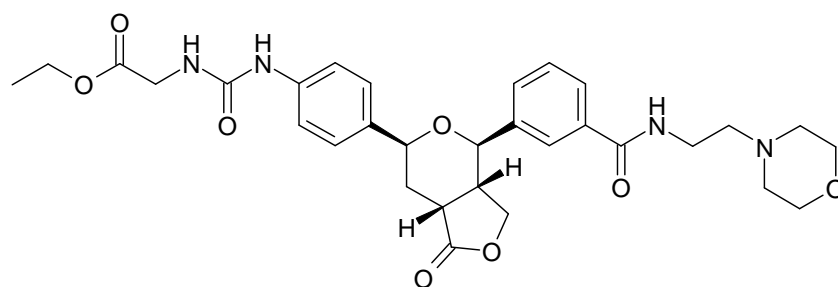
*cis-78*

569.66

 $C_{33}H_{35}N_3O_6$ 

Yield of *cis-78*: 58 mg (>100 %, based on 90% loading, still some water inside). RP-HPLC (acetonitrile/H<sub>2</sub>O, 4 min,  $\lambda=214$  nm):  $t_R = 2.32$  min. <sup>1</sup>H-NMR (300 MHz, DMSO):  $\delta$  (M+H<sup>+</sup>) 10.27 (s, 1H), 9.70 (s, 1H), 8.79 (s, 1H), 7.97-7.93 (m, 3H), 7.85 (d,  $J = 7.91$  Hz, 1H), 7.78-7.70 (m, 3H), 7.62-7.49 (m, 4H), 7.36 (d,  $J = 8.67$  Hz, 2H), 4.41 (d,  $J = 11.11$  Hz, 2H), 4.24 (m, 1H), 3.98-3.15 (m, 14H), 2.81 (m, 1H), 2.23-1.98 (m, 2H). ESI-MS  $m/z$  (positive ion mode):  $[C_{33}H_{35}N_3O_6 + H]^+ = 570.29$ .

**[3-(4-{4-[3-(2-Morpholin-4-yl-ethylcarbamoyl)-phenyl]-1-oxo-hexahydro-furo[3,4-c]pyran-6-yl}-phenyl)-ureido]-acetic acid ethyl ester (79)**



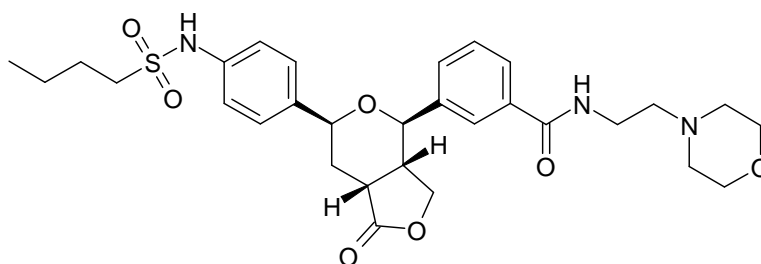
*cis*-**79**

594.67

$C_{31}H_{38}N_4O_8$

Yield of *cis*-**79**: 49 mg (>100 %, based on 90% loading, still some water inside). RP-HPLC (acetonitrile/H<sub>2</sub>O, 4 min,  $\lambda=214$  nm):  $t_R = 1.96$  min. <sup>1</sup>H-NMR (300 MHz, DMSO):  $\delta$  (M+H<sup>+</sup>) 9.68 (s, 1H), 8.85-8.77 (m, 2H), 7.95 (s, 1H), 7.84 (d,  $J = 7.91$  Hz, 1H), 7.69 (d,  $J = 7.72$  Hz, 1H), 7.52 (t,  $J = 7.72$  Hz, 1H), 7.37 (d,  $J = 8.67$  Hz, 2H), 7.23 (d,  $J = 8.67$  Hz, 2H), 6.47 (t,  $J = 5.84$  Hz, 1H), 4.39-4.20 (m, 3H), 4.10 (q,  $J = 7.10$  Hz, 2H), 4.02-3.14 (m, 16H), 2.79 (m, 1H), 2.18-1.96 (m, 2H), 1.19 (t,  $J = 7.06$  Hz, 3H). ESI-MS  $m/z$  (positive ion mode): [ $C_{31}H_{38}N_4O_8 + H$ ]<sup>+</sup> = 595.30.

**3-{6-[4-(Butane-1-sulfonylamino)-phenyl]-1-oxo-hexahydro-furo[3,4-c]pyran-4-yl]-N-(2-morpholin-4-yl-ethyl)-benzamide (80)**



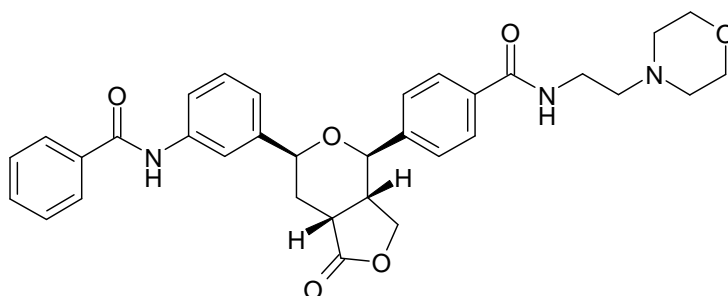
*cis*-**80**

585.73

$C_{30}H_{39}N_3O_7S$

Yield of *cis*-**80**: 12 mg (29 %, based on 90% loading). RP-HPLC (acetonitrile/H<sub>2</sub>O, 4 min,  $\lambda=214$  nm):  $t_R = 2.32$  min. <sup>1</sup>H-NMR (300 MHz, DMSO):  $\delta$  (M+H<sup>+</sup>) 9.79-9.73 (m, 2H), 8.80 (t,  $J = 5.65$  Hz, 1H), 7.95 (s, 1H), 7.84 (d,  $J = 7.72$  Hz, 1H), 7.69 (d,  $J = 7.72$  Hz, 1H), 7.52 (t,  $J = 7.63$  Hz, 1H), 7.33 (d,  $J = 8.48$  Hz, 2H), 7.18 (d,  $J = 8.48$  Hz, 2H), 4.37 (m, 2H), 4.23 (m, 1H), 4.02-3.01 (m, 16H), 2.79 (m, 1H), 2.19-1.95 (m, 2H), 1.61 (m, 2H), 1.32 (m, 2H), 0.80 (t,  $J = 7.44$  Hz, 3H). ESI-MS  $m/z$  (positive ion mode): [C<sub>30</sub>H<sub>39</sub>N<sub>3</sub>O<sub>7</sub>S + H]<sup>+</sup> = 586.27.

**4-[6-(3-Benzoylamino-phenyl)-1-oxo-hexahydro-furo[3,4-c]pyran-4-yl]-N-(2-morpholin-4-yl-ethyl)-benzamide (81)**

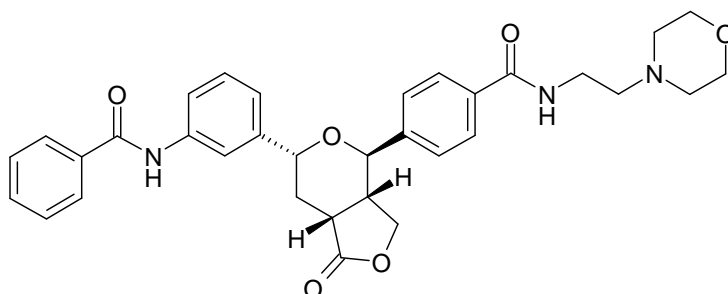


*cis*-**81**

569.66

C<sub>33</sub>H<sub>35</sub>N<sub>3</sub>O<sub>6</sub>

Yield of *cis*-**81**: 4 mg (10 %, based on 90% loading). RP-HPLC (acetonitrile/H<sub>2</sub>O, 4 min,  $\lambda=214$  nm):  $t_R = 2.36$  min. <sup>1</sup>H-NMR (300 MHz, DMSO):  $\delta$  (M+H<sup>+</sup>) 10.27 (s, 1H), 9.70 (s, 1H), 8.76 (t,  $J = 5.65$  Hz, 1H), 7.96-7.50 (m, 11H), 7.34 (t,  $J = 8.01$  Hz, 1H), 7.11 (d,  $J = 7.72$  Hz, 1H), 4.44 (m, 2H), 4.24 (m, 1H), 4.02-3.14 (m, 14H), 2.78 (m, 1H), 2.25-1.93 (m, 2H). ESI-MS  $m/z$  (positive ion mode): [C<sub>33</sub>H<sub>35</sub>N<sub>3</sub>O<sub>6</sub> + H]<sup>+</sup> = 570.34.



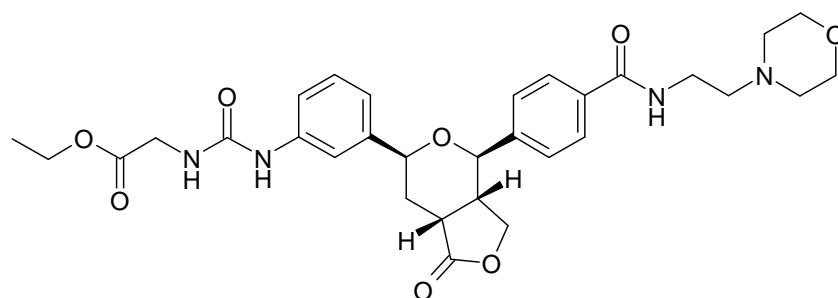
*trans*-**81**

569.66

C<sub>33</sub>H<sub>35</sub>N<sub>3</sub>O<sub>6</sub>

Yield of *trans*-**81**: 35.5 mg (86 %, based on 90% loading). RP-HPLC (acetonitrile/H<sub>2</sub>O, 4 min,  $\lambda=214$  nm):  $t_R = 2.28$  min. <sup>1</sup>H-NMR (300 MHz, DMSO):  $\delta$  (M+H<sup>+</sup>) 10.25 (s, 1H), 9.66 (s, 1H), 8.75 (t,  $J = 5.56$  Hz, 1H), 7.95-7.49 (m, 11H), 7.32 (t,  $J = 7.91$  Hz, 1H), 7.09 (d,  $J = 7.72$  Hz, 1H), 5.01 (d,  $J = 5.46$  Hz, 1H), 4.65 (m, 1H), 4.42 (m, 1H), 4.20 (m, 1H), 4.02-3.14 (m, 14H), 2.28-1.89 (m, 2H). ESI-MS  $m/z$  (positive ion mode): [C<sub>33</sub>H<sub>35</sub>N<sub>3</sub>O<sub>6</sub> + H]<sup>+</sup> = 570.33.

**[3-(3-{4-[4-(2-Morpholin-4-yl-ethylcarbamoyl)-phenyl]-1-oxo-hexahydro-furo[3,4-c]pyran-6-yl}-phenyl)-ureido]-acetic acid ethyl ester (**82**)**

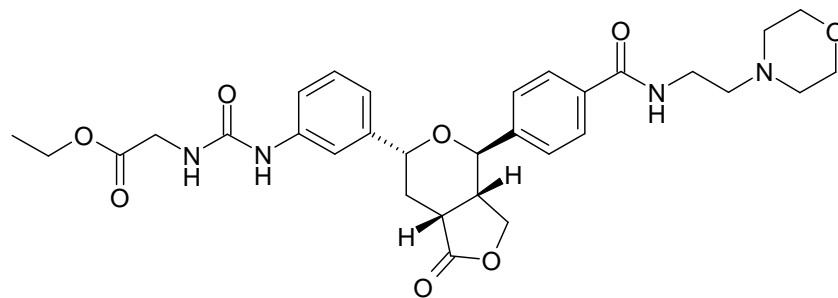


*cis*-**82**

594.67

C<sub>31</sub>H<sub>38</sub>N<sub>4</sub>O<sub>8</sub>

Yield of *cis*-**82**: 8.9 mg (20 %, based on 90% loading). RP-HPLC (acetonitrile/H<sub>2</sub>O, 4 min,  $\lambda=214$  nm):  $t_R = 1.98$  min. <sup>1</sup>H-NMR (300 MHz, DMSO):  $\delta$  (M+H<sup>+</sup>) 9.77 (s, 1H), 8.87 (d,  $J = 10.74$  Hz, 1H), 8.76 (t,  $J = 5.65$  Hz, 1H), 7.89 (d,  $J = 7.72$  Hz, 2H), 7.61 (m, 2H), 7.45 (d,  $J = 16.01$  Hz, 1H), 7.30-7.16 (m, 2H), 6.90 (m, 1H), 6.48 (t,  $J = 5.65$  Hz, 1H), 4.98 (d,  $J = 5.46$  Hz, 1H), 4.61-3.15 (m, 20H), 2.76 (m, 1H), 2.19-1.89 (m, 2H), 1.20 (m, 3H). ESI-MS  $m/z$  (positive ion mode): [C<sub>31</sub>H<sub>38</sub>N<sub>4</sub>O<sub>8</sub> + H]<sup>+</sup> = 595.34.

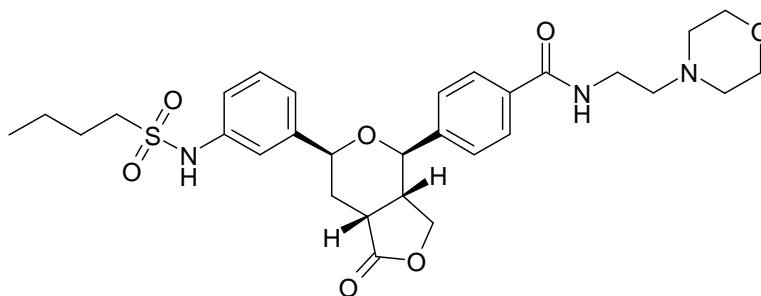
*trans*-**82**

594.67

 $C_{31}H_{38}N_4O_8$ 

Yield of *trans*-**82**: 38.6 mg (90 %, based on 90% loading). RP-HPLC (acetonitrile/H<sub>2</sub>O, 4 min,  $\lambda=214$  nm):  $t_R = 1.93$  min. <sup>1</sup>H-NMR (300 MHz, DMSO):  $\delta$  (M+H<sup>+</sup>) 9.65 (s, 1H), 8.83 (s, 1H), 8.75 (t,  $J = 5.65$  Hz, 1H), 7.89 (d,  $J = 8.29$  Hz, 2H), 7.60 (d,  $J = 8.48$  Hz, 2H), 7.43 (s, 1H), 7.28-7.16 (m, 2H), 6.90 (d,  $J = 7.54$  Hz, 1H), 6.45 (t,  $J = 5.75$  Hz, 1H), 4.98 ( $J = 5.28$  Hz, 1H), 4.61-3.15 (m, 21H), 2.20-1.85 (m, 2H), 1.20 (t,  $J = 7.16$  Hz, 3H). ESI-MS  $m/z$  (Positive ion mode): [ $C_{31}H_{38}N_4O_8 + H$ ]<sup>+</sup> = 595.35.

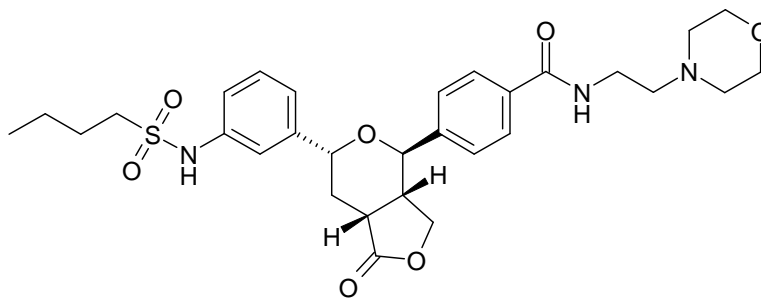
**4-{6-[3-(Butane-1-sulfonylamino)-phenyl]-1-oxo-hexahydro-furo[3,4-c]pyran-4-yl}-N-(2-morpholin-4-yl-ethyl)-benzamide (83)**

*cis*-**83**

585.73

 $C_{30}H_{39}N_3O_7S$ 

No pure *cis*-**83** could be isolated. Only a mixture of *cis*-/*trans*-**83** was isolated. Yield: 1.5 mg (4%, based on 90% loading). RP-HPLC (acetonitrile/H<sub>2</sub>O, 4 min,  $\lambda=214$  nm):  $t_R = 2.35$  min. ESI-MS  $m/z$  (positive ion mode): [ $C_{30}H_{39}N_3O_7S + H$ ]<sup>+</sup> = 586.30.

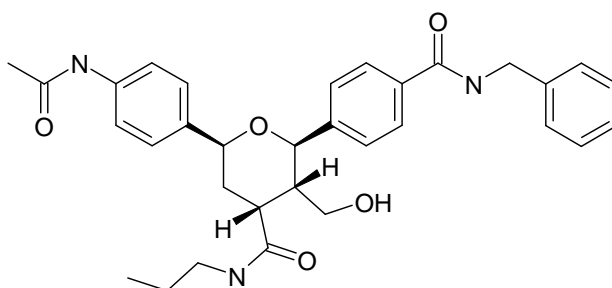
*trans*-**83**

585.73

 $C_{30}H_{39}N_3O_7S$ 

Yield of *trans*-**83**: 8.1 mg (19 %, based on 90% loading). RP-HPLC (acetonitrile/H<sub>2</sub>O, 4 min,  $\lambda=214$  nm):  $t_R = 2.29$  min. <sup>1</sup>H-NMR (300 MHz, DMSO):  $\delta$  (M+H<sup>+</sup>) 9.76-9.69 (m, 2H), 8.76 (t,  $J = 5.75$  Hz, 1H), 7.89 (d,  $J = 8.29$  Hz, 2H), 7.59 (d,  $J = 8.48$  Hz, 2H), 7.28 (t,  $J = 7.82$  Hz, 1H), 7.21 (s, 1H), 7.09 (m, 1H), 4.95 (d,  $J = 5.84$  Hz, 1H), 4.67 (m, 1H), 4.38 (m, 1H), 4.20-3.02 (m, H), 2.23 (m, 1H), 1.94 (m, 1H), 1.61 (m, 2H), 1.32 (m, 2H), 0.80 (t,  $J = 7.35$  Hz, 3H). ESI-MS  $m/z$  (positive ion mode):  $[C_{30}H_{39}N_3O_7S + H]^+ = 586.32$ .

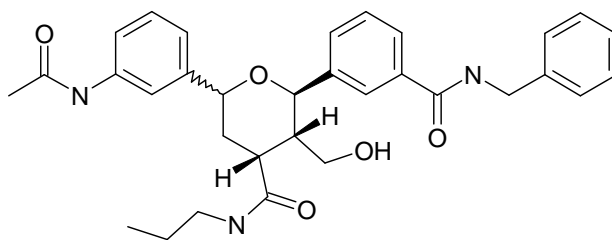
**6-(4-Acetylamino-phenyl)-2-(4-benzylcarbamoyl-phenyl)-3-hydroxymethyl-tetrahydro-pyran-4-carboxylic acid propylamide (84) and 6-(3-Acetylamino-phenyl)-2-(3-benzylcarbamoyl-phenyl)-3-hydroxymethyl-tetrahydro-pyran-4-carboxylic acid propylamide (85)**

**84**

543.67

 $C_{32}H_{37}N_3O_5$ 

No pure **84** could be isolated. Only an impure fraction was isolated. Yield: 2.6 mg (9%, based on 90% loading). RP-HPLC (acetonitrile/H<sub>2</sub>O, 4 min,  $\lambda=214$  nm):  $t_R = 2.36$  min. ESI-MS  $m/z$  (positive ion mode):  $[C_{33}H_{37}N_3O_5 + H]^+ = 544.29$ .

**85**

543.67

 $C_{32}H_{37}N_3O_5$ 

No pure **85** could be isolated. RP-HPLC (acetonitrile/H<sub>2</sub>O, 4 min,  $\lambda=214$  nm):  $t_R = 2.66$  min.  
ESI-MS  $m/z$  (positive ion mode):  $[C_{33}H_{37}N_3O_5 + H]^+ = 544.28$ .



#### 6.4.14 Cellular Assays (K562 Cells)

##### Material:

Penicillin-Streptomycin solution stabilised (Sigma CatN° P4333)

L-Glutamine, 200mM (Sigma CatN° G7513)

0.25% Trypsin-EDTA solution (Sigma CatN° T4049)

FCS (serum), (Gibco-Invitrogen, CatN° 10270-106)

Dimethyl Sulphoxide (DMSO) HYBRI-MAX® (Sigma CatN° D2650)

Pipettes (10ml) (Falcon advantage 35-6551) single sealed (any brand).

Set of sterile micropipette tips (filtered)

Cryotubes (any brand).

Culture flasks: (distributor Millian)

Nunclon, Easyflask 25 V/C CatN° 156340

Nunclon, Easyflask 75 FILT CatN° 156499

Culture medium:

RPMI-1640; (Sigma CatN° R8758)

DMEM-Dulbecco's Modified Eagle Medium ; (Sigma CatN° D6546)

PBS (Sigma CatN° D8537)

5% Javel solution for waste neutralisation.

##### Culture medium supplementation:

K562 cells (suspension):

500ml bottle RPMI-1640 (contains L-glutamine and NaHCO<sub>3</sub>) supplemented with 55ml FCS and 5.5 ml Penicillin-Streptomycin solution. Mix well and store at 4°C for up to 1 month.

##### **Sub culturing the cells:**

##### Suspension cells:

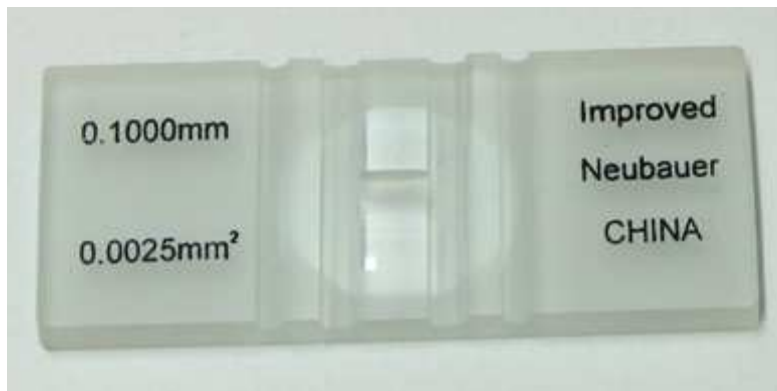
1. Prepare an appropriate amount of pre-warmed culture medium.
2. Transfer cell suspension to a 50 ml Falcon tube and centrifuge at 1100-1200 rpm for 2-3 min. at RT.

3. Discard supernatant (by pouring off or aspirating)
4. Re-suspend cell pellet in 5 ml fresh pre-warmed culture medium (use pipetman) and count cells.

### Drug treatment and Cell-Counting:

For drug treatments, cell were grown to 80% confluence (over the weekend) and then split into the appropriate number of culture flasks (Dilution 10X).

The cells were counted under the microscope using a hemacytometer. A hemacytometer (also spelled hemocytometer, see Figure 6.1) is an etched glass chamber with raised sides that will hold a quartz coverslip exactly 0.1 mm above the chamber floor. The counting chamber is etched in a total surface area of 9 mm<sup>2</sup> (see Figures 6.1 and 6.2). Calculation of concentration is based on the volume underneath the cover slip. One large square (see 1 to 5 in Figure 6.2) has a volume of 0.0001 ml (length x width x height; i.e., 0.1 cm x 0.1 cm x 0.01 cm).



**Figure 6.1.** Reusable hemacytometer cell counting chamber for counting cell densities. Cell depth: 0.100 mm; Volume: 0.1 Microliter.<sup>10</sup>

The cell concentration was calculated by counting the number of cells in the four outer squares (see Figure 6.2, squares 1 to 4). Then the cell concentration was calculated as follows:

$$\text{Cell concentration per millilitre} = \frac{\text{Total cells counted in 4 squares} \times 2500 \times \text{dilution factor}}{\text{factor}}$$

Since no dilution was used, the calculation was simplified by leaving out the dilution factor. So the cell concentration was calculated by multiplying the total cells counted in 4 squares by 2500.

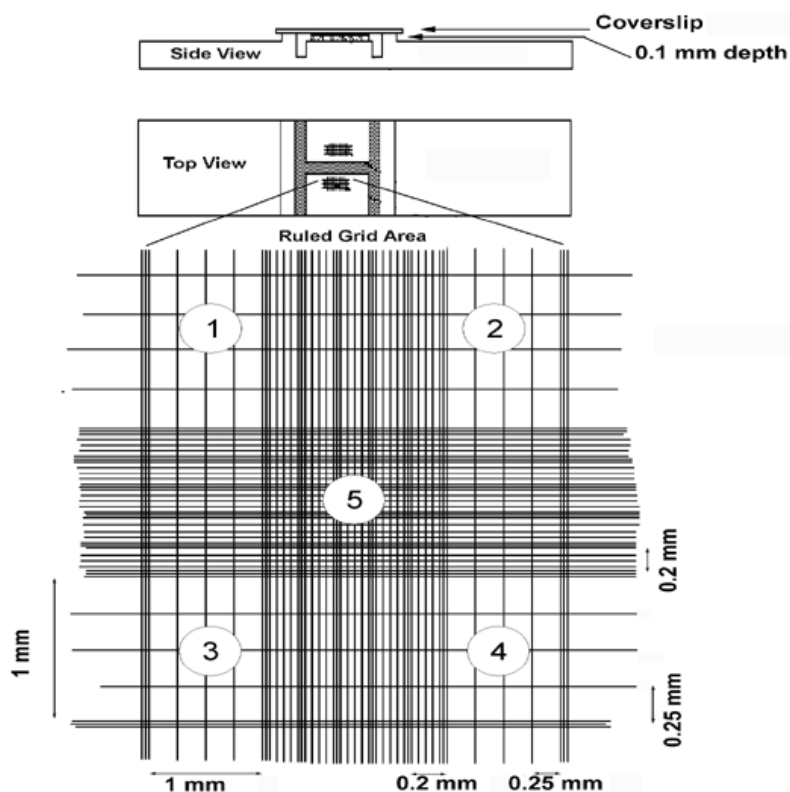


Figure 6.2. Improved Neubauer hemacytometer.<sup>11</sup>

Starting from a concentration of about 90'000 cells per ml each cell culturing vessel was prepared containing 9 ml of culture medium, 10  $\mu$ l of the corresponding DMSO solution and 1 ml cell suspension (see Figure 6.3). Finally this gave a drug concentration of 50  $\mu$ M. After 17 h, 42 h, 66 h, and 90 h the cell concentration was determined by using a hemacytometer as described above. The experiment was performed twice and independent from each other. The results were identical and so only one experiment is presented in detail.

For K562, start new culture at  $1 \times 10^5$  viable cells/ml. Subculture at  $1 \times 10^6$  cells/ml (source: ECACC.org). Consult this cell line repository or ATCC for other cell lines.



Figure 6.3. Picture of K562 cells in culture medium after 90 h. From left to right: untreated cells only with DMSO, with DMSO solution of compound **3g**, with DMSO solution of compound **3f**, with DMSO solution of compound **16**.

## 6.5 References for Chapter 6

- [1] H.E. Gottlieb, V. Kotlyar, A. Nudelman, *J. Org. Chem.* **1997**, *62*, 7512-7515.
- [2] Stoe. (2005). X-Area V1.26 & X-RED32 V1.26 Software. Stoe & Cie GmbH, Darmstadt, Germany.
- [3] Sheldrick, G. M. (1990) "SHELXS-97 - Program for Crystal Structure Determination", *Acta Crystallogr.*, *A46*, 467-473.
- [4] Sheldrick, G. M. (1999) "SHELXL-97", Universität Göttingen, Göttingen, Germany.
- [5] Spek, A.L. (2003), *J. Appl. Cryst.*, *36*, 7-13.
- [6] L. A. Carpino, G. Y. Han, *J. Org. Chem.* **1972**, *37*, 3404-3409.
- [7] a) C. A. Fuhrer, R. Messer, R. Häner, *Tetrahedron Lett.* **2004**, *45*, 4297-4300 (and references therein); b) Cyril Fuhrer, *Stereoselektive Synthese von Pyranofuranonen mittels intramolekularer hetero Diels-Alder Reaktion*, Diplomarbeit **2003**, Universität Bern, Schweiz (and references therein).
- [8] Florian Garo, *Trennung der Enantiomere eines biologisch aktiven Furo[3,4-c]pyranons durch die Synthese von Diastereomeren*, Bachelorarbeit **2006**, Universität Bern, Schweiz.
- [9] Sandro Manni, *Stereoselektive Synthese von Furo[3,4-c]pyranonen mittels intramolekularer hetero-Diels-Alder-Reaktion zur Durchführung einer Struktur-Aktivitäts-Beziehungs Studie in neoplastischen Zellen*, Bachelorarbeit **2006**, Universität Bern, Schweiz.
- [10] [http://www.thesciencefair.com/Merchant2/merchant.mvc?Screen=PROD&Product\\_Code=B-4005&Category\\_Code=BS](http://www.thesciencefair.com/Merchant2/merchant.mvc?Screen=PROD&Product_Code=B-4005&Category_Code=BS)
- [11] <http://homepages.gac.edu/~cellab/chpts/chpt1/figure8.html>

## 7. Appendix

### 7.1 Abbreviations

A549	human nonsmall cell lung cancer cells
Acetyl-CoA	acetyl-Coenzyme A
ADME	absorption, distribution, metabolism, elimination/excretion
AIDS	acquired immune deficiency syndrome
BAL	backbone amide linker
Bn	benzyl
BnBr	benzyl bromide
<i>n</i> -BuLi	<i>n</i> -butyllithium
<i>t</i> -Bu	<i>tert</i> -butyl
°C	degrees Celsius
CA-4	combretastatin A-4
Caco-2	human colon cancer cells
CDCl <sub>3</sub>	deuterated chloroform
CH <sub>2</sub> Cl <sub>2</sub>	dichloromethane
CH <sub>3</sub> CN	acetonitrile
CDKs	cyclin-dependent kinases
CML	chronic myeloid leukaemia
COSY	correlation spectroscopy
COX	cyclo-oxygenase
Cs <sub>2</sub> CO <sub>3</sub>	cesium carbonate
CVDs	cardiovascular diseases
δ	chemical shift
d	day; doublet
DA	Diels-Alder
DCM	dichloromethane
DIPEA	N-ethyldiisopropylamine
DMA	N,N-dimethylacetamide
DMAP	4-dimethylaminopyridine
DMAPP	dimethylallyl diphosphate
DMF	N,N-dimethylformamide
DMSO	dimethyl sulphoxide
DNA	deoxyribonucleic acid
DOS	diversity-oriented synthesis

---

DOX	doxorubicin
$\varepsilon$	extinction coefficient
EI-MS	Electron-Ionization Mass Spectrometry
eq.	equivalent
ESI	Electrospray Ionization
EtOAc	ethyl acetate
EtOH	ethanol
EWG	electron withdrawing group
FMO	frontier molecular orbital theory
Fmoc	9-fluorenylmethyloxycarbonyl
Fmoc-Cl	9-fluorenylmethyloxycarbonylchloride; 9-Fluorenylmethyl chloroformate
g	gram(s)
GC	gas chromatography
GPP	geranyl diphosphate
GTP	guanosine triphosphate
$h$	Planck constant $\approx 6.63 \times 10^{-34}$ Js
h	hour(s)
HCl	hydrogen chloride
HCT-116	human colon adenocarcinoma cells
HCTU	1H-benzotriazolium 1-[bis(dimethylamino)methylene]-5-chloro- ,hexafluorophosphate (1-),3-oxide
HDA	<i>hetero</i> Diels-Alder
HeLa S3	human epithelial cancer cell line
HIV	human immunodeficiency virus
HL-60	human myeloid leukaemia cells
HMDS	1,1,1,3,3,3-hexamethyldisilazane
HMEC-1	human microvascular endothelial cells
HOBT	1-hydroxybenzotriazole
H <sub>2</sub> O	water
HOMO	highest occupied molecular orbital
HPLC	high performance liquid chromatography
HRMS	high-resolution mass spectrometry
HT-29	colon adenocarcinoma cells
HTS	high-throughput screening
HV	high vacuum
Hz	hertz

---

IC <sub>50</sub>	inhibitory concentration 50%, the concentration required for 50% inhibition
IPP	isopentenyl diphosphate
IR	infrared
<i>J</i>	coupling constant
KB31	human cervix carcinoma cells
K562	human caucasian chronic myelogenous leukaemia cells
$\lambda$	wavelength
l	liter(s)
L1210	murine leukaemia cell line
LC	liquid chromatography
LDL-C	low-density lipoprotein cholesterol
Log P	partition coefficient; see P
LSD	lysergic acid diethylamide
LUMO	lowest unoccupied molecular orbital
$\mu$	micro
m	multiplet; meter(s); milli
M	moles per liter
MCF-7	breast carcinoma cells
MDM2	murine double-minute 2; a protein involved in the regulation process of the p53 tumor suppressor protein
MDR	multidrug resistance
MeOH	methanol
MHz	megahertz
min	minute(s)
mol	mole(s)
mp	melting point
MRI	magnetic resonance imaging
MS	mass spectrometry
MW	molecular weight
<i>m/z</i>	mass to charge ratio
$\nu$	frequency
n	nano
NaCl	sodium chloride
N <sub>2</sub>	nitrogen
NaBH <sub>4</sub>	sodium borohydride
NaBH <sub>3</sub> CN	sodium cyanoborohydride

---

NaHCO <sub>3</sub>	sodium hydrogencarbonate
Na <sub>2</sub> SO <sub>4</sub>	sodium sulfate
NSAID	non-steroidal anti-inflammatory drugs
NH <sub>4</sub> Cl	ammonium chloride
NEt <sub>3</sub>	triethylamine
NMP	1-methyl-2-pyrrolidone
NMR	nuclear magnetic resonance
NOE	nuclear Overhauser enhancement
NP	normal phase
P	partition coefficient; a measure of a drug's hydrophobic character determined as the drug's relative distribution in an <i>n</i> -octanol/water mixture; usually quoted as log P.
p53 protein	important protein that monitors the health of the cell and the integrity of its DNA. Important to the apoptosis process.
PAL	peptide amide linker
PDGF	platelet-derived growth factor
PEG	polyethylene glycol
Ph	phenyl
P(OEt) <sub>3</sub>	triethyl phosphite
PS	polystyrene
psi	pounds per square inch
PTFE	polytetrafluoroethylene
q	quadruplet
QSAR	quantitative structure-activity relationships
R <sub>f</sub>	retention factor
Ras protein	rat sarcoma protein; a small G-protein that plays an important role in the signal transduction pathways leading to cell growth and division
ref.	reference(s)
RIF	radiation induced fibrosarcoma
RP	reversed phase
rt	room temperature
s	singlet; second
SAR	structure-activity relationship
sat.	saturated
t <sub>R</sub>	retention time
TFA	trifluoroacetic acid



TGF- $\alpha$	transforming growth factor $\alpha$
TGF- $\beta$	transforming growth factor $\beta$
THF	tetrahydrofuran
TLC	thin layer chromatography
UV	ultraviolet

## 7.2 X-Ray Crystallography of Compound 3g

Suitable crystals of **3g** were obtained as colourless by slow evaporation of a solution in methanol. The intensity data were collected at 173K (-100°C) on a Stoe Mark II-Image Plate Diffraction System\* equipped with a two-circle goniometer and using MoK $\alpha$  graphite monochromated radiation. Image plate distance 100 mm,  $\omega$  rotation scans 0 - 180° at  $\phi$  0°, and 0 - 77° at  $\phi$  90°, step  $\Delta\omega = 1.0^\circ$ , with an exposure time of 3 mins per image,  $2\theta$  range 2.29 - 59.53°,  $d_{\min} - d_{\max} = 17.779 - 0.716 \text{ \AA}$ .

The structure was solved by Direct methods using the programme SHELXS.† The refinement and all further calculations were carried out using SHELXL-97.‡ The H-atoms were located from Fourier difference maps and refined isotropically. The non-H atoms were refined anisotropically, using weighted full-matrix least-squares on  $F^2$ .

The molecular structure and crystallographic numbering scheme are illustrated in the PLATON§ drawing, Figure 7.1.

---

\* Stoe. (2005). *X-Area V1.26 & X-RED32 V1.26: IPDS Software*. Stoe & Cie GmbH, Darmstadt, Germany.

† Sheldrick, G. M. (1990) "SHELXS-97 - Program for Crystal Structure Determination", *Acta Crystallogr.*, **A46**, 467-473.

‡ Sheldrick, G. M. (1999) "SHELXL-97", Universität Göttingen, Göttingen, Germany.

§ Spek, A.L. (2003), *J. Appl. Cryst.*, **36**, 7-13.

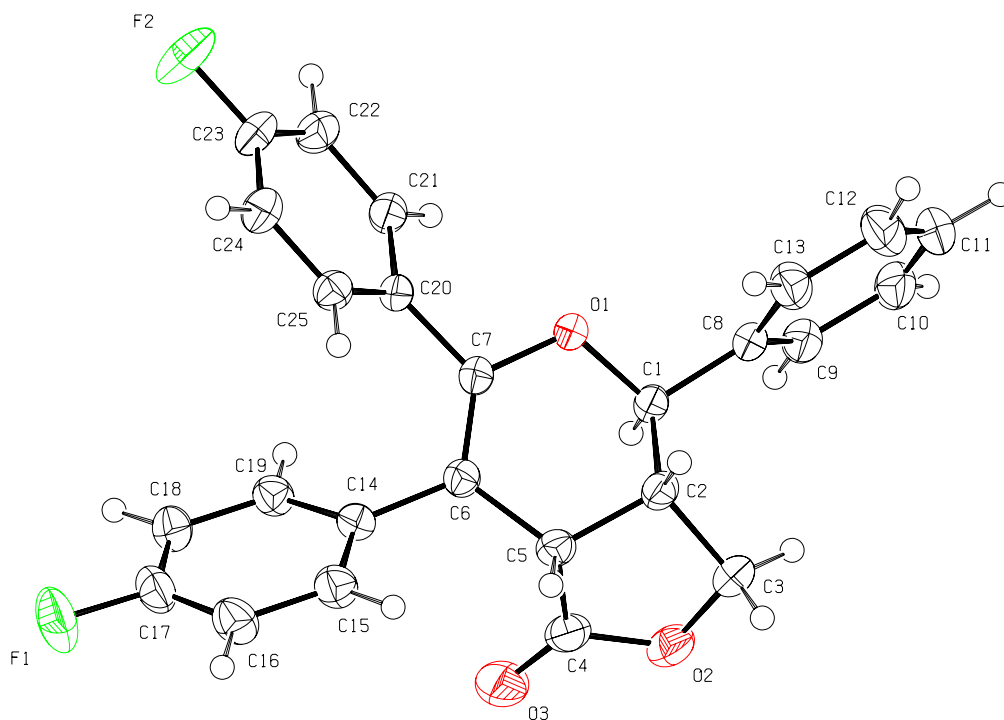


Figure 7.1. X-ray structure of **3g**.

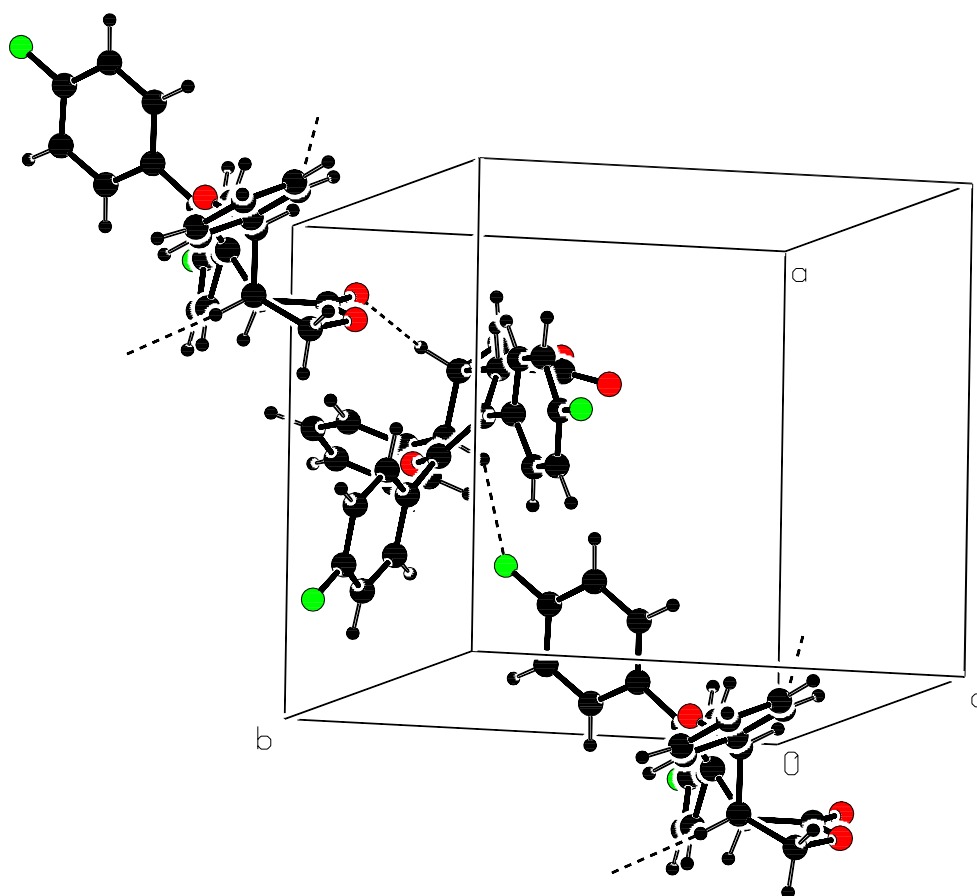


Figure 7.2. Crystal packing of **3g** showing the C-H...O and C-H...F hydrogen bonding as dashed lines.

**Table 7.1.** Crystal Data and Details of the Structure Determination  
for: **3g** P 21/n R = 0.04

Crystal Data			
Formula		C25	H18 F2 O3
Formula Weight			404.39
Crystal System			Monoclinic
Space group		P21/n	(No. 14)
a, b, c [Angstrom]	10.9685(6)	11.2602(6)	15.6882(8)
alpha, beta, gamma [deg]	90	91.671(4)	90
V [Ang**3]			1936.79(18)
Z			4
D(calc) [g/cm**3]			1.387
Mu(MoKa) [ /mm ]			0.103
F(000)			840
Crystal Size [mm]		0.28 x	0.50 x 0.50
Data Collection			
Temperature (K)			173
Radiation [Angstrom]		MoKa	0.71073
Theta Min-Max [Deg]			2.2, 29.2
Dataset		-15: 15 ; -15: 15 ; -21: 21	
Tot., Uniq. Data, R(int)		26170, 5230,	0.038
Observed data [I > 2.0 sigma(I)]			4363
Refinement			
Nref, Npar			5230, 344
R, wR2, S		0.0397, 0.1063,	1.01
w = 1/[\s^2^(Fo^2^)+(0.0581P)^2^+0.3906P] where P=(Fo^2^+2Fc^2^)/3			
Max. and Av. Shift/Error			0.00, 0.00
Min. and Max. Resd. Dens. [e/Ang^3]			-0.19, 0.34

### 7.3 X-Ray Crystallography of Compound 41

Suitable crystals of **41** were obtained as colourless rods by slow evaporation of a solution in methanol. The intensity data were collected at 173K (-100°C) on a Stoe Mark II-Image Plate Diffraction System\* equipped with a two-circle goniometer and using MoK $\alpha$  graphite monochromated radiation. Image plate distance 135mm,  $\omega$  rotation scans 0 - 180° at  $\phi$  0°, and 0 - 83° at  $\phi$  90°, step  $\Delta\omega = 1.2^\circ$ , with an exposure time of 3 mins per image,  $2\theta$  range 1.70 - 51.55°,  $d_{\min} - d_{\max} = 23.995 - 0.817 \text{ \AA}$ .

The structure was solved by Direct methods using the programme SHELXS.† The refinement and all further calculations were carried out using SHELXL-97.‡ The H-atoms were located from Fourier difference maps and refined isotropically. The non-H atoms were refined anisotropically, using weighted full-matrix least-squares on  $F^2$ .

The molecular structure and crystallographic numbering scheme are illustrated in the PLATON§ drawing, Figure 7.3.

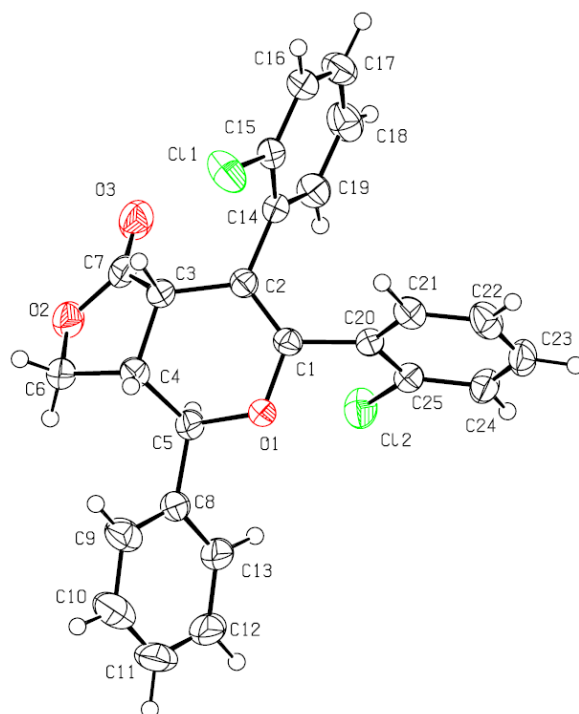
---

\* Stoe. (2005). *X-Area V1.26 & X-RED32 V1.26: IPDS Software*. Stoe & Cie GmbH, Darmstadt, Germany.

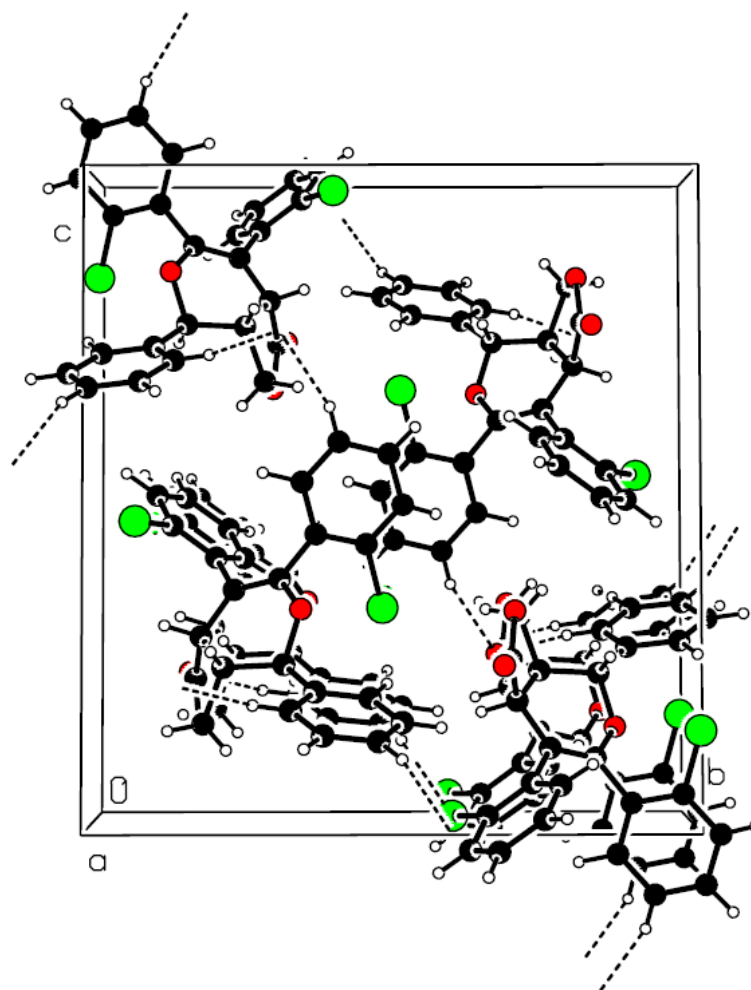
† Sheldrick, G. M. (1990) "SHELXS-97 - Program for Crystal Structure Determination", *Acta Crystallogr.*, **A46**, 467-473.

‡ Sheldrick, G. M. (1999) "SHELXL-97", Universität Göttingen, Göttingen, Germany.

§ Spek, A.L. (2003), *J. Appl. Cryst.*, **36**, 7-13.



**Figure 7.3.** X-ray structure of **41**. Thermal ellipsoid at the 50% probability level.



**Figure 7.4.** View of the crystal packing of **41** along the *a* axis, showing the C-H...O hydrogen bonds as dashed lines.

**Table 7.2.** Crystal data table for **41**.

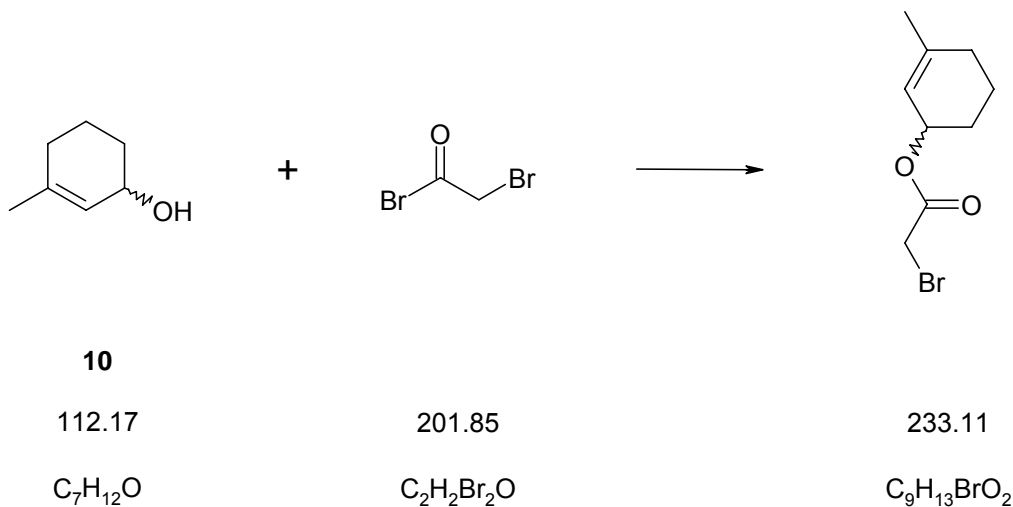
---

Identification code	<b>41</b>
Crystal shape	rod
Crystal colour	colourless
Crystal size	0.50 x 0.35 x 0.27 mm
Empirical formula	C <sub>25</sub> H <sub>18</sub> Cl <sub>2</sub> O <sub>3</sub>
Formula weight	437.29
Crystal system	Monoclinic
Space group	P 2 <sub>1</sub> /n
Unit cell dimensions	a = 7.2820(4) Å    alpha = 90 deg. b = 15.9643(13) Å    beta = 94.204(5) deg. c = 17.4021(11) Å    gamma = 90 deg.
Volume	2017.6(2) Å <sup>3</sup>
Cell refinement parameters	
Reflections	16235
Angle range	1.73 < theta < 25.59
Z	4
Density (calculated)	1.440 g/cm <sup>3</sup>
Radiation used	MoK $\alpha$
Wavelength	0.71073 Å
Linear absorption coefficient	0.347 mm <sup>-1</sup>
Temperature	173(2) K

---

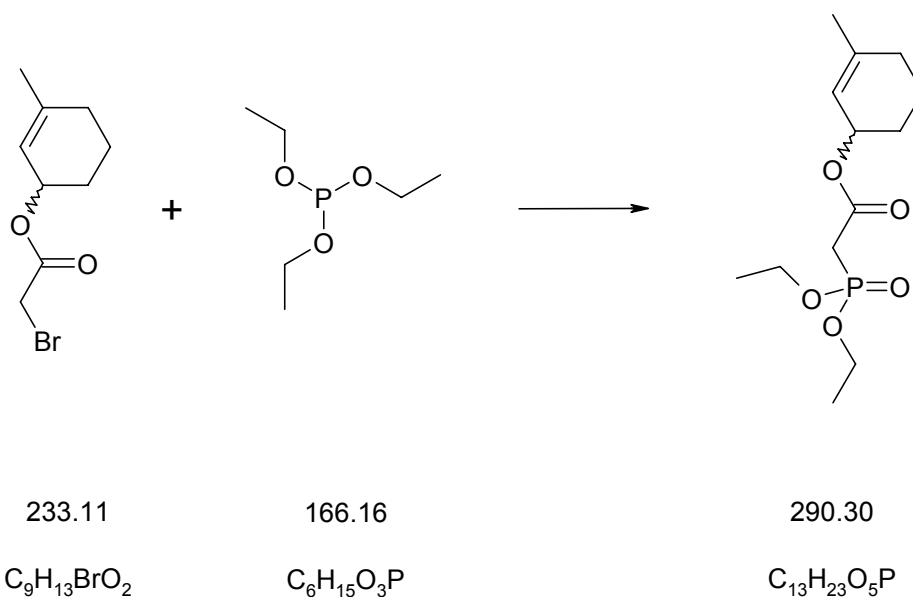
## 7.4 Synthesis of (E/Z)-4-Oxo-3,4-diphenyl-but-2-enoic acid 3-methyl-cyclohex-2-enyl ester

### Bromo-acetic acid 3-methyl-cyclohex-2-enyl ester

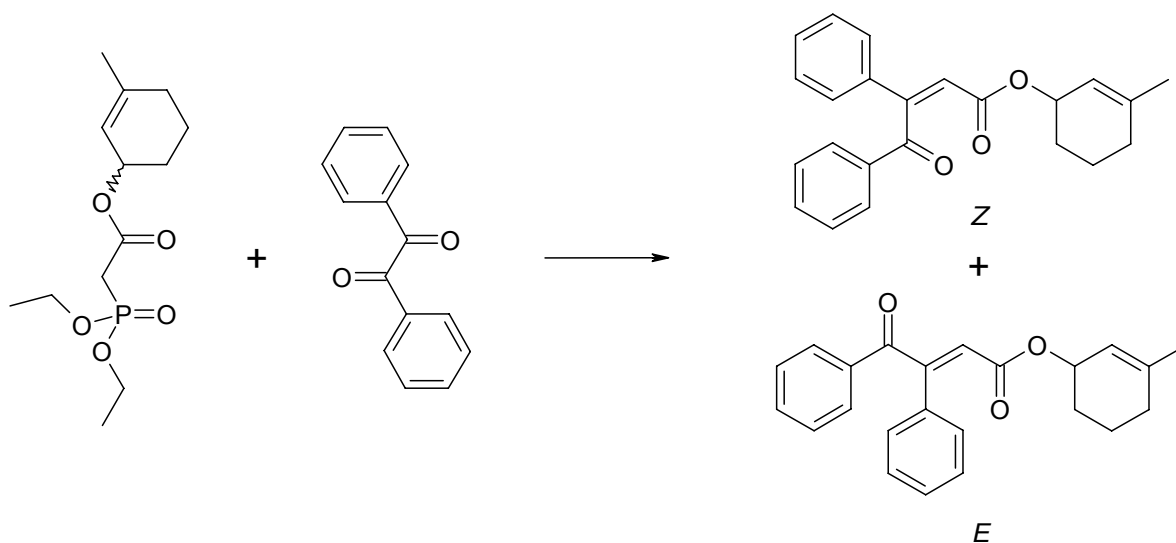


A solution of bromoacetyl bromide (0.78 ml, 8.9 mmol) in  $CH_2Cl_2$  (2 ml) was added dropwise to a stirred solution of racemic 3-methyl-2-cyclohexen-1-ol (**10**, 1.06 ml, 8.9 mmol) and pyridine (0.79 ml, 9.8 mmol) in  $CH_2Cl_2$  (10 ml) at  $0^\circ C$  under a nitrogen atmosphere. Directly after the addition of bromoacetyl bromide the colour changed to white, later yellow and formation of a solid was visible. The obtained suspension was allowed to warm to room temperature during one hour. The mixture was poured onto saturated aqueous ammonium chloride and extracted three times with  $CH_2Cl_2$ . The combined organic phases were dried ( $Na_2SO_4$ ) and concentrated. The liquid product was separated from a small amount of brown residue by removal with a pipette. The obtained bromoacetic acid 3-methyl-cyclohex-2-enyl ester (1.72 g, 83%) was used without further purification. TLC (EtOAc/hexane, 1:9):  $R_f$  0.63.  $^1H$ -NMR (300 MHz,  $CDCl_3$ ):  $\delta$  5.47 (m, 1H), 5.29 (br, 1H), 3.81 (s, 2H), 1.99-1.61 (m, 9H).  $^{13}C$ -NMR (75 MHz,  $CDCl_3$ ):  $\delta$  167.1, 142.3, 119.2, 71.2, 30.0, 27.8, 26.7, 23.9, 18.9. EI-MS  $m/z$  (%): 232 ( $[C_9H_{13}O_2^{81}Br]^+$ , weak), 234 ( $[C_9H_{13}O_2^{79}Br]^+$ , weak), 153 (65), 111 (66), 93 (72), 79 (89), 55 (100).



**(Diethoxy-phosphoryl)-acetic acid 3-methyl-cyclohex-2-enyl ester**

Triethyl phosphite (0.90 ml, 5.2 mmol) was added to a solution of bromoacetic acid 3-methyl-cyclohex-2-enyl ester (800 mg, 3.4 mmol) in dry THF (10 ml) under a nitrogen atmosphere. The light brown solution was stirred and refluxed for 20 h. Then THF and triethyl phosphite were removed *in vacuo*. (Diethoxy-phosphoryl)-acetic acid 3-methyl-cyclohex-2-enyl ester (922 mg, 93%) was isolated and used without further purification.  $^1H$ -NMR (300 MHz,  $CDCl_3$ ):  $\delta$  5.45 (m, 1H), 5.27 (s, 1H, br), 4.15 (m, 4H), 2.93 (d,  $^2J_{HP}=21.5$  Hz, 2H), 2.00-1.56 (m, 9H), 1.32 (t,  $J=7.1$  Hz, 6H).  $^{13}C$ -NMR (75 MHz,  $CDCl_3$ ):  $\delta$  165.7 (d, 1C,  $^2J_{CP}=5.6$  Hz), 141.6, 119.6, 70.3, 62.7 (d, 2C,  $^2J_{CP}=6.2$  Hz), 34.8 (d, 1C,  $^1J_{CP}=133.6$  Hz), 30.0, 27.9, 23.8, 19.0, 16.4 (2d, 2C,  $^3J_{CP}=6.2$  Hz).  $^{31}P$ -NMR (121 MHz,  $CDCl_3$ ):  $\delta$  20.1 (s, 1P). EI-MS  $m/z$  (%): 290 ( $[C_{13}H_{23}PO_5]^+$ , 1), 123 (85), 79 (100).

**(E/Z)-4-Oxo-3,4-diphenyl-but-2-enoic acid 3-methyl-cyclohex-2-enyl ester**

290.30

210.23

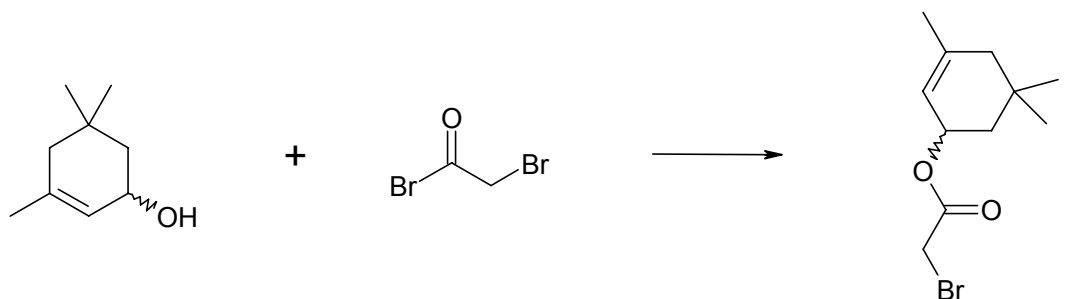
346.43

 $C_{13}H_{23}O_5P$  $C_{14}H_{10}O_2$  $C_{23}H_{22}O_3$ 

HMDS (0.35 ml, 1.7 mmol) was added slowly to a stirred solution of *n*-butyllithium (0.95 ml, 1.5 mmol, 1.6 M solution in hexane) in dry THF (5 ml) at 0°C under a nitrogen atmosphere. After half an hour, (diethoxy-phosphoryl)-acetic acid 3-methyl-cyclohex-2-enyl ester (400 mg, 1.4 mmol) dissolved in dry THF (1 ml) was added to the solution. Then the solution was cooled down to -78°C and benzil (320 mg, 1.5 mmol) dissolved in dry THF (1 ml) was added slowly. For the final half hour the cooling bath was removed. After 3.5 hours, the solution was poured onto saturated aqueous ammonium chloride and extracted three times with EtOAc. The combined organic phases were dried ( $Na_2SO_4$ ) and concentrated. The crude product was purified by column chromatography (EtOAc/hexane, 1:9) and (E/Z)-4-oxo-3,4-diphenyl-but-2-enoic acid 3-methyl-cyclohex-2-enyl ester (424 mg, 88%) was isolated as a yellow oily liquid. The ratio of the *E*- and *Z*-isomer was about 1:2 (as determined by NMR). TLC (EtOAc/Hexane, 1:9):  $R_f$  0.33 (both *E*- and *Z*-isomer).  $^1H$ -NMR (300 MHz, DMSO, mixture of isomers):  $\delta$  7.95-7.31 (m, 20H), 6.68 (s, 1H, *E*), 6.34 (s, 1H, *Z*), 5.34-5.02 (m, 4H), 1.82-1.24 (m, 18H). EI-MS  $m/z$  (%): 346 ( $[C_{23}H_{22}O_3]^+$ , 1), 105 (96), 77 (100), 51 (97).

## 7.5 Synthesis of (E/Z)-4-Oxo-3,4-diphenyl-but-2-enoic acid 3,5,5-trimethyl-cyclohex-2-enyl ester

### Bromo-acetic acid 3,5,5-trimethyl-cyclohex-2-enyl ester

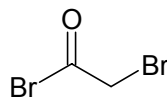


**11**

140.23

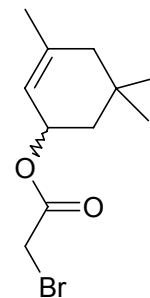
C<sub>9</sub>H<sub>16</sub>O

+



201.85

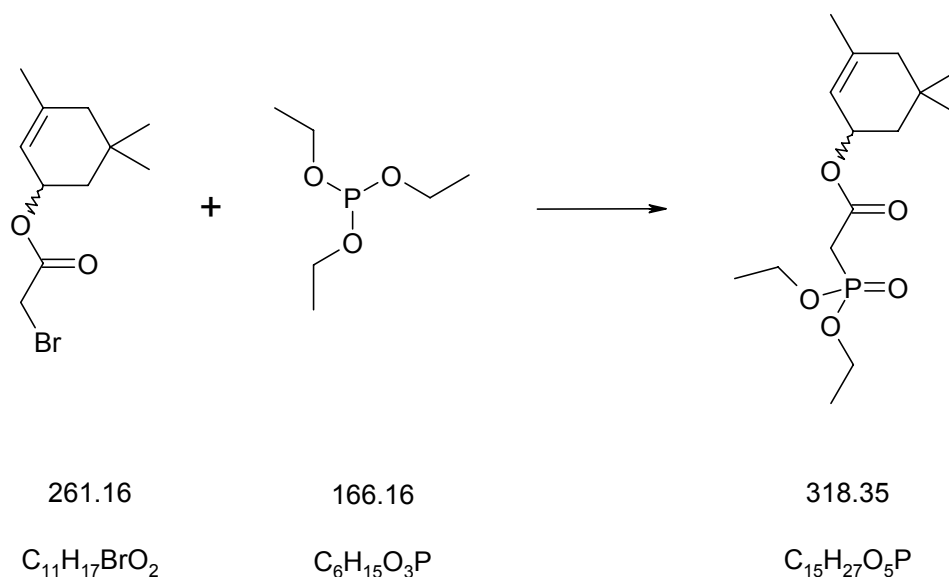
C<sub>2</sub>H<sub>2</sub>Br<sub>2</sub>O



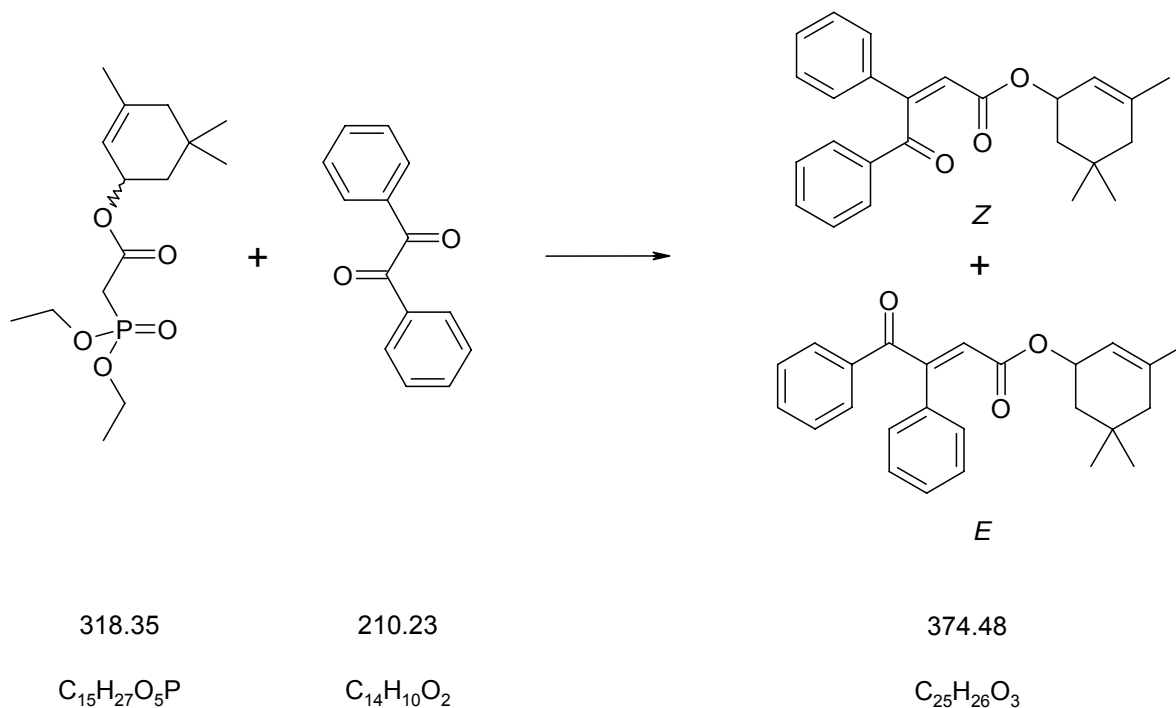
261.16

C<sub>11</sub>H<sub>17</sub>BrO<sub>2</sub>

A solution of bromoacetyl bromide (1.24 ml, 14.3 mmol) in CH<sub>2</sub>Cl<sub>2</sub> (3 ml) was added dropwise to a stirred solution of racemic 3,5,5-trimethyl-2-cyclohexen-1-ol (**11**, 2.20 ml, 14.3 mmol) and pyridine (1.26 ml, 15.7 mmol) in CH<sub>2</sub>Cl<sub>2</sub> (10 ml) at 0°C under a nitrogen atmosphere. Directly after the addition of bromoacetyl bromide the colour changed to white, later yellow and formation of a solid was visible. The obtained suspension was allowed to warm to room temperature during one hour. The mixture was poured onto saturated aqueous ammonium chloride and extracted three times with CH<sub>2</sub>Cl<sub>2</sub>. The combined organic phases were dried (Na<sub>2</sub>SO<sub>4</sub>) and concentrated. The crude product was purified by column chromatography (EtOAc/hexane, 1:10) and bromoacetic acid 3,5,5-trimethyl-cyclohex-2-enyl ester (1.64 g, 45%) was isolated as a light yellow liquid. TLC (EtOAc/hexane, 1:9): *R<sub>f</sub>* 0.65. <sup>1</sup>H-NMR (300 MHz, CDCl<sub>3</sub>): δ 5.39 (m, 2H), 3.80 (s, 2H), 1.90-1.64 (m, 6H), 1.44 (m, 1H), 1.00 (s, 3H), 0.93 (s, 1H). <sup>13</sup>C-NMR (75 MHz, CDCl<sub>3</sub>): δ 167.2, 139.5, 118.4, 72.5, 44.1, 40.4, 30.7, 30.3, 27.3, 26.5, 23.8. EI-MS *m/z* (%): 260 ([C<sub>11</sub>H<sub>17</sub>O<sub>2</sub><sup>81</sup>Br]<sup>+</sup>, weak), 262 ([C<sub>11</sub>H<sub>17</sub>O<sub>2</sub><sup>79</sup>Br]<sup>+</sup>, weak), 121 (92), 107 (100), 91 (90).

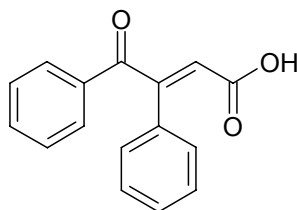
**(Diethoxy-phosphoryl)-acetic acid 3,5,5-trimethyl-cyclohex-2-enyl ester**

Triethyl phosphite (0.80 ml, 4.6 mmol) was added to a solution of bromoacetic acid 3,5,5-trimethyl-cyclohex-2-enyl ester (800 mg, 3.1 mmol) in dry THF (9 ml) under a nitrogen atmosphere. The light brown solution was stirred and refluxed for 25 h. Then THF and triethyl phosphite were removed *in vacuo*. (Diethoxy-phosphoryl)-acetic acid 3,5,5-trimethyl-cyclohex-2-enyl ester (977 mg, 99%) was isolated and used without further purification.  $^1H$ -NMR (300 MHz,  $CDCl_3$ ):  $\delta$  5.36 (m, 1H, br), 4.15 (m, 4H), 2.93 (d,  $^2J_{HP}=21.5$  Hz, 2H), 1.88-1.63 (m, 6H), 1.40 (m, 1H), 1.33 (t,  $J=7.1$  Hz, 6H), 0.98 (s, 3H), 0.91 (s, 3H).  $^{31}P$ -NMR (121 MHz,  $CDCl_3$ ):  $\delta$  20.1 (s, 1P). EI-MS  $m/z$  (%): 318 ( $[C_{15}H_{27}PO_5]^+$ , 1), 123 (76), 107 (100), 91 (87), 79 (67).

**(E/Z)-4-Oxo-3,4-diphenyl-but-2-enoic acid 3,5,5-trimethyl-cyclohex-2-enyl ester**

HMDS (0.24 ml, 1.1 mmol) was added slowly to a stirred solution of *n*-butyllithium (0.64 ml, 1.0 mmol, 1.6 M solution in hexane) in dry THF (4 ml) at 0°C under a nitrogen atmosphere. After half an hour, (diethoxy-phosphoryl)-acetic acid 3,5,5-trimethyl-cyclohex-2-enyl ester (300 mg, 0.9 mmol) dissolved in dry THF (1 ml) was added to the solution. Then the solution was cooled down to -78°C and benzil (217 mg, 1.0 mmol) dissolved in dry THF (1 ml) was added slowly. For the final half hour the cooling bath was removed. After 3.5 hours, the solution was poured onto saturated aqueous ammonium chloride and extracted three times with EtOAc. The combined organic phases were dried (Na<sub>2</sub>SO<sub>4</sub>) and concentrated. The crude product was purified by column chromatography (EtOAc/hexane, 1:10) and (E/Z)-4-oxo-3,4-diphenyl-but-2-enoic acid 3,5,5-trimethyl-cyclohex-2-enyl ester (281 mg, 80%) was isolated as a yellow oily liquid. The ratio of the *E*- and *Z*-isomer was about 1:2 (as determined by NMR). TLC (EtOAc/Hexane, 1:10): *R<sub>f</sub>* 0.39 (both *E*- and *Z*-isomer). <sup>1</sup>H-NMR (300 MHz, CDCl<sub>3</sub>, mixture of isomers): δ 8.00-7.33 (m, 20H), 6.49 (s, 1H, *E*), 6.27 (s, 1H, *Z*), 5.36-5.19 (m, 4H), 1.83-1.57 (m, 14H), 0.93-0.84 (3s, 12H). EI-MS *m/z* (%): 374 ([C<sub>25</sub>H<sub>26</sub>O<sub>3</sub>]<sup>+</sup>, 1), 105 (100), 77 (94), 51 (96).

The same reaction was carried out at 0°C instead of -78°C. In this case the product was isolated with a yield of 83% and the ratio of *E*- to *Z*-isomer changed to about 1:1 as determined by NMR spectroscopy.

**7.6 4-Oxo-3,4-diphenyl-but-2-enoic acid (12)****12**

252.27

 $C_{16}H_{12}O_3$ 

Carboxylic acid **12** was isolated after tried thermal cyclisation reaction of (*E/Z*)-4-oxo-3,4-diphenyl-but-2-enoic acid 3-methyl-cyclohex-2-enyl ester and of (*E/Z*)-4-oxo-3,4-diphenyl-but-2-enoic acid 3,5,5-trimethyl-cyclohex-2-enyl ester. The reaction was carried out in an autoclave which was heated in an oil bath at 200°C for 18 h (inside temperature: 180-183°C). Toluene was used as solvent. After removing the solvent *in vacuo*, followed by column chromatography (EtOAc/hexane, 1:4), the carboxylic acid **12** (up to 55 mg, up to 36%) was isolated as a white solid.  $^1\text{H-NMR}$  (300 MHz,  $\text{CDCl}_3$ ):  $\delta$  7.61-7.30 (m, 10H), 6.46 (s, 1H), COOH not visible. EI-MS *m/z* (%): 252 ( $[\text{C}_{16}\text{H}_{12}\text{O}_3]^+$ , 36), 224 (42), 105 (100), 102 (84), 77 (82), 51 (42).

## 7.7 Cellular Assays (KB31 and A549 Cells)

Description of the assay: Cells are seeded into 96-well plates ( $3 \times 10^3$  cells per well) and grown over night in an incubator. Cells are then treated for 72 h with the indicated concentrations of compound. Effect of inhibitors on viability and onset of apoptosis is assessed by the YO-PRO-1 assay as described.\* Briefly, after the treatment period of 72 h with compounds, a 25  $\mu$ L aliquot of a solution containing 100 mM sodium citrate, pH 4.0, 134 mM sodium chloride and 12.5  $\mu$ M YO-PRO-1 dye (YO-PRO-1 iodide, #Y3603, Molecular Probes) is directly added to the 100  $\mu$ L medium in the wells of the 96-well plate to a final dye concentration of 2.5  $\mu$ M. The plate is incubated for 10 min at ambient temperature in the dark. The uptake of the YO-PRO-1 dye into cells is assessed by a first measurement using a Cytofluor II fluorescence plate reader (PerSeptive Biosystems; instrument settings: excitation 485/20nm, emission 530/25nm, gain 75). After the first reading, 25  $\mu$ L of lysis buffer consisting of 20 mM sodium citrate, pH 4.0, 26.8 mM sodium chloride, 0.4 % NP40, 20 mM EDTA and 20 mM is added to each well. Upon completion of cell lysis after incubation for 30 min at room temperature, the total amount of YO-PRO-1 bound to DNA is determined by a second measurement using the Cytofluor II fluorescence plate reader with the identical setting as described above.

Data evaluation: The raw data obtained with the Cytofluor II fluorescence plate reader are transferred as 96-well-matrix to an EXCEL-template. EXCEL-routines are used for calculation of means and standard deviations of the triplicates. The percentage of apoptotic cells is calculated using the formula:

$$[(\text{values of the first reading})/(\text{values of the second reading})] \times 100 = \% \text{ apoptotic cells.}$$

To determine the anti-proliferative effect of a compound, the corresponding value of the second reading representing totally bound YO-PRO-1 dye is expressed as percentage of the value of the control cells set as 100 %. IC<sub>50</sub> values are then calculated from dose response curves according to the following formula, considering the region around 50 % inhibition to be a straight line (half-logarithmic plot):

$$10[\log C_1 + (50\% - I_1) \cdot (\log C_2 - \log C_1) / (I_2 - I_1)] = IC_{50}$$

where:

C <sub>1</sub>	=	concentration resulting in inhibition just below 50 %
C <sub>2</sub>	=	concentration resulting in inhibition just above 50 %
I <sub>1</sub>	=	% inhibition measured at C <sub>1</sub>
I <sub>2</sub>	=	% inhibition measured at C <sub>2</sub>

\* T. Idziorek, J. Estaquier, F. De Bels, J. C. Ameisen, *J.Immunol.Methods* **1995**, 185, 249-258.

## 7.8 Cell Cycle Analysis (KB31 and A549 Cells)

Cell cycle stages were analyzed by laser-scanning cytometry (LSC, CompuCyte, Cambridge, MA).<sup>\*</sup> Briefly, KB31 and A549 cells ( $3.0 \times 10^5$  cells) were plated out in 100 mm dishes and grown over night. After treatment for 24h with compounds **3f** (Figures 7.5 and 7.6) and **3g** (Figure 7.7) using the indicated concentrations, cells were collected, fixed using ice-cold 70% ethanol and stained with propidium iodide (PI) following standard protocols.

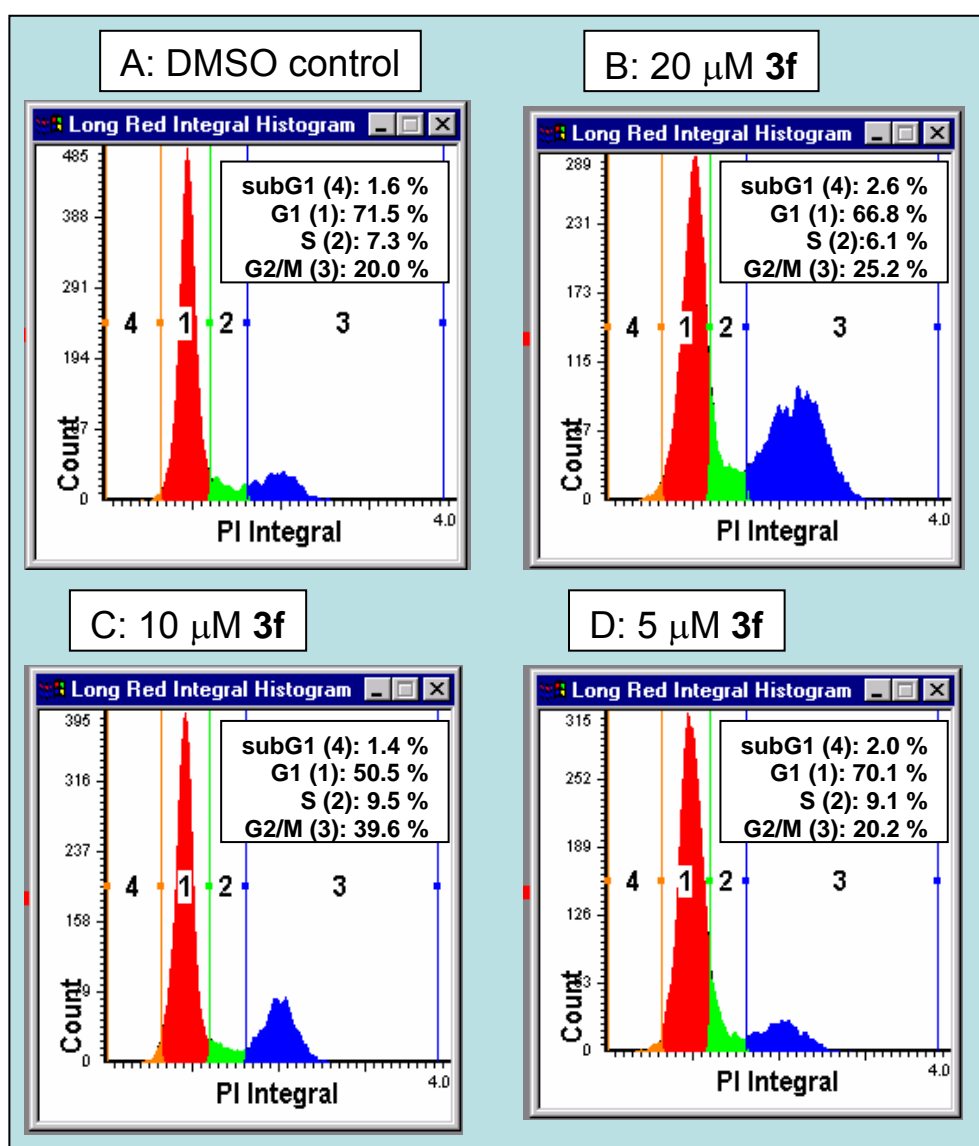


Figure 7.5: DNA profile of KB31 cells treated with compound **3f**.

<sup>\*</sup> E. Luther, L. Kamensky, M. Henriksen, E. Holden, *Methods Cell Biol.*, **2004**, *75*, 185-218.



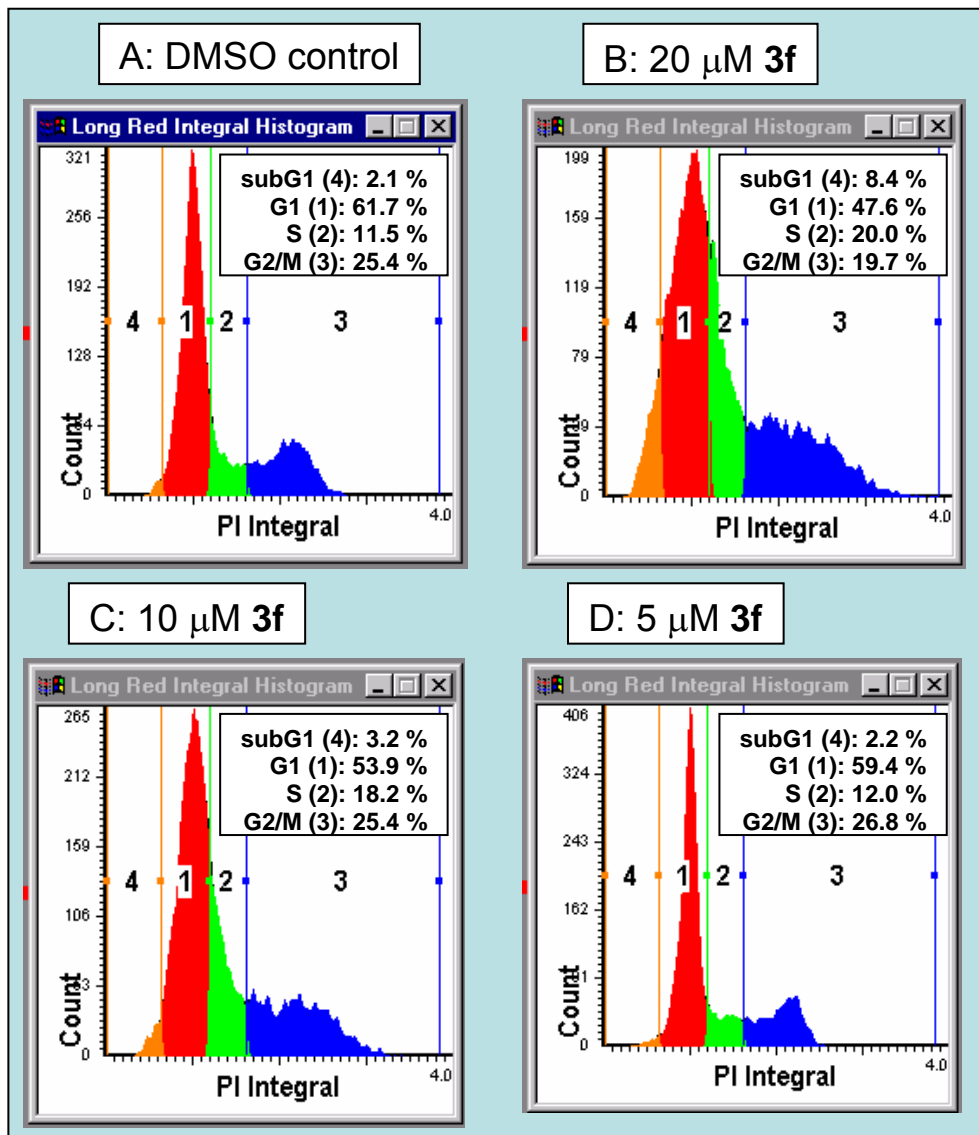


Figure 7.6: DNA profile of A549 cells treated with compound 3f.

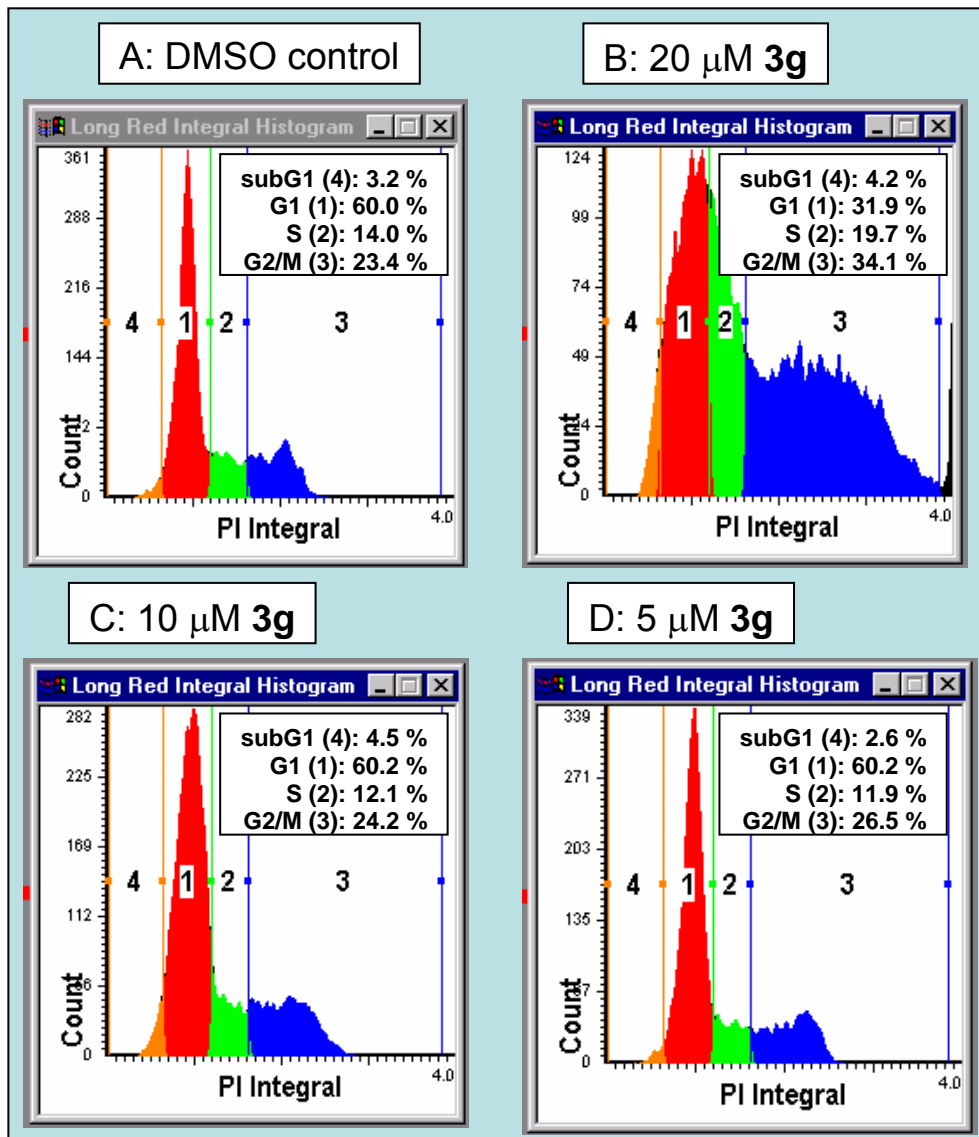


Figure 7.7: DNA profile of A549 cells treated with compound 3g.

E-Mail: [c.fuhrer@hispeed.ch](mailto:c.fuhrer@hispeed.ch)

# Cyril A. Fuhrer

## Curriculum Vitae



### Personal Information

Date of Birth : 23 November 1976  
 Marital Status : single  
 Nationality : Swiss

### Degrees

- Dissertation in the field of Medicinal Chemistry with Prof. Dr. R. Häner, University of Bern, Switzerland Feb 2004  
- Nov 2007  
 - *organic synthesis, solid phase chemistry*  
 - *cell culture, in vitro analysis, Flow Cytometry*  
 - *HPLC, NMR, MS, IR, UV-VIS, fluorescence spectroscopy*
- Master Degree in Chemistry (Dipl. Chem. UniBE), University of Bern, Switzerland Dec 2003  
 - *title of the diploma thesis: „Stereoselektive Synthese von Pyranofuranonen mittels intramolekularer hetero Diels-Alder Reaktion“*
- Federal Graduated Teacher of Physical Education, University of Bern, Switzerland Dec 2001
- Grammar School Diploma, Type C, Städtisches Realgymnasium Bern-Neufeld, Switzerland Jun 1996

### Professional Experience

- Assistant Lecturer, University of Bern, Switzerland: Feb 2004  
- Nov 2007  
 - *assistant in practical courses for chemistry students*  
 - *supervision of Bachelor and Master students*  
 - *training and supervision of apprentices*  
 - *occasional presentations of lectures for Prof. Dr. R. Häner*  
 - *collaborator in Novartis Pharma related projects*
- Teacher of Physical Education at the Oberstufenschule Uettligen, Switzerland: Aug 2001  
- Jul 2004  
 - *teacher of physical education and several representations concerning other school subjects*
- Assistant Course Instructor for „Selbstverteidigung und psychologische Verhaltensschulung für die Schutzbeamtinnen und Schutzbeamten des Tag- und Nachtdienstes der Schutzorganisation“, Federal Police Agency, Bern, Switzerland. Sep 1998  
- Mar 2003
- Temporary employment at two security companies from Bern and Freiburg, Switzerland since 1997

- Several temporary positions (e.g. courier, cinema operator, handyman) in different companies 1992 - 2001
- 

### Languages

- German: mother tongue  
➤ Englisch: very good  
➤ French: very good  
➤ Italian: basic knowledge
- 

### Computer Skills

- Microsoft Office and operating systems and experiences with Macintosh:  
- *Office: Word, Excel, Outlook, Powerpoint*  
- *Operating Systems: Windows 95, 98, Me, NT, 2000, XP*  
- *Flow Cytometry Software: Cell Quest (Mac), FlowJo*
- Macromedia Dreamweaver, BuddyW  
- *Webmaster of the Häner Group: <http://www.dcb.unibe.ch/groups/haener/index.htm>*
- Microsoft Small Business Server 2003  
- *Administrator of the Häner Group*
-